5-2009

Engineering the Nanoparticle Surface for Protein Recognition and Applications

Mrinmoy De
University of Massachusetts Amherst, mrinmoyde@gmail.com

ENGINEERING THE NANOPARTICLE SURFACE FOR PROTEIN RECOGNITION AND APPLICATIONS

A Dissertation Presented

By

MRINMOY DE

Submitted to the Graduate School of the
University of Massachusetts Amherst in partial fulfillment
of the requirements for the degree of

DOCTOR OF PHILOSOPHY

May 2009

Department of Chemistry

ENGINEERING THE NANOPARTICLE SURFACE FOR PROTEIN RECOGNITION AND APPLICATIONS

A Dissertation Presented

by

MRINMOY DE

Approved as to style and content by:

_____
Vincent M. Rotello, Chair

_____
Sankaran Thayumanavan, Member

_____
Robert Weis, Member

_____
Scott C. Garman, Member

_____
Bret E. Jackson, Department Head,
Department of Chemistry

DEDICATION

To my Parents, Brother and Wife, whose love and support made this possible.

ACKNOWLEDGMENTS

I would like to express my deep and sincere gratitude to my advisor, Prof. Vincent M. Rotello, Charles A. Goessmann Professor of Chemistry, for his understanding and constant encouragement. His personal care and guidance lead me from synthetic chemistry to the world of bio-nanotechnology and make it possible to finish this thesis.

I am also extremely thankful to my research committee members, Prof. Sankaran Thayumanavan, Prof. Robert Weis and Prof. Scott C. Garman, for their detailed and constructive comments and constant academic support throughout this work. Other than their generous help it was impossible to finish this thesis.

I wish to express my warm and sincere gratitude to Prof. Bogdan Dragnea and his research group, especially to Dr. Marie-Christine Felicie Daniel in Indiana University for such a successful and productive collaboration on virus like particle preparation.

I thank my past and present group members in Rotello's group for their friendship and wonderful collaboration throughout my Ph.D years. I specifically like to thank Dr. Chang-Cheng You for his great support at my early stage of Ph.D life. Also my warm thanks to the Nick, Ayush, Rui, Gang, Rocky, Brian, Bappa, Partha, Debu, Sarit, Oscar, Handan and Subinoy for their teamwork. I also cordially thank Greene Carol, for her untiring help.

I would like to thank the Department of Chemistry, NMR facilities and the Graduate School of the University of Massachusetts at Amherst.

I want to thank my entire family over the sea that I haven't seen in last 3 and ½ years but their love and constant support was with me always in my difficult moments. Most importantly, I thankful to my wife, Debalina, for her endless support and encourage through out my research life and in writing my thesis. It was impossible to complete this thesis in time without her help.

ABSTRACT

ENGINEERING THE NANOPARTICLE SURFACE FOR PROTEIN RECOGNITION AND APPLICATIONS

MAY 2009

MRINMOY DE, B.Sc., VIDYASAGAR UNIVERSITY, INDIA

M. Sc., INDIAN INSTITUTE OF TECHNOLOGY, BOMBAY, INDIA

Ph.D., UNIVERSITY OF MASSACHUSETTS AMHERST

Directed by: Prof. Vincent M. Rotello

Proteins and nanoparticles (NPs) provide a promising platform for supramolecular interaction. We are currently exploring both fundamental and applied aspects of this interaction. On the fundamental side, we have fabricated a series of water-soluble anionic and cationic NPs to interact with cationic and anionic proteins respectively. A Varity of studies such as, activity assay, fluorescence titration, isothermal titration calorimetry etc. were carried out to quantify the binding properties of these functional NPs with those proteins. Those studies reveal the prospect of tuning the affinity between the nanoparticles and proteins by the surface modification. On the application side, we have used this protein-nanoparticle interaction in protein refolding where we successfully refolded the thermally denatured proteins toward its native structure. We have also applied this particle-protein recognition to create a biocompatible protein sensor using a protein-NP conjugate. Green fluorescent protein and a series of cationic NPs were used for a protein sensor for the identification of protein analytes through displacement process. We have extended this application even in sensing the proteins in human serum.

CONTENTS

LIST OF TABLES

LIST OF FIGURES

LIST OF SCHEMES

CHAPTER 1

NANOPARTICLES IN PROTEIN SURFACE RECOGNITION

1.1 Introduction

The recognition of proteins surfaces is an important issue in biomaterials,[1] where controlled detection of protein surfaces presents a major challenge for the creation of materials for biomedical applications.[2, 3] On the other hand, protein-surface interactions can provide a model for protein-protein interactions, origin of a number of cellular processes, such as cellular signal transduction, DNA transcription, and protein antigen/antibody recognition.[4, 5] Additionally engineered protein-surface interactions are central of diverse bio-applications such as biosensing,[6] biocatalysis,[7] protein purification[8] and controlled culturing of cells.[9] For example, Herceptin:Her2/neu interaction,[10] have many therapeutic implications Interruption of this protein-protein interactions has been used by Chmielewski[11] to inhibit the dimerization and hence activity of HIV-1 protease. In other example Fletchera *et. al.* demonstrated that the Bcl-2-like proteins bind in small proportion of apoptotic Bax protein molecules with an exposed BH3 domain on the mitochondrial membrane, to prevent Bax-imposed cell death and hence can control the programmed cell death (apoptosis) process.[12] Therefore the ability to modify and control the protein interaction by modulating surface chemistry provides a means for probing these interactions in a systematic fashion which is almost inaccessible using purely protein-based systems.

1.2 Protein Surface Recognition using Synthetic Receptors

Protein surface recognition is an emerging target in chemotherapeutics[13] and provides a potent tool for the regulation of protein-protein interactions central to a number of cellular processes as mentioned above. Clearly, control and recognize the protein-protein interactions are a fertile target for the fields of chemical biology and pharmaceutical science.

In general protein-protein interaction involves three kinds of interfaces (Figure 1.1). The first one is surface-surface interactions,[14] which observed in the majority of protein-protein interactions. The second is surface-loop binding,[15] as it is observed in well known p53-MDM2 interaction and the least observed is complementary α-helices interaction.[16]

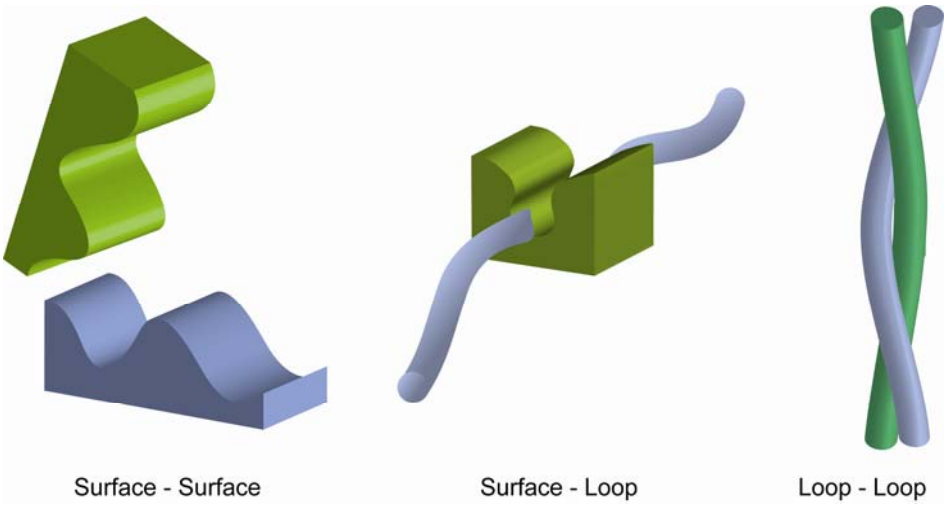

Figure 1.1. Motifs for protein-protein interactions (reproduced from Alberts *et al* in *Molecular Biology of the Cell, 3rd ed.* p 217).

Recognition of protein surfaces using synthetic receptors is based on noncovalent host-guest interaction as observed in small molecule systems. However the regulation of biomolecules remains a far more significant challenge. This challenge is

primarily due to two basic requirements for an effective recognition between a biomacromolecule and its receptor. First of all, a large biomacromolecule-receptor contact area is required. For example, relatively large surface areas are required for effective binding of protein surfaces (which are solvent exposed) to successfully inhibit the active site. Insight into this requirement comes from examination of protein-protein interactions, which reveals that a surface area of more than 6 nm^2 per protein are typically involved in such interactions.[17, 18]

A number of "small molecule" systems[19] and macromolecular scaffolds have been used to address this challenge for protein surface recognition. Most of the research in the creation of receptors targeted to protein surfaces has focused on peptides[20] and peptidomimetic structures,[21] where protein self-assembly assists in the creation of large constructs featuring controlled structure. Recent "small molecule" systems include the receptors Hamilton has developed on calixarene and porphyrin scaffolds,[22, 23] cyclodextrin dimers synthesized by Breslow,[24] and Mallik's transition metal complexes targeted against surface-exposed histidines.[25] Another very productive method for the creation of protein surface receptors uses macromolecular scaffolding. In this aspect, Kiessling has used ring opening metathesis polymerization (ROMP) to create libraries of macromolecular receptors possessing partially-constrained backbones.[26, 27] Such systems demonstrate a certain level of success in modulation of biomolecular function; but the question of protein surface recognition still remains indistinct.

The second challenge for protein surface recognition is the complexity of the surfaces involved,[28] in terms of their multiple electrostatic,[29] hydrophobic[30] and topological features.[31, 32] Direction for the design of receptors can be obtained from

examination of protein-protein interactions. From these studies, it is clear that proper presentation of surface elements is required for the effective recognition of the "hot spot",[33] present in protein-protein interfaces. Creation of systems complementary to these hotspots, however, is an essentially open question, in particular in the area of surface-surface interactions.

1.3 Nanoparticles as Scaffolds for Recognition

Nanoparticle based receptors, however, offer a platform for biomolecular surface recognition which is unique and distinctive in its own way. In this respect nanoparticles are promising materials for the creation of artificial receptor for the following reasons. The size of the nanoparticle core can be tuned from 1.5 to more than 10 nm which can provides a suitable platform for the interaction of nanoparticles with proteins and other biomolecules (Figure 1.2).[34]

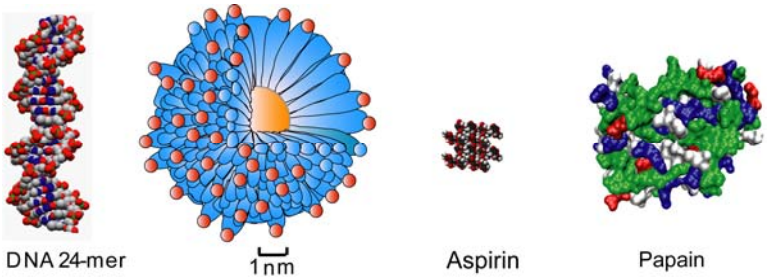

Figure 1.2. Schematic representation for relative size of a 2 nm gold nanoparticle with 11-mercaptoundecanoic acid monolayer and aspirin crystal (small molecule), papain (protein), and a 24 mer DNA duplex.

Secondly nanoparticles can be fabricated with a wide range of surface functionality thus providing a versatile system for creation of surface-specific receptors. The third important feature is the range of metal and semiconductor cores can be generated featuring useful properties and application (Table 1.1).[35] From table 1.1

metallic nanoparticle (i.e. Au, Ag etc.) are become more popular for molecular recognition, delivery and sensing where as semiconductor and magnetic nanoparticles are drawing the interest as an imaging agent.[36]

Table 1.1. Characteristics and corresponding ligand for various metal and semiconductor materials as nanometer-sized scaffold (reproduced from reference no. 36).

Core material	Characteristics	Ligand(s)	Applications
Au	Optical absorption, fluorescence and fluorescence quenching, stability	Thiol, disulfide, phosphine, amine	Biomolecular recognition, delivery, sensing
Ag	Surface-enhanced fluorescence	Thiol	Sensing
Pt	Catalytic property	Thiol, phosphine, amine, isocyanide	Bio-catalyst, sensing
CdSe	Luminescence, photo-stability	Thiol, phosphine, pyridine	Imaging, sensing
Fe_2O_3	Magnetic property	Diol, dopamine derivative, amine	MR imaging and biomolecule purification
SiO_2	Biocompatibility	Alkoxysilane	Biocompatible by surface coating

Finally, the self-template nature of this system to guest molecules is allowing an increase in the affinity and selectivity upon incubation with the guest molecules. Applying these characteristic to the selective recognition of biomacromolecules, however, requires suitable surface functionality which can be solved by using reported synthetic methods.[37]

There are several applications on nanoparticle-biomolecule interactions have been reported based on various biological and diagnostic applications.[36] Nanoparticles can be made-up with a diverse array of metal, alloy, oxide and semiconductor materials, using standard reported procedure available in literatures which already mention before (Table 1.1). As an example Brust and coworkers have developed a widely used particle preparation procedure for metallic nanoparticles by the reduction of metal salt in the

presence surfactant and coating ligands (Figure 1.3a)[38] Using this method various metallic nanoparticles (such as Ag, Pt, Pd, Cu etc.) have been prepared. In this protocol the size of the particle can be controlled by varying the metal-ligand ratio and reaction conditions. For efficient biological applications, the most important requirements of the nanoparticle are surface functionality and water-solubility.

To introduce the surface functionality, the most acceptable method is the Murray's place-exchange process (Figure 1.3a),[39] where the initial ligands on the nanoparticle surface are replaced by external ligands of similar functionality as an instance, thiol or disulfide ligands for gold and silver particle. The other well known method is direct synthesis of metallic nanoparticles in presence of corresponding ligand to generate monolayer-protected clusters (MPCs) and mixed monolayer-protected clusters (Nanoparticles). According to the necessity further functionality can be introduced through conventional organic protocols.[40] Recently, another kind of water-soluble functionalized nanoparticles were reported by the incorporation of hydrophobic nanoparticles into the hydrophobic interiors of surfactant micelles.[41, 42] To improve the biocompatibility oligo(ethylene glycol) (OEG) and poly(ethylene glycol) (PEG) are commonly incorporated into the monolayers.[43] The OEG or PEG are hydrophilic in nature to improve the water solubility with the added benefit these ligand resist the nonspecific interactions with biomolecules. Therefore the slandered nanoparticle for controlled biomolecular interactions consists of hydrophobic interior, an OEG or PEG layer, and recognition elements on the surface (Figure 1.3b).

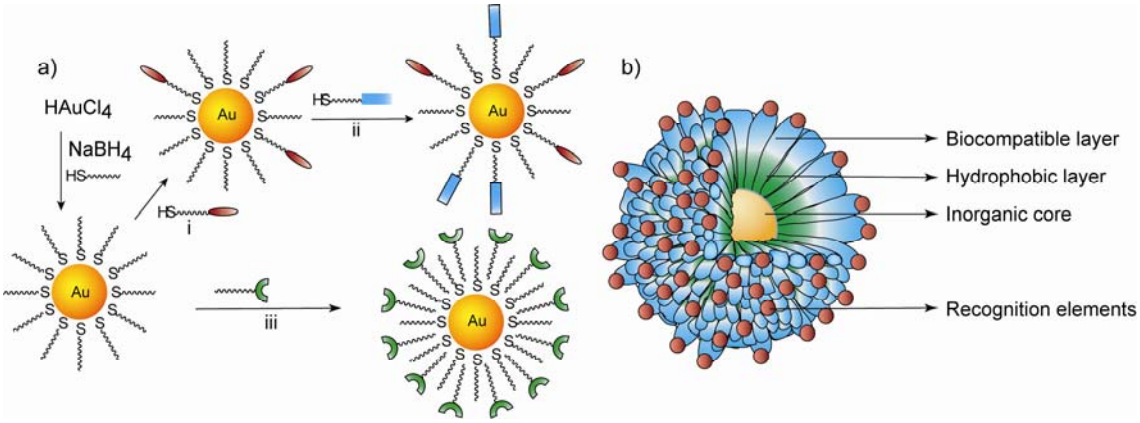

Figure 1.3. a) Construction of nanoparticles through Brust reduction and subsequent modification such as Murray place-exchange reaction (i), (ii) and encapsulation of hydrophobic MPCs into surfactant micelles (iii). b) Multifunctional particle monolayers featuring a hydrophobic core for stability, OEG or PEG layer for biocompatibility, and recognition elements on the surface for interaction with biomolecules.

1.4 Applications of Nanoparticles in Biology

Applications of nanometrials in biotechnology merge the interface between material science and biology. The development of biocompatible nanometrials for enhancing or modifying the bio-properties is the new challenge in the biotechnology field. Here I will highlight few recent research activities involving the use and diverse applications of nanoparticles in biology. Those applications can be classified in four main categories, a) biomolecular interactions, b) application in drug and gene delivery, c) biosensing and d) bioimaging.

1.4.1 Recognition of Biomolecules

Based on the surface functionality and properties bio-macromolecules can be sub-divided into two categories, nucleic acid and proteins. Binding of DNA with receptors can be happen in three ways, surface binding, groove binding and intercalation.[44] A number of small synthetic and natural receptors have been utilized to

bind specific DNA sequences,[45] and to inhibit[46] or activate[47] DNA transcription. Similar to naturally occurring protein-nucleic acid interactions, nanoparticles with large surface area and multivalent recognition unit can serve as an attractive receptor for nucleic acids.[48] The binding between nanoparticles and DNA can be achieved in three ways. First, nanoparticles can be functionalized with a highly selective complementary single strand of DNA, which can display excellent sequence specificity (Figure 1.4a).[49] Secondly, we can use complementary electrostatic interactions to promote high affinity of nanoparticle-DNA binding. As the nucleic acids are negatively charged due to its phosphate backbone, inserting appropriate cationic ligands onto nanoparticle surface can provides effectual receptors for DNA, for example the use of **NP1** to recognize a 37-mer DNA duplex (Figure 1.4b) by our group.[50] The binding of the DNA inhibited transcription by T7 RNA polymerase, indicating the high affinity of the NP-DNA complex, and pointing out a potential use of these systems in gene delivery into cells and the protection of DNA from enzymatic cleavage.[51] Intercalation provides another mechanism for DNA binding, as demonstrated by Murray *et al*. by useing ethidium bromide (Eb) as a means of binding cationic and anionic gold nanoparticles to DNA.[52]

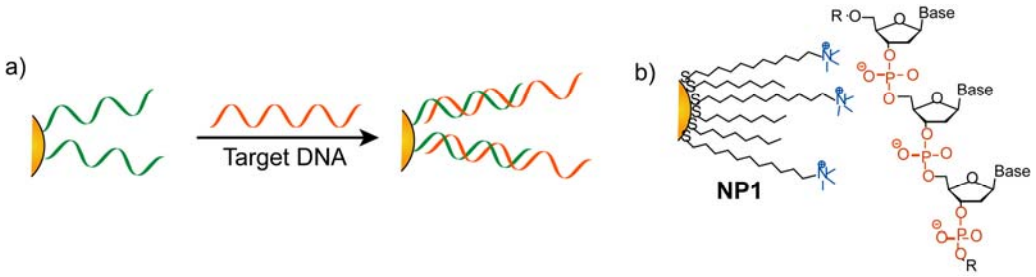

Figure 1.4. The DNA-nanoparticle interactions. a) Binding of DNA through complementary oligonucleotide hybridization. b) Structure of **NP1** scaffold and the DNA backbone. The interaction is directed by electrostatic interaction.

The interaction of protein with nanoparticles is more complex compare to the DNA, due to its diverse shape, size and charge on the surface. The complexation between protein and nanoparticle can be achieved either by noncovalent interaction (e.g. electrostatic, hydrophobic, p-p stacking etc.) or by specific interaction (e.g. antigen-antibody interaction, metal complex formation etc.) (Figure 1.5). The noncovalent complexation can be achieved by electrostatic interaction by using oppositely charged nanoparticle in respect to protein. One system that has been explored is the binding of α-chymotrypsin (ChT), utilizing the ring of cationic residues around active site of ChT (Figure 1.5a).[53] The inhibition of ChT activity was observed upon incubation with negatively charged **NP 2**.[54] A two-step binding process with a fast reversible association followed by a slower irreversible denaturation was established by our group. The above conception of complementary electrostatic interaction was also used for positively charged nanoparticles with negatively charged proteins. Positively charged nanoparticle bind with negatively charged protein such as β-Galactosidase (β-Gal), and inhibits its activity which was again reactivated by the addition of glutathione.

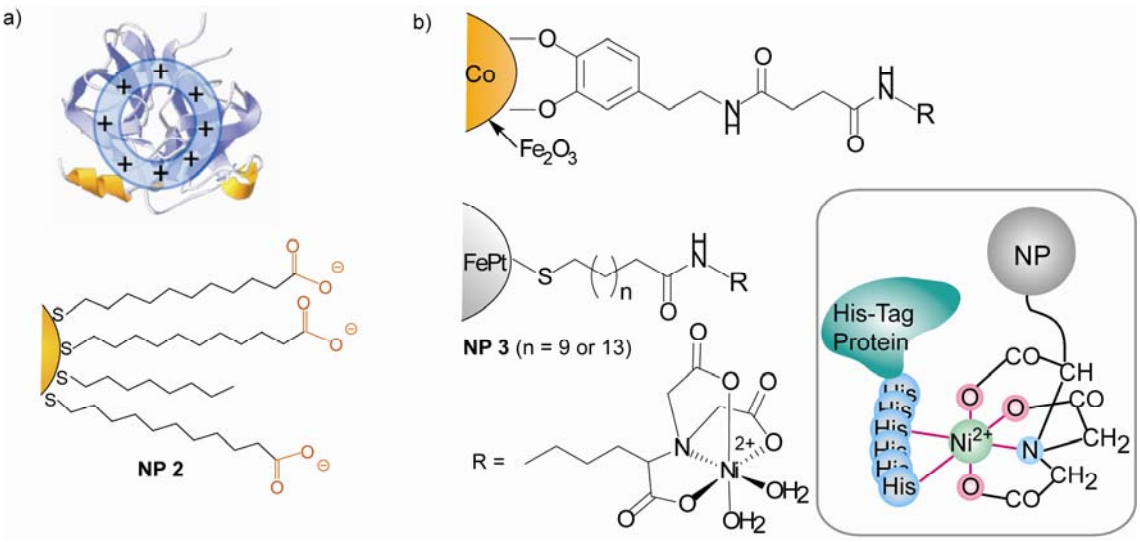

Figure 1.5. Protein-nanoparticle conjugation. a) Electrostatic targeting of ChT by anionic **NP 2** b) Structure of NTA-modified magnetic nanoparticles and the NTA-Ni^{2+} functionalized magnetic nanoparticles selectively bind to histidine-tagged proteins.

As nanoparticles can be fabricated with numerous ligands in a small volume, they can use as a multivalent receptor to enhance low affinity interactions such as carbohydrate-protein interactions.[55] As an example, Lin *et al.* prepared mannose functionalized gold nanoparticle[56] and it was found that the nanoparticles showed high affinity to Con A in compare to single mannose (binding constant: $10^7 – 10^8$ dm^3 mol^{-1}, 10-100-fold higher affinity than that of monovalent mannose ligands).

Specific biomacromolecular interactions such as streptavidin/biotin complementarity ($K_a \sim 10^{14}$ M^{-1}) have been used to provide specific protein-NP binding.[57] Biotin functionalized quantum dots (QDs) were used for specific protein binding in time-resolved fluoroimmunoassay.[58] Another way to specifically bind proteins is through the use of transition metal complexes that can bind with surface-exposed histidines of proteins. Xu *et al.* fabricated FePt magnetic nanoparticle **NP 3**, with nickel-terminated nitrilotriacetic acid (NTA).[59] These NPs show high affinity and

specificity towards histidine-tagged proteins (proteins with six consecutive histidine residues) (Figure. 1.5b).

1.4.2 Application in Targeted Delivery

For successful delivery, carriers must: 1) form condensed complexes with therapeutic molecules, 2) reach the target position, 2) facilitate penetration of the cell membrane and (3) unload their payloads inside of cells. In this aspect nanoparticles can be used as potential DDSs due to its advantageous characteristics as mentioned previously. Nanoparticle based drug delivery can be presented in two categories: 1) delivery using surface property or surface bounded drug molecules and 2) nanoparticles as a delivery vehicle. Here three interesting studies are highlighted where nanoparticles are used to deliver drug, gene and protein. According to the first category Mixed monolayer protected gold clusters were exploited for *in vitro* delivery of a hydrophobic fluorophore (BODIPY); an analog of hydrophobic drugs, and release of the fluorogenic ligand in a controlled fashion.[60] Cationic nature of the nanoprticles facilitates the penetration of cell membrane and the release was triggered by intracellular glutathione (GSH) since the concentration of GSH inside the cells is around 1000 fold more than extracellular environment.

RNA technology has appeared in twenty first century as a potential tool for curing disease at early stage. Gene can be efficiently silenced by small interfering RNA (siRNA), generally consists of 19-21 base pairs. This siRNA has been conjugated by a thiol linker with variety of nanoparticles, such as gold,[61] quantum dots,[62] or iron oxide for *in vitro* delivery.[63] Moore *et al.* designed a superparamagnetic nanoparticle to

perform multiple functions such as, carry the siRNA, deliver in a site-specific manner and probe the delivery by magnetic resonance imaging as well as optical imaging.[63] The multifunctional nanoparticle was effective for in vitro and in vivo gene silencing via a specific pathway.

Protein delivery has emerged as a complementary to nucleic acids delivery in the field of biomedicine. Nanoparticles can efficiently recognize protein, and hence create the opportunity of using them as protein delivery systems. Lin *et al* have fabricated MCM-41 type mesoporous silica nanoparticles (MSN) as protein carriers (Figure 1.6).[64] These MSN can incorporate cytochrome *c*, a membrane-impermeable protein, into their large pores (diameter = 5.4 nm), and slowly release the proteins in active form under physiological conditions. The particles were also effective in delivery of cytochrome *c* human cervical cancer cells (HeLa).

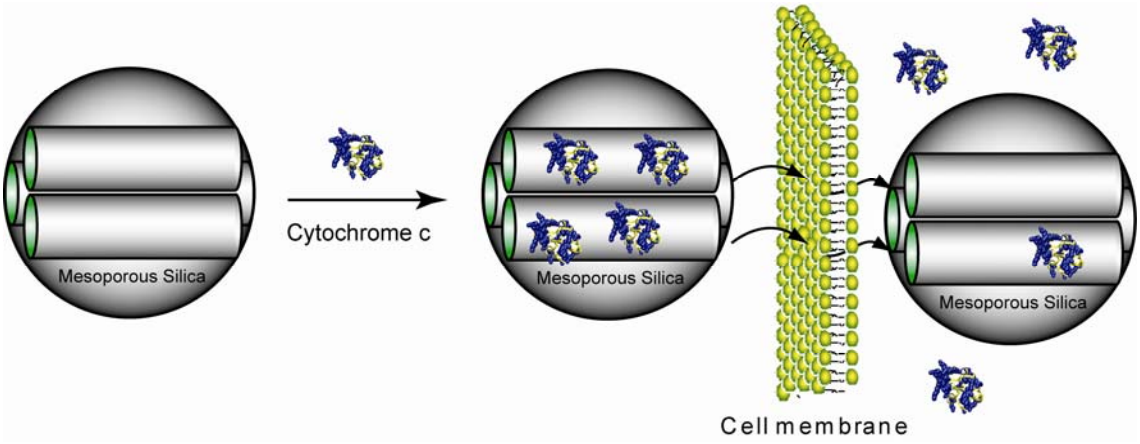

Figure 1.6. Schematic illustration of cellular delivery of cytochrome *c* using mesoporous silica nanoparticles.

1.4.3 Nanoparticles in Bio-Sensing

A sensor generally consists of two components: 1) recognition element for target binding and 2) transduction element for signaling the binding event. The large surface-

to-volume ratio with the electronic and optical properties makes the nanoparticles as a potential system in sensor application. Nanoparticles are applied in the detection of various biomolecules such as, oligonucleotides, proteins, and microorganisms. Based on the regulating properties such as absorbance, quenching, conductivity etc. the nanoparticle based biological sensing can be sub-categorized in several group, such as, 1) colorimetric Sensing, 2) fluorescence Sensing 3) electrochemical Sensing etc. Some of the very interesting studies of each kind have been highlighted here. In first kind of sensing is the controlled assembly of nanomaterials alters the interparticle surface plasmon coupling, resulting in a visual color change. Using this control aggregation of the particles, a range of biomolecules from polynucleotides to proteins are detected.[65] DNA functionalized nanoparticles have been assembled or aggregates with complementary DNA strand through Watson-Crick base pairing which is first described by Mirkin *et al.* in 1996.[49] After that, the oligonucleotide mediated nanoparticle aggregation process was extensively used for the development of simple and highly sensitive colorimetric biosensors for oligonucleotides.[66, 67] The general procedure for the detection of the oligonucleotides was done by the fabrication of the nanoparticles with two complementary single strands DNA of the both ends of targeted oligonucleotides. According to the Figure 1.7, the particles are aggregated and changed the color of the solution. Using this method oligonuceotides are detected at subpicomolar level without the assistance of polymerase chain reaction (PCR).[68]

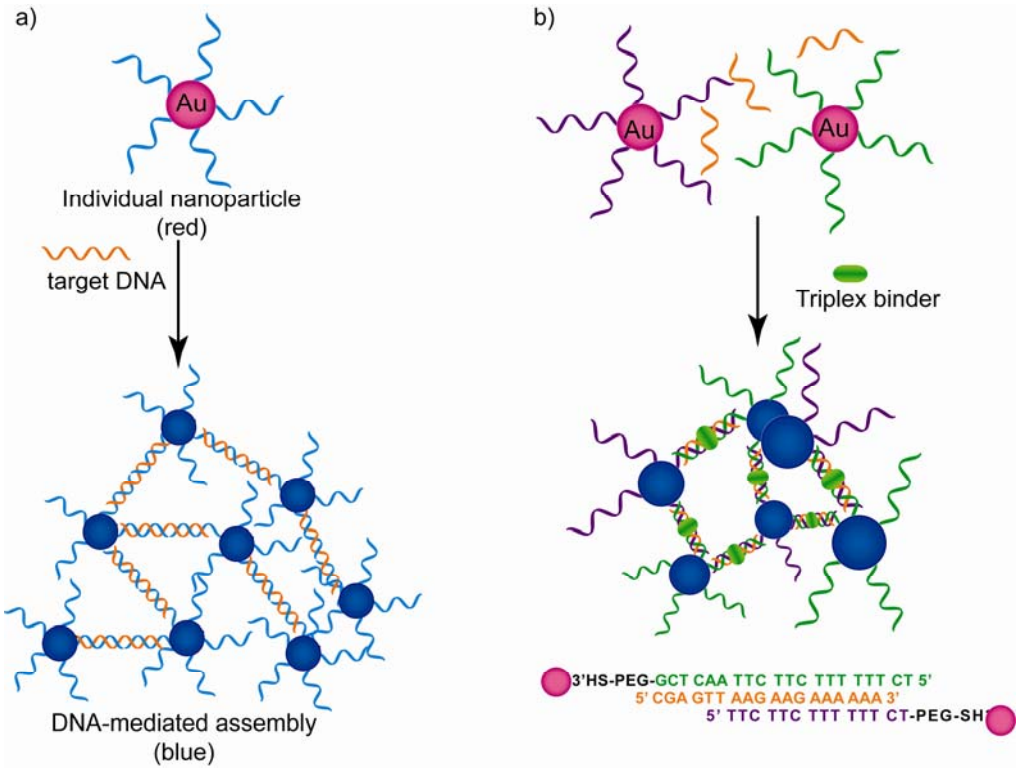

Figure 1.7. Schematic illustration of a) DNA-induced nanoparticle aggregation and b) sensing of DNA triplex binder using DNA-directed AuNP assembly.

The high quenching ability of gold nanoparticles was used for molecular beacons construction for sensing the DNA strands using the intensity of fluorescence responses.[69] According to the reported design, initially the dye molecule remains close to the nanoparticle surface due to hairpin structure of the attached DNA, resulting in an effective fluorescence quenching through FRET. As shown in the hybridization of target DNA opens up the hairpin structure and increase the distance between nanoparticle and dye, results in a significant increase in fluorescence. As the fluorescent intensity was only depends on the concentration of the target DNA, this system was used for DNA sensing. A range of ssDNA and DNA cleavages ware detected using this molecular beacon approach.[70]

1.4.4 Nanoparticles in Bio-Imaging

Based on the imaging techniques there are two different types of nanoparticles are well known, one is luminescent nanoprobes for OI and the other one is magnetic nanoparticles for MRI. There are also hybrid nanoparticles are reported which can concurrently detected both by OI and MRI.[71] These nanoparticles are composed of luminescent agent and paramagnetic materials.

The nanoparticle based optical imaging agent can be subdivided into two categories, the most popular one is quantum dots (QDs) and the other one is dye doped nanoparticles. The use of QDs for cell imaging was first reported by Nie[72] and Alivisatos groups in 1998.[73] An attractive example of self-illuminating QD conjugate was reported by So et al. for *in vivo* imaging.[74] The requirement of external excitation for QDs sometimes limits their *in vivo* application due to opacity. They overcome this problem by designing this self-illuminating QD which can luminesce without the need for external excitation. They prepared this QD conjugets by coupling with carboxylate modified QDs to a mutant of the bioluminescent protein Renilla luciferase. The energy released by luciferase-catalyzed substrate catabolism was transferred to QDs via resonance energy transfer; end up with the emission from QD (Figure 1.8).

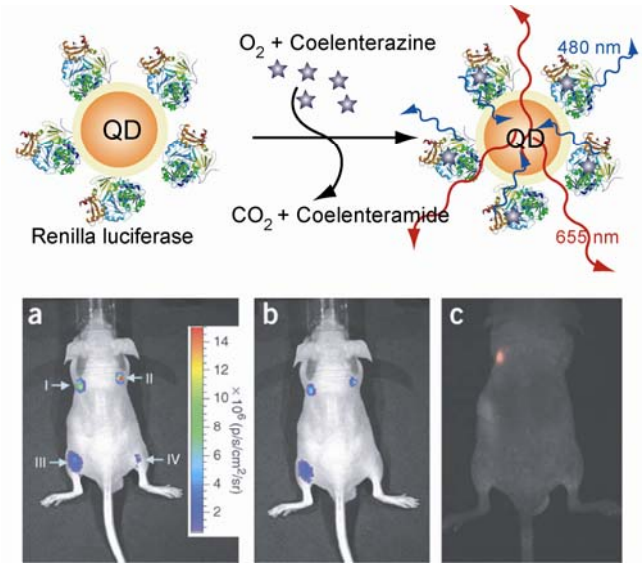

Figure 1.8. Conjugation of QDs with luciferase proteins. The luminescence released from QD during the luciferase catalyzed oxidation of coelenterazine is tranfered to the QD. Bioluminescence and fluorescence imaging of QD and luciferase protein injected at indicated sites (I and III QD, II and IV luciferase protein). (a) Without filters. (b) With 575- to 650-nm filter. (c) Fluorescence imaging with filter, 503–555 nm. Adapted from reference no. 74.

On the other hand the dye doped silica nanoparticle solves the problem of rapid photo-bleaching of organic dyes. This dye doped silica particles are biocompatible and non-toxic.[75]

Another important non-invasive imaging technique is MRI. This is a very potential method to image in cellular and subcellular level. The MRI technique is based on the nuclear magnetic resonance of the interacting protons with each other and with the surrounding molecules. With recent development of molecular MRI the magnetic particles are used not only as a targeted imaging agent but also can image local enzyme activity and develop the multispectral MRI techniques.[76] At present monodisperse, cross-linked iron oxide (CLIO) nanoparticles reported by R. Weissleder group are popular for the MRI.[77] The CLIO nanoparticles are highly stable and a large variety of

ligands can be conjugated on the surface. This monodisperse, surface modified iron oxide nanoparticle CLIO-Cy5.5 and convenient 'clickable' nanoparticles ware used for targeted imaging with high cellular uptake.[78]

Taking the advantage of both OI and MRI, multimodal imaging agents such as magnetofluroscent nanoparticles is now gaining the more popularity.[79, 80] A realistic procedure for development of targeted magnetofluorescent nanoparticles is well described in a recent report by R. Weissleder's group. According to that protocol first need to discover or choose the targeting ligands using high-throughput screening techniques. Then functionalization of the targeting ligands on the surface of the magnetofluorescent nanoparticles needs to do to enhance the target specificity.

Overall nanoparticles present a prospective platform for the diverse biological applications. The surface and core properties of these systems can be engineered for multipurpose applications. Other than biomolecular recognition, therapeutic delivery, biosensing and bioimaging based applications; various well known applications are also reported. As an example, Scrimin's group reported a peptide functionalized nanoparticles which show enzyme-like structure and properties. Those particles not only have a good esterolytic catalytic activity but also you can regulate its activity like natural enzymes.[81]

1.5 Perspective of Fundamental Studies of Protein-Surface Interactions

Fundamental studies on protein nanoparticle interaction are always an attractive point of interest, because it can explore the nature of the interaction which can be used for control recognition. Study of protein-surface interactions on planar surfaces,

however, is complicated by the inherent limitations in characterizing surface-bound proteins. While adsorption kinetics can be readily quantified using Quartz Crystal Microbalance (QCM)[82] and Surface Plasmon Resonance (SPR) methods,[83] the limited quantity of material contained in a monolayer can make assessing the activity of enzymes difficult. Spectroscopic characterization of adsorbed proteins is likewise difficult, with available methods generally limited to IR[84] and fluorescence spectroscopy,[85] and techniques such as CD and NMR difficult or impossible to apply. Of equal importance is the inherent difficulty of applying powerful thermochemical techniques as Isothermal Titration Calorimetry (ITC) to surface recognition processes.

Nanoparticles provide a highly useful tool for studying protein-surface interactions. The high surface area and optical properties of these systems allow ready application of CD and fluorescence methods.[86] Recent studies have also used unfunctionalized silica particles for Differential Scanning Calorimetry (DSC),[87] though interestingly ITC has not been applied to these systems. Clearly, integration of these spectroscopic and calorimetric techniques with the structural diversity that can be generated using nanoparticles (*vide infra*) can provide a powerful tool for understanding and protein-surface interactions. Moreover, these interactions can be harnessed in a controlled fashion for a wide variety of applications such as protein refolding and sensing.

1.6 Reference

1 Mrksich, M.; Whitesides, G. M., *Annu. Rev. Biophys. Biomol. Struct.* **1996,** *25*, 55-78.

2 Horne, W. S.; Gellman, S. H., *Acc. Chem. Res.* **2008,** *41*, 1399-1408.

3 Wei, G. B.; Ma, P. X., *Adv. Funct. Mater.* **2008,** *18*, 3568-3582.

4 Ron, D.; Walter, P., *Nat. Rev. Mol. Cell Biol.* **2007,** *8*, 519-529.

5 Addadi, L.; Rubin, N.; Scheffer, L.; Ziblat, R., *Acc. Chem. Res.* **2008,** *41*, 254-264.

6 Willner, I.; Katz, E., *Angew. Chem., Int. Ed.* **2000,** *39*, 1180-1218.

7 Zhong, D. P., *Curr. Opin. Chem. Biol.* **2007,** *11*, 174-181.

8 Duellman, S. J.; Burgess, R. R., *Protein Expression Purif.* **2009,** *63*, 128-133.

9 Khademhosseini, A.; Jon, S.; Suh, K. Y.; Tran, T. N. T.; Eng, G.; Yeh, J.; Seong, J.; Langer, R., *Adv. Mater.* **2003,** *15*, 1995-2000.

10 Eigenbrot, C.; Randal, M.; Presta, L.; Carter, P.; Kossiakoff, A. A., *J. Mol. Biol.* **1993,** *229*, 969-995.

11 Shultz, M. D.; Chmielewski, J., *Bioorg. Med. Chem. Lett.* **1999,** *9*, 2431-2436.

12 Fletchera, J. I.; Meusburger, S.; Hawkins, C. J.; Riglar, D. T.; Lee, E. F.; Fairlie, W. D.; Huang, D. C. S.; Adams, J. M., Proc. Natl. Acad. Sci. U. S. A. 2008, *105*, 18081-18087.

13 Lindsley, C. W.; Barnett, S. F.; Yaroschak, M.; Bilodeau, M. T.; Layton, M. E., *Current Topics in Medicinal Chemistry* **2007,** *7*, 1349-1363.

14 Braig, K.; Otwinowski, Z.; Hegde, R.; Boisvert, D. C.; Joachimiak, A.; Horwich, A. L.; Sigler, P. B., *Nature* **1994,** *371*, 578-586.

15 Kussie, P. H.; Gorina, S.; Marechal, V.; Elenbaas, B.; Moreau, J.; Levine, A. J.; Pavletich, N. P., *Science* **1996,** *274*, 948-953.

16 Harrison, C. J.; Bohm, A. A.; Nelson, H. C. M., *Science* **1994,** *263*, 224-227.

17 Lo Conte, L.; Chothia, C.; Janin, J., *J. Mol. Biol.* **1999,** *285*, 2177-2198.

18 Nadassy, K.; Wodak, S. J.; Janin, J., *Biochemistry* **1999,** *38*, 1999-2017.

19 Park, H. S.; Lin, Q.; Hamilton, A. D., *Proc. Natl. Acad. Sci. U. S. A.* **2002,** *99*, 5105-5109.

20 Robinson, J. A., *Acc. Chem. Res.* **2008,** *41*, 1278-1288.

21 Hanessian, S.; Auzzas, L., *Acc. Chem. Res.* **2008,** *41*, 1241-1251.

22 Wilson, A. J.; Groves, K.; Jain, R. K.; Park, H. S.; Hamilton, A. D., *J. Am. Chem. Soc.* **2003,** *125*, 4420-4421.

23 Ernst, J. T.; Becerril, J.; Park, H. S.; Yin, H.; Hamilton, A. D., *Angew. Chem., Int. Ed.* **2003,** *42*, 535-540.

24 Leung, D. K.; Yang, Z. W.; Breslow, R., *Proc. Natl. Acad. Sci. U. S. A.* **2000,** *97*, 5050-5053.

25 Fazal, M. A.; Roy, B. C.; Sun, S. G.; Mallik, S.; Rodgers, K. R., *J. Am. Chem. Soc.* **2001,** *123*, 6283-6290.

26 Gordon, E. J.; Sanders, W. J.; Kiessling, L. L., *Nature* **1998,** *392*, 30-31.

27 Gestwicki, J. E.; Cairo, C. W.; Strong, L. E.; Oetjen, K. A.; Kiessling, L. L., *J. Am. Chem. Soc.* **2002,** *124*, 14922-14933.

28 de Rinaldis, M.; Ausiello, G.; Cesareni, G.; Helmer-Citterich, M., *J. Mol. Biol.* **1998,** *284*, 1211-1221.

29 Golumbfskie, A. J.; Pande, V. S.; Chakraborty, A. K., *Proc. Natl. Acad. Sci. U. S. A.* **1999,** *96*, 11707-11712.

30 Lijnzaad, P.; Argos, P., *Proteins-Structure Function and Genetics* **1997,** *28*, 333-343.

31 Di Cera, E., *Chem. Rev.* **1998,** *98*, 1563-1591.

32 Mammen, M.; Choi, S. K.; Whitesides, G. M., *Angew. Chem., Int. Ed.* **1998,** *37*, 2755-2794.

33 Bogan, A. A.; Thorn, K. S., *J. Mol. Biol.* **1998,** *280*, 1-9.

34 Hostetler, M. J.; Wingate, J. E.; Zhong, C. J.; Harris, J. E.; Vachet, R. W.; Clark, M. R.; Londono, J. D.; Green, S. J.; Stokes, J. J.; Wignall, G. D.; Glish, G. L.; Porter, M. D.; Evans, N. D.; Murray, R. W., *Langmuir* **1998,** *14*, 17-30.

35 Ferrando, R.; Jellinek, J.; Johnston, R. L., *Chem. Rev.* **2008,** *108*, 845-910.

36 De, M.; Ghosh, P. S.; Rotello, V. M., *Adv. Mater.* **2008,** *20*, 4225 - 4241.

37 Euliss, L. E.; DuPont, J. A.; Gratton, S.; DeSimone, J., *Chem. Soc. Rev.* **2006,** *35*, 1095-1104.

38 Brust, M.; Walker, M.; Bethell, D.; Schiffrin, D. J.; Whyman, R., *J. Chem. Soc.-Chem. Commun.* **1994**, 801-802.

39 Templeton, A. C.; Wuelfing, M. P.; Murray, R. W., *Acc. Chem. Res.* **2000,** *33*, 27-36.

40 Rothrock, A. R.; Donkers, R. L.; Schoenfisch, M. H., *J. Am. Chem. Soc.* **2005,** *127*, 9362-9363.

41 Fan, H. Y.; Chen, Z.; Brinker, C. J.; Clawson, J.; Alam, T., *J. Am. Chem. Soc.* **2005,** *127*, 13746-13747.

42 Fan, H. Y.; Leve, E. W.; Scullin, C.; Gabaldon, J.; Tallant, D.; Bunge, S.; Boyle, T.; Wilson, M. C.; Brinker, C. J., *Nano Lett.* **2005,** *5*, 645-648.

43 Kanaras, A. G.; Kamounah, F. S.; Schaumburg, K.; Kiely, C. J.; Brust, M., *Chem. Commun.* **2002**, 2294-2295.

44 Armitage, B. A., Cyanine dye-DNA interactions: Intercalation, groove binding, and aggregation. In *DNA Binders and Related Subjects*, 2005; Vol. 253, pp 55-76.

45 Fechter, E. J.; Olenyuk, B.; Dervan, P. B., *Angew. Chem., Int. Ed.* **2004,** *43*, 3591-3594.

46 Gearhart, M. D.; Dickinson, L.; Ehley, J.; Melander, C.; Dervan, P. B.; Wright, P. E.; Gottesfeld, J. M., *Biochemistry* **2005,** *44*, 4196-4203.

47 Arndt, H. D.; Hauschild, K. E.; Sullivan, D. P.; Lake, K.; Dervan, P. B.; Ansari, A. Z., *J. Am. Chem. Soc.* **2003,** *125*, 13322-13323.

48 Mahtab, R.; Harden, H. H.; Murphy, C. J., *J. Am. Chem. Soc.* **2000,** *122*, 14-17.

49 Mirkin, C. A.; Letsinger, R. L.; Mucic, R. C.; Storhoff, J. J., *Nature* **1996,** *382*, 607-609.

50 McIntosh, C. M.; Esposito, E. A.; Boal, A. K.; Simard, J. M.; Martin, C. T.; Rotello, V. M., *J. Am. Chem. Soc.* **2001,** *123*, 7626-7629.

51 Han, G.; Martin, C. T.; Rotello, V. M., *Chemical Biology & Drug Design* **2006,** *67*, 78-82.

52 Wang, G. L.; Zhang, J.; Murray, R. W., *Anal. Chem.* **2002,** *74*, 4320-4327.

53 Blow, D. M., *Acc. Chem. Res.* **1976,** *9*, 145-152.

54 Fischer, N. O.; McIntosh, C. M.; Simard, J. M.; Rotello, V. M., *Proc. Natl. Acad. Sci. U.S.A.* **2002,** *99*, 5018-5023.

55 Lee, Y. C., *FASEB J.* **1992,** *6*, 3193-3200.

56 Lin, C. C.; Yeh, Y. C.; Yang, C. Y.; Chen, G. F.; Chen, Y. C.; Wu, Y. C.; Chen, C. C., *Chem. Commun.* **2003**, 2920-2921.

57 Zheng, M.; Huang, X. Y., *J. Am. Chem. Soc.* **2004,** *126*, 12047-12054.

58 Hildebrandt, N.; Charbonniere, L. J.; Beck, M.; Ziessel, R. F.; Lohmannsroben, H. G., *Angew. Chem., Int. Ed.* **2005,** *44*, 7612-7615.

59 Xu, C. J.; Xu, K. M.; Gu, H. W.; Zhong, X. F.; Guo, Z. H.; Zheng, R. K.; Zhang, X. X.; Xu, B., *J. Am. Chem. Soc.* **2004,** *126*, 3392-3393.

60 Hong, R.; Han, G.; Fernandez, J. M.; Kim, B. J.; Forbes, N. S.; Rotello, V. M., *J. Am. Chem. Soc.* **2006,** *128*, 1078-1079.

61 Oishi, M.; Nakaogami, J.; Ishii, T.; Nagasaki, Y., *Chem. Lett.* **2006,** *35*, 1046-1047.

62 Derfus, A. M.; Chen, A. A.; Min, D. H.; Ruoslahti, E.; Bhatia, S. N., *Bioconjugate Chem.* **2007,** *18*, 1391-1396.

63 Medarova, Z.; Pham, W.; Farrar, C.; Petkova, V.; Moore, A., *Nature Medicine* **2007,** *13*, 372-377.

64 Slowing, II; Trewyn, B. G.; Lin, V. S. Y., *J. Am. Chem. Soc.* **2007,** *129*, 8845-8849.

65 Rosi, N.; Mirkin, C. A., *Chem. Rev.* **2005,** *105*, 1547-1562.

66 Chakrabarti, R.; Klibanov, A. M., *J. Am. Chem. Soc.* **2003,** *125*, 12531-12540.

67 Storhoff, J. J.; Lucas, A. D.; Garimella, V.; Bao, Y. P.; Muller, U. R., *Nat. Biotechnol.* **2004,** *22*, 883-887.

68 Reynolds, R. A.; Mirkin, C. A.; Letsinger, R. L., *J. Am. Chem. Soc.* **2000,** *122*, 3795-3796.

69 Dubertret, B.; Calame, M.; Libchaber, A. J., *Nat. Biotechnol.* **2001,** *19*, 365-370.

70 Ray, P. C.; Fortner, A.; Darbha, G. K., *J. Phys. Chem. B* **2006,** *110*, 20745-20748.

71 Schellenberger, E. A.; Sosnovik, D.; Weissleder, R.; Josephson, L., *Bioconjugate Chem.* **2004,** *15*, 1062-1067.

72 Chan, W. C. W.; Nie, S. M., *Science* **1998,** *281*, 2016-2018.

73 Bruchez, M.; Moronne, M.; Gin, P.; Weiss, S.; Alivisatos, A. P., *Science* **1998,** *281*, 2013-2016.

74 So, M. K.; Xu, C. J.; Loening, A. M.; Gambhir, S. S.; Rao, J. H., *Nat. Biotechnol.* **2006,** *24*, 339-343.

75 Jin, Y. H.; Kannan, S.; Wu, M.; Zhao, J. X. J., *Chem. Res. Toxicol.* **2007,** *20*, 1126-1133.

76 Sosnovik, D. E.; Weissleder, R., *Curr. Opin. Biotechnol.* **2007,** *18*, 4-10.

77 Wunderbaldinger, P.; Josephson, L.; Weissleder, R., *Academic Radiology* **2002,** *9,* S304-S306.

78 Sosnovik, D. E.; Nahrendorf, M.; Weissleder, R., *Circulation* **2007,** *115*, 2076-2086.

79 Gerion, D.; Herberg, J.; Bok, R.; Gjersing, E.; Ramon, E.; Maxwell, R.; Kurhanewicz, J.; Budinger, T. F.; Gray, J. W.; Shuman, M. A.; Chen, F. F., *J. Phys. Chem. c* **2007,** *111*, 12542-12551.

80 Lee, J. H.; Jun, Y. W.; Yeon, S. I.; Shin, J. S.; Cheon, J., *Angew. Chem., Int. Ed.* **2006,** *45*, 8160-8162.

81 Pengo, P.; Baltzer, L.; Pasquato, L.; Scrimin, P., *Angew. Chem., Int. Ed.* **2007,** *46*, 400-404.

82 Ross, M.; Gerke, V.; Steinem, C., *Biochemistry* **2003,** *42*, 3131-3141.

83 Wegner, G. J.; Lee, N. J.; Marriott, G.; Corn, R. M., *Anal. Chem.* **2003,** *75*, 4740-4746.

84 Koffas, T. S.; Kim, J.; Lawrence, C. C.; Somorjai, G. A., *Langmuir* **2003,** *19*, 3563-3566.

85 Wada, A.; Mie, M.; Aizawa, M.; Lahoud, P.; Cass, A. E. G.; Kobatake, E., *J. Am. Chem. Soc.* **2003,** *125*, 16228-16234.

86 Karlsson, M.; Martensson, L. G.; Jonsson, B. H.; Carlsson, U., *Langmuir* **2000,** *16*, 8470-8479.

87 Larsericsdotter, H.; Oscarsson, S.; Buijs, J., *J. Colloid Interface Sci.* **2001,** *237*, 98-103.

CHAPTER 2

TUNABLE INHIBITION AND DENATURATION OF α-CHYMOTRYPSIN WITH AMINO ACID-FUNCTIONALIZED GOLD NANOPARTICLES

2.1 Introduction

2.1.1 Importance of Protein Surface Binding

Protein surface binding and recognition by synthetic receptors is an emerging field in drug discovery and in medicinal chemistry. Surface recognition by artificial receptor is an alternative method to control the activation or inhibition of enzymatic process which greatly extends the number of protein targets for therapeutic development.[1]

Biomolecular interactions are controller of a number of biological activities such as, cell enzyme activity,[2] surface recognization,[3] protein-protein interactions and protein- nucleic acid interactions.[4] In recent examples, a direct physical interaction between the G protein-coupled A(2A) receptor (A(2A)R) and the receptor tyrosine kinase fibroblast growth factor receptor (FGFR) was observed where concomitantly activate these two classes of receptors, but not individual activation of either one alone. caused a robust activation of the MAPK/ERK pathway, which activate the signal transduction pathway that couples intracellular responses to the binding of growth factors to cell surface receptors. Hence by control on this interaction can open new avenues for therapeutic.[5] Clearly, the control the protein- protein interactions by protein surface recognition represents an important target for chemical biology and pharmaceutical science. For the efficient binding by surface recognition we need to

consider some obstacles during designing synthetic receptors. The difficulty can be summarized by two basic requirements for an effective protein surface recognition. The first difficulty is high surface area of receptor-target interface. Insight into the requirements for receptor-protein contact area comes from examination of protein-protein interactions,[6] where a recent survey by Jones and Thornton[7] of non-homologous protein dimers found that > 6 nm^2 of surface area per protein is typically buried. The second difficulty is proper presentation of multivalent recognition elements including topological, hydrophobic, electrostatic and polar features.[8]

2.1.2 Nanoparticle as an Artificial Receptor

Nanoparticle based receptors, however, offer a potential platform for biomacromolecular surface recognition which is unique and distinctive in its own way.[9] The use of core-shell nanoparticle systems, such as monolayer protected clusters (MPCs) and mixed monolayer protected clusters (MMPCs) possess some distinctive and significant features that make them promising scaffolds for creation of receptors targeted to biomacromolecular surfaces. The first important feature is the size of the nanoparticle core can be tuned from 1.5 to 8 nm with overall diameters of 2.5-11 nm.[10] This variability of core sizes provides a suitable platform for the interaction of nanoparticles with biomacromolecules on comparable size scales (Chapter 1, Figure 1.1). The second useful property of nanoparticles is that they can be fabricated with a wide range of surface functionality thus providing a versatile route to creation of surface-specific receptors. MPCs are easily synthesized in one step via the Brust-Schiffrin[11] reduction forming monolayer protected clusters (MPCs). The selection of

thiols used during synthesis controls the functionality of the monolayer surface, while the stoichiometry controls the particle size.[12] Mixed monolayer protected clusters (MMPCs) are easily fabricated using the Murray place displacement reaction[4] via incubation of functional thiols and MPCs (Chapter 1, Figure 1.2). This provides a unique tool for achieving efficient and specific recognition of protein surface via complementary surface interaction. The third important feature of MMPCs is that a range of metal and semiconductor cores can be generated featuring useful electronic, fluorescence, and magnetic properties which allow for use as probes and/or diagnostic agents. Finally, these systems have been shown to self-template to guest molecules allowing an increase in the affinity and selectivity upon incubation with the guest molecules (Figure 2.1).[13, 14] MPCs and MMPCs provide a definite advantage over the conventionally used synthetic receptors, which are limited in their ability to mimic biological interactions due to their inherent rigidity.

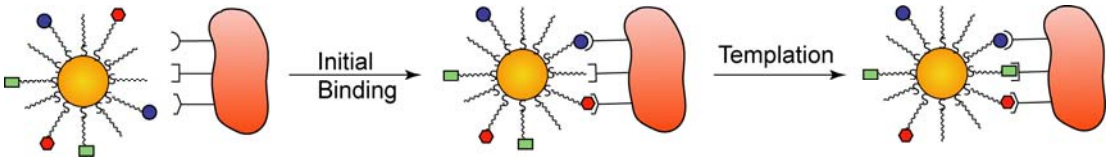

Figure 2.1. Schematic representation of ligand mobility on nanoparticle surface.

2.1.3 α-Chymotrypsin - A Model Protein

We decided α-chymotrypsin (ChT) as a model protein for our protein surface recognition by using nanoparticles as a receptor. ChT, a serine protease of molecular weight 25kDa,[15] was used for protein surface recognition for several reasons.[16] First ChT is well characterized photolytic enzyme with well established activity assessment. A series of substrates are already developed to monitor the enzymatic activity by using

either absorbance or fluorescence measurement.[15] Second the structure of the protein is well explored. According to the structural analysis a ring of cationic residue is present surrounding the active site ("hot spot") of the enzyme (Figure 2.2).[17] The center of the ring, active site of ChT has an abundance of hydrophobic and aromatic residues. Hence this "hot spot" is an ideal target for the nanoparticles surface with anionic and hydrophobic residues for fundamental studies on surface binding based on complementary electrostatic and hydrophobic interactions. Third the change of secondary structure can be easily monitored by comparing with well established circular dichroism (CD)[18] and tryptophan fluorescence response.[19] Furthermore the size of this enzyme (~ 5 nm diameter) is well appropriate with the range of nanoparticles which can be easily synthesized and fabricated.

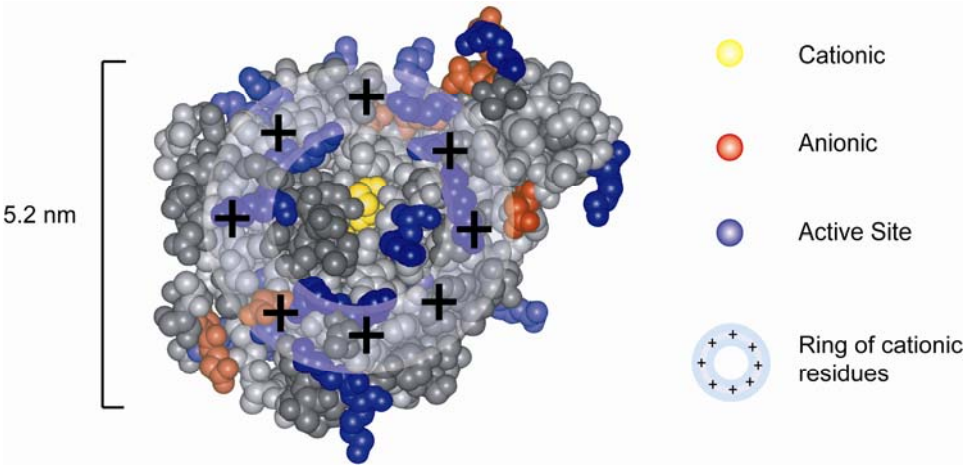

Figure 2.2. Surface residues on ChT. The ring of cationic residues situated around the active site.

2.1.4 Inhibition of α-Chymotrypsin using Anionic Nanoparticles

Anionically functionalized nanoparticle (**NP 1**) was fabricated to target the positive circle surrounding the active site channel of ChT.[20] Time-dependent inhibition

of ChT was observed with anionic particles; however cationic control particles (**NP 2**) had no effect. From initial rate studies (Figure 2.3b), it was determined that between four to five ChTs were inhibited per nanoparticle (Binding ratio of nanoparticle:ChT is 1:4 to 5). The electrostatic nature of the interactions was supported by the fact of little or no interaction was observed with cationic proteins such as elastase or β-galactosidase. Moreover, dynamic light scattering (DLS) studies confirm that inhibition proceeds with only protein nanoparticle interaction without any extended aggregation.

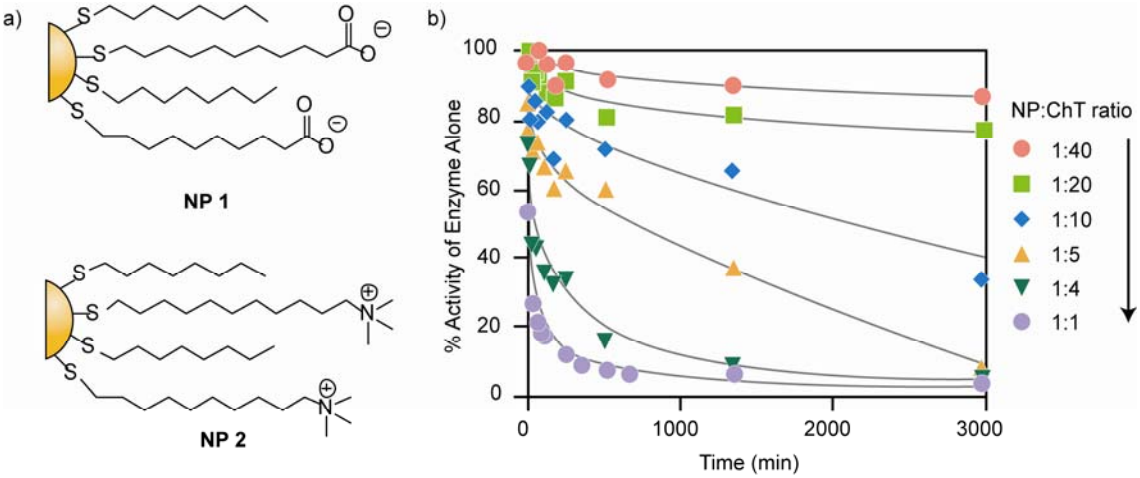

Figure 2.3. a) Anionic and cationic nanoparticle **NP 1** and **NP 2**, respectively. b) Initial velocities for ChT hydrolysis of benzoyl tyrosine p-nitroanilide (BTNA).

After that circular dichroism (CD) analysis was used to follow structural changes occurring upon protein-nanoparticle binding (Figure 2.4a). From these studies, it is clear that the secondary structure of chymotrypsin is dramatically changed with time after incubation with **NP 1**. The conformation of chymotrypsin (3.2 μM) was measured after initial mixing with **NP 1** and at various time intervals at room temperature. Addition of either 0.8 or 2.1 μM nanoparticle affected a substantial increase in the intensity of the minimum at 202 nm. But in all cases the characteristic

minimum at 230 nm for native ChT was not observed. Upon further incubation, this minimum was shifted to lower wavelengths, indicating a conformational shift toward random coil.

To determine the binding and denaturation rate the inhibition kinetics of the nanoparticle were determined. The kinetic study indicated an initial inhibition followed by a second phase of time-dependent inhibition. Progress curves were studied at different concentrations of nanoparticle, providing the pseudo first-order rate constant (k_{obs}) for each concentration of nanoparticle while keeping chymotrypsin and substrate concentrations fixed at 10 nM and 150 mM, respectively. Fitting these data provided a $K_{i(app)}$ of the nanoparticle of 10.4±1.3 nM. The zero intercept of this fitted curve indicates, as expected, that the inhibition is irreversible. A double reciprocal plot of these data results in a non-zero intercept, confirming the two-step mechanism of inactivation (Figure 2.4b).[21]

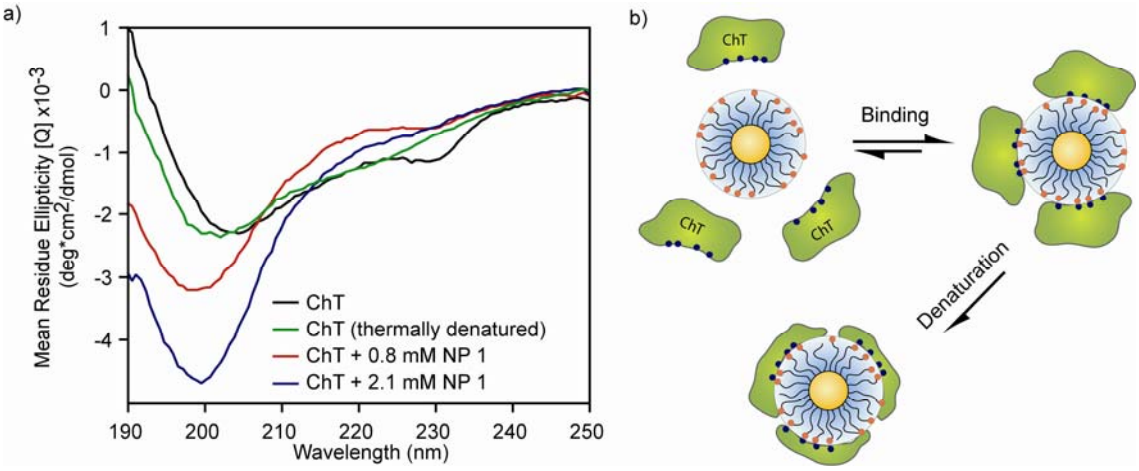

Figure 2.4. a) Circular dichroism of chymotrypsin ([ChT]=3.2 μM) after 24 h incubation with **NP 1** and after thermal denaturation b) Schematic representation of two-step inactivation and denaturation mechanism.

2.1.5 Stabilization of Protein Structure by Tailored Nanoparticles

The above nanoparticle protein interaction results in protein denaturation. In practical many applications need to retain the native enzyme structure upon binding. According to the proposed hypothesis, the first reversible binding event is electrostatic in nature, while the denaturation process results from nonspecific interaction of internal hydrophobic residues of protein with the nanoparticle monolayer.

One way to inhibit the denaturation process during protein-nanoparticle binding would be to create a "barrier" between the hydrophobic nanoparticle interior and the exterior electrostatic recognition elements. This barrier would have the added benefit of enhancing the specificity of the receptor by reducing non-specific hydrophobic interactions between the nanoparticle and other proteins. Ethylene glycol oligomers provide a likely candidate to serve as a barrier. PEG-based functionality has been widely used to impart biocompatibility and antifouling properties on planar substrates[22] and nanoparticles.[23] Previous studies have shown that the use of a sandwich structure in which a PEG chain is appended to an alkanethiol provides robust particles.[24]

To established this hypothesis, 3 nm core CdSe nanoparticles featuring composite alkanethiol-tetra(ethylene glycol) (TEG) monolayers were prepared.[25] For comparison, CdSe nanoparticles are similar to their Au counterparts, with somewhat less well-packed monolayers. Also the similar behavior CdSe nanoparticles extend the applicability of this system in different core materials with other potential properties. In the studies, three different sidechains: hydroxyTEG (**NP 3**), carboxyTEG, (**NP 4**), and mercaptoundecanoic acid (**NP 5**) (Figure 2.5) were used to probe the effect of TEG spacer. The interaction between **NP 3**-**NP 5** and ChT was explored via kinetic assay,

fluorescence assay, and CD. As expected, **NP 3** did not interact with ChT, as evidenced by the lack of inhibition, and the absence of change in the tryptophan fluorescence and CD signatures of ChT. **NP 4** behaved in similar fashion to its counterpart **NP 1**, with rapid inhibition observed. This inhibition was accompanied by a 20 nm red shift in the tryptophan fluorescence over a five-hour time span, indicative of dramatic reorganization of protein secondary structure. Most eloquently, this reorganization is mirrored in the shift in the CD, including the loss of the diagnostic minimum at 230 nm, and shift of the minimum from 207 nm to 199 nm, indicative of essentially complete denaturation.

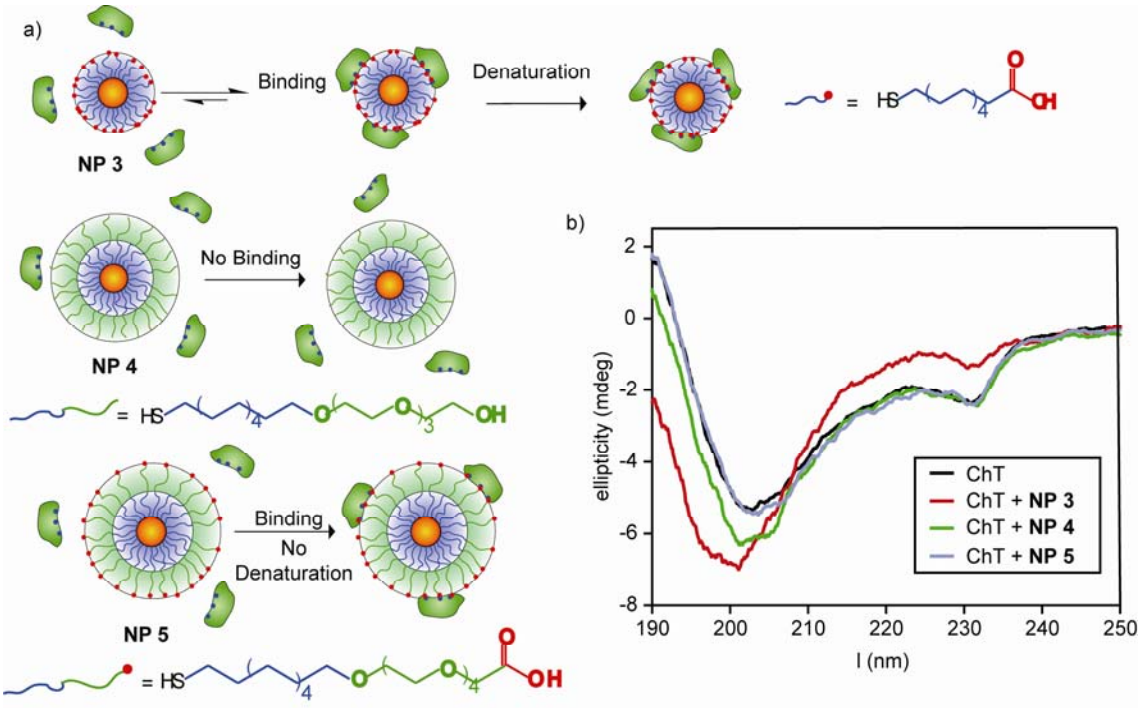

Figure 2.5. a) Behavior of nanoparticle **NP 3-NP 5** with chymotrypsin. b) CD spectra of ChT-nanoparticle mixtures.

Of particular interest is **NP 4**, which appends a terminal recognition element to the TEG protective layer. As with **NP 5**, **NP 4** demonstrates a time-dependent

inhibition, although over a much longer period. Structural studies, however, indicate little change in protein conformation upon binding. A relatively modest red shift is observed in the tryptophan fluoresence, with a shift of only 6 nm observed when maximal inhibition is achieved. The retention of native conformation was confirmed by CD, where essentially no change in either maxima observed over the 24 hr study. Taken together, the results observed with **NP 4** indicate that inhibition can be decoupled from denaturation.

Now, from this above study the complexation between nanoparticle and protein is only govern by electrostatic interaction, but if we consider the natural protein-protein interaction, that is involved along with electrostatic interaction other noncovalent interaction such as hydrophobic interaction, π-π stacking and hydrogen bonding. One of the goals of creating nanoparticle based artificial receptor is the possible multifunctionality on the surface. Hence the following analysis[26, 27] was carried out to answer the following two important questions: 1) what level of specificity can we obtain through choice of surface functionality and 2) what factors contribute to stabilization/denaturation of nanoparticle-bound proteins?

2.2 Amino Acids Fabricated Nanoparticle as a Recognition Scaffold

Amino acids provide an attractive means for generating structural diversity.[28] In the current study, we have fabricated a series of L-amino acids functionalized gold nanoparticles and examined their interaction with ChT (Figure 2.6). The amino acid-decorated surfaces represent the simplest mimics of protein surfaces. Their interaction with proteins thus exhibits much more resemblance with the naturally occurring

protein-protein systems. In this study, we have found that the interactions between ChT and these nanoparticles depend on the surface composition of nanoparticles. Significantly, the binding affinity as well as the stability of the protein is regulated by the charge and the hydrophobicity of amino acid side chains in the nanoparticles. Therefore, it is possible to control the association/dissociation and stabilization/denaturation of the protein at the nanoparticle interfaces through variation of the extra functionality in the vicinity of carboxylic acid recognition elements.

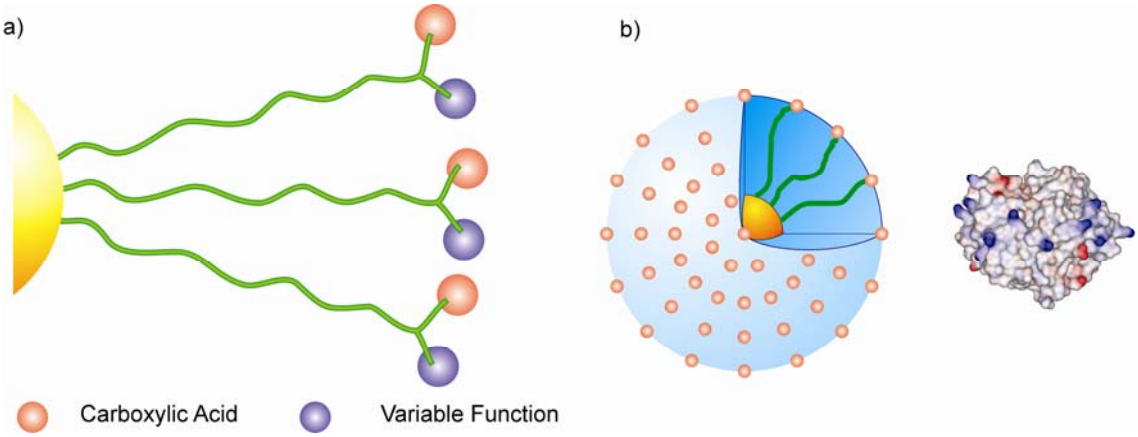

Figure 2.6. a) Amino acid-decorated nanoparticle surface that consist of carboxylic acid recognition elements as well as extra functions for perturbation. b) The relative sizes of amino acid-functionalized gold nanoparticles and ChT. The surface of ChT is patterned with the electrostatic surface potential, showing basic and acidic domains on protein surface.

2.2.1 Result and Discussion

2.2.1.1 Fabrication of Amino Acid-Functionalized Gold Nanoparticles

ω-functionalized *n*-alkanethiols have been widely used as building blocks in self-assembled monolayers on gold for various applications for several years.[29] While a number of oligopeptide functionalized thioligands have been designed and synthesized,[30, 31] amino acid terminated thioligands have hardly been reported so far.[32]

Eventually, the latter can provide more fundamental information on the monolayer construction as well as the corresponding application in either material or biological technology. For example, variation in amino acid side chain structure will allow us to probe the effect of hydrophobic groups (e.g. Leu, Val), additional anionic functionality (e.g. Asp, Glu), cationic groups (e.g. Arg), and hydrogen bonding functionality (e.g. Asn, Gln).

Carboxylic acid terminated nanoparticle clusters have proven to be able to bind ChT and inhibit its activity through complementary electrostatic interaction.[20] The additional tetra(ethylene glycol) tethers in the nanoparticles, however, minimizes the nonspecific protein adsorption and preserve the secondary structure of proteins as well.[25] In this context, trityl protected 26-mercapto-3,6,9,12,15-pentaoxahexacosan-1-oic acid **1** was prepared according to Houseman and Mrksich's protocol[33] and used as the starting compound for the preparation of amino acid functionalized thioligands. As shown in Scheme 2.1, two methods were used to synthesize aminoacid terminated thiol ligands. In first method, target thioligands **4** were synthesized by the reaction of **1** with L-amino acid *tert*-butyl esters in dry dichloromethane through the activation of carboxylic acid function by dicyclohexylcarbodiimide (DCC), followed by removal of trityl and *tert*-butyl groups in trifluoroacetic acid (TFA) with triisopropylsilane as a hydride donor.[34] Alternatively, the coupling reaction of **1** with *N*-hydroxysuccinimide afforded corresponding active ester, which was further reacted with free L-amino acids in a mixed solvent of THF and H_2O and treated with TFA to give the amino acid ligands **4**. Detailed synthetic procedures are described in experimental section.

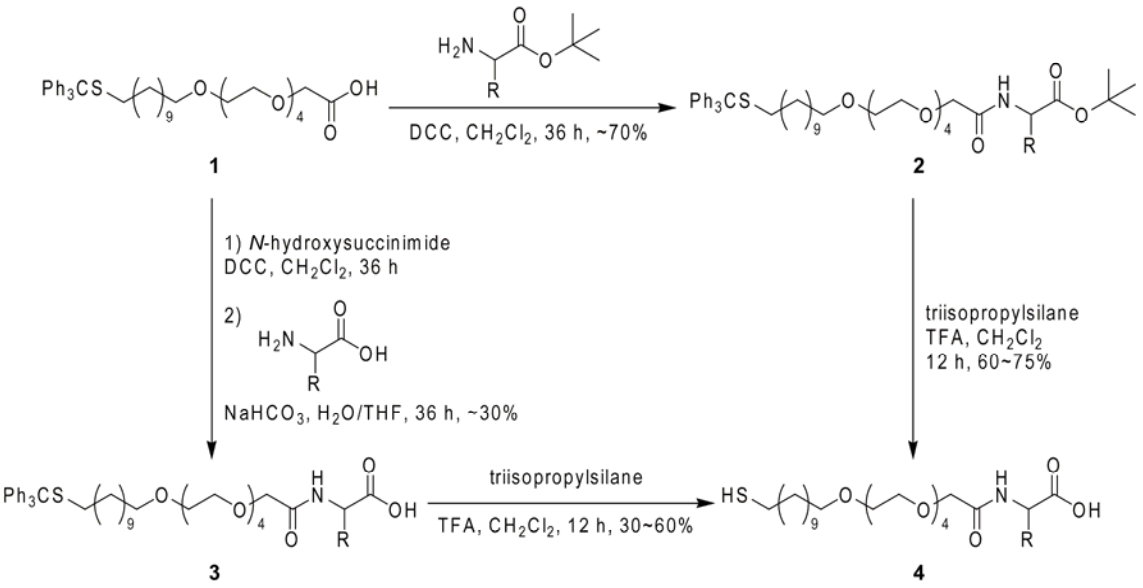

Scheme 2.1. Synthesis of L-amino acid-terminated thioligands

Once the amino acid functionalized alkanethiols were obtained, they were subject to the well-established ligand exchange reaction[10] with 1-pentanethiol coated gold nanoparticle (C_5-NP, $d \sim 2.0$ nm).[11] While C_5-NP is highly soluble in dichloromethane, the ligand exchanged nanoparticles were fully precipitated from the solution. Thus, the nanoparticles were conveniently collected by centrifugation. All of the resultant nanoparticles show good solubility in water. Scheme 2.2 illustrates the fabrication of amino acid decorated gold nanoparticles and their structures and corresponding IDs. As Murray and coworkers' research has demonstrated that place exchange proceeds in a 1:1 stoichiometry,[35] ~100 amino acid ligands are estimated to be present on our 2 nm core particles.

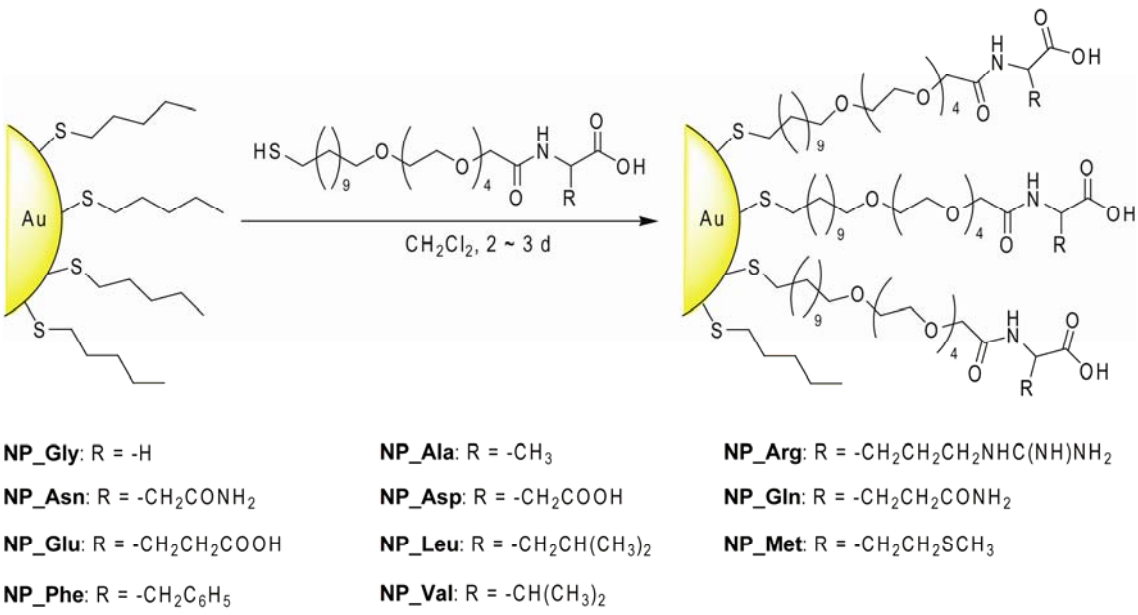

Scheme 2.2. Fabrication of L-amino acid decorated gold nanoparticles through place-exchange reaction.

2.2.1.2 ChT Activity Assays and Binding Affinity

It was previously established that negatively charged nanoparticles can block the active site and subsequently diminish the accessibility of negatively charged substrates to the catalytic center as the ChT active site is surrounded by cationicresidues, resulting in the inhibition of ChT activity.[20,25] In order to probe the effect of various amino acid residues on nanoparticle, the ChT-catalyzed hydrolysis of SPNA were firstly examined in the presence of various concentrations of nanoparticles. The activities of ChT in the presence of nanoparticles were normalized to that of free ChT.

The results show that the nanoparticles exhibit quite different degree of inhibition on the activity of ChT. For most amino acid decorated gold nanoparticles, the rate of ChT-catalyzed hydrolysis of SPNA decreased upon the increase of nanoparticle concentration. This phenomenon clearly suggested the activity inhibition through complex formation. The residual activity reached saturation at higher NP/ChT

ratio. The only exception is Arg terminated gold nanoparticle, which has no inhibition on the activity of ChT, indicating that no significant interaction exists between ChT and **NP_Arg**. By contrast, slight superactivity of ChT was observed in the presence of **NP_Arg**. Apparently, the guanidine side chain of L-arginine might generate a positively charged shell at the surface of the nanoparticle, so that the electrostatic interaction between ChT and **NP_Arg** is unfavorable. All the other hydrophobic, neutral polar or negatively charged amino acids decorated gold nanoparticles show considerable inhibition of ChT activity, substantially suggesting that the complementary electrostatic interaction dominates the formation of ChT-NP complexes. The normalized activity of ChT (3.2 μM) in the presence of NPs (0.8 μM) with variable side chains is represented in Figure 2.7a

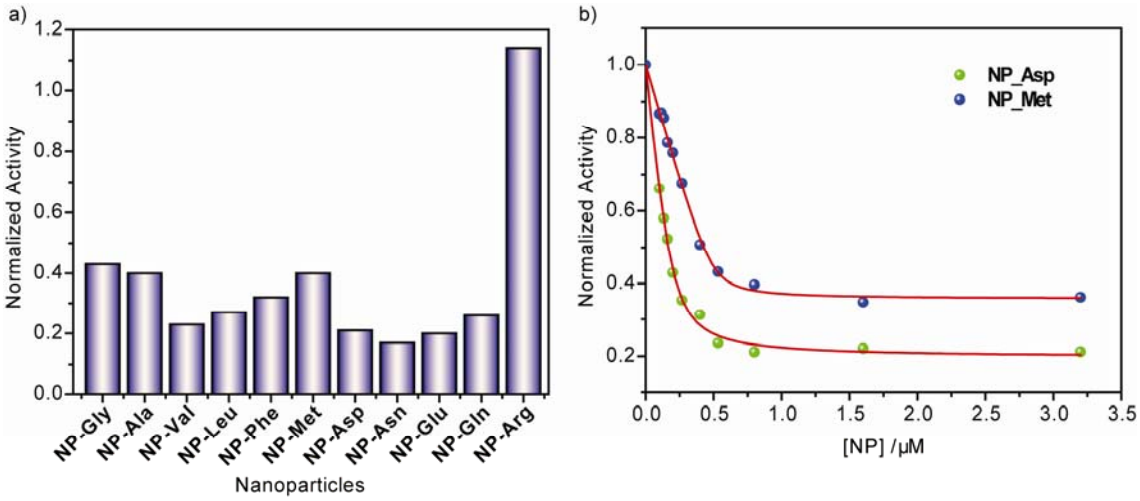

Figure 2.7. Normalized activity of ChT (3.2 μM) with nanoparticles (0.8 μM) bearing various amino acid side chains. b) Nonlinear least-squares curve-fitting analysis of the activity assay data ([ChT] = 3.2 μM).

From Figure 2.7a, we also noticed that the inhibition of ChT activity depends critically on the side chain properties of nanoparticles. While no inhibition effect was observed for **NP_Arg**, the nanoparticles with polar side chains, e.g. **NP_Asp**, **NP_Asn**

and **NP_Glu**, showed the strongest inhibition of around 80%. Whereas, the nanoparticles with hydrophobic side chains exhibited less pronounced inhibition, e.g. **NP_Met** and **NP_Ala** showed only 60% inhibition. This observation is presumably attributed to the hydrophobicity difference of ChT active site in the presence of different nanoparticles. Upon interaction with nanoparticles bearing hydrophobic side chains, the hydrophobic pockets of ChT active sites were also extended to a certain extent in addition to the disadvantageous block of them. Such hydrophobic active sites are considered to be more accessible by SPNA in comparison with that surrounded by nanoparticles bearing polar side chains, since the phenylalanine residue in the substrate need first to be bound into the active site during the enzyme-promoted cleavage of peptide bonds. As a result, more residual activity of ChT was detected even in the presence of higher concentration nanoparticles.

The activity assay results were further analyzed by curve fitting analysis to assess the association strength between ChT and nanoparticles. For that we assumed that nanoparticles have a number of identical and independent binding sites. The *microscopic* binding constants (K_S) and binding ratios (n) can be simultaneously estimated by using nonlinear least-squares curve-fitting analysis on the data of activity assays (details in experimental section). Representative fitting curves are shown in Figure 2.7b, in which no serious deviations are observed and the excellent curve fits indicate the reliability of the binding model. The binding constants and binding ratios are summarized in Table 2.1.

Table 2.1. Microscopic binding constant (K_S), Gibbs free energy Change ($-\Delta G$), and binding ratio (n) for the complexation of ChT with nanoparticles in phosphate buffer (5 mM, pH 7.4) at 30 °C. The error of binding constants was usually less than 20%.

Nanoparticle	K_S / 10^6 M^{-1}	$-\Delta G$ / kJ mol^{-1}	n
NP_Gly	2.9	37.5	7.3 ±1.5
NP_Ala	7.8	40.0	6.2 ±0.2
NP_Asn	2.7	37.3	6.7 ±0.9
NP_Asp	2.2	36.8	13.1 ±0.3
NP_Gln	3.0	37.6	6.8 ±0.5
NP_Glu	2.4	37.0	9.1 ±0.7
NP_Leu	5.9	39.3	6.4 ±0.4
NP_Met	13.1	41.3	6.4 ±0.2
NP_Phe	7.1	39.8	6.8 ±0.7
NP_Val	8.1	40.1	7.6 ±0.2

Like activity inhibition, the binding constants are also dependent on the nature of the side chains of the nanoparticles. For nanoparticles with hydrophilic amino acid side chains the binding constants are around 3×106 M^{-1}, comparable to that of NP_Gly. Whereas for nanoparticles with hydrophobic amino acid side chains, considerably enhanced binding affinity is observed. For NP_Met, the highest binding constant of 1.3×107 M^{-1} was obtained, which is four times of that for reference nanoparticle NP_Gly. This result also indicates that the hydrophobic side chain might aid the interaction between nanoparticles and ChT. To correlate the hydrophobicity effect the Gibbs free energy changes for the complexation of ChT with various nanoparticles were tentatively plotted against the hydrophobicity index[36] of amino acid side chains. The correlation suggest that the binding affinity of nanoparticles increases according to the hydrophobicity increase of amino acid side chains (Figure 2.8).

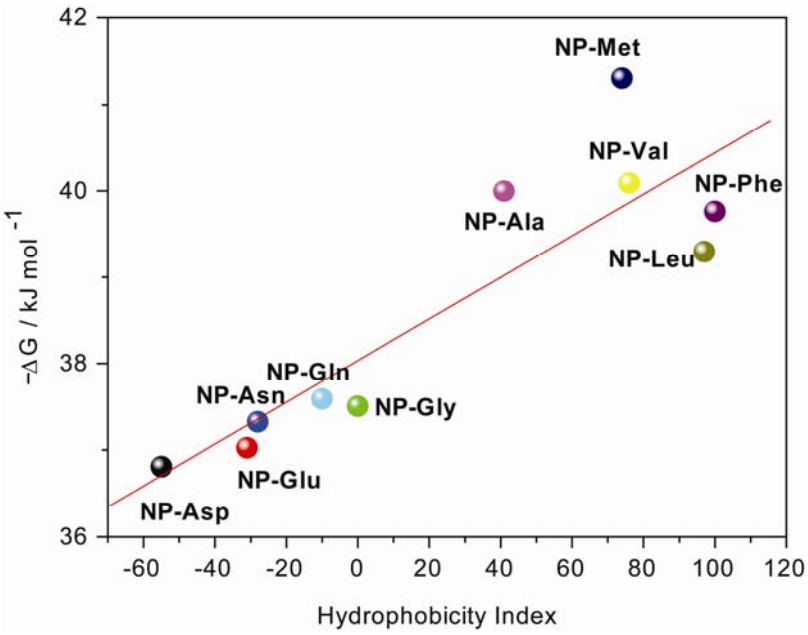

Figure 2.8. Correlation between Gibbs free energy changes and hydrophobicity index of amino acid side chains. Trend line represents the linear fit of the correlation data.

As is well known, the surface of ChT consists of both cationic and hydrophobic patches.[37] Therefore, in addition to the well-characterized electrostaltic interactions, the hydrophobic amino acid side chains are proposed to be able to selectively interact with the hydrophobic patches on the ChT surface when the nanoparticles approach to the surface of ChT. Such supplementary hydrophobic interaction enhances the stability of ChT-NP complexes. However, electrostatic interaction is still the major driving force. For **NP_Met**, for instance, only 10% of the Gibbs free energy change originates from the hydrophobic interaction. At this point it is noteworthy that these binding affinities lie still at the lower limit for many enzyme-inhibitor complexes (e.g. 10^7 to 10^{13} M^{-1}),[38] probably due to the fact that the geometric compensation between the current artificial receptors and the protein is not as good as that in the natural systems.

2.2.1.3 Gel Electrophoresis and Binding Ratio

From the curve fitting analysis it should be noted that most nanoparticles have binding stoichiometries of around 7, except for **NP_Asp** and **NP_Glu** that have considerably higher values (13 and 9, respectively). This curve fitting analysis unambiguously was supported by the gel electrophoresis results of the ChT-NP complexation. Also the narrow bands observed for the ChT-NP complex suggest the formation of discrete complexes rather than extended ChT-NP aggregates. Additionally, the gel electrophoresis experiments clearly show that the binding stoichiometry of monobasic amino acid functionalized nanoparticle **(NP_Asn)** and ChT is 1:7, while the value for **NP_Asp** and ChT is 1:12 (Figure 2.9). The gel electrophoresis studies on the other nanoparticle/ChT systems gave concurrent results with activity assays.

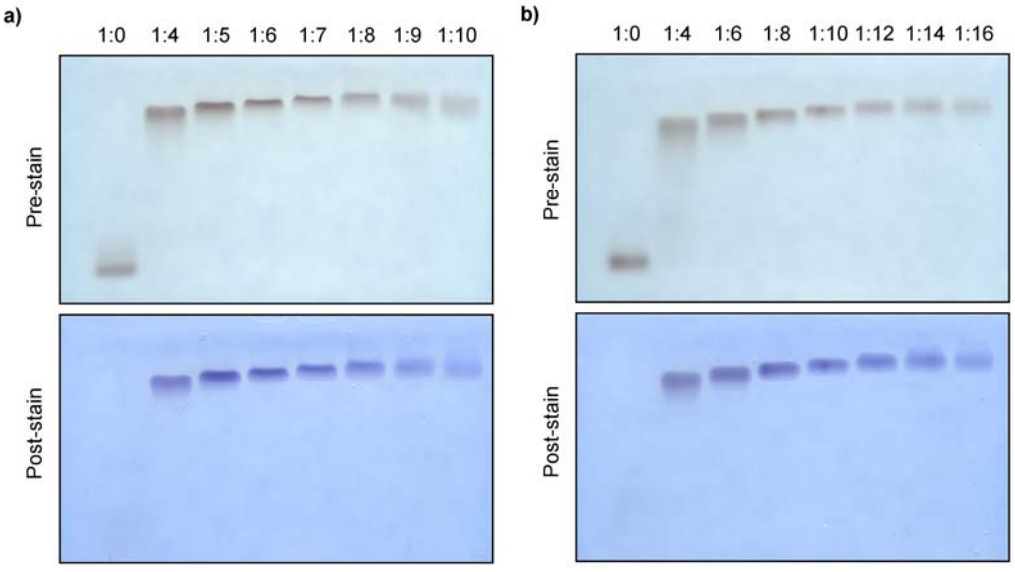

Figure 2.9. Gel electrophoresis of ChT and NP_Asn (a) and NP_Asp (b). Nanoparticle concentrations were varied at a constant ChT concentration (50 μM).

Our previous study revealed that the binding ratio **NP 1**:ChT is 1:4 to get the complete inhibition of ChT (**NP 1** - 11-mercaptoundencanoic acid capped gold nanoparticle, d = 5.5 nm). The diameters of current nanoparticles are significantly larger than **NP 1** by 4.5 nm (2 nm Au core + ~8 nm for the ligand chain), along with an increase in surface area of more than 3-folds.

As the binding stoichiometry is critically dependent on the area of nanoparticle surface, then all the nanoparticles should have a binding ratio of 1:>12. But this binding ratio is not fitted with all nanoparticles. From the structural point of view, the number of carboxylates in **NP_Asp** and **NP_Glu** are twice than the other nanoparticles. Then, it seems that the surface charge density also affect the binding ratio. X-Ray single crystal analysis revealed that 12 positively charged residues (L-Lys and L-Arg) are located on the same side of ChT surface (Figure 2.1),[17, 37] which are considered to take part in the electrostatic interaction with nanoparticles. On the other hand, it has been demonstrated that roughly 100 ligands surround the Au core in 2 nm gold nanoparticles.[35] Therefore, if the electrostatic interaction takes place in a 1:1 negative/positive charge ratio, **NP_Asn** and other monocarboxylic amino acid functionalized nanoparticles can bind 8 ChT molecules, while **NP_Asp** and **NP_Glu** have the capacity of associating 16 ChT molecules. These values are quite closed to the observed binding stoichiometry.

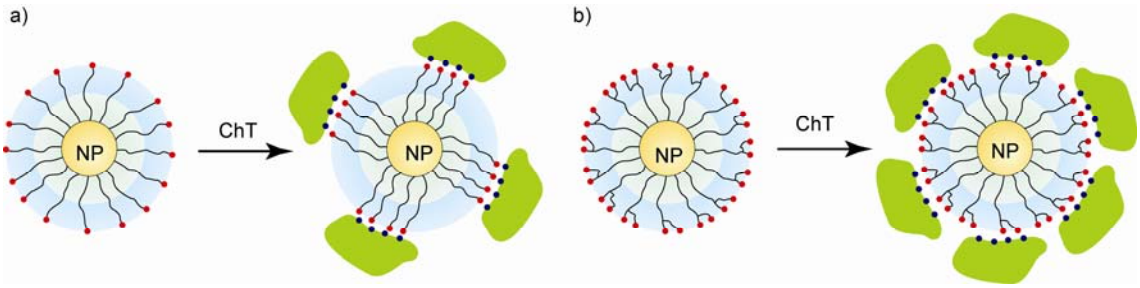

Figure 2.10. Schematic representation for the binding modes of ChT with NP_Asn (a) and NP_Asp (b). In the former case, the surface carboxylate functions are proposed to reorganize to maximize the electrostatic interactions.

To get direct evidence on the surface charge disparity of these two nanoparticles, ζ potentials were measured in 100 mM sodium phosphate buffer solution (pH 7.4) at 25.0 °C. The ζ potentials of **NP_Asn** and **NP_Asp** are –26.2 mV and –32.5 mV, respectively, explicitly showing that the latter possesses a more negatively charged surface. In this situation, one rational explanation for the variant binding ratio is that the flexible nanoparticle surfaces would adopt allosteric conformations to achieve the maximal amount of electrostatic interactions during the complexation process (Figure 1.10). The surface of **NP_Asn** is less saturated than that of **NP_Asp** by the protein, since the former has fewer recognition elements (i.e. carboxylates) on the surface. The charge complementary interaction between ChT and NP is therefore not only dependent on the relative surface areas, but also the number of recognition units.

2.2.1.4 Circular Dichroism Study

Circular dichroism (CD) spectra have been extensively used to explore the absolute conformation of biological macromolecules. This powerful tool enables us to get much primary information about the effect of nanoparticle association on the secondary structure of ChT. Figure 1.11 illustrates the CD spectra of ChT and ChT

with different nanoparticles after 24 h incubation. It is interesting that the CD spectra of ChT are significantly regarded to the amino acid side chains of nanoparticles. While almost no change in the CD spectrum of ChT was observed with **NP_Leu**, nanoparticles with Asn and Asp side chains induced different levels of CD spectral changes of ChT, i. e. the impairment of the characteristic minimum at 232 nm and the hypochromic shift of the minimum at 204 nm. The analysis explored that ChT are little influenced by the presence of nanoparticles bearing hydrophobic amino acid side chains such as **NP_Phe** or **NP_Leu**, while ChT experiences considerable CD spectral changes in the presence of nanoparticles bearing polar amino acid side chains, e. g. **NP_Gln**, **NP_Asp** etc. **NP_Arg** does not perturb the CD spectrum of ChT. This phenomenon is reasonable since no complexation exists between these two species as demonstrated by activity assay. The spectral changes are found time-dependent, suggesting that the polar amino acid side chains induced the conformational changes of ChT, whereas the hydrophobic amino acid side chains promote the retention of ChT structure.

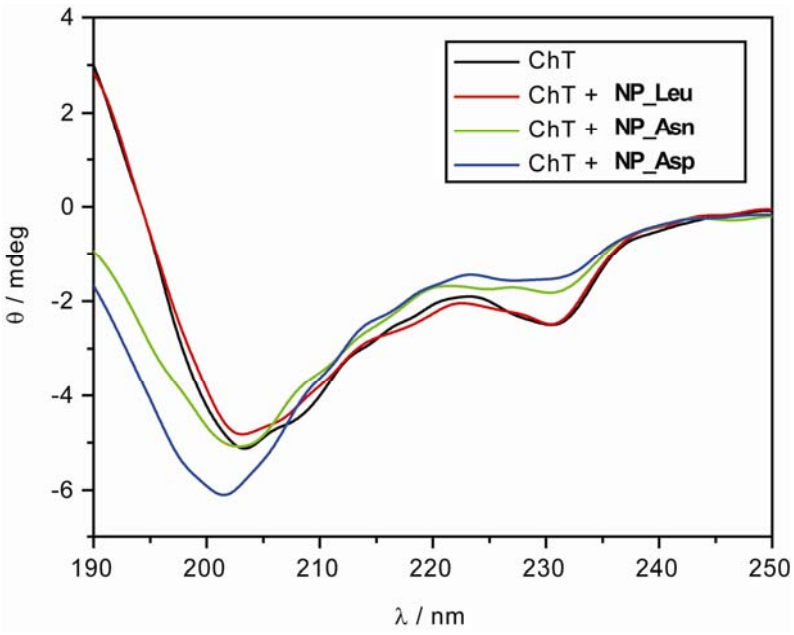

Figure 2.11. Circular dichroism spectra of ChT (3.2 μM) and ChT with nanoparticles (0.8 μM) after 24 h incubation.

The amounts of secondary structure in proteins, including α-helices, β-sheets, β-turns and random coils, could be evaluated from the far-UV CD spectra *via* a number of well-established algorithms.[39] The current far-UV CD spectra were subject to analyze by using CDSSTR method in the CDPro package. Spectral deconvolution of native ChT spectrum in buffer solution showed 6.5% of α-helices, 32.5% of β-sheets, 26% of β-turns and 33.8% of random coils, very similar to previously reported values obtained through X-ray crystal methods.[40] Because no significant CD spectral changes have been observed for the interaction between ChT and nanoparticles with hydrophobic amino acid side chains and **NP_Arg**, the calculated compositions of the secondary structure were also essentially the same as that of native ChT. Nevertheless, the interaction with nanoparticles bearing hydrophilic amino acid side chains led to evident changes in the secondary structure of ChT. Representatively, the spectral deconvolution results for ChT in the presence of **NP_Asp** showed decreases of α-

helices and β-turns to 4.2% and 23.7%, respectively, and increases of both β-sheets and random coils to 35.3% (For the secondary structure compositions of ChT in the presence of other nanoparticles, see Supporting Information). As is well known that the hydrophobic interaction between amino acid side groups in the protein's interior supports the formation of α-helices, the decrease in the α-helix content indicates the destabilization of such interaction. Besides the surface electrostatic interaction with ChT, the hydrophilic amino acid side chains are feasible to competitively form hydrogen-bonds with the amino acid residues in α-helices, resulting in the destabilization of α-helices and the increase of β-sheets and random coils. By contrast, the hydrophobic amino acid side chains might interact with the hydrophobic patches of ChT and stabilize the protein's globular geometry through favorable hydrophobic interaction.

2.2.1.5 Fluorescence and Denaturation Kinetics

To obtain insight into the denaturation process of ChT in the presence of nanoparticles, the characteristic fluorescence of tryptophan residues in ChT was further investigated using steady-state fluorescence spectrometry. As shown in Figure 1.12, the intrinsic emission of ChT shows a maximum at 331 nm in buffer solution. However, significant bathochromic shifts and peak broadening were observed after incubation with nanoparticles for 24 h. The maximal fluorescence shift of 23 nm was observed for the ChT incubated with **NP_Asp**, with concomitant broadening of half-maximal amplitude from 52 nm to 68 nm. These phenomena indicate that the initially buried tryptophan residues were rather exposed to more polar environment due to the

destructure of the protein.[41] The denaturation extent of ChT is reflected by the different values of fluorescence shift, which is again regard to the properties of amino acid side chains in nanoparticles.

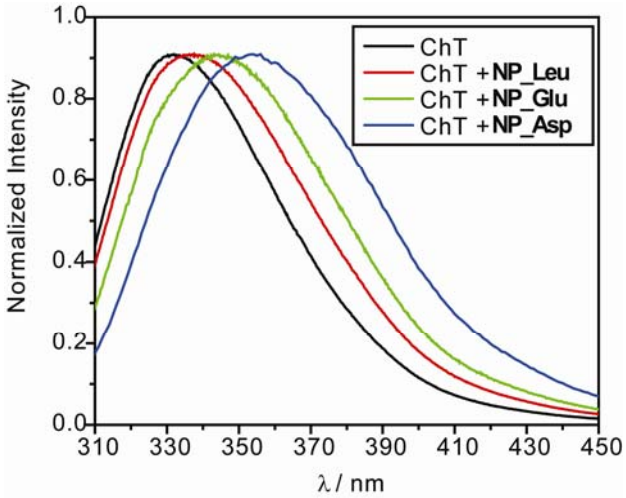

Figure 2.12. Fluorescence spectra of ChT (3.2 μM) and ChT with nanoparticles (0.8 μM) after 24 h incubation.

The denaturation of ChT should occur in a two-state process as described in equation (1):

$$\mathrm{ChT}-N \xrightarrow{k} \mathrm{ChT}-D \qquad (1)$$

where ChT-*N* is the native form and ChT-*D* the denatured form, *k* denotes the rate constant. In principle, the denaturation should follow a first-order reaction profile.

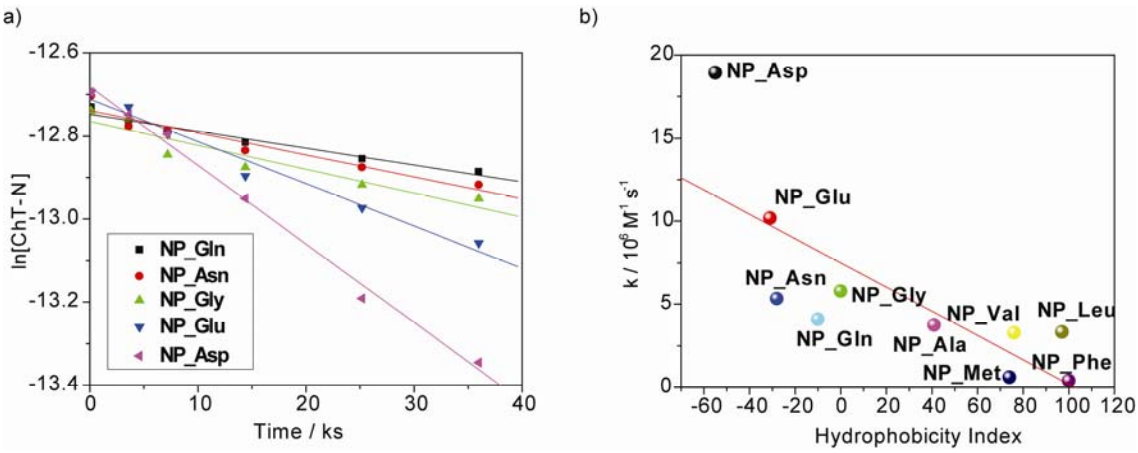

Figure 2.13. a) Linear plots for the first-order chymotrypsin denaturation in the presence of different nanoparticles in 5 mM sodium phosphate buffer (pH 7.4). b) Correlation between the denaturation rate constants (*k*) of ChT and the hydrophobicity index of amino acid side chains in nanoparticles.

In Figure 2.13a, the logarithm of native ChT concentration was plotted against time. Good linear regressions were found for all systems, unambiguously confirming the first-order denaturation profiles. Interestingly, the rate of denaturation decreases significantly with the increase of the hydrophobicity of amino acid side chains. The rate constants obtained by the linear regression are listed in Table 2.2

Table 2.2. Rate constants of the denaturation of ChT in the presence of different nanoparticles.

Nanoparticles	k / 10^{-6} M^{-1} s^{-1}
NP_Gly	5.79
NP_Ala	3.73
NP_Asn	5.33
NP_Asp	18.92
NP_Gln	4.08
NP_Glu	10.18
NP_Leu	3.31
NP_Met	0.61
NP_Phe	0.41
NP_Val	3.27

From Table 2.2, it can be seen that the denaturation rates are in accordance with the extent of final fluorescence shifts after 24 h incubation. **NP_Asp** induces the fast

denaturation of ChT with a rate constant of 1.89×10^{-5} M^{-1} s^{-1}. For **NP_Asn**, the rate constant drops by two thirds to 5.33×10^{-6} M^{-1} s^{-1}. Similarly, for the L-Glu/L-Gln counterparts, the rate constants decrease from 1.02×10^{-5} M^{-1} s^{-1} to 4.08×10^{-6} M^{-1} s^{-1}. Glycine decorated nanoparticle shows an intermediate denaturation rate constant, although it has the highest hydrophobicity among the five amino acids. The observation strongly suggests that the carboxylate functions tend to facilitate the denaturation. As pointed out previously, the competitive hydrogen-bonding formation may destabilize the α-helices in ChT and spoil its initial secondary structure. Furthermore, these phenomena are most probably attributed to the fact that the salt bridge (i.e. between the *N*-terminus of Ile16 and the Asp194 side chain) in the protein is more easily broken by the charged side chains. Indeed, the observed denaturation rates for **NP_Asp** and **NP_Glu** are comparable to the denaturation rate of ChT at pH 11.0 (i.e. $k = 1.43\times10^{-5}$ M^{-1} s^{-1}),[42] where hydroxide ions are believed involving in the breakage of salt bridges.[43]

In accordance with the previous observations, the hydrophobic amino acid side chains are able to aid in the retention of ChT secondary structure. **NP_Phe**, the nanoparticle bearing the most hydrophobic side chain, gives a denaturation rate constant of only 4.1×10^{-7} M^{-1} s^{-1}, decreasing by 50 times in comparison with **NP_Asp**. Both CD and fluorescence studies revealed that the hydrophobicity of amino acid side chains affect the denaturation of ChT. Therefore, the denaturation rate constants of ChT in diverse nanoparticles were again plotted against the hydrophobicity index of amino acid side chains in Figure 2.13b. This correlation strongly suggests that the hydrophobicity of amino acid side chains in nanoparticles plays a vital role in preserving ChT structure.

Our previous study has shown that the alkyl interior in **NP 1** induces the drastic denaturation of ChT, whereas the current hydrophobic amino acid side chains might stabilize the bound ChT. One plausible interpretation for these phenomena is that in the former case the alkyl chain nonspecifically interacts with the whole surface of ChT and therefore destabilizes the protein. In the latter, however, the hydrophobic amino acid side chains specifically interact with the hydrophobic patches in ChT and preserve the protein structure much as in the natural protein-protein interaction. Indeed, selective introduction of hydrophobic groups near the hydrophobic region on protein surface has proven to be one method of choice for improving protein stabilization.

2.2.2 Conclusion

In summary, we have demonstrated that the functionality of monolayer protected gold nanoparticles could be readily tailored by introducing diverse terminal functions. By incorporating simple L-amino acids, nanoparticles exhibit distinctly different inhibition ability on ChT activity. Complementary electrostatic interaction between nanoparticles and ChT has proven to be the predominant driving force contributing to the complex formation, but the hydrophobic interaction between the hydrophobic patches of receptors and proteins might enhance the complex stability to certain extents. The binding ratio lies not only on the surface areas of nanoparticle receptors, but also on their surface charge density. The surface recognition elements are proposed to reorganize to achieve the maximal electrostatic interaction upon complexation with ChT. Most importantly, the hydrophobicity of amino acid side chains shows great influence on the secondary structure of ChT. The hydrophobic side chains might stabilize the ChT structure, while the hydrophilic side chains display serious negative

effects. Taken together, the control over association/dissociation as well as stabilization/denaturation of ChT at the nanoparticle interfaces has been conveniently accomplished by introducing additional functions in the vicinity of carboxylic acid functions. These fundamental insight into the interaction between proteins and artificial receptors with nanoparticle scaffolds offer opportunities for developing novel core/shell receptors with highly specific protein-surface recognition ability, which would possess promising applications in protein stabilization, alteration, and delivery.

2.3 Antipodal Effect of Exterior and Interior Hydrophobic Moieties

Previously we have reported that carboxylate-terminated gold nanoparticles are able to target α-chymotrypsin (ChT). Significantly, we found that nanoparticle (**NP 1)** featuring simple alkyl carboxylate ligands rapidly denatured the bound ChT molecules, while the incorporation of tetra(ethylene glycol) (TEG) spacers onto nanoparticle monolayer (**NP 5**) reduced considerably the extent of denaturation.The denaturation of ChT at the interface was presumably ascribed to the nonspecific hydrophobic interactions of the protein with the alkyl interior of the monolayer. From the above study we also observed that the amino acid-decorated surfaces results both electrostatic and hydrophobic interactions between the hydrophobic patches of receptors and the protein contribute to the complex stability. The microscopic binding constants for these receptor-protein complexes are $10^6 \sim 10^7$ dm^3 mol^{-1}, which roughly increase with the hydrophobicity index of amino acid side chains (Figure 12b). This binding affinity of amino acid-functionalized Nanoparticles toward ChT is comparable to the naturally occurring protein-inhibitor interaction.[44] But more interestingly, the hydrophobic amino acids have little effect on the native structure of the bound ChT, while hydrophilic

(especially dianionic) amino acids destabilize the protein. Hence the effects of exterior and interior hydrophobicity are opposite in nature. To explore this antipodal effect, we build a family of 30 L-amino acid-functionalized nanoparticles (Figure 2.14) with variant length of oligo(ethylene glycol) (OEG) tethers and explore their interaction with ChT. OEG units are well-known to resist nonspecific interaction with biomolecules and have extensitively been deposited onto various substrates to afford biocompatible monolayers. Hence the varible amino acids at the periphery of nanoparticles allow us to detect the side chain effect upon interaction with ChT where the OEG with variable chain length can control the nonspecific interaction from hydrophobic monolayer. More attractively, we can predict that the effect of various amino acid properties and diverse OEG tethers in nanoparticles through organic chemistry offers us a new opportunity to gain control over the structure of bound proteins at interface.

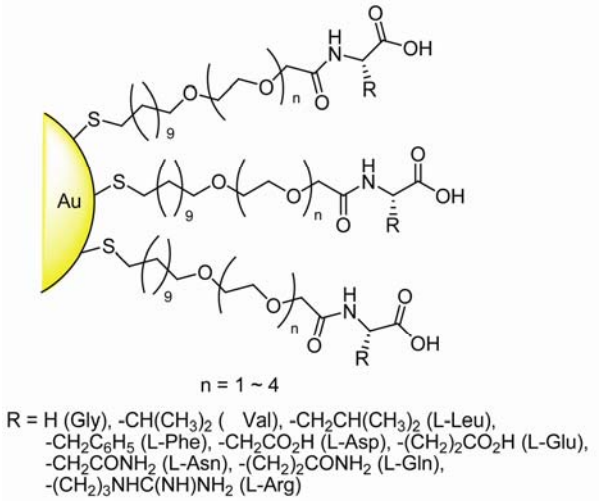

Figure 2.14. Chemical structure of amino acid-functionalized nanoparticles with variable OEG spacer.

2.3.1 Result and Discussion

2.3.1.1 Activity Assay

Inhibitory potencies of these nanoparticles were first conducted to evaluate the inhibitory potencies by activity assay. With *N*-succinyl-L-phenylalanine *p*-nitroanilide (SPNA) as substrate, the acitivity of ChT was drastically depressed upon addition of most nanoparticless (Figure 1.15). As expected only Arg functionalized nanoparticles exhibited no inhibition due to their positively charged side chains. Consequently, the complementary electrostatic interaction between ChT and nanoparticles plays the vital role in the complex formation. The enzymatic activity of ChT typically decreased ca. 60% to 85% upon incubation with excess nanoparticles.

The binding strength between ChT and Nanoparticles was quantified by analyzing the activity assay data through nonlinear least-squares curve-fitting using an equal *K* model where the Nanoparticles were assumed to possess *n* identical and independent binding sites. The results show that microscopic binding constants for complexations between ChT and Nanoparticles are between 10^6 to 10^7 M^{-1} (Table 2.4).[45]

Table 2.3. The binding constants (K_S) and binding ratios (n) estimated from activity assays for the complexation of ChT with nanoparticles in phosphate buffer (5 mM, pH 7.4) at 30 °C.

Nanoparticle	K_S / M^{-1}	n	Residual activity at 4:1 (ChT to NP) ratio
NP_1EG_Gly	1.3×10^7	7.8±1.2	0.29
NP_2EG_Gly	1.1×10^7	7.4±0.8	0.28
NP_3EG_Gly	8.9×10^6	6.2±0.3	0.21
NP_4EG_Gly	2.9×10^6	7.3±1.5	0.43
NP_1EG_Asn	6.9×10^6	8.3±0.6	0.27
NP_2EG-Asn	3.6×10^6	7.8±1.0	0.37
NP_3EG-Asn	2.5×10^6	6.0±0.5	0.29
NP_4EG-Asn	2.7×10^6	6.7±0.9	0.17
NP_1EG-Asp	7.9×10^6	13.2±0.9	0.21
NP_2EG-Asp	1.6×10^7	11.0±0.4	0.16
NP_3EG-Asp	9.5×10^6	11.3±0.5	0.22
NP_4EG-Asp	2.2×10^6	13.1±0.3	0.22
NP_1EG-Glu	6.9×10^6	11.9±1.4	0.22
NP_2EG-Glu	6.0×10^6	12.8±1.1	0.24
NP_3EG-Glu	4.9×10^6	9.0±0.5	0.26
NP_4EG-Glu	2.4×10^6	9.1±0.7	0.20
NP_1EG-Leu	5.9×10^6	7.3±0.4	0.26
NP_2EG-Leu	4.2×10^6	7.7±0.8	0.25
NP_3EG-Leu	9.9×10^6	6.2±0.1	0.20
NP_4EG-Leu	5.9×10^6	6.4±0.4	0.27
NP_1EG-Phe	8.5×10^7	8.4±0.6	0.38
NP_2EG-Phe	2.7×10^7	8.0±0.3	0.34
NP_3EG-Phe	1.9×10^7	6.2±0.2	0.19
NP_4EG-Phe	7.1×10^6	6.8±0.8	0.32
NP_1EG-Val	5.2×10^6	7.5±0.8	0.25
NP_2EG_Val	4.7×10^6	7.8±0.5	0.21
NP_3EG_Val	9.5×10^6	8.1±0.3	0.24
NP_4EG_Val	8.1×10^6	7.6±0.2	0.23

Interestingly, the length of OEG tethers shows considerable influence on the complex stability of ChT and nanoparticles. For most nanoparticles the affinity

increases with decreasing length of OEG tether. One plausible interpretation for this phenomenon is that the shorter linkers are more pre-organized, decreasing the entropic cost of binding.

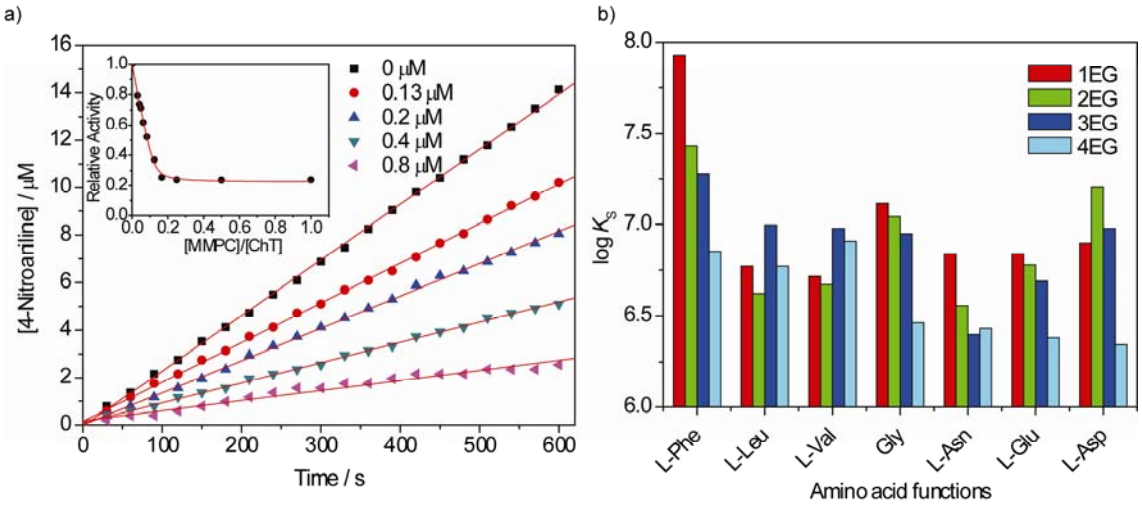

Figure 2.15. a) Progress curves for the hydrolysis of SPNA in the presence of ChT and various concentrations of NP_3EG_Val. [ChT] = 3.2 μM and SPNA [2 mM].[46] (Inset) Normalized activity of ChT in the presence of varying concentrations of NP_3EG_Val. b) Binding constants (logK_S) between ChT and Nanoparticles bearing various amino acid side chains and OEG tethers, estimated from activity assays.

Both activity assays and gel electrophoresis studies showed that the binding capacity of ditopic amino acid terminated Nanoparticles is higher than that of monotopic amino acid-functionalized Nanoparticles, in accordance with our previous studies.[26] For example, the binding stoichiometries of all four L-Asp functionalized Nanoparticles are ~11-13, while the binding stoichiometries of monotopic amino acid (e.g. L-Leu) functionalized Nanoparticles are ~6-8. Surprisingly, the binding capacity is essentially irrespective of the length of OEG tethers for the tested nanoparticles. These reults suggest that the binding ratios are dependent on the surface 'hot spots' (i.e. carboxylates) rather than proportional to the surface area, which is expected to decrease from 300 to 180 nm^2 going from the 4EG to the 1EG spacer. In this context, the

association between ChT and these Nanoparticles is proposed to operate through intermolecular ion pairs and the highly mobile carboxylates on the MMPC periphery tend to cluster together to realize the maximal electrostatic interaction with ChT through cooperative interactions.

2.3.1.2 Circular Dichroism Study

Circular dichroism (CD) spectra of ChT with various nanoparticles were subsequently recorded to determine the impact of amino acid side chains as well as the OEG tethers on the protein structure. Figure 2.16 shows the CD spectra of ChT upon incubation with a series of L-Leu terminated nanoparticles for 24 h. While ChT that was incubated with **NP_4EG_Leu** showed negligible CD spectral changes, the protein displayed different levels of CD spectral changes upon incubation with L-Leu nanoparticles that bear shorter OEG tethers. Among the four nanoparticles, **NP_1EG_Leu** that possesses the shortest OEG tether induced the most significant spectral changes, i.e. the decrease of the characteristic minimum at 230 nm and the blue-shift of the minimum at 204 nm. The spectral changes were found time-dependent This phenomenon clearly shows that the initial structure of ChT is strongly modified by nanoparticles. Deconvolution of the circular dichroism spectra revealed that the contents of α-helices drastically decreased along with the augmentation of β-sheets. The deconvolution using CONTINLL protocol showed that the α-helices in ChT decreased from 16.8% to 6.9%, whereas β-sheets enriched from 30.2% to 36.7% upon incubation with **NP_1EG_Leu**.[47] The OEG length-related denaturation indicates that OEG tethers can aid in the retention of ChT secondary structure. The amino acid side chains also

displayed different levels of influence on the protein structure. Compared with hydrophobic amino acids like L-Phe, L-Leu and L-Val, hydrophilic amino acids such as L-Asp, L-Glu, L-Asn, L-Gln and Gly with the same tethers always induced more significant CD spectral changes. In other words, the hydrophilic residues facilitate the denaturation of the proteins.

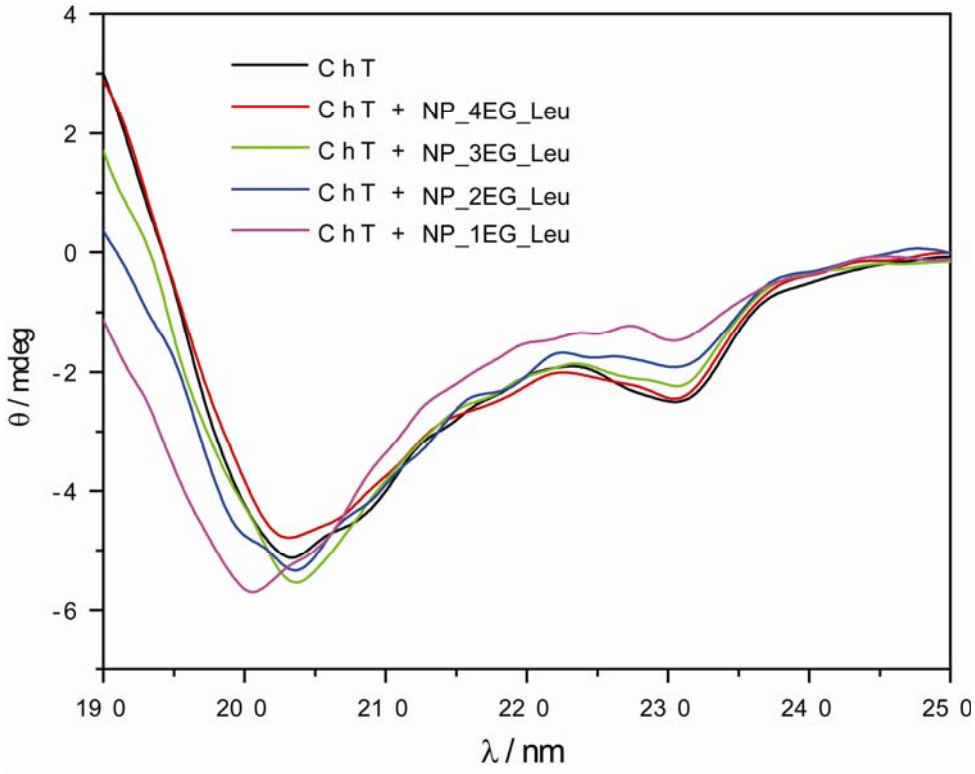

Figure 2.16. CD spectra of ChT (3.2 μM) in the absence and presence of l-Leu functionalized MMPCs (0.8 μM) with different OEG tethers in 5 mM sodium phosphate buffer (pH 7.4) after 24 h incubation.

2.3.1.3 Fluorescence spectrometry

Fluorescence spectrometry was used to provide kinetic information on the conformational changes of ChT in the presence of nanoparticles. As shown in Figure 2.17a, the steady-state fluorescence spectrum of ChT exhibits a maximum at 331 nm with a half-maximal amplitude of 54 nm. Upon incubation with nanoparticles for 24 h, significant bathochromic shifts of fluorescence maxima as well as peak broadenings

were observed. For **NP_1EG_Val**, the fluorescence maximum was red-shifted to 352 nm ($\Delta\lambda$ = 21 nm) with concomitant broadening of half-maximal amplitude to 68 nm. These phenomena indicate that the initially buried tryptophan residues were exposed to more polar environment (i.e. water) due to the unfolding of the protein.[41] The denaturation extent of ChT was found to be governed by both the properties of amino acid side chains and the length of OEG tethers in nanoparticles.

The denaturation of ChT follows a first-order reaction profile. In Figure 2.17b, the logarithm of native ChT concentration is plotted against the incubation period with L-Leu functionalized nanoparticles. Good linear regressions are obtained, confirming the first-order reaction. It can be seen from Figure 2.17b that the denaturation rates decrease with the length increase of OEG linkage, i.e. 1EG > 2EG > 3EG > 4EG, which is in accordance with the CD study.

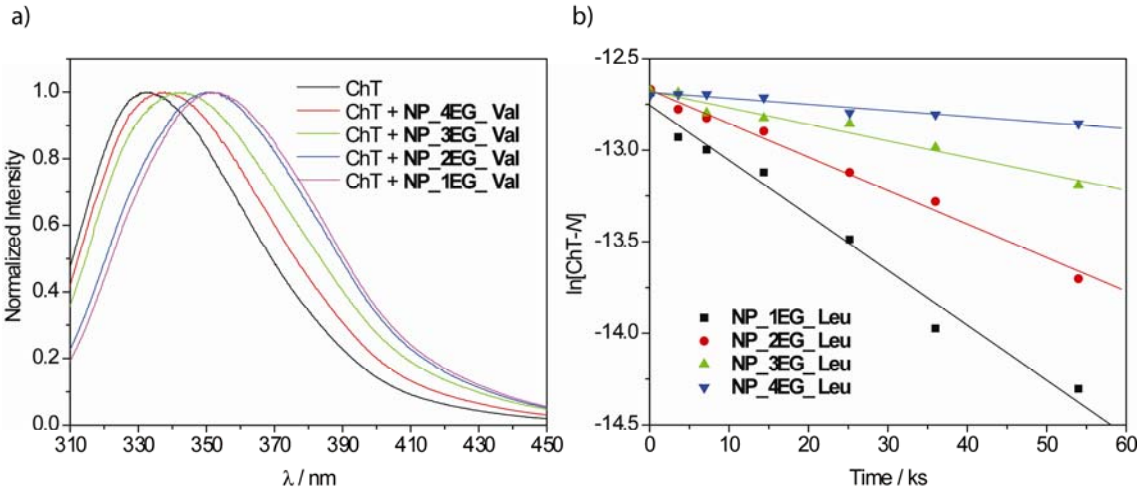

Figure 2.17. a) Fluorescence spectra of ChT (3.2 μM) in the absence and presence of L-Val decorated nanoparticles with different OEG tethers after 24 h incubation. b) Linear plots for the first-order ChT denaturation in the presence of L-Leu terminated nanoparticles with different OEG tethers. The experiment was run in 5 mM sodium phosphate buffer (pH 7.4).

The denaturation rate constants of ChT in the presence of various nanoparticles were calculated from their kinetic curves and compiled in Figure 2.18. The denaturation rate constants vary within a broad range, e.g. from 4.1×10^{-7} M^{-1} s^{-1} for **NP_4EG_Phe** to 3.1×10^{-5} M^{-1} s^{-1} for **NP_1EG_Asp**. The difference in denaturation rates of 3EG and 4EG particles with ChT decreases with increasing hydrophobicity of the amino acid termini. This trend suggests that the hydrophobic side chains of amino acids only marginally affect the structure of the bound protein, while the hydrophilic (especially the anionic) side chains promote denaturation. For the series of 1EG and 2EG, however, drastic denaturation of ChT was observed for all amino acids. Such results are presumably attributed to the exposing of the interior alkyl chains to the protein surface, which accelerates the conformational mutation of the protein through nonspecific hydrophobic interaction.[48] The denaturation rates of nanoparticles that bear the same amino acid function but different OEG length constantly increase in the order: 4EG < 3EG < 2EG < 1EG. The spacers of three or more EG units significantly reduce the nonspecific interaction of proteins with interior hydrophobic shell and preserve the native structure of proteins.

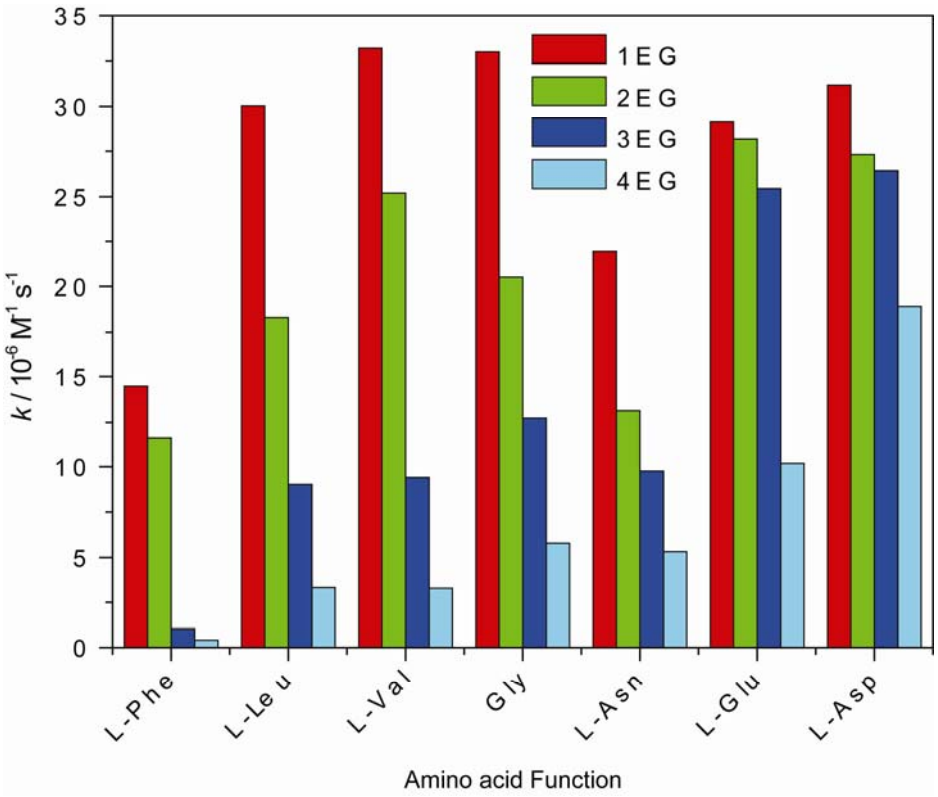

Figure 2.18. Histograms of first-order denaturation rate constants of ChT upon incubation with nanoparticles bearing various amino acid side chains and OEG tethers in 5 mM sodium phosphate buffer (pH 7.4).

2.3.2 Conclusion

In summary, we have demonstrated that in the amino acid-functionalized nanoparticles the hydrophobic amino acid side chains favor the retention of the protein structure. The interior alkyl chains, however, spoil the protein secondary structure due to nonspecific hydrophobic interactions, which can be significantly impaired by introducing tethers with three or more EG units. Therefore, the tunable denaturation of protein is achievable by adjusting either the recognition elements (amino acids) or the linkers.

2.4 Experimental Section

2.4.1 General

α-Chymotrypsin (type II from bovine pancreas, ChT), *N*-succinyl-L-phenylalanine *p*-nitroanilide (SPNA), and *tert*-butyl esters of amino acids (Gly, L-Phe, L-Ala, L-Val, L-Leu, L-Met, and L-Glu) were purchased from Sigma and used as received. All the other chemicals were obtained from Aldrich unless otherwise stated. Trityl protected acid **1** was prepared according to the procedure described by Houseman and Mrksich.[33] The purification of all intermediates and ligands was performed on flash chromatography (SiO_2, particle size 0.032 - 063 mm). Pentanethiol capped gold nanoparticle ($d \sim 2$ nm) was prepared according to the reported method.[11]

2.4.2 Synthesis of Ligands and Nanoparticles

General procedure for the preparation of 2_Amino acid. Trityl protected thioacid **1** (680 mg, 1.0 mmol) was dissolved in dry dichloromethane (20 mL) that was placed in an ice-bath. When the temperature reached about 0 °C, corresponding amino acid *tert*-butyl ester hydrochloride (1.0 mmol), DCC (1.5 mmol) and sodium bicarbonate (1.0 mmol) were added successively. The mixture was stirred at room temperature for 36 h. The insoluble stuff was removed by suction filtration. The filtrate was concentrated and charged on SiO_2 column for purification. The yields were around 70%.

General procedure for the preparation of 3_Amino acid. Trityl protected thioacid **1** (2.7 g, 4.0 mmol) was dissolved in dry dichloromethane (50 mL) placed in an ice-bath, followed by the addition of *N*-hydroxysuccinimide (690 mg, 6.0 mmol) and DCC

(1.25 g, 6.0 mmol). The reaction was allowed to rise automatically to room temperature and stirred for 36 h. The insoluble stuff was removed by filtration. The filtrate was concentrated and the crude ester was dissolved in THF (30 mL). Sodium bicarbonate (420 mg, 5.0 mmol) was then dissolved in water (30 mL) in another round-bottom flask, followed by the addition of the corresponding amino acid (5.0 mmol). Subsequently, the above prepared *N*-hydroxysuccinimide ester solution in THF was added dropwise to the reaction flask. The reaction proceeded at room temperature for another 36 h. The insoluble materials were removed by suction filtration. Most THF in the filtrate was evaporated under a reduced pressure. Subsequently, the residue was chilled with ice-bath and the pH value was adjusted to ca. 2 with 1 M HCl. The resultant emulsion was extracted with ethyl acetate for 4 times. The organic layers were combined and washed thoroughly with brine and dried over anhydrous sodium sulfate. After filtration, the solvent was evaporated and the residue was charged on SiO_2 column for purification. The overall yields were typically around 30%.

General procedure for the preparation of 4_Amino acid. Trityl protected thioligands **2** or **3** were dissolved in dry dichloromethane and stoichiometric trifluoroacetic acid was added under stirring. The color of the solution was immediately turned to yellow. Subsequently, triisopropylsilane was added. The color of the solution recovered slowly to colorless. The reaction was allowed to proceed at room temperature for 12 h. The solvent and excess trifluoroacetic acid and triisopropylsilane were removed under reduced pressure. The residue was charged on SiO_2 column for purification. The yields were from 30% to 75%.

General procedure for ligand exchange. 1-Pentanethiol coated gold nanoparticles (d = 2 nm) were prepared according to the previously reported protocol. Place-exchange reactions were conducted to replace the 1-pentanethiol ligand on the nanoparticle surface with amino acid functionalized ligands **4**. Typically, 20 mg of 1-pentanethiol coated gold nanoparticles were added to a solution of 50 mg ligand **4** in dichloromethane. The mixture were stirred at room temperature for 2~3 days. The ligand-exchanged nanoparticles precipitated from the solution automatically and were collected by centrifugation. The nanoparticles were washed thoroughly with dichloromethane and dried under high vacuum. The amino acid decorated gold nanoparticles are highly soluble in methanol and water, but insoluble in less polar solvents like chloroform and toluene (which are good solvents for the precursor C_5-NP). As compared with the ligand precursor, the ^{1}H NMR signals of nanoparticles are significantly broadening. No signals of free ligands are observed in all ^{1}H NMR spectra.

2.4.3 Activity Assays

All of the experiments were performed in sodium phosphate buffer (5 mM, pH 7.4) with [ChT] = 3.2 μM and variant NP concentrations. The enzymatic hydrolysis reaction was initiated by adding a SPNA stock solution (16 μL) in ethanol to a preincubated ChT-NP solution (184 μL) to reach a final SPNA concentration of 2 mM. Enzyme activity was followed by monitoring product formation every 15 s for 15 min at 405 nm with a microplate reader (EL808IU, Bio-Tek Instruments, Winooski, VT). Control experiment showed that the autohydrolysis of SPNA was negligible during the

time course of activity assay. The assays were performed in duplicates or triplicates, and the averages are reported. The standard deviation was usually less than 10%.

Estimation of the Binding Constants from Activity Assay. Assuming that one nanoparticle has *n* identical and independent binding sites that are able to bind one ChT molecule each, the complexation of ChT with nanoparticles could be expressed by equation S1.

$$\text{Site} + \text{ChT} \underset{}{\overset{K_S}{\rightleftharpoons}} \text{Site}\cdot\text{ChT} \qquad \text{(S1)}$$

where K_S denotes the microscopic binding constant. Because the activity decrease of ChT is attributed to the complexation with nanoparticles, the activity difference (ΔZ) is assumed to be proportional to the concentration of complexed ChT, i.e. $\Delta Z=\alpha\cdot$[Site·ChT]. The proportionality coefficient α reflects the activity difference of unit ChT before and after complexation. Then K_S could be defined as:

$$K_S = \frac{[\text{Site}\cdot\text{ChT}]}{[\text{Site}][\text{ChT}]} = \frac{\Delta Z/\alpha}{([\text{Site}]_0 - \Delta Z/\alpha)([\text{ChT}]_0 - \Delta Z/\alpha)} \qquad \text{(S2)}$$

Where $[\text{Site}]_0$ and $[\text{ChT}]_0$ denote the initial concentrations of binding sites and ChT, repectively. The relationship between the concentrations of binding sites and nanoparticles is describable by $[\text{Site}]_0=n[\text{NP}]_0$. After a few manipulation, equation S2 is solved for ΔZ to give equation S3:

$$\Delta Z = \frac{\alpha}{2}\cdot\{([\text{ChT}]_0 + n[\text{NP}]_0 + 1/K_S) - \sqrt{([\text{ChT}]_0 + n[\text{NP}]_0 + 1/K_S)^2 - 4n[\text{ChT}]_0[\text{NP}]_0}\} \qquad \text{(S3)}$$

On the base of Equation S3, microscopic binding constants (K_S) and binding ratios (i.e. the number of nanoparticles' binding sites) could be readily determined by

using the nonlinear least-squares curve-fitting analysis. The curve-fitting analysis was done on PC using Origin 7.0 program (OriginLab Co., Northampton, USA).

2.4.4 Gel Electrophoresis

Agarose gels were prepared in 5 mM sodium phosphate buffer at 1% final agarose concentration. Appropriately sized wells (40 μL) were generated by placing a comb in the center of the gel. A ChT stock solution of 100 μM in 5 mM sodium phosphate buffer (pH 7.4) was used to prepare 30 μL samples at the appropriate ChT/NP ratios ([ChT] = 50 mM). After a 30 min incubation period at room temperature, 3 μL of 80% glycerol was added to ensure proper well loading (30 μL) and a constant voltage (100 V) was applied for 30 min for sufficient separation. Gels were placed in staining solution (0.5% Coomassie blue, 40% methanol, 10% acetic acid aqueous solution) for 1 h, followed by extensive destaining (40% methanol, 10% acetic acid aqueous solution) until protein bands were clear. Gels were scanned on a flatbed scanner both prior to and after staining to separately visualize particle and ChT bands.

2.4.5 Zeta Potential

Amino acid-functionalized gold nanoparticles were dissolved in PBS buffer (20mM potassium phosphate and 100mM sodium chloride, pH 7.8) to make a 1 μM solution and their zeta potentials were measured on a MALVERN Zetasizer Nano ZS instrument. Three rounds of assays have been performed and the average values were reported.

Table 2.4. Zeta-potentials for various amino acid-functionalized gold nanoparticles in PBS buffer (20 mM potassium phosphate and 100 mM sodium chloride, pH 7.8) at 25.0 °C

Nanoparticle	zeta-potential / mV	nanoparticle	zeta-potential / mV
NP_Gly	–25.8±1.5	**NP_Glu**	–32.2±0.7
NP_Ala	–24.7±2.1	**NP_Leu**	–25.6±1.5
NP_Asn	–26.2±0.5	**NP_Met**	–25.4±2.0
NP_Asp	–32.5±0.4	**NP_Phe**	–25.7±1.8
NP_Gln	–23.5±1.2	**NP_Val**	–26.4±1.6

2.4.6 Circular Dichroism

Far-UV circular dichroism (CD) spectra of ChT (3.2 μM) were measured on a JASCO J-720 spectropolarimeter with quartz cuvettes of 1 mm path length at 20 °C. The spectra were recorded from 190 to 250 nm as an average of 3 scans at a rate of 20 nm/min. The concentration of NP is 0.8 μM and their CD spectra were subtracted to eliminate background effects. Quantitative analyses of the secondary structure content were done by deconvolution of the far-UV CD spectra using the CDSSTR method in the CDPro program package.

2.4.7 Fluorescence

Fluorescence spectra were measured in a conventional quartz cuvette (10 × 10 × 40 mm) on a Shimadzu RF-5301 PC spectrofluorophotometer at room temperature (ca. 20 °C). The samples were excited at 295 nm, and the emission spectra were recorded from 300 to 450 nm. For the denaturation study, the sample concentrations are the same as that in CD study.

Complexation Study by Using Fluorescence Titration. To corroborate the observed binding strength, the complexation of ChT with NP_l-Leu was further investigated by fluorescence titration experiment. As shown in Figure 2.19, the

addition of NP_l-Leu drastically quenched the intrinsic fluorescence of ChT. Because the gold nanoparticles are intense absorbers at the excitation and the emission wavelengths (i.e. 295 and 330 nm, respectively), this fluorescence quenching is at least partially due to their absorption. In this context, the quenching of ChT by tetra(ethylene glycol) terminated gold nanoparticle, which has been proven to not complex with ChT, was measured to dispel the effect of nanoparticles' absorption. From the quenching process of tetra(ethylene glycol) terminated gold nanoparticle, absorbance correction factors (θ) that reflect the emission quenching due to nanoparticle absorbance at the exciting and emission wavelengths could be determined. The raw and the corrected fluorescence intensities of ChT at 330 nm in the presence of NP_Leu are depicted in the inset of Figure 4. The corrected fluorescence changes are unambiguously attributed to the production of ChT-NP complex, where an energy-transfer from the tryptophan residues in ChT to the gold core is responsible for the fluorescence quenching. The binding constant could be roughly estimated by the analysis of the fluorescence titration data. For the system of ChT and NP_Leu, a binding constant of 5.3×106 M-1 was obtained, which is in accordance with the value estimated from the activity assay.

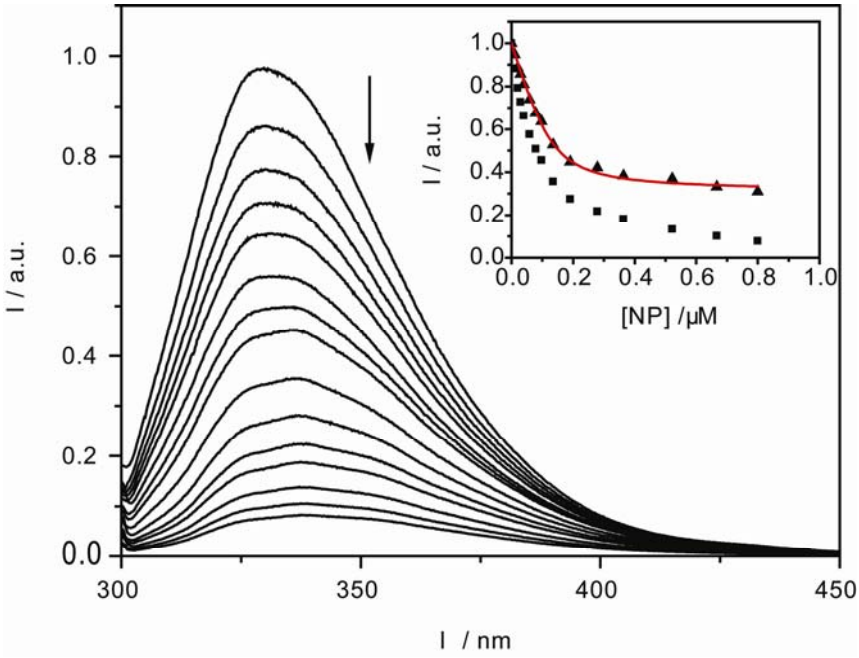

Figure 2.19. Fluorescence quenching of ChT (1 μM) in the presence of NP_L-Leu (0 ~ 0.8 μM). (Inset) The fluorescence intensities monitored at 330 nm (■) and the corrected intensities (▲).

2.4 References

1 Pulido, R.; van Huijsduijnen, R. H., *Febs Journal* **2008,** *275*, 848-866.

2 Karaman, M. W.; Herrgard, S.; Treiber, D. K.; Gallant, P.; Atteridge, C. E.; Campbell, B. T.; Chan, K. W.; Ciceri, P.; Davis, M. I.; Edeen, P. T.; Faraoni, R.; Floyd, M.; Hunt, J. P.; Lockhart, D. J.; Milanov, Z. V.; Morrison, M. J.; Pallares, G.; Patel, H. K.; Pritchard, S.; Wodicka, L. M.; Zarrinkar, P. P., *Nat. Biotechnol.* **2008,** *26*, 127-132.

3 Grueninger, D.; Treiber, N.; Ziegler, M. O. P.; Koetter, J. W. A.; Schulze, M. S.; Schulz, G. E., *Science* **2008,** *319*, 206-209.

4 Selmer, M.; Dunham, C. M.; Murphy, F. V.; Weixlbaumer, A.; Petry, S.; Kelley, A. C.; Weir, J. R.; Ramakrishnan, V., *Science* **2006,** *313*, 1935-1942.

5 Flajolet, M.; Wang, Z. F.; Futter, M.; Shen, W. X.; Nuangchamnong, N.; Bendor, J.; Wallach, I.; Nairn, A. C.; Surmeier, D. J.; Greengard, P., *Nat. Neurosci.* **2008,** *11*, 1402-1409.

6 Lo Conte, L.; Chothia, C.; Janin, J., *J. Mol. Biol.* **1999,** *285*, 2177-2198.

7 Jones, S.; Thornton, J. M., *Proc. Natl. Acad. Sci. U. S. A.* **1996,** *93*, 13-20.

8 Fairlie, D. P.; West, M. L.; Wong, A. K., *Curr. Med. Chem.* **1998,** *5*, 29-62.

9 Sperling, R. A.; Gil, P. R.; Zhang, F.; Zanella, M.; Parak, W. J., *Chem. Soc. Rev.* **2008,** *37*, 1896-1908.

10 Hostetler, M. J.; Wingate, J. E.; Zhong, C. J.; Harris, J. E.; Vachet, R. W.; Clark, M. R.; Londono, J. D.; Green, S. J.; Stokes, J. J.; Wignall, G. D.; Glish, G. L.; Porter, M. D.; Evans, N. D.; Murray, R. W., *Langmuir* **1998,** *14*, 17-30.

11 Brust, M.; Walker, M.; Bethell, D.; Schiffrin, D.J.; Whyman, R. *Chem. Commun.* **1994**, 801-802.

12 Stavens, K. B.; Pusztay, S. V.; Zou, S. H.; Andres, R. P.; Wei, A., *Langmuir* **1999,** *15*, 8337-8339.

13 Boal, A. K.; Rotello, V. M., *J. Am. Chem. Soc.* **2000,** *122*, 734-735.

14 Verma, A.; Nakade, H.; Simard, J. M.; Rotello, V. M., *J. Am. Chem. Soc.* **2004,** *126*, 10806-10807.

15 Hedstrom, L., *Chem. Rev.* **2002,** *102*, 4501-4524.

16 Wroblowski, B.; Diaz, J. F.; Schlitter, J.; Engelborghs, Y., *Protein Eng.* **1997,** *10*, 1163-1174.

17 Capasso, C.; Rizzi, M.; Menegatti, E.; Ascenzi, P.; Bolognesi, M., *J. Mol. Recognit.* **1997,** *10*, 26-35.

18 Schechter, N. M.; Eng, G. Y.; Selwood, T.; McCaslin, D. R., *Biochemistry* **1995,** *34*, 10628-10638.

19 Desie, G.; Boens, N.; Deschryver, F. C., *Biochemistry* **1986,** *25*, 8301-8308.

20 Fischer, N. O.; McIntosh, C. M.; Simard, J. M.; Rotello, V. M., *Proc. Natl. Acad. Sci. U.S.A.* **2002,** *99*, 5018-5023.

21 Copeland, R. A. *Enzymes: A Practical Introduction to Structure, Mechanism, and Data Analysis*, John Wiley & Sons, Inc.: New York, **2000**, pp. 318-349.

22 Ostuni, E.; Grzybowski, B. A.; Mrksich, M.; Roberts, C. S.; Whitesides, G. M., *Langmuir* **2003,** *19*, 1861-1872.

23 Oyewumi, M. O.; Liu, S. Q.; Moscow, J. A.; Mumper, R. J., *Bioconjugate Chem.* **2003,** *14*, 404-411.

24 Kanaras, A. G.; Kamounah, F. S.; Schaumburg, K.; Kiely, C. J.; Brust, M., *Chem. Commun.* **2002**, 2294-2295.

25 Hong, R.; Fischer, N. O.; Verma, A.; Goodman, C. M.; Emrick, T.; Rotello, V. M., *J. Am. Chem. Soc.* **2004,** *126*, 739-743.

26 You, C. C.; De, M.; Han, G.; Rotello, V. M., *J. Am. Chem. Soc.* **2005,** *127*, 12873-12881.

27 You, C. C.; De, M.; Rotello, V. M., *Org. Lett.* **2005,** *7*, 5685-5688.

28 Coppola, G. M.; Schuster, H. F. *Asymmetric Synthesis. Construction of Chiral Molecules Using Amino Acids*; Wiley: New York, 1987.

29 Witt, D.; Klajn, R.; Barski, P.; Grzybowski, B. A., *Curr. Org. Chem.* **2004,** *8*, 1763-1797.

30 Pengo, P.; Broxterman, Q. B.; Kaptein, B.; Pasquato, L.; Scrimin, P., *Langmuir* **2003,** *19*, 2521-2524.

31 Roberts, C.; Chen, C. S.; Mrksich, M.; Martichonok, V.; Ingber, D. E.; Whitesides, G. M., *J. Am. Chem. Soc.* **1998,** *120*, 6548-6555.

32 Nissink, J. W. M.; van der Maas, J. H., *Appl. Spectrosc.* **1999,** *53*, 33-39.

33 Houseman, B. T.; Mrksich, M., *J. Org. Chem.* **1998,** *63*, 7552-7555.

34 Greene, T. W.; Wuts, P. G. M. *Protective Groups in Organic Synthesis*, 3rd ed., John Wiley & Sons, New York, 1999.

35 Hostetler, M. J.; Templeton, A. C.; Murray, R. W., *Langmuir* **1999,** *15*, 3782-3789.

36 Monera, O. D.; Sereda, T. J.; Zhou, N. E.; Kay, C. M.; Hodges, R. S., *J. Pept. Sci.* **1995,** *1*, 319-29.

37 Tsukada, H.; Blow, D. M., *J. Mol. Biol.* **1985,** *184*, 703-711.

38 Jones, S.; Thornton, J. M., *Proc. Natl. Acad. Sci. U. S. A.* **1996,** *93*, 13-20.

39 Greenfield, N. J., *Numerical Computer Methods, Pt D* **2004,** *383*, 282-317.

40 Provencher, S. W.; Glockner, J., *Biochemistry* **1981,** *20*, 33-37.

41 Ladokhin, A. S. In *Encyclopedia of Analytical Chemistry*; Meyers, R. A., Ed.; John Wiley & Sons Ltd., Chichester, U.K., 2000; pp 5762−5779.

42 Wu, H. L.; Lace, D. A.; Bender, M. L., *Proceedings of the National Academy of Sciences of the United States of America-Biological Sciences* **1981,** *78*, 4118-4119.

43 Wroblowski, B.; Diaz, J. F.; Schlitter, J.; Engelborghs, Y., *Protein Eng.* **1997,** *10*, 1163-1174.

44 H. Fukada, K. Takahashi and J. M. Sturtevant, *Biochemistry*, 1985, **24**, 5109−5115; C. Chen, C.-H. Hsu, N.-Y. Su, Y.-C. Lin, S.-H. Chiou and S.-H. Wu, *J. Biol. Chem.*, 2001, **276**, 45079−45087.

45 Chen, C. P.; Hsu, C. H.; Su, N. Y.; Lin, Y. C.; Chiou, S. H.; Wu, S. H., *J. Biol. Chem.* **2001,** *276*, 45079-45087.

46 Strater, N.; Sun, L.; Kantrowitz, E. R.; Lipscomb, W. N., *Proc. Natl. Acad. Sci. U. S. A.* **1999,** *96*, 11151-11155.

47 Sreerama, N.; Woody, R. W., *Anal. Biochem.* **2000,** *287*, 252-260.

48 Prime, K. L.; Whitesides, G. M., *J. Am. Chem. Soc.* **1993,** *115*, 10714-10721.

CHAPTER 3

BIOMIMETIC INTERACTIONS OF PROTEINS WITH FUNCTIONALIZED NANOPARTICLES: A THERMODYNAMIC STUDY

3.1 Introduction

3.1.1 Biomimetic Systems

Inspired by biological systems, there are numerous chemical systems were developed.[1] These systems are studied by controlling chemical process in a well-defined nanoscale environment, but they have the potential to extend into advanced devices for nanofluidics[2] and nanochemistry applications.[3] Biomimetic system also provides a valuable tool for the understanding of biological processes as well as tool for the creation of advanced functional synthetic systems. On the other hand proteins provide an important target for the creation of biomimetic systems. Considering this target a vast array of protein and metallprotein active site model systems have been developed.[4, 5] As example, Cyclodextrin derivatives containing trifluoromethyl groups at C6 of the A and D rings were synthesized by Bjerre *et. al.* for the purpose of creating artificial enzymes.[6]

In contrast to active site models, there have been far fewer efforts to model the surface of proteins, in particular their interactions with other biomacromolecules. Effective mimicking of protein surfaces would provide fundamental insight into issues such as protein-protein and protein-nucleic acid interactions. Additionally, replication of protein surface behavior provides access to useful catalysts,[7] sensors,[8] and therapeutics.[9, 10]

3.1.2 Nanoparticle as a Biomimetic scaffold

Nanoparticles provide excellent systems for modeling protein surfaces. In particular, they can be readily fabricated with dimensions comparable to biological macromolecules.[11] Moreover, the synthetic control we can exert on the ligands can be used to tune the structure and dynamics of the monolayer surface. For example, peptide-functionalized NPs have been constructed to function as artificial proteins and enzymes,[12] glyconanoparticles have been used as useful models of cell adhesion,[13, 14] and a variety of functionalized particles have been used for recognition in aqueous media.[15], [16] Likewise, nanoparticle-protein interactions have found promising applications in modulation of enzymatic activity,[17] biosensing,[18] separation,[19] and production of hybrid materials.[20]

Two distinct approaches have been used to engineer the protein-nanoparticle interface. The first strategy uses the direct introduction of highly specific binding moieties onto the particle surface. For example, biotin-tagged NPs exhibit high affinity interactions with proteins of avidin family.[21] An alternative approach is to utilize the nanoparticle as a multivalent scaffold for the presentation of simple ligands. With this approach the structural attributes of the nanoparticle are brought to bear, including the ability to generate the multiple electrostatic, hydrophobic and hydrogen-bonding interactions that are found in typical protein-protein interactions.[22]

Amino acids present a readily accessed source of the electrostatic, hydrogen bonding and hydrophobic elements found in proteins. Our previous investigations have demonstrated that amino acid-terminated gold NPs can effectively interact with positively charged proteins, showing tunable inhibition of the enzymatic activity.[23]

From binding assays, we observed that complementary electrostatic interactions and hydrophobic interactions between nanoparticles and proteins govern complex formation.

3.1.3 Thermodynamic analysis of protein interactions

In biological system proteins are interacting with DNA,[24] protein, peptide,[25] small molecules[26] and metal ion[27] for numerous cellular processes. Proper understanding of the development of these interactions can lead us to multiple biological applications.[28] To monitor the interaction of proteins with other biomolecules, the conventional methods are mostly based on imaging,[29] optical analysis (eg. Förster Resonance Energy Transfer (FRET))[30] and X-ray crystal structure analysis.[31] In this regard determination of the thermodynamic parameters can explore the mechanism in protein-bimolecular complexation which can be used for control the interaction.[32] For example, the thermodynamic parameters obtained from inhibitors, that target the SH2 domain-binding site, show dramatic enthalpy/entropy compensation. These data suggest that the v-Src SH2 domain does not have a highly specific secondary-binding site, which presents a major difficulty as well as the direction to design selective inhibitors.[33] As mentioned before, compare to other artificial receptor nanomaterials can provide a highly useful tool for studying protein-surface interactions. Fundamental studies on protein-nanoparticle interaction are always an attractive point of interest, because it can explore the nature of the interaction which can be used for control recognition. Incidentally, understanding of thermodynamics behind these interactions can help to design proper receptor. Recent studies have used

unfunctionalized silica particle-protein interaction for Differential Scanning Calorimetry (DSC),[34] though interestingly ITC has not been well studied. Clearly, the application calorimetric techniques in protein-nanoparticle system can provide a powerful tool for understanding the protein-surface interactions.

3.2 Protein-Nanoparticle Complexation: A Thermodynamic Study

In this chapter, we investigate the thermodynamics of nanoparticle-protein interactions using isothermal titration calorimetry (ITC). As shown in Figure 3.1, we choose structurally diverse anionic amino acid-functionalized gold particles as the protein receptors, and explored their interactions with three positively charged proteins: α-chymotrypsin (ChT),[35] histone,[36] and cytochrome *c* (CytC).[37] We choose these three model proteins to estimate the effect of both size and charge of the protein molecules. If we consider the molecular weight (MW) and overall charge (pI) of these three proteins, they are varied with charge and size (Figure 3.1). If we compare between ChT and histone, the size is similar but histone is more positively charged. So the thermodynamic analysis can explore the effect of charge on the protein. On the other hand comparison between Histone and CytC can see the sights of size effect when the overall charges are comparable.

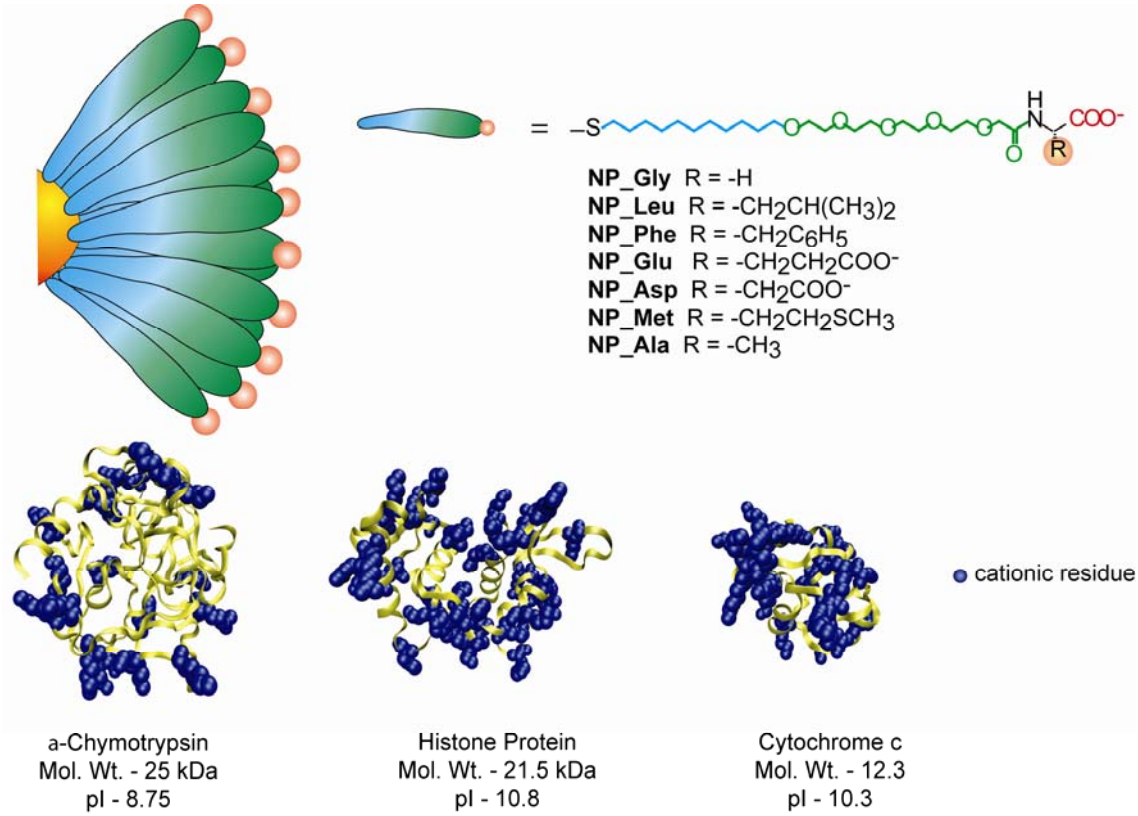

Figure 3.1. Structural features and relative sizes of amino acid-functionalized gold nanoparticles and proteins. The blue overlapping spheres in the proteins represent the positively charged residues on their surface.

3.2.1 Results and Discussion

3.2.1.1 Isothermal Titration Calorimetry

Thermodynamic parameters of particle protein interaction are highly effective for determining the nature of interactions. In this respect ITC can provide useful thermodynamic parameters of particle-protein interactions, which a highly effective for determining the origin and pattern of interactions. Using ITC the equilibrium constants (K_S), the molar entropy changes (ΔS) and the molar enthalpy changes (ΔH) can be determined simultaneously from a single titration curve. While differential scanning calorimetry (DSC) has been used to characterize NP-protein systems, this technique

provides only partial information on binding thermodynamics.[38] ITC has been extensively used to investigate biomacromolecular interactions, directly providing the free energy and enthalpy of association, and the entropy from the former two values.[39]

We have demonstrated that ChT associates with anionic NPs through complementary surface charge interaction. We fabricated several anionic gold NPs bearing various L-amino acid functionalities to examine their interactions with ChT, histone, and CytC. These proteins have an overall positive charge, albeit with different surface characteristics (ref. Figure 3.1). ITC experiments were carried out at 30 ^{o}C by titrating protein solutions into the sample cell containing nanoparticles. As can be seen from the titration curves (Figure 3.2), the three NP-protein systems exhibit distinctly different heat change profiles. The complexation of ChT with **NP_Phe** is exothermic, while the complexation of histone with **NP_Ala** or CytC with **NP_Glu** involves endothermic processes. The heat changes can be fitted into isothermal functions to quantify the corresponding thermodynamic parameters of NP-protein interactions. Interestingly, the complexation of NPs with both ChT and histone can be fitted using the mode of single set of identical binding sites. By contrast, the complexation of NPs with CytC can only been assessed using a binding mode of two sets of binding sites.

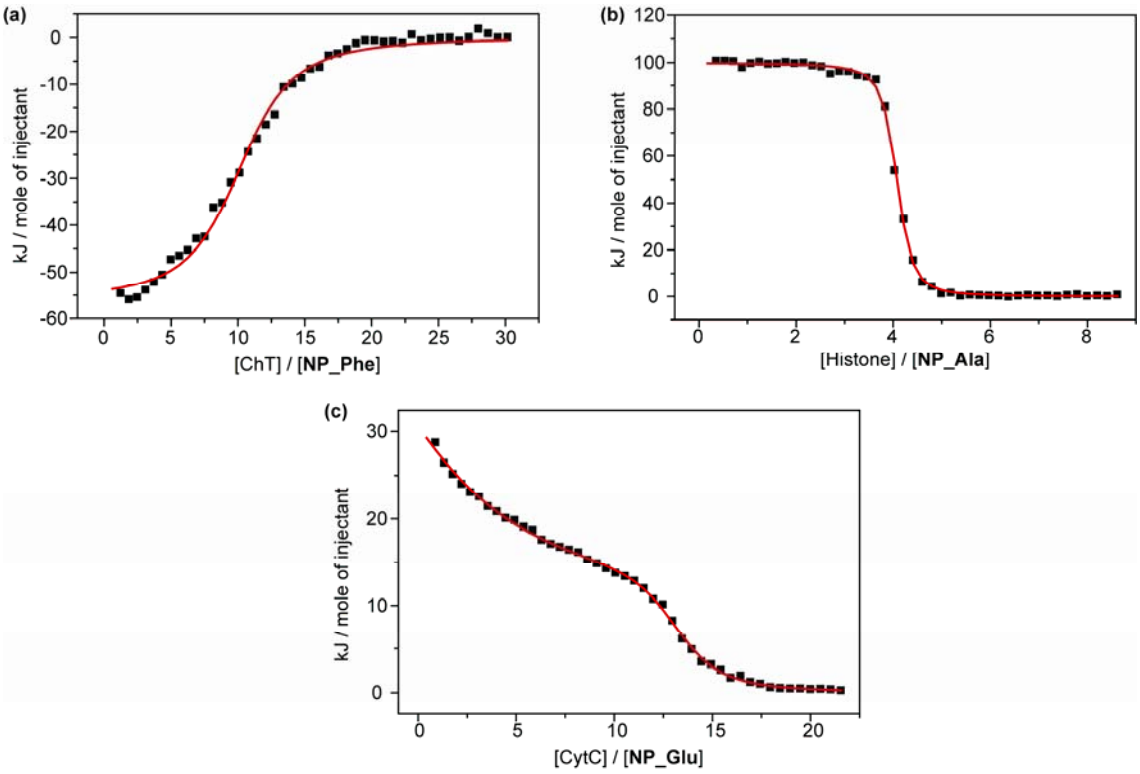

Figure 3.2. ITC analyses for the complexation of (a) ChT with **NP_Phe**, (b) histone with **NP_Ala**, and (c) CytC with **NP_Glu** in 5 mM sodium phosphate buffer (pH = 7.4). The squares represent the integrated heat changes during complex formation and the red solid lines the curve fit to the binding isothermal functions.

After the perfect fitting of the curve with the corresponding model (single set or double set of identical binding sites), the binding constants (K), enthalpy changes (ΔH) and binding ratios are determined from curve fitting analysis. By using the standard thermodynamic equations $\Delta G = -RT\ln K$ and $\Delta G = \Delta H - T\Delta S$ (assuming the parameters are independent on temperature), the Gibbs free energy changes (ΔG) and entropy Changes (ΔS) were calculated. The thermodynamic parameters for the complexation protein-nanoparticles are summarized in table 3.1.

Table 3.1. Complex stability constants (K_S), Gibbs free energy changes (ΔG), enthalpy changes (ΔH), entropy changes ($T\Delta S$), and binding stoichiometries (n) for the complexation of ChT, histone, and CytC with various amino acid-functionalized gold NPs (5 mM sodium phosphate, pH 7.4) at 30 °C.

Protein	NPs	First binding event					Second binding event				
		K_{S1} / M^{-1}	$-\Delta G$ / kJ mol^{-1}	ΔH / kJ mol^{-1}	$T\Delta S$ / kJ mol^{-1}	n	K_{S2} / M^{-1}	$-\Delta G$ / kJ mol^{-1}	ΔH / kJ mol^{-1}	$T\Delta S$ / kJ mol^{-1}	n
ChT	**NP_Glu**	5.2×10^5	33.2	-52.1	-18.9	23.6	–	–	–	–	–
	NP_Gly	3.6×10^5	32.2	-38.7	-6.4	7.3	–	–	–	–	–
	NP_Leu	7.8×10^5	34.2	-48.1	-13.9	9.7	–	–	–	–	–
	NP_ Phe	8.6×10^5	34.4	-56.2	-21.7	10.2	–	–	–	–	–
Histone	**NP_Ala**	6.8×10^7	45.6	90.1	135.7	3.5	–	–	–	–	–
	NP_Gly	6.2×10^7	45.1	100.7	145.8	4.0	–	–	–	–	–
	NP_Met	1.2×10^8	46.9	92.6	139.5	3.5	–	–	–	–	–
CytC	**NP_Ala**	1.0×10^7	40.7	51.6	92.3	1.8	4.5×10^5	32.8	15.7	48.6	5.5
	NP_Glu	1.1×10^7	41.0	56.5	97.5	2.0	3.1×10^6	37.6	12.5	50.1	11.1
	NP_Gly	1.0×10^7	40.7	107.7	148.3	2.2	2.0×10^5	30.6	88.7	119.3	4.2
	NP_Met	1.0×10^7	40.7	24.2	64.9	1.9	2.9×10^5	31.7	24.5	56.2	5.9
	NP_Phe	1.8×10^7	42.1	29.0	71.1	1.9	6.2×10^5	33.6	23.2	56.8	9.6

3.2.1.2 Protein Dependent Binding Ratio

According to table 3.1 nanoparticles afford drastically different binding stoichiometries with the proteins that depend on both the functionality of NPs and the protein type. For example, ChT and histone possess similar molecular sizes, but the latter exhibits significantly lower binding ratios to the NPs. On the other hand, the binding capacity of **NP_Glu** with ChT is almost twice that of other NPs, although they have comparable surface area. Structurally, histone has more positively charged residues in comparison with ChT (62 versus 17),[35, 36] while **NP_Glu** possesses double anionic carboxylate functionalities. Taking this information into account, it is reasonable to conclude that the complexation stoichiometries are determined by the ion pairs involved in electrostatic interactions. In other words, if the particle has more electrostatic recognition elements (i.e. carboxylates) it can bind more proteins; likewise if the protein has more cationic residues on surface it requires more NP partners to form

supramolecular complexes. In contrary, the complexation of NPs with CytC features two distinct binding processes, with markedly differing affinities. For nanoparticle-CytC complexation, the first interaction involves a ~2:1 binding ratio of CytC to NP with binding constants ~ 10^7 M^{-1}, with the subsequent binding much weaker with binding stoichiometries from 4 to 11. By considering the isotropic surfaces of NPs against ChT and histone, it seems that the observed phenomena arise from the unique structural features of CytC. It has been demonstrated that with an increase in protein concentration CytC molecules undergo reorientation on the surface of citrate-coated silver NPs to facilitate interprotein interactions.[40] In this context, the orientation change and interprotein attraction/repulsion may account for the binding modes of CytC to NPs. The two CytC molecules initially bound may orient themselves opposite from each other to afford the highest binding affinity. Further bound CytC would generate unfavorable interprotein interactions due to electrostatic repulsion (Figure 3.3). A second explanation can be provided by the monolayer model recently proposed by Stellacci *et al.* In this model, the ligands on two hemispheres of the particle feature opposing tilt angles, resulting in the appearance of two poles with distinct ligand arrangement.[41] Thus, an alternative explanation for the binding stoichiometries of NP to CytC could be that the first two CytC molecules bind to the NP in the two topologically distinct 'polar' regions. It is noteworthy that the nanoparticle-protein ratios all are in feasible range. Based on a model of smaller spheres packing on the surface of a larger sphere, the maximum binding stoichiometries of the nanoparticles (r ~ 5 nm) with α-chymotrypsin (r ~ 2.5 nm), cytochrome *c* (r ~ 1.8 nm), and histone (r ~ 2.1 nm) are evaluated as 28, 48, and 37, respectively.[42]

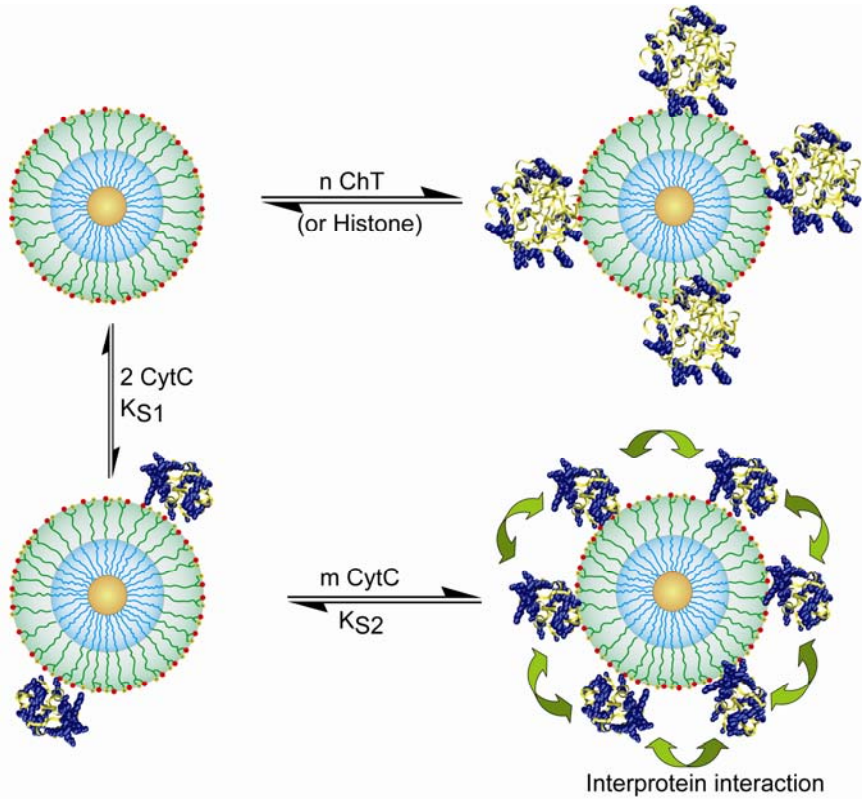

Figure 3.3. Schematic illustration for the binding modes of CytC with amino acid-functionalized NPs in comparison with that of ChT and histone.

3.2.1.3 Binding Thermodynamics of NP-Protein Interactions

The thermodynamic data, i.e. change of enthalpy and entropy (ΔH and ΔS) obtained from all protein nanoparticle interaction can be used for detection the nature of the interaction. We also observed from Table 3.1 that those data not only differ from protein to protein but also vary with nanoparticle functionality. For the complexation of ChT with all particles features a favorable enthalpy change ($\Delta H < 0$), which is offset partially by unfavorable entropy loss ($\Delta S < 0$), affording overall free energy changes (ΔG) ranging from -32.2 to -34.4 kJ mol^{-1}. By contrast, the complexation of NPs with histone and CytC is endothermic, providing an unfavorable enthalpic contribution (ΔH

> 0) to the free energy of association. The binding of histone and CytC is as a result dominated by a large favorable entropy change ($\Delta S > 0$). The complexation behavior of proteins is a complex process that involves not only the synergetic work of noncovalent forces including electrostatic, hydrophobic, hydrogen bonding and π-π stacking, but also features the desolvation of both NPs and proteins and solvation of newly formed complexes. The complexation process may be described in a simplified fashion using Equation 3.1.

$$\mathrm{Protein} \cdot m\mathrm{H_2O} + \mathrm{NP} \cdot p\mathrm{H_2O} \Leftrightarrow [\mathrm{Protein} \cdot \mathrm{NP}] \cdot (m + p - x)\mathrm{H_2O} + x\mathrm{H_2O} \qquad (3.1)$$

According to Equation 3.1, the thermodynamics of complexation depend on two simultaneous processes featuring noncovalent bond formation and solvent reorganization. From an enthalpic viewpoint, the formation of noncovalent bonds is exothermic ($\Delta H_{\mathrm{intrinsic}} < 0$) while the disruption of structurally well-defined solvent shells is endothermic ($\Delta H_{\mathrm{desolv}} > 0$). In this context, the intrinsic bond formation (or namely protein-particle interaction) plays a predominant role in the complex formation of ChT with NPs according to the observed negative enthalpy changes. It has been proposed that during protein-ligand interactions solvent reorganization accounts for great contributions to enthalpy changes.[43] Nevertheless, the complex formation generally reduces the solvent accessible surface area, resulting in the release of highly ordered solvent molecules into bulk solution. Consequently, the observed enthalpy changes are the compensatory outcomes of unfavorable desovlation enthalpy and favorable intrinsic enthalpy.[44]

Water molecules at interfaces can sometimes enhance the complementarity of the interacting surfaces,[45, 46] however the negative entropy changes do not necessarily

indicate that the hydration of the complex interface remains unchanged or increases in comparison with that of the free proteins or protens and particles. Another important unfavorable contribution to the entropy change may arise from the conformational restriction of the flexible amino acid residues in both partners upon complexation. When the entropy increase due to desolvation is not large enough to remedy the entropy loss due to solute freedom reduction, overall unfavorable entropy changes are observed for the complexation of NPs with ChT.

In the complexation of NPs with histone and CytC, the large positive entropy change unambiguously indicates the disordering of molecules upon complex formation, presumably arising from the release of a large amount of the water of hydration from the binding interface. In comparison with ChT, histone and CytC possess more charged residues. Consequently, the corresponding interaction interfaces involve significantly more polar surface. The large entropic increase for the NP-histone and NP-CytC interactions may arise from either the release of more water of hydration or the dissociation of water molecules from a more ordered initial state.[47] Meanwhile, the breakage of well-defined solvent-protein and/or solvent-NP bonds leads to the unfavorable enthalpy changes, which counteract a portion of entropy contribution to the complex stability. It is also necessary to mention that the binding constants for NP-ChT interactions are around ~10-fold lower than those obtained from enzyme activity assays,[23] presumably due to the fact that in the latter case (i) the final solution contained 8% (v/v) of ethanol-DMSO (90:10) in the 5 mM phosphate buffer, (ii) 2 mM of *N*-succinyl-L-phenylalanine *p*-nitroanilide (SPNA) was presented as an enzyme substrate would be expected to interfere in the protein-NP interactions, (iii) the protein

concentrations for the ITC are higher than those used in the activity assay, which would be expected to raise the ionic strength of the solution due to the polyelectrolyte nature of the protein and finally (iv) the nanoparticle concentrations were calculated on the basis of their average molecular weights as described in experimental section. Thus, also the binding stoichiometrics between NPs and ChT differ slightly from the previously reported ones,[23] where the NP concentrations were calibrated according to the UV absorbance of the gold core.[48]

3.2.1.4 Effect of Hydrophobic in NP-Protein Complexation

As we observe from the above study that different NPs interact with same protein with different extent according to thermodynamic parameters, which lead us to the investigation for the effect of head group. Complex stability between particles and ChT increases in the order of **NP_Glu** < **NP_Leu** < **NP_Phe** i.e the complex stability increases with increasing hydrophobicity.[49] These trends track well with the hydrophobicity of the particle surfaces. As we know that ChT has hydrophobic patches on the protein surface, these observations indicate the role of hydrophobic interactions along with electrostatic interactions in complex formation. However this correlation is not observed in case of other two proteins, i.e. Cyt c and histone. This can be explainable if we consider the nature of surface of the later proteins in compare to ChT (Figure 3.1). For the Cyt c, it has 21 positively charged residues (19 Lys and 2 Arg)[37] with minor hydrophobic patches on the surface. Also for the histone protein, it has 62 positively charged residues (56 Lys and 6 Arg).[36] On the other hand for the ChT has lot of hydrophobic patches along with positively charged residue (14 Lys and 3 Arg).[35]

Thus the complexation of Cyt c and histone protein with NPs is dominated by complementary electrostatic interaction. But for the ChT although electrostatic interaction plays the mail role in stable complex formation the hydrophobic interaction also act as an accessory binding force.

To probe the hydrophobic effect, we investigated particle-ChT interactions at varying ionic strengths, since the electrostatic forces should be attenuated by the presence of competitive ions.[50] ITC experiments at various salt concentrations were carried out to quantify the corresponding thermodynamic parameters. The thermodynamic quantities for the complexation of ChT with three amino acid-functionalized NPs at various salt concentrations are summarized in Table 3.2.

Table 3.2. Thermodynamic parameters for the complexation of ChT with different amino acid-functionalized nanoparticles in various phosphate buffered NaCl solutions (5 mM sodium phosphate, pH 7.4) at 30 °C.

NP	Salt conc.	K_S / 10^5 M^{-1}	ΔG / kJ mol^{-1}	ΔH / kJ mol^{-1}	ΔS / J mol^{-1} K^{-1}	n
NP_Phe	0	8.6	-34.4	-56.2	-71.5	10.2
	25	6.3	-33.7	-35.2	-5.7	9.5
	35	4.2	-32.7	-22.8	32.4	9.5
	50	2.0	-30.8	-17.8	43.1	8.2
NP_Leu	0	7.8	-34.2	-48.1	-46.0	9.7
	25	4.8	-32.9	-28.2	15.6	9.0
	35	1.9	-30.7	-17.7	43.1	6.9
	50			ND[a]		
NP_Glu	0	5.2	-33.2	-52.1	-62.3	23.6
	25	2.8	-31.6	-21.7	32.8	22.4
	35			ND[a]		
NP_Gly	0	3.6	-32.2	-38.7	-21.2	7.3

[a] Not detectable

We can see from Table 3.2 that the thermodynamic quantities depend critically on the monolayer components of NPs as well as the salt concentrations. For the demonstration for the correlation of thermodynamic parameters (ΔG, ΔH and ΔS) with salt concentration we plotted those data in Figure 3.4a.

As expected, the Gibbs free energy changes ($-\Delta G$) decrease with increasing salt concentration for all three NPs owing to the attenuation of electrostatic interactions. No binding was detectable for ChT-**NP_Glu** in 35 mM and ChT-**NP_ Leu** in 50 mM or higher concentrations of NaCl solution, respectively. For **NP_Phe**, however, considerable complex stability is still preserved at 50 mM NaCl. In all cases, the binding constants increase in the order: **NP_Glu** < **NP_Leu** < **NP_Phe**. **NP_Phe** always affords higher binding affinity to ChT than **NP_Leu** does, although they have similar hydrophobicity indices. One plausible explanation is that the surface area of L-Phe is larger than that of L-Leu and can thus provide more efficient hydrophobic interactions with the protein. Additionally, there exist the possibility of CH-π interaction and π-π stacking of L-Phe with residues in ChT active pocket.[51]

The similar observation also obtained from activity assay study. The inhibition of ChT activity toward SPNA by three NPs at increasing ionic strengths show different trend according to surface functionality on nanoparticle surface. As shown in Figure 3.4b, three ChT-NP complexes exhibit different profiles of activity restoration upon addition of salt, resulting in the activity recovery in the order **NP_Glu** > **NP_Leu** > **NP_Phe**. This supports that amino acid side chains play an important role in the binding process. Taking the structure into account, the observation is similar to ITC analysis and that again attributed to the presence of hydrophobic interaction between the

protein and L-Leu and L-Phe residues whose effect is amplified along with the attenuation of electrostatic forces.

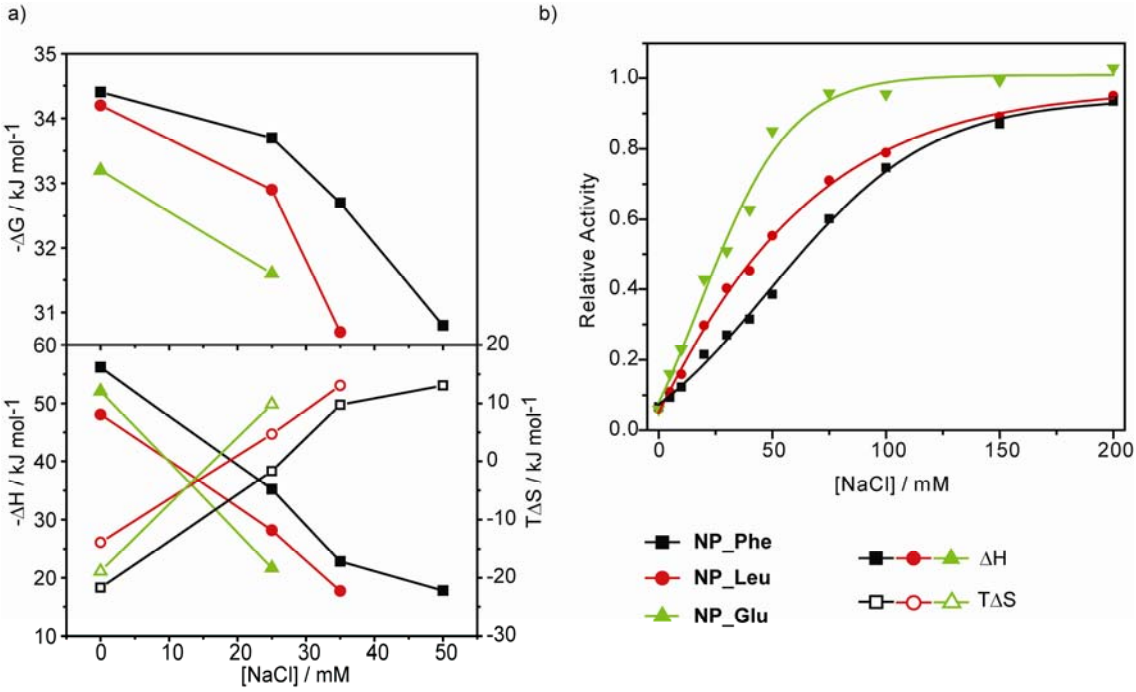

Figure 3.4. a) Thermodynamic parameters for the complexation of ChT with amino acid-functionalized NPs at various salt concentrations. b) Activity of ChT plotted as a function of salt concentration in the presence of anionic amino acid-functionalized NPs. The activity is normalized to that of ChT at respective salt concentrations.

At low salt concentrations, ChT-NP complexation is driven by enthalpy. With increasing salt concentration, the favorable enthalpic components decrease, whereas entropy changes become more favorable. In 50 mM of NaCl solution, the enthalpic and entropic contributions to the formation of ChT-**NP_Phe** complex are comparable. As hydrophobic interactions at room temperature are generally dominated by entropic effects,[52] the more positive entropic changes at higher salt concentrations presumably originate from hydrophobic interactions. Hydrophobic interactions, however, are not strong enough to maintain the complexes at higher ionic strength where electrostatic interaction is fully diminished.

3.2.1.5 Enthalpy-Entropy Compensation

The opposing trends of enthalpy and entropy change with increasing ionic strength for NP-ChT interaction as well as comparable DG values for protein-NP complexation (For ChT-NP complex 30 to 34 kJ mol^{-1}, for Histone-NP complex 45 to 46 kJ mol^{-1} and for Cyt c-NP complex, first binding 40 to 42 kJ mol^{-1}, second binding 31 to 37 kJ mol^{-1}) indicate enthalpy-entropy compensation. Although no explicit relationship between the enthalpic and the entropic terms can be deduced from fundamental thermodynamics, the compensation effect has been observed universally in host-guest complexation.[53, 54] However, the origin of this extrathermodynamic relationship is still under controversy, complicated in part by experimental concerns regarding the quality of the data.[53, 55, 56] In the current study, it should be noted that the use of ITC eliminates issues associated with van't Hoff approximations. Additionally, the wide spread of free energy values provides an excellent benchmark for assessing compensation.[53]

The physical significance of enthalpy-entropy compensation has been discussed in terms of cooperative interaction[57] and thermodynamic functions.[58] Inoue *et al.* have carried out quantitative correlation analyses of compensatory enthalpy-entropy relationships using a wide variety of molecular recognition systems.[59] In these analyses, the $T\Delta S$ value was linearly correlated with the ΔH value to give equation 3.2. When equation 2 is introduced to Gibbs-Helmholtz equation followed by differential, equation 3.3 is obtained.

$$T\Delta S = \alpha\Delta H + T\Delta S_0 \qquad (3.2)$$

$$\delta\Delta G = (1-\alpha)\delta\Delta H \qquad (3.3)$$

According to equation 3.3, the slope (α) of ΔH-$T\Delta S$ plots reflects the contribution of enthalpic gains ($\delta\Delta H$) induced by alterations in host, guest, and/or solvent to the free energy change ($\delta\Delta G$), as some enthalpy has been canceled by the accompanying entropic loss ($\delta\Delta S$).[59] The intercept ($T\Delta S_0$) represents the inherent complex stability (ΔG) obtained at $\Delta H = 0$, which means that the complex is stabilized even in the absence of enthalpic stabilization in case of positive $T\Delta S_0$ terms. By employing this correlation approach, the entropy changes ($T\Delta S$) listed in Table 1 and Figure 4 are plotted against corresponding enthalpy changes (ΔH) for the particle-protein systems studied. As shown in Figure 3.5a, an excellent linear relationship is obtained for these thermodynamic quantities with a correlation coefficient of 0.998. The compensation plot for protein-protein and protein nanoparticle interactions is also represented in Figure 3.5b for comparison.

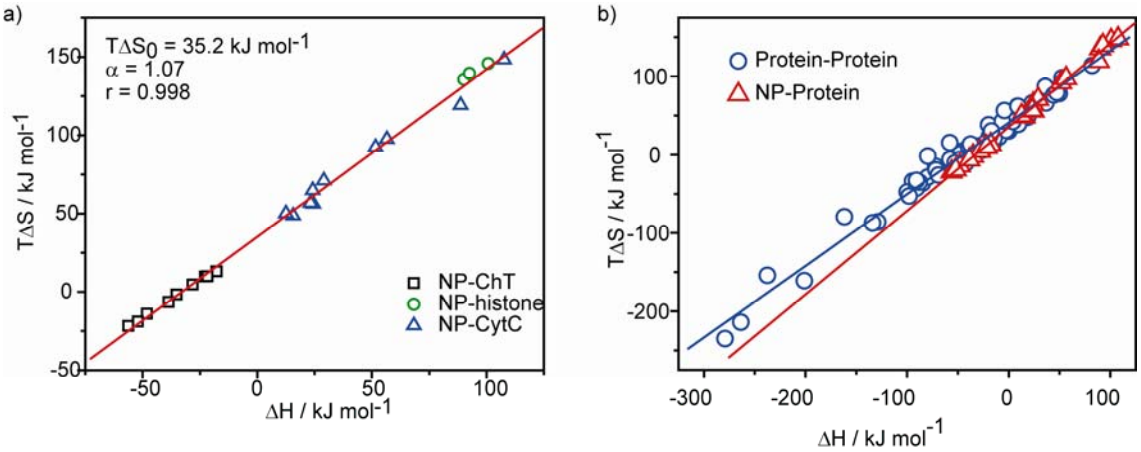

Figure 3.5. Plots of entropy (TΔS) versus enthalpy (ΔH) for (a) NP-protein (number of data set n = 23) and (b) the overlap of compensation plots for protein-protein (number of data set n = 70) and NP-protein interactions.

Using correlation analyses, it has been suggested that the slope (α) and the intercept ($T\Delta S_0$) can be empirically used as a quantitative measure of the conformational

change and the desolvation upon complex formation, respectively.[59] In Table 3.3, the slope and intercept values of ΔH-$T\Delta S$ plots for various host-guest complexation, protein-nonpeptide ligand, protein-peptide and protein-protein interactions are compared with that of NP-protein interaction. The ΔH-$T\Delta S$ plots for protein-protein, protein-nonpeptide molecule and protein peptide interactions are presended in Appendix 2 with all thermodynamic values. As expected, rigid hosts such as cryptands and metal porphyrins give smallest slope values, whereas flexible hosts such as glymes and lariat crown ethers shows largest slope values. The α value of particle-protein interaction is comparable to that of glyme-cation and substituted cyclodextrin-organic molecule interactions, and somewhat larger than that of protein-protein interaction (Figure 3.6). For the four systems involving protein partners, the α values increase in the order of nonpeptide ligand < protein < peptide < nanoparticle. This result indicates that the NP-protein couple undergoes large conformational changes during the complexation process. Such conclusion is in good accordance with the structural features of monolayer-protected NPs as the flexible ligands are expected to reorganize on the NP surface to attain a maximum complex stability.[60]

Table 3.3. Slope (α) and Intercept ($T\Delta S_0$) of Enthalpy-Entropy Compensation Plots for Various Host-Guest Systems.

Host	Guest	α	$T\Delta S_0$ / kJ mol^{-1}	Data set (n)	r
Glyme/podand[a]	Metal ion	1.02	15.9	150	0.98
Lariat crown ether[a]	Metal ion	0.98	18.6	132	0.96
Crown ether[a]	Metal ion	0.83	14.2	744	0.92
Cryptand[a]	Metal ion	0.44	13.6	160	0.65
Metal porphyrin[a]	Pyridine/imidole	0.63	8.4	49	0.94
Cyclophane/calixarene[a]	Small organic molecule	0.84	15.6	77	0.92
Native cyclodextrin[a]	Small organic molecule	0.82	10.2	1091	0.90
Substituted cyclodextrin[a]	Small organic molecule	1.02	16.7	182	0.97
Cyclodextrin[b]	Small organic molecule	1.06	14.6	–	–
Organic host[b]	Small organic molecule in water	0.96	13.2	–	–
Organic host[b]	Small organic molecule in organic solvent	1.30	17.4	–	–
Protein	Nonpeptide ligand	0.89	26.1	277	0.97
Protein	Peptide	0.96	32.7	252	0.98
Protein	Protein	0.92	44.1	70	0.99
Nanoparticle	Protein	1.07	35.2	23	0.99

[a] see reference [61]. [b] Recalculated from reference 53 by assuming a temperature of 298.15 K, which presumably causes the deviation from the values obtained from reference 61.

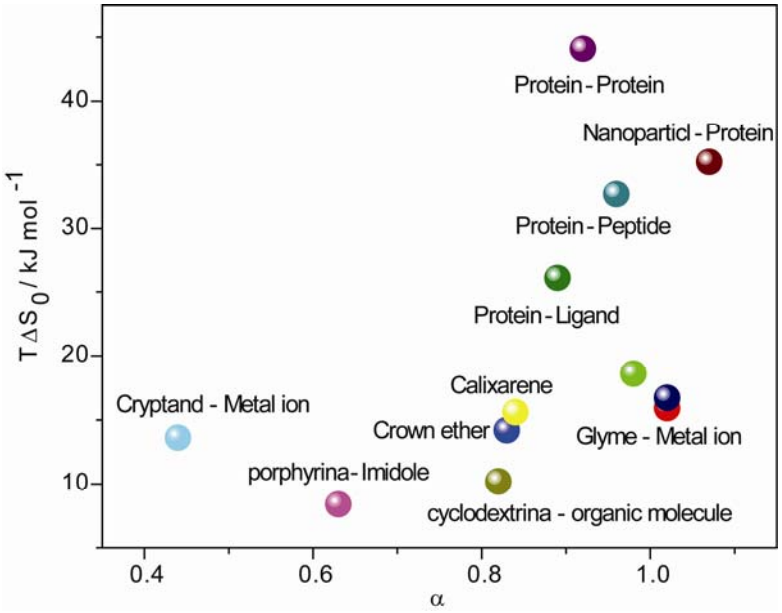

Figure 3.6. Slope (α) and intercept ($T\Delta S_0$) values for various host-guest systems. Protein-ligand interactions have been divided into protein-peptide and protein-other (protein-ligand) interactions.

While a number of host-guest systems feature slopes similar to protein-protein interactions, dramatic differences are observed in the intercept values ($T\Delta S_0$) of protein-partner interactions and other host-guest systems. For the protein-partner interactions, the intercept values ($T\Delta S_0$) increase in the order of nonpeptide ligand < peptide < nanoparticle < protein. The intercept for the particle-protein interactions is substantially more positive than that of the other 'small molecule' interactions and is comparable to protein-protein/peptide interactions. Protein surface recognition involves large surface contact area and the rearrangement of water of hydration around the binding interface. Therefore, the large intercepts explicitly indicate that the complexation of proteins with both native partners (i.e. proteins) and artificial receptors (i.e. NPs) experiences significant desolvation. As a consequence, the complex formation can be readily driven by the positive entropy changes due to the desolvation effect even in the absence of an enthalpic gain (i.e. $\Delta H = 0$). Obviously, for the protein-small ligand interactions, such desolvation effect is not as significant as that of protein-protein and protein-particle interactions, as there is less desolvation process in this system although proteins serve also as a complexation partner.

Collectively, the enthalpy-entropy compensation analysis reveals the large conformational changes and extensive desolvation during the formation of NP-protein complexes, consistent with the prototypical protein-protein interactions. Nanoparticles thus provide an excellent biomimetic system that affords both large surface area and multivalent binding features.

3.2.3 Conclusion

In summary, we have demonstrated that electrostatic and hydrophobic interactions cooperatively control the complexation of amino acid-functionalized NPs with proteins, which depends on the surface distributions of charged and hydrophobic residues in the protein. The thermodynamic parameters obtained from ITC studies revealed dramatic differences in the mode of interaction, with the complexation of NPs with ChT enthalpy-driven while the complexation with histone and CytC is entropy-driven. With ChT as a model protein, it is demonstrated that the electrostatic and hydrophobic contributions to the complex stability can be tuned by varying system ionic strengths. The validity of enthalpy-entropy compensation has been examined for the NP-protein system. An excellent linear relationship is obtained for the ΔH-$T\Delta S$ plot with a near unit slope and a large intercept. These quantitative measurements indicate the significant conformational changes and substantial dehydration of the partners. These studies also point to strategies that can be used to further optimize synthetic receptors for proteins, namely the reduction of the slope (α) value while maintaining or enhancing the intercept ($T\Delta S_0$) value. But significantly, the compensation coefficients of nanoparticle-protein binding closely resemble that of natural protein-protein interactions, demonstrating the biomimetic nature of these systems.

3.3 Size Dependent Protein-Nanoparticle Self-Assembly

Protein-nanoparticle conjugates have numerous applications in biology and material science. Along with numerous biological applications,[62, 3] assemblies of proteins with nanoparticles also provide building blocks for the creation of hybrid

bionanomaterials.[63, 64] The wide range of sizes and charges of protein molecules provide access to a broad range of biomaterials with controlled interparticle spacing,[65] magnetic properties[66] and overall structure of the nanocomposites. Each of these applications rely extensively on the fundamental aspects of protein-nanoparticle interactions. Monolayer-functionalized nanoparticles provide a tunable surface for binding with target molecules, enabling controlled nanoparticle-protein interactions. A fundamnetal understanding of the thermodynamic parameters of these protein-nanoparticle interactions provides an important foundation for the application of these systems in biological and material applications.

As we can see from the above experiments, ITC provides a powerful tool for investigating the thermodynamics and stoichiometry of supramolecular processes.[67] ITC analysis can be used in nanoparticle-protein assemblies to determine: i) binding stoichiometry, ii) stability of the conjugates, and iii) solublility or aggregation of the conjugates etc. Likewise, ITC analysis of protein nanoparticle complexation can determine the nature of binding (entropic vs. enthalpic), and the effect of surface functionality and envioronmental conditions on binding ratios and affinities.[68, 69]

Here we want to develop the thermodynamic characterization on the interaction of proteins of three different sizes with nanoparticles using ITC to probe the effect of relative particle-protein size in complexation (Figure 3.7b). For our studies we used 2 nm core gold nanoparticles (~8 nm overall diameter) with variable cationic functionality (hydrophobic, hydrophilic and aromatic, Figure 3.7a). The selected proteins are anionic in nature to allow sufficient electrostatic interaction. For the protein, we choose three anionic proteins of distinctly different size (Fig. 3.7b). Green

fluorescence protein (GFP) is the smallest beta barrel shaped protein among these: 3.0 nm x 4.0 nm (MW = 27 kDa, pI = 5.92).[70] Bovine serum albumin (BSA) is the triangular prismatic protein with comparable size to the nanoparticle: 8.4 nm x 8.4 nm x 8.4 nm x 3.1 nm (MW = 66.3 kDa, pI = 4.8).[71] The third protein is acid phosphatase (PhosA), which is orthorhombic shaped and larger than the receptors: 12.6 nm x 20.7 nm x 7.3 nm (MW = 110 kDa, pI = 5.2).[72]

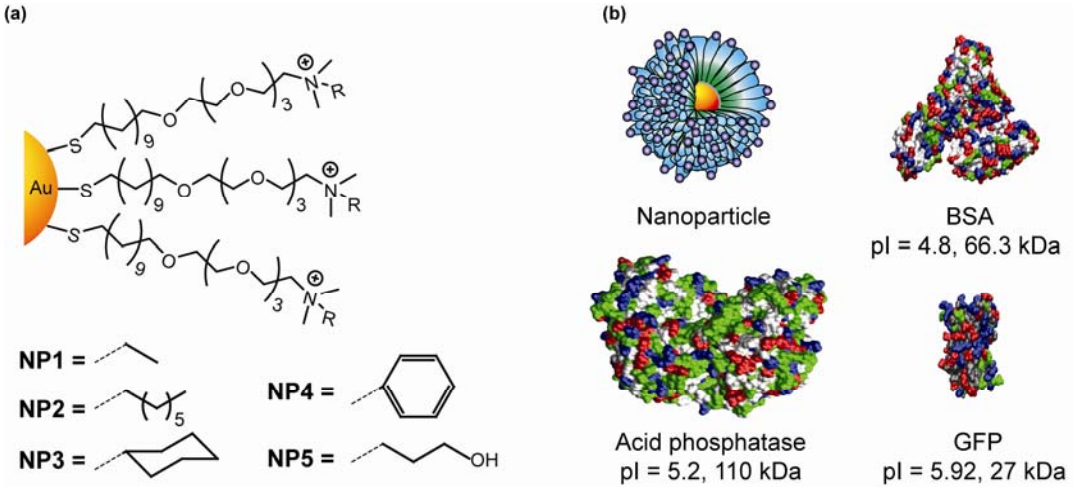

Figure 3.7. a) Chemical structure of the cationic gold nanoparticles (**NP1-NP5**). b) Surface structural features and relative size of three negatively charged proteins used in the ITC study. Colour scheme for the proteins: basic residues (blue), acidic residues (red), polar residues (green) and nonpolar residues (grey).

3.3.1 Result and Discussion

3.3.1.1 Isothermal titration Calorimetry

The ITC experiments were carried out at 30 ^{o}C by titrating protein solutions into the nanoparticle solution in the isothermal cell. For our experimental purpose we first standardize the relative concentration of nanoparticle and protein to get the suitable heat change response. Depending on the protein structure we observed three different types of heat change profile from the titration curves (Figure 3.8).

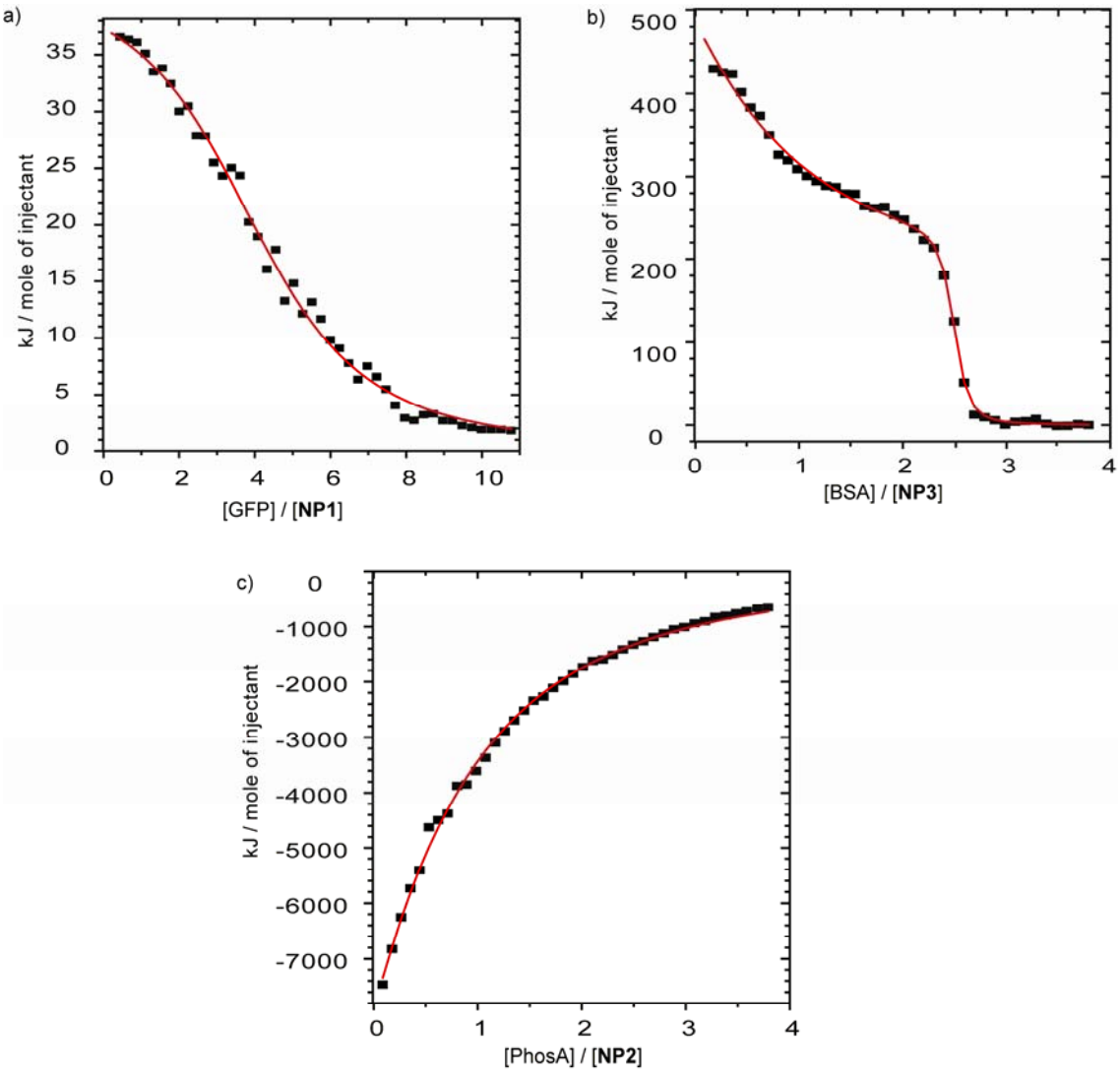

Figure 3.8. ITC analysis for the complexation of (a) GFP with **NP1**, (b) BSA with **NP3**, and (c) PhosA with **NP2** in 5 mM sodium phosphate buffer (pH = 7.4). The squares represent the integrated heat changes during complex formation and the lines the curve fit to the binding isothermal functions.

The complexation of GFP and BSA with all nanoparticles is endothermic in nature, while the complexation of PhosA with nanoparticles exhibits exothermic processes. We tried to fit this heat change into various isothermal functions to determine the various binding parameter corresponding to NP-protein interactions. Interestingly, the complexation of NPs with both GFP and PhosA can be fitted using the mode of single

set of identical binding sites which are either smaller or larger than the size of the nanoparticles. In contrast, the BSA with comparable size to nanoparticles, can only be assessed using a binding mode of two sets of binding sites. We also observed the precipitation at the end of titration in disparity with other two proteins. Using the isothermal curve fitting analysis various thermodynamic parameters such as, binding constants (K_S), enthalpy changes (ΔH) and binding stoichiometries (n) were determined. The Gibbs free energy changes (ΔG) and entropy changes (ΔS) were calculated by using the standard thermodynamic equations : $\Delta G = -RT\ln K_S$ and $\Delta G = \Delta H - T\Delta S$. These quantities for the corresponding nanoparticle-protein interactions are summarized in Table 3.4.

Table 3.4. Complex stability constants (K_S), Gibbs free energy changes (ΔG), enthalpy changes (ΔH), entropy changes ($T\Delta S$), and binding stoichiometries (n) for the complexation of GFP, BSA and PhosA with various gold NPs (5 mM sodium phosphate, pH 7.4) at 30 °C.

Protein	NPs	First binding event					Second binding event				
		K_{S1} / M^{-1}	$-\Delta G$ / kJ mol^{-1}	ΔH / kJ mol^{-1}	$T\Delta S$ / kJ mol^{-1}	n	K_{S2} / M^{-1}	$-\Delta G$ / kJ mol^{-1}	ΔH / kJ mol^{-1}	$T\Delta S$ / kJ mol^{-1}	n
GFP	**NP1**	1.74×10^{6}	36.22	42.26	78.48	4.39	–	–	–	–	–
BSA	**NP1**	3.66×10^{7}	43.89	18.70	62.59	1.71	1.21×10^{8}	46.91	1133.86	1180.77	0.36
	NP2	9.63×10^{7}	46.33	223.43	269.76	1.89	10.4×10^{8}	52.33	615.05	667.38	0.39
	NP3	10.7×10^{7}	46.60	187.02	233.62	2.11	3.13×10^{8}	49.30	1087.84	1137.14	0.34
	NP4	26.5×10^{7}	48.88	247.27	296.15	2.27	1.04×10^{8}	52.33	732.20	775.53	0.39
	NP5	5.86×10^{7}	45.08	164.43	209.51	1.97	8.46×10^{8}	51.81	623.42	675.23	0.32
PhosA	**NP1**	2.03×10^{5}	30.80	-11171	-11140	0.43	–	–	–	–	–
	NP2	1.47×10^{5}	29.99	-31380	-31350	0.45	–	–	–	–	–
	NP3	1.89×10^{5}	30.62	-29664	-29633	0.43	–	–	–	–	–
	NP4	1.69×10^{5}	30.34	-35103	-35073	0.39	–	–	–	–	–
	NP5	3.16×10^{5}	31.92	-21171	-21139	0.44	–	–	–	–	–

3.3.1.2. Exothermic vs. Endothermic Process

The thermodynamic quantities listed in Table 3.4 reveals that the complexation of proteins involves not only the electrostatic interaction but also the other noncovalent forces including hydrophobic, hydrogen bonding and π-π stacking interaction as obtained from surface functionality of the nanoparticles. This result suggests that the nanoparticle-protein interaction can be controlled by surface modification of artificial receptors. Further examination on the change of enthalpy and entropy values explore that the complexation of GFP and BSA involves unfavorable enthalpy change ($\Delta H > 0$) which is compensated by favorable entropy gain ($\Delta S > 0$), resulting in overall negative free energy changes (ΔG). On the other hand, the interaction with the larger protein is exothermic process with highly negative change in enthalpy ($\Delta H < 0$), although this favorable gain partially offset by unfavorable entropy loss ($\Delta S < 0$). This enthalpy or entropy controlled process can be easily explained if we consider the overall complexation process as described in Equation 3.6, which is the combination of two simultaneous processes (Equations 3.4 and 3.5).

$$Protein + NP \Leftrightarrow [Protein.NP] \quad (3.4)$$

$$xH_2Op + yH_2On \Leftrightarrow (x+y-z)\ H_2Op.n + zH_2O \quad (3.5)$$

$$Protein.xH_2Op + NP.yH_2On \Leftrightarrow [Protein.NP](x+y-z)H_2Op.n + zH_2O \quad (3.6)$$

Where, H_2Op, H_2On, $H_2Op.n$ – water molecule associated with protein, nanoparticle and protein-nanoparticle complex respectively.

The first process is noncovalant complex formation, where ΔH and ΔS both are negative i.e. exothermic process. In contrast, the solvent reorganization process involves the disruption of the well defined solvent shells to end up with endothermic process (ΔH

> 0 and $\Delta S > 0$). Depending on the contribution of these two processes, the final complexation (Equation 3) will be either exothermic (1st process predominant) or endothermic (2nd process predominant). In complexation of smaller proteins, GFP and BSA, higher degree of surface interaction is occurring which results from the release of a large amount of the water of hydration from the binding interface. This process is evident from the large positive entropy changes. On the other hand, protein-nanoparticle interaction plays the main role for the PhosA indicated by the observed negative enthalpy changes.

3.3.1.3 Diverse Binding Ratio

Another important observation from the Table 3.4 is the binding ratios and binding mode between protein and nanoparticles which are drastically different depending on protein size. In case of smaller protein the nanoparticle:GFP binding ratio is ~1:4 indicating the nanoparticle is surrounded by proteins. In contrast for the bigger protein, the nanoparticles surround the protein molecule. The similar size protein has different binding mode than other two proteins. In case of first binding mode, the binding is similar to GFP where each nanoparticle is surrounded by two BSA. The following binding involves nanoparticle-protein aggregation and precipitation with nanoparticle:BSA binding ratio 1:3. This extended aggregation and precipitation is supported by the large positive entropy change ($T\Delta S$ = 667 – 1180 kJ mol^{-1}) due to the release of large amount of bound water molecules (Figure 3.9). This aggregation was further established by dynamic light scattering (DLS) study (Figure3.13 in experimental section), where aggregates of ~150 nm were formed initially between **NP1** and BSA, with larger aggregates and concomitant precipitation observed over time. Hence, by

controlling the relative protein-nanoparticle concentration we can control the pattern of protein-nanoparticle aggregation.

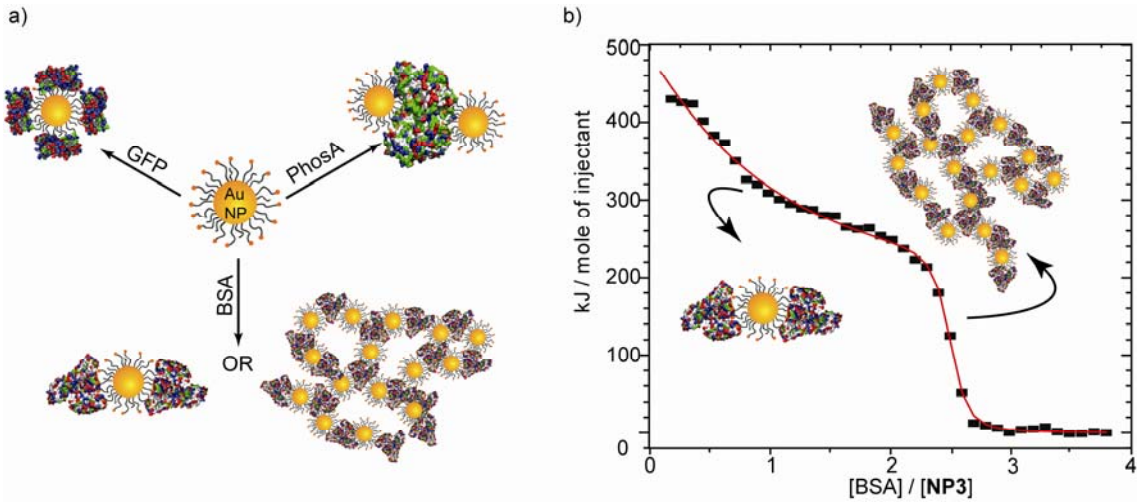

Figure 3.9. a) Schematic depiction of particle-protein assemblies observed in this study. b) ITC analysis of BSA-nanoparticle complexation and concentration dependant different protein-nanoparticle conjugation.

3.3.1.4 Consistent Enthalpy-Entropy Compensation

We also observed from table 1 that enthalpy and entropy changes are always balanced to get the favorable free energy changes ($\Delta G < 0$). This indicates enthalpy-entropy compensation, which is commonly observed for many host-guest complexes.[53] The physical significance of enthalpy-entropy compensation is determined from the linear correlation using the relation $T\Delta S = \alpha\Delta H + T\Delta S_0$, where α is the slop and $T\Delta S_0$ is the intercept. The slope and intercept of compensation plots have been related to the conformational change and desolvation during complexation, respectively.[59] As shown in Figure 3.10, an excellent linear relationship is obtained for these thermodynamic quantities with a correlation coefficient of 0.999. Herein, near-unit slopes ($\alpha = 1.00$ for protein-NP and 0.94 for protein-protein) suggest that significant conformational

changes occur at the interaction interface, which is unambiguously true for similar kind of flexible systems. For the nanoparticle systems, the reorganization of flexible surface ligands provides a target-responsive system to afford optimal binding affinity.[60] Large positive intercept values ($T\Delta S_0$ = 46.2 kJ mol^{-1} for protein-NP and 41.5 kJ mol^{-1} for protein-protein) are also obtained for these interactions, reflecting the extensive desolvation during complexation. This means that the complex formation can take place even in the absence of an enthalpic gain (i.e. ΔH = 0 kJ mol^{-1}). Such situation may arise when the entropic contribution from the desolvation process becomes major factor for the protein-nanoparticle complexation.

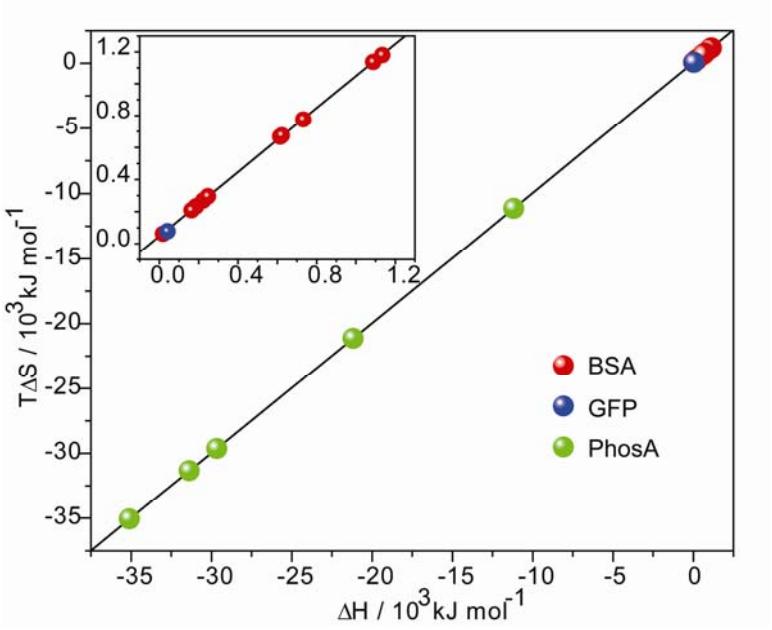

Figure 3.10. Plot of entropy (TΔS) versus enthalpy (ΔH) for protein-nanoparticle interaction. Inset shows magnification of the correlation data for the BSA and GFP.

3.3.2 Conclusion

In summary, we have demonstrated that the thermodynamic properties for complexation between protein and nanoparticles depends on the relative size of

proteins. In case of smaller and larger proteins the binding mode is similar but the arrangements of protein and nanoparticle are in contrary. The most interesting phenomenon is observed for protein with comparable size to nanoparticle where the binding mode is different than others. We also observed that the complexation exclusively depends on the relative concentration of proteins in solutions. In addition, we established the potentiality of the ITC study as a powerful tool to resolve the nature of supramolecular interaction by determining the thermodynamic parameters which is very crucial for further applications.

3.4 Experimental Section

3.4.1 Materials

All the reagents, α-Chymotrypsin (Type II from bovine pancreas, ChT), cytochrome *c* (from equine heart), histone (Type III-S from calf thymus, an isolated lysine rich fraction)bovine serum albumin (BSA) and acid phosphatase (PhosA, from potato) were purchased from Sigma and used as received. Green fluorescence protein (GFP) was expressed according to the known procedure from the Starter cultures from a glycerol stock of GFP (Enhanced GFP (eGFP) was cloned into the pET21d vector (Novagen) where Hisx6 tag was located at N-terminus) in BL21 (DE3).[73] Amino acid-functionalized gold nanoparticles (NPs) were prepared by place-exchange of corresponding thiol ligands with 1-pentanethiol capped gold NPs (diameter ~ 2 nm) according to the published procedure.[23] The cationic nanoparticles are prepared according to our published procedure.[18] Disodium hydrogen and sodium dihydrogen

phosphate were dissolved in 18 MΩ water to make a 5 mM phosphate buffer solution of pH 7.4, which was used as solvent in isothermal titration calorimetries.

3.4.2 Determination of Molecular weight of Nanoparticles

TEM measurements on **NP_Ala** revealed an average particle size of 2.1±0.4 nm (Figure 3.11a). TGA revealed that the weight percentage of organic ligands in the NPs is 36% (Figure 3.11b). Based on that, the average molecular weight of the NP is estimated as 100 kDa, which was used for the preparation of NP solutions. The detail procedure for TEM and TGA are as follows:

Transmission Electron Microscopy (TEM). The nanoparticle film was drop-cast by putting a drop of aqueous nanoparticles on a 300 mesh carbon-coated copper grid. The solvent was evaporated at room temperature (ca. 20 °C). The TEM images were taken on a JEOL 200 instrument operated at 200 keV (Figure 3.11a).

Thermogravimetric analysis (TGA). TGA was performed using a TGA 2950 high-resolution thermo-gravimetric analyzer (TA Instruments, Inc., New Castle, DE), which was equipped with an open platinum pan and an automatically programmed temperature controller. The TGA curves were recorded as follows: about 3.5 mg of nanoparticles was placed in the TGA pan and heated in a nitrogen atmosphere at a rate of 10 °C / min up to 600 °C.

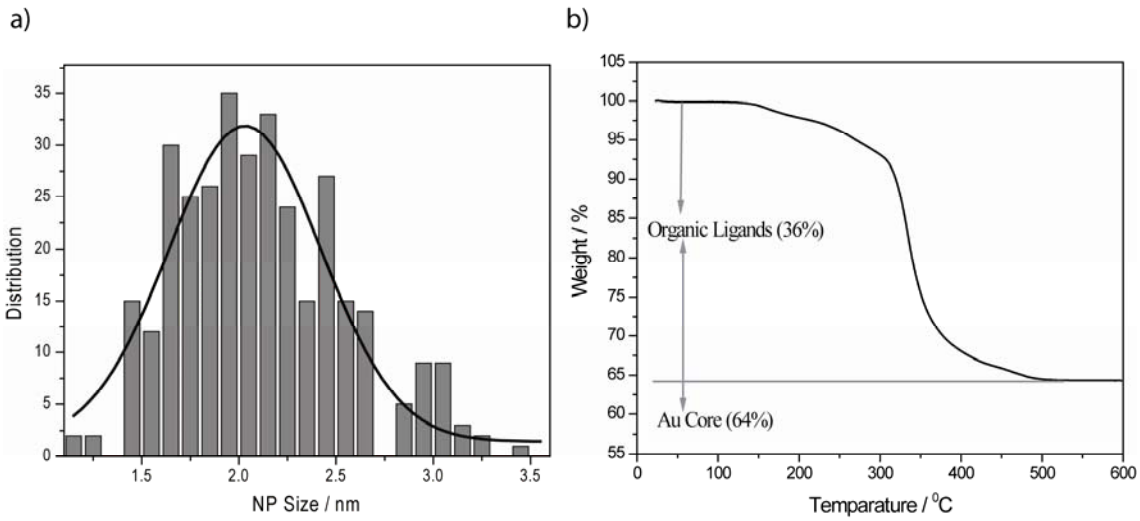

Figure 3.11. a) Histogram of size distribution of **NP_Ala** (333 counts) from TEM image. The average diameter is 2.1±0.4 nm. b)Thermal gravimetric analysis (TGA) curve of **NP_Ala**.

3.4.3 Isothermal Titration Calorimetry

An isothermal calorimeter (ITC), purchased from Microcal Inc. (Northampton, MA), was used in all microcalorimetric experiments operated at 30 °C. Each microcalorimetric titration experiment consisted of 30-45 successive injections of a constant volume (6 μL/injection) of ChT, Cyt-c, Histone, GFP, BSA or PhosA solution (100 μM to 400 μM according to binding ratio) into the reaction cell (1.4 mL) charged with a NP solution (1.0 to 2.5 μM) in the same buffer. The heat of dilution of the protein solutions when added to the buffer solution in the absence of NPs was determined in each run, using the same number of injections and concentration of proteins as in the titration experiments. The dilution enthalpies determined in these control experiments were subtracted from the enthalpies measured in the titration experiments. The Origin program supplied by Microcal Inc. was used to calculate the binding constant (K_S) and molar enthalpy change (ΔH) of reaction from the titration

curve. The molar Gibbs free energy changes (ΔG) and entropies (ΔS) of reaction were calculated from the experimentally determined K_S and ΔH values.

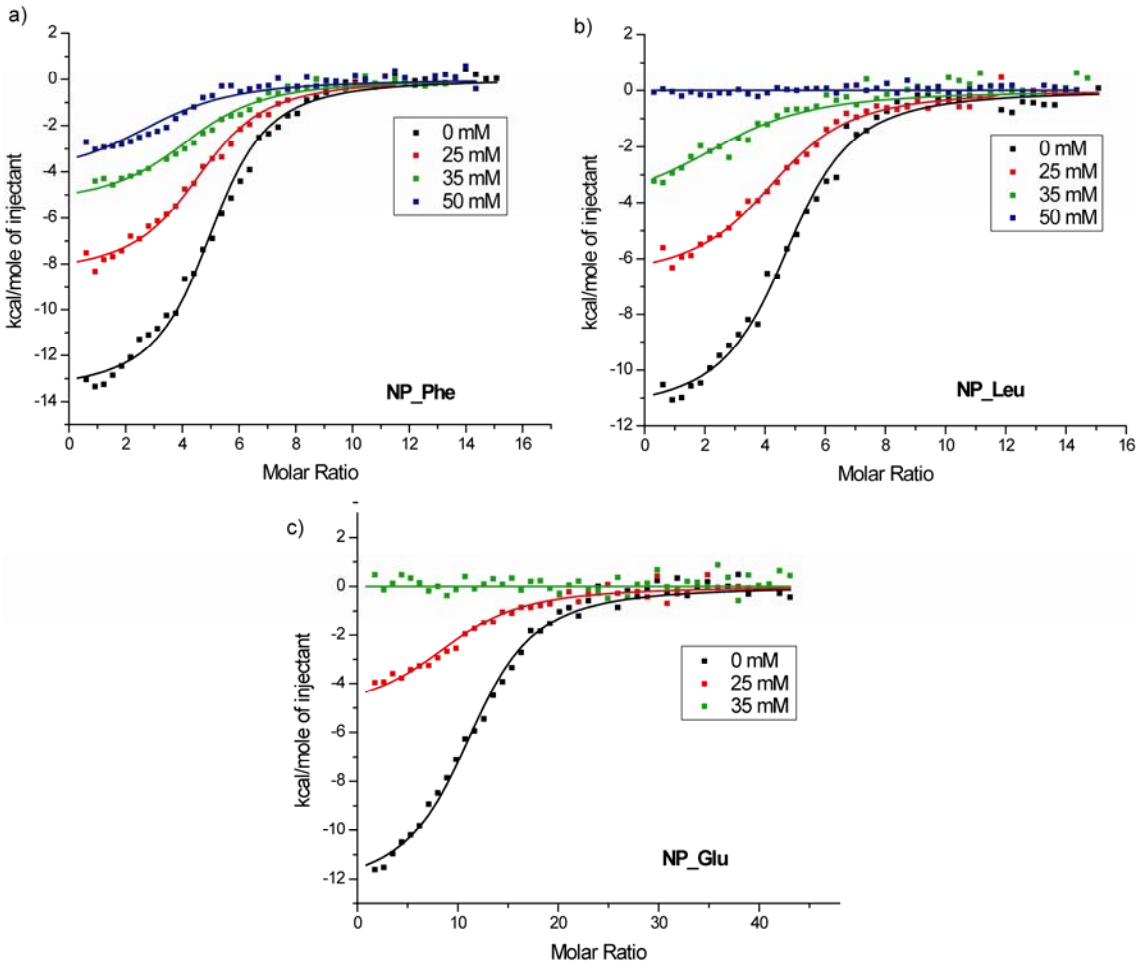

Figure 3.12. ITC analysis of the interaction of ChT with phenylalanine-functionalized nanoparticles (a) leucine-functionalized nanoparticles (b) and glutamic acid-functionalized nanoparticles (c) in 5 mM sodium phosphate buffer (pH = 7.4) at various NaCl concentrations

3.4.4 Activity Assays

α-Chymotrypsin (3.48 μM) was incubated with amino acid-functionalized nanoparticles (1.74 μM) in 5 mM sodium phosphate buffer (pH 7.4) at varying NaCl concentrations (0 mM-200 mM) for 4 h. Thereafter, 184 μL of the above solutions were introduced into a 96-well flat bottom microplate followed by the addition of 16 μL of

25.9 mM SPNA dissolved in ethanol, resulting in final concentrations of 3.2 μM for ChT, 1.6 μM for NPs and 2.0 mM for SPNA. Activity was followed by monitoring the absorption changes at 405 nm with an Ultra Microplate Reader (EL808 Bio-Tek Instruments, Inc.). The obtained activity was normalized to that of ChT without NPs at respective salt concentrations. Each sample was measured in triplicate and the average was reported.

3.4.5 Dynamic Light Scattering (DLS)

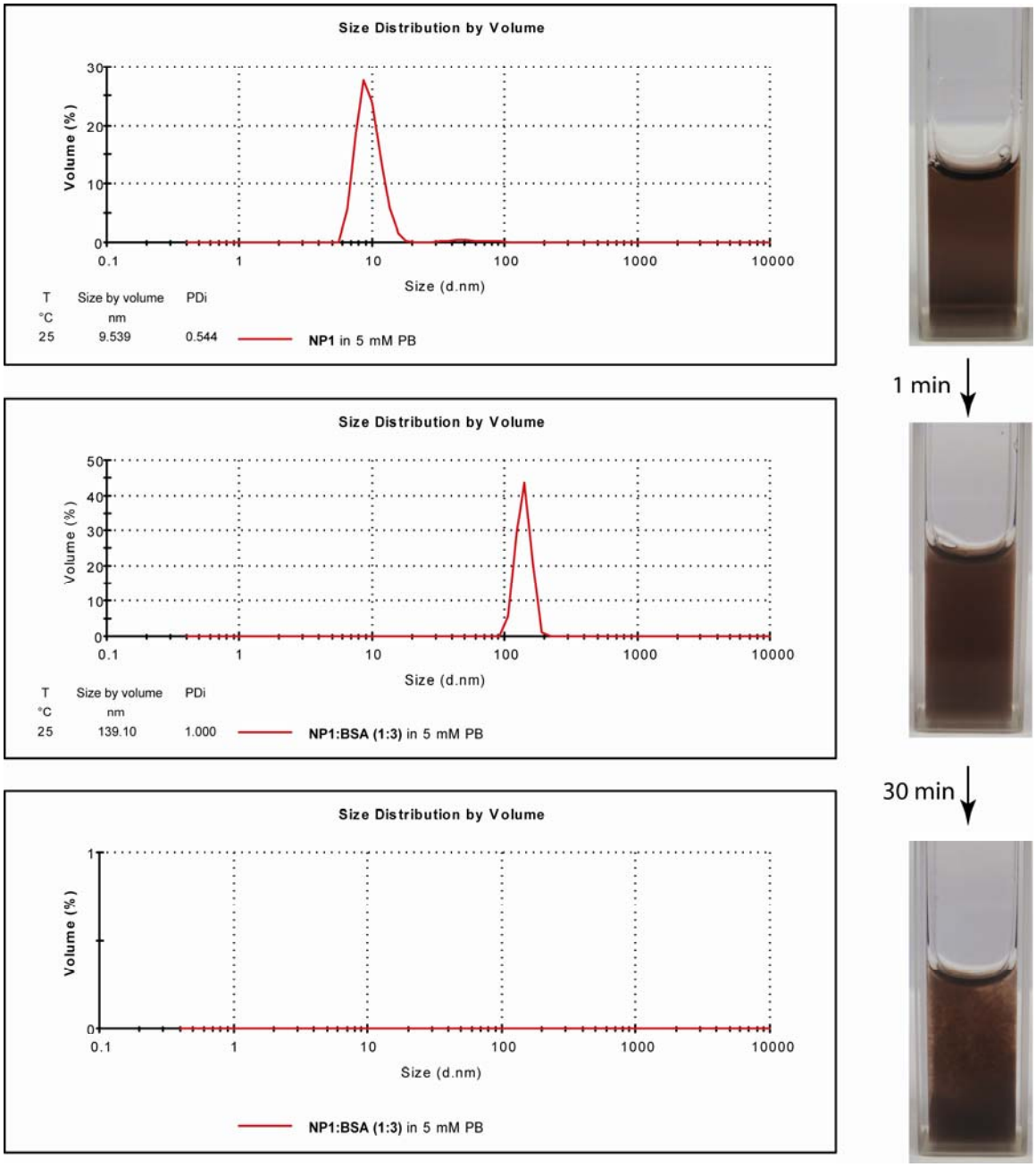

Figure 3.13. The DLS analysis for the complexation of NP 1 with BSA at variable time scale.

Gold nanoparticles were dissolved in 5 mM sodium phosphate buffer, pH 7.4 to make a 2 μM solution and their size was measured on a MALVERN Zetasizer Nano ZS

instrument. The similar experiment was repeated with the mixture of 2 μM nanoparticle and 6 μM BSA. Just after the addition of BSA the aggregation was started and the average diameter was 139 nm. After 15 minute the solution becomes cloudy and the measurement was not possible any more. After 2 hours we saw the complete precipitation of the protein nanoparticle conjugates.

3.5 References

1 Karlsson, M.; Davidson, M.; Karlsson, R.; Karlsson, A.; Bergenholtz, J.; Konkoli, Z.; Jesorka, A.; Lobovkina, T.; Hurtig, J.; Voinova, M.; Orwar, O., *Annu. Rev. Phys. Chem.* **2004,** *55*, 613-649.

2 Prakash, S.; Piruska, A.; Gatimu, E. N.; Bohn, P. W.; Sweedler, J. V.; Shannon, M. A., *Ieee Sensors Journal* **2008,** *8*, 441-450.

3 De, M.; Ghosh, P. S.; Rotello, V. M., *Adv. Mater.* **2008,** *20*, 4225 - 4241.

4 Breslow, R. Ed. *Artificial Enzymes*, Wiley-VCH, Weinheim, 2005.

5 Thomas, C. M.; Ward, T. R., *Chem. Soc. Rev.* **2005,** *34*, 337-346.

6 Bjerre, J.; Fenger, T. H.; Marinescu, L. G.; Bols, M., *Eur. J. Org. Chem.* **2007**, 704-710.

7 Thordarson, P.; Bijsterveld, E. J. A.; Rowan, A. E.; Nolte, R. J. M., *Nature* **2003,** *424*, 915-918.

8 Favero, G.; Campanella, L.; Cavallo, S.; D'Annibale, A.; Perrella, M.; Mattei, E.; Ferri, T., *J. Am. Chem. Soc.* **2005,** *127*, 8103-8111.

9 Yoshida, R., *Curr. Org. Chem.* **2005,** *9,* 1617-1641.

10 Ma, P. X., *Adv. Drug Delivery Rev.* **2008,** *60*, 184-198.

11 Hostetler, M. J.; Wingate, J. E.; Zhong, C. J.; Harris, J. E.; Vachet, R. W.; Clark, M. R.; Londono, J. D.; Green, S. J.; Stokes, J. J.; Wignall, G. D.; Glish, G. L.; Porter, M. D.; Evans, N. D.; Murray, R. W., *Langmuir* **1998,** *14*, 17-30.

12 Pengo, P.; Baltzer, L.; Pasquato, L.; Scrimin, P., *Angew. Chem., Int. Ed.* **2007,** *46*, 400-404.

13 De Souza, A. C.; Kamerling, J. P., *Methods Enzymol.* **2006,** *417*, 221-243.

14 de la Fuente, J. M.; Barrientos, A. G.; Rojas, T. C.; Rojo, J.; Canada, J.; Fernandez, A.; Penades, S., *Angew. Chem., Int. Ed.* **2001,** *40*, 2257-2261.

15 Rosi, N.; Mirkin, C. A., *Chem. Rev.* **2005,** *105*, 1547-1562.

16 Nam, J. M.; Stoeva, S. I.; Mirkin, C. A., *J. Am. Chem. Soc.* **2004,** *126*, 5932-5933.

17 You, C. C.; Agasti, S. S.; De, M.; Knapp, M. J.; Rotello, V. M., *J. Am. Chem. Soc.* **2006,** *128*, 14612-14618.

18 You, C. C.; Miranda, O. R.; Gider, B.; Ghosh, P. S.; Kim, I. B.; Erdogan, B.; Krovi, S. A.; Bunz, U. H. F.; Rotello, V. M., *Nature Nanotechnology* **2007,** *2*, 318-323.

19 Xu, C. J.; Xu, K. M.; Gu, H. W.; Zhong, X. F.; Guo, Z. H.; Zheng, R. K.; Zhang, X. X.; Xu, B., *J. Am. Chem. Soc.* **2004,** *126*, 3392-3393.

20 Cheon, J.; Lee, J. H., *Acc. Chem. Res.* **2008,** *41*, 1630-1640.

21 Oh, E.; Hong, M. Y.; Lee, D.; Nam, S. H.; Yoon, H. C.; Kim, H. S., *J. Am. Chem. Soc.* **2005,** *127*, 3270-3271.

22 Stites, W. E., *Chem. Rev.* **1997,** *97*, 1233-1250.

23 You, C. C.; De, M.; Han, G.; Rotello, V. M., *J. Am. Chem. Soc.* **2005,** *127*, 12873-12881.

24 Benjamin, L. R.; Chung, H. J.; Sanford, S.; Kouzine, F.; Liu, J. H.; Levens, D., *Proc. Natl. Acad. Sci. U. S. A.* **2008,** *105*, 18296-18301.

25 Marsili, V.; Lupidi, G.; Berellini, G.; Calzuola, I.; Perni, S.; Cruciani, G.; Gianfranceschi, G. L., *Peptides* **2008,** *29*, 2232-2242.

26 Backes, A. C.; Zech, B.; Felber, B.; Klebl, B.; Muller, G., *Expert Opinion on Drug Discovery* **2008,** *3*, 1409-1425.

27 Zambelli, B.; Turano, P.; Musiani, F.; Neyroz, P.; Ciurli, S., *Proteins-Structure Function and Bioinformatics* **2009,** *74*, 222-239.

28 Russell, R. B.; Aloy, P., *Nature Chemical Biology* **2008,** *4*, 666-673.

29 Granneman, J. G.; Moore, H. P. H.; Granneman, R. L.; Greenberg, A. S.; Obin, M. S.; Zhu, Z. X., *J. Biol. Chem.* **2007,** *282*, 5726-5735.

30 Merchant, K. A.; Best, R. B.; Louis, J. M.; Gopich, I. V.; Eaton, W. A., *Proc. Natl. Acad. Sci. U. S. A.* **2007,** *104*, 1528-1533.

31 Di Fiore, A.; Monti, S. M.; Hilvo, M.; Parkkila, S.; Romano, V.; Scaloni, A.; Pedone, C.; Scozzafava, A.; Supuran, C. T.; De Simone, G., *Proteins-Structure Function and Bioinformatics* **2009,** *74*, 164-175.

32 Olsson, T. S. G.; Williams, M. A.; Pitt, W. R.; Ladbury, J. E., *J. Mol. Biol.* **2008,** *384*, 1002-1017.

33 Taylor, J. D.; Ababou, A.; Fawaz, R. R.; Hobbs, C. J.; Williams, M. A.; Ladbury, J. E., *Proteins-Structure Function and Bioinformatics* **2008,** *73*, 929-940.

34 Larsericsdotter, H.; Oscarsson, S.; Buijs, J., *J. Colloid Interface Sci.* **2001,** *237*, 98-103.

35 Birktoft, J. J.; Blow, D. M., *J. Mol. Biol.* **1972,** *68*, 187-&.

36 Johns, E. W., *Biochem. J.* **1964,** *92*, 55-&.

37 Tsukihara, T.; Aoyama, H.; Yamashita, E.; Tomizaki, T.; Yamaguchi, H.; ShinzawaItoh, K.; Nakashima, R.; Yaono, R.; Yoshikawa, S., *Science* **1996,** *272*, 1136-1144.

38 Larsericsdotter, H.; Oscarsson, S.; Buijs, J., *J. Colloid Interface Sci.* **2005,** *289*, 26-35.

39 Joshi, H.; Shirude, P. S.; Bansal, V.; Ganesh, K. N.; Sastry, M., *J. Phys. Chem. B* **2004,** *108*, 11535-11540.

40 Macdonald, I. D. G.; Smith, W. E., *Langmuir* **1996,** *12*, 706-713.

41 DeVries, G. A.; Brunnbauer, M.; Hu, Y.; Jackson, A. M.; Long, B.; Neltner, B. T.; Uzun, O.; Wunsch, B. H.; Stellacci, F., *Science* **2007,** *315*, 358-361.

42 Qi, K.; Ma, Q. G.; Remsen, E. E.; Clark, C. G.; Wooley, K. L., *J. Am. Chem. Soc.* **2004,** *126*, 6599-6607.

43 Battistuzzi, G.; Borsari, M.; Ranieri, A.; Sola, M., *Journal of Biological Inorganic Chemistry* **2004,** *9*, 781-787.

44 Shimokhina, N.; Bronowska, A.; Homans, S. W., *Angew. Chem., Int. Ed.* **2006,** *45*, 6374-6376.

45 Holdgate, G. A.; Tunnicliffe, A.; Ward, W. H. J.; Weston, S. A.; Rosenbrock, G.; Barth, P. T.; Taylor, I. W. F.; Pauptit, R. A.; Timms, D., *Biochemistry* **1997,** *36*, 9663-9673.

46 Li, Z.; Lazaridis, T., *J. Phys. Chem. B* **2005,** *109*, 662-670.

47 Makhatadze, G. I.; Privalov, P. L., *J. Mol. Biol.* **1993,** *232*, 639-659.

48 Link, S.; Wang, Z. L.; El-Sayed, M. A., *J. Phys. Chem. B* **1999,** *103*, 3529-3533.

49 Monera, O. D.; Sereda, T. J.; Zhou, N. E.; Kay, C. M.; Hodges, R. S., *J. Pept. Sci.* **1995,** *1*, 319-29.

50 Verma, A.; Simard, J. M.; Rotello, V. M., *Langmuir* **2004,** *20*, 4178-4181.

51 Shimohigashi, Y.; Nose, T.; Yamauchi, Y.; Maeda, I., *Biopolymers* **1999,** *51*, 9-17.

52 Israelachvili, J. N. *Intermolecular and Surface Forces*, 2nd Ed., Academic Press, London, 1992.

53 Houk, K. N.; Leach, A. G.; Kim, S. P.; Zhang, X., *Angew. Chem. Int. Ed.* **2003,** *42*, 4872 – 4897.

54 Liu, L.; Guo, Q. X., *Chem. Rev.* **2001,** *101*, 673-695.

55 Linert, W., *Chem. Phys.* **1989,** *129*, 381-393.

56 Sharp, K., *Protein Sci.* **2001,** *10*, 661-667.

57 Williams, D. H.; Stephens, E.; O'Brien, D. P.; Zhou, M., *Angew. Chem., Int. Ed.* **2004,** *43*, 6596-6616.

58 Dunitz, J. D., *Chem. Biol.* **1995,** *2*, 709-712.

59 Rekharsky, M. V.; Inoue, Y., *Chem. Rev.* **1998,** *98*, 1875-1917.

60 Boal, A. K.; Rotello, V. M., *J. Am. Chem. Soc.* **2000,** *122*, 734-735.

61 Liu, Y.; You, C.-C.; Zhang, H.-Y. in *Supramolecular Chemistry: Molecular Recognition and Assembly of Synthetic Receptors*; Nankai University Press: Tianjin, 2001; pp 454-596 (in Chinese), ISBN 7-310-01641-6.

62 Murphy, C. J.; Gole, A. M.; Stone, J. W.; Sisco, P. N.; Alkilany, A. M.; Goldsmith, E. C.; Baxter, S. C., *Acc. Chem. Res.* **2008,** *41*, 1721-1730.

63 McMillan, R. A.; Paavola, C. D.; Howard, J.; Chan, S. L.; Zaluzec, N. J.; Trent, J. D., *Nat. Mater.* **2002,** *1*, 247-252.

64 Hu, M. H.; Qian, L. P.; Brinas, R. P.; Lymar, E. S.; Hainfeld, J. F., *Angew. Chem., Int. Ed.* **2007,** *46*, 5111-5114.

65 Verma, A.; Srivastava, S.; Rotello, V. M., *Chem. Mater.* **2005,** *17*, 6317-6322.

66 Srivastava, S.; Samanta, B.; Jordan, B. J.; Hong, R.; Xiao, Q.; Tuominen, M. T.; Rotello, V. M., *J. Am. Chem. Soc.* **2007,** *129*, 11776-11780.

67 Jelesarov, I.; Bosshard, H. R., *J. Mol. Recognit.* **1999,** *12*, 3-18.

68 De, M.; You, C. C.; Srivastava, S.; Rotello, V. M., *J. Am. Chem. Soc.* **2007,** *129*, 10747-10753.

69 Lindman, S.; Lynch, I.; Thulin, E.; Nilsson, H.; Dawson, K. A.; Linse, S., *Nano Lett.* **2007,** *7*, 914-920.

70 Tsien, R. Y., *Annu. Rev. Biochem.* **1998,** *67*, 509-544.

71 Ferrer, M. L.; Duchowicz, R.; Carrasco, B.; de la Torre, J. G.; Acuna, A. U., *Biophys. J.* **2001,** *80*, 2422-2430.

72 Kruzel, M.; Morawiecka, B., *Acta Biochim. Pol.* **1982,** *29*, 321-330.

73 De, M.; Rana, S.; Rotello, V. M., *Macromol. Biosci.* **2009,** *9*, DOI: 10.1002/mabi.200800289.

CHAPTER 4

SYNTHETIC "CHAPERONES": NANOPARTICLE-MEDIATED REFOLDING OF THERMALLY DENATURED PROTEINS

4.1 Introduction

4.1.1 Molecular Chaperones in Protein Refolding

One of the key hurdles in biotechnology is the rescue of misfolded proteins obtained by *in vitro* or bacterial expression.[1, 2] The molecular chaperones play the role at this part by recognizing and selectively binding nonnative proteins to form relatively stable complexes.[3] This complex help to refold the protein to its original active form then the complexes are dissociated by the binding and hydrolysis of ATP. In this context, chaperons are not only prevent irreversible aggregation of nonnative conformations and keep proteins on the productive folding pathway, but also maintain newly synthesized proteins in an unfolded conformation suitable for translocation across membranes and bind to nonnative proteins during cellular stress and other functions.[4] Now why chaperons are so important at cellular environment? It is well known that depending on amino acid sequence the unfolded or expressed proteins are folded to the native protein by a spontaneous process determine by the global free energy minimum. But for this process the key factors are time, concentrations and temperature which are unusual at physiological condition. In cellular environment the temperature is ambient (~37 °C), where the hydrophobic effect will be stronger and thus protein denaturation and aggregation will be bigger problem and the concentration with other proteins and metabolites is very high.[5] Thus there is the need for additional factors for the successful

folding of many proteins in *vivo* with the following prerequisite: i) to prevent aggregation and misfolding during the folding of newly expressed proteins, ii) to prevent nonproductive interactions with other cell components, iii) to direct the assembly of larger proteins and multiprotein complexes and iv) after the proper folding the folded protein will be released without any surplus effects.

Cells have solved the problem of misfolding and aggregation, to a considerable extent at least, through the participation of molecular chaperones in the *in vivo* folding process.[6] Many investigations in the past few years have established the decisive role of molecular chaperones in protein folding, which predominantly involved the recognition of hydrophobic residues of newly expressed proteins.[7, 8] This noncovalent interaction needs a large surface compare to the target protein. Hence based on the size the chaperones are classified as follows, 40-kDa heat shock protein (HSP40; the DnaJ family), 60-kDa heat shock protein [HSP60; including GroEL and the T-complex polypeptide 1 (TCP-1) ring complexes], 70-kDa heat shock protein (HSP70), and 90-kDa heat shock protein (HSP90).[9, 10] Although the fundamental mechanism is similar for all chaperones, but their activity is varied from each other. As example, the HSP70 (DnaK in *Escherichia coli*) bind to nascent polypeptide chains on ribosomes, preventing their premature folding, misfolding, or aggregation, as well as to newly synthesized proteins in the process of translocation from the cytosol into the mitochondria and the endoplasmic reticulum (ER).[11] The GroEL family of chaperones has been intensively studied, especially in the context of in vitro protein folding, yet it is not clear just how important a role this family play in the folding of most proteins in the cell.

Although the folding at cellular environment is not exactly similar to *in vitro* folding, but both *in vivo* and *in vitro*, proteins fold remarkably rapidly, indicating that the folding pathway is directed in some way. Many studies have revealed intermediates during in vitro protein folding experiments; it is not clear, and is very difficult to establish experimentally, whether these are on- or off-pathway species.[12] Although it is becoming apparent that in some cases these may be off-pathway species,[13] some appear to be true intermediates on the productive folding pathway.[14] It was also evident that small proteins under appropriate conditions, fold to the native state within a few tens of milliseconds with no detectable intermediates.[15] On the other hand, the presence of partially folded intermediates during folding was detected for larger proteins which take longer to achieve the native state (seconds or longer).[16]

In general the protein folding processes can be summarized as described in Figure 4.1. According to that the earliest stages of folding involve hydrophobic collapse to a relatively compact state and formation of metastable secondary structure. It is not clear if collapse or secondary structure occur simultaneously or if one precedes the other. It is most likely that both proceed concurrently. Following the metastable state, condensation will lead to one or more particularly stable intermediates; which consist of a core of nativelike structure with the remainder of the protein in varying degrees of disorder.[17] Depending on the particular protein, the intermediate(s) will have regions of unique structure, especially in terms of the compactness, amount of secondary structure, and topology. It was also observed that the metastable and the equilibrium intermediates have high tendency to aggregate, particularly at high cellular concentration.[18] It is likely that a significant factor in the formation of in vivo

aggregates, such as inclusion bodies, is a lack of available molecular chaperones, usually due to the rapid rate of protein synthesis, the formation of long-lived folding intermediates, or a combination of both. Either situation could lead to saturation of the available chaperones which inhibit the protein aggregation and allow proper folding. These folded proteins then release, which is mediated by a conformational change in the chaperone driven by ATP hydrolysis.

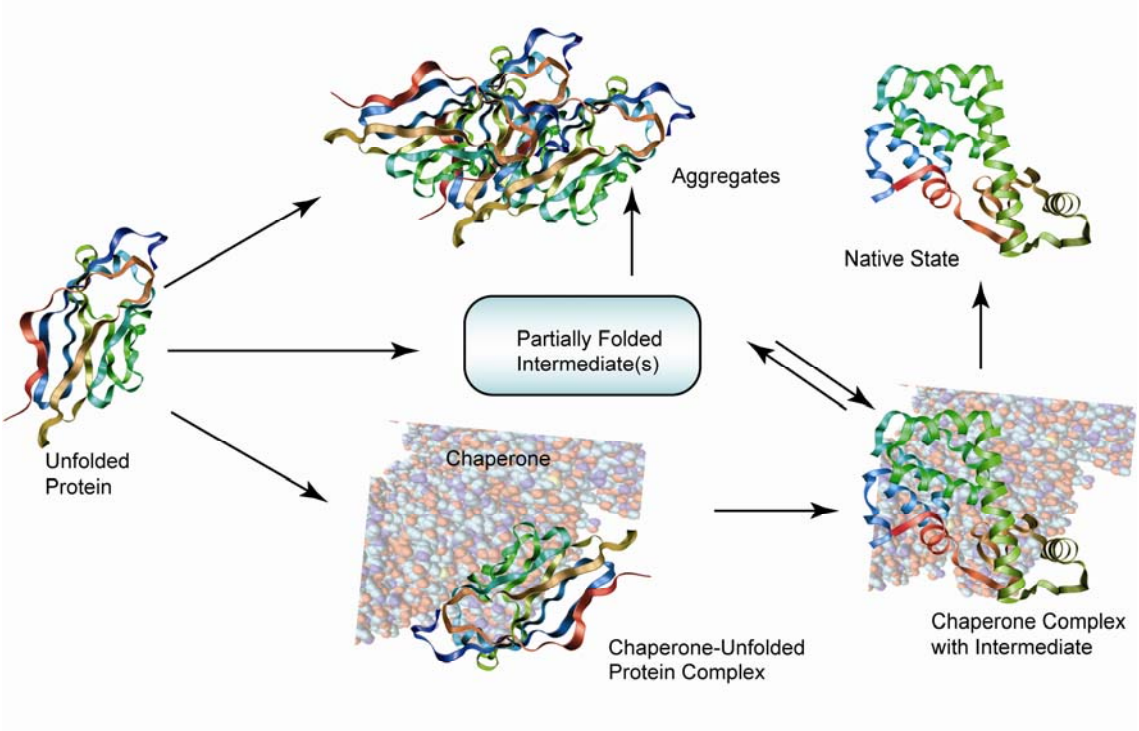

Figure. 4.1. General outline of chaperone-mediated protein folding.

4.1.2 Rescue of Misfolded Proteins Using Artificial 'Chaperones'

Proper rescue of the misfolded protein can greatly widen the range of proteins available for medical and biotechnological applications. Of the issues associated with protein expression, aggregation is the main obstacle hindering proper folding of denatured proteins; self-association is often favorable relative to proper folding, resulting in significant losses in active protein yield. The importance of proper protein

folding has spurred research in developing artificial chaperones and other in vitro folding aids. The majority of these approaches proceed in a two-step manner: prevention of aggregation followed by proper folding. The most conventional methods include solubilization with either urea or guanidine HCl, relying on methods such as additives, pH and redox buffers to effect folding.[19] Other simplified approaches include the addition of polyamines,[20] amino acids,[21] and polyetheylene glycol.[22]

In the cellular environment, machinery in the form of molecular chaperones, such as the bacterial GroEL, are used to sequester unfolded proteins to hinder aggregation, allowing subsequent folding in a controlled manner.[23] Grossly oversimplifying their mechanism of action, chaperonins such as GroEL use large hydrophobic patches in their interior to bind and unfold misfolded proteins. These proteins then refold upon release, which is mediated by a conformational change in the chaperone driven by ATP hydrolysis.[24] The mechanism of action of molecular chaperones has spurred the design and implementation of a variety of biomimetic refolding strategies. Rozema and Gellman presented a two-step method using surfactants to prevent aggregation, followed by the addition of β-cyclodextrin to strip the surfactant and facilitate folding.[25, 26] This approach can lead to successful protein refolding at concentrations below 1mg/mL, although this value was heavily dependent on the model protein used in the studies. Based on these initial reports, many groups have tested numerous surfactant and β-cyclodextrin combinations. For example, as reported by Cavalieri et. al., the hydrophobized nanoparticles assist carbonic anhydrase B (CAB) refolding in a manner similar to the mechanism of molecular chaperones. Irreversible CAB thermal denaturation is prevented by nanoparticle complexation and

recovery of almost 100% of enzymatic activity is triggered by the ability of β-cyclodextrin to interact with the hydrophobic moieties (Figure 4.2).[27] Other interesting modifications of this approach include using linear dextrins,[28] hydrophobized carbohydrate nanogels,[29] stimuli-responsive polymers,[30] and liposomes.[31]

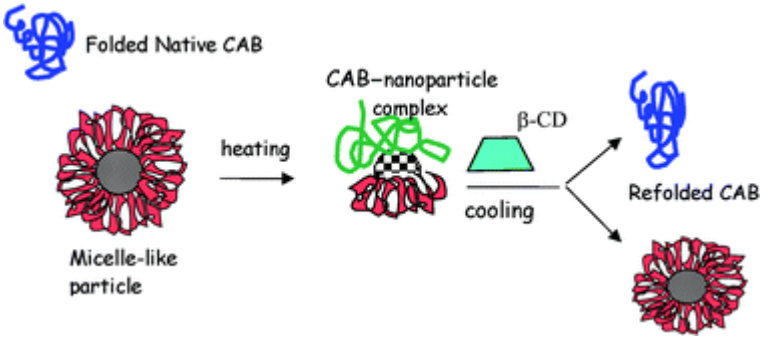

Figure 4.2. Schematic illustration of hypothetical mechanism of nanoparticle induced refolding of CAB protein. The figure is adapted from reference no. 27.

4.1.3 Reversible Binding and Folding of Protein Using Nanoparticles

External control of the scaffold-protein interaction to either initiate or disrupt the binding event is a useful tool for both fundamental and applied biomedical investigations.[32] Extension of this strategy to surface recognition extends the applicability of this methodology to a wide array of cellular processes. Previously, we demonstrated that noncovalent inhibition of chymotrypsin by nanoparticles is initially mediated by electrostatic complementarity between the cationic residues on ChT and the anionic surface of the carboxylate-functionalized nanoparticles. Given the unique characteristics of the nanoparticle monolayer we anticipated that the "irreversible" inhibition could be reversed through surface modification of the nanoparticle after enzyme inhibition has been accomplished. Cationic surfactant derivatives (Figure 4.3a) would be expected to bury their hydrophobic segments into the monolayer, exposing the

cationic head groups. As a result, the anionic surface charge of the monolayer would be attenuated, disrupting the electrostatic interaction between the nanoparticle and ChT and releasing the protein.

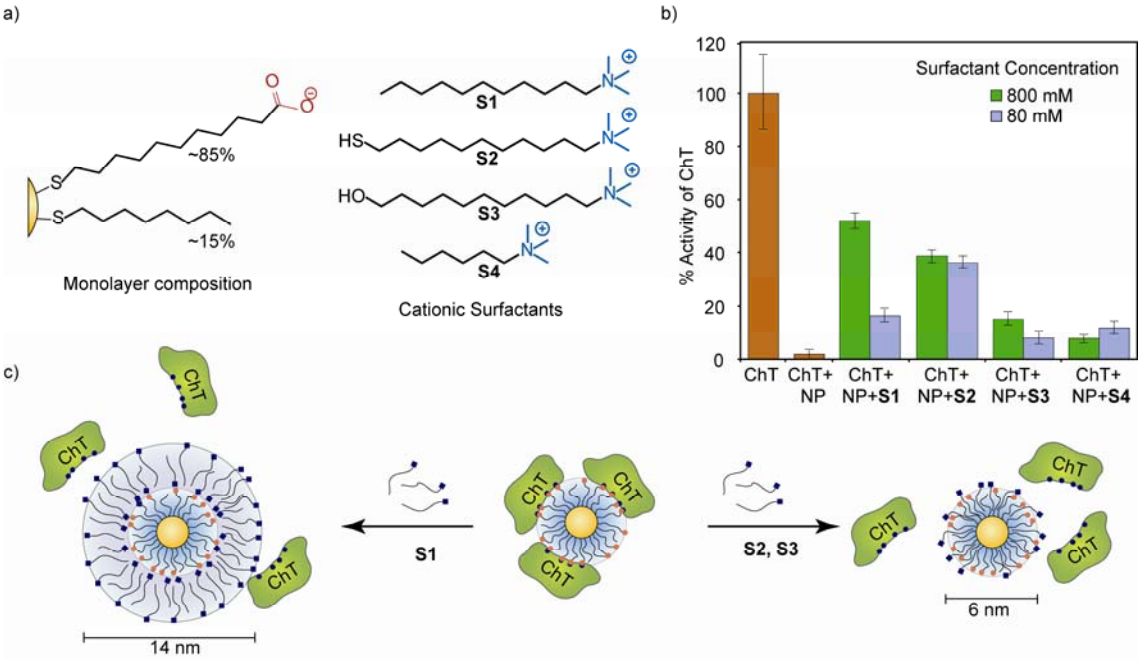

Figure 4.3. a) Chemical structure of anionic nanoparticle and four cationic surfactants used for monolayer modification. b) Reactivation of ChT (3.2 μM) and MMPC (0.8 μM) after preincubation for 16 hours at room temperature followed by surfactant. c) Proposed mechanism of ChT rescue by various surfactants as evident from hydrodynamic radius.

For the inhibition of chymotrypsin on the nanoparticle surface, a buffered solution of ChT and anionic nanoparticle was incubated at room temperature for 16 hours, at which time essentially complete inhibition was observed (Figure 4.3b).[33] Four cationic surfactants were then added: C11 alkane **S1**, thiol **S2**, alcohol **S3**, and C6 alkane **S4** (Figure 4.3a). Addition of surfactants resulted in almost immediate restoration of enzyme activity. Long chain derivatives, however, were required for any substantial reactivation, with the shorter C6 alkane showing only marginal reactivation (Figure 4.3b). The strongest reactivation observed upon addition of the C11 alkane **S1**

was attributed to the formation of bilayer-type structures.[34] Interestingly, the thiol chains show substantial reactivation at the lower concentration, suggesting that the favorable thiol-gold interaction augment the modification process. The formation of either bilayer or mixed monolayer was attributed from dynamic light scattering (DLS) study.

We have also described previously that anionic nanoparticles without ethylene glycol spacer eventually denature the protein structure. The rescue of ChT activity by the addition of surfactants **S1**-**S3**, suggest that ChT is partially refold to regain the enzymatic activity. Further structural investigation by fluorescence analysis suggests that the released ChT from nanoparticle surface are partially refolded towards its native structure.

4.2 Refolding of the Thermally Denatured Protein

Most of the native proteins have a hydrophobic core and charged or polar group on the surface. The hydrophobic core helps to stabilize the tertiary structure of protein where the outer polar surfaces interact with the environment for the biological activity. Denatured proteins are responsible for numerous diseases such as Creutzfeldt-Jakob disease, Bovine spongiform encephalopathy (mad cow disease), and amyloid-related illnesses such as Alzheimer's diseases.[35,36] Also various medical and biotechnological applications require the rescue of misfolded proteins produced by *in vitro* or *in vivo* genetic expression.[37] Therefore, the requirements of proper protein folding have prompted research in developing artificial chaperones and other *in vitro* folding aids.

In the cellular environment, chaperone machinery, such as the bacterial GroEL and GroES, are used to stabilize unfolded proteins to hinder aggregation, allowing subsequent folding in a controlled manner. From the established mechanism of the molecular chaperone machinery, a variety of biomimetic refolding strategies are introduced. Rozema and Gellman presented a most popular method in protein refolding process in a two-step manner: (i) the capture step, in which denatured protein bind with ionic detergent to prevent aggregation and (ii) the releasing step, where detergents are removed from refolded proteins by some additives.[26] The most conventional methods consider either urea or guanidine-HCl as an ionic detergent and relying on various additives, pH and redox buffers to effect folding. Additional interesting modifications of this approach include using linear dextrins, hydrophobized carbohydrate nanogels, stimuli-responsive polymers, and liposomes.[28, 29] Alternative reported methods include the addition of polyamines, amino acids, and polyethylene glycol.[20,38]

Recent advance in nanoparticle applications encouraged us to exploit these materials in protein refolding. In our previous studies we were able to denature α-chymotrypsin (ChT) using anionic gold nanoparticles and then sequentially refolded and restored ChT activity by the addition of cationic surfactants as a releasing agent.[33] We have shown that 2-(10-mercapto-decyl)-malonic acid functionalized nanoparticle (**NP_MA**) (Figure 4.4a) can form strong complex with ChT and denature the protein and upon addition of NaCl it releases the protein with almost complete restoration of activity.[39] Considering this effect, **NP_MA** can be used as a refolding agent by interacting with denatured cationic proteins, allowing to partial refolding and preventing the possible aggregation. After the partial refolding of the proteins, it will be released

from **NP_MA** by the increase of ionic strength of the solution by increasing the NaCl concentration since the electrostatic forces should be attenuated by the presence of competitive ions (Figure 4.4b).[40] The partially refolded proteins will then be renatured to its native structure. To establish this idea we consider three cationic proteins, ChT, Lysozyme and Papain as model proteins (Figure 4.4c).

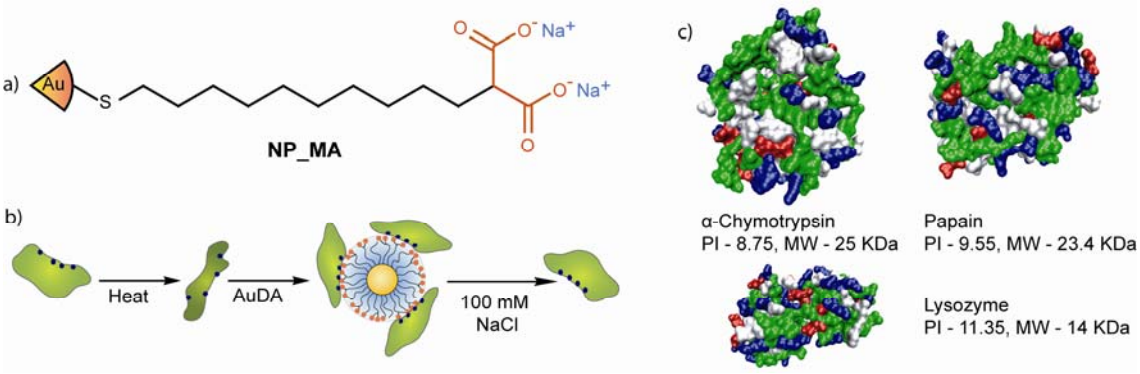

Figure 4.4. a) Schematic representation of the structure of AuDA and b) thermal denaturation followed by NP mediated refolding of proteins. c) Surface structural features of three positively charged proteins used in the refolding study. Color scheme for the proteins: basic residues (blue), acidic residues (red) polar residues (green) and nonpolar residues (grey).

4.2.1 Result and Discussion

4.2.1.1 Rescue of Enzymatic Activity

Protein can be denatured chemically in the presence of denaturing agents or thermally by heating or cooling. Here we denatured the protein solution in 5 mM sodium phosphate buffer (pH 7.4) by heating at suitable temperature. The NP_MA was prepared by Murray's place exchange reaction. The detail procedure is described in experimental section.

The enzymetic activity of the proteins are changed or diminished with the alteration of secondary structure of protein. As the ChT and papain are serine and

cysteine protease respectively, the enzymatic activity of denatured and refolded ChT and papain was studied to determine the extent of refolding. ChT and papain denatured by heating at 80°C for 30 min in 5mM sodium phosphate buffer at pH 7.4 while the lysozyme heated at 60°C for 30 min. For refolding the protein the **NP_MA** was added and the mixture was allowed to stand for one hour. 100 mM NaCl was then added to release the refolded protein by disrupting the electrostatic interaction. With this resultant solution the activity of ChT and papain was measured. The activity of ChT was monitored using *N*-succinyl-l-phenylalanine *p*-nitroanilide (SPNA) as a substrate in compare with native ChT in 5mM sodium phosphate buffer at 7.4 pH. The enzymatic activity of thermally denatured ChT and in the presence of **NP_MA** is also measured. The concentration of protein and nanoparticles ware fixed at 3.2μM and 0.8 μM respectively. As expected **NP_MA** exhibits inhibition on residual activity of denatured protein but upon release by 100mM NaCl solution highly efficient (~93%) restoration of activity was observed with **NP_MA**, while little activity restoration was observed in the absence of nanoparticle (Figure 4.5). The restoration of activity suggests that in presence of the nanoparticle, the thermally denatured ChT refolds. This refolding take place *via* binding with the nanoparticles with positively charged residues on the surface of the ChT and subsequent release by 100 mM NaCl which exposes its active site to the substrate. The similar enzymatic study was done with papin using Nα-benzoyl-L-arginine *p*-nitroanilide (BAPNA) as a substrate in presence of β-mercaptoethanol as an activator. The concentration of nanoparticle and protein are same as the earlier at same buffer. Similar to ChT, the enzymatic activity of thermally denatured protein increases to ~97% in presence of **NP_MA** compared to the native protein.

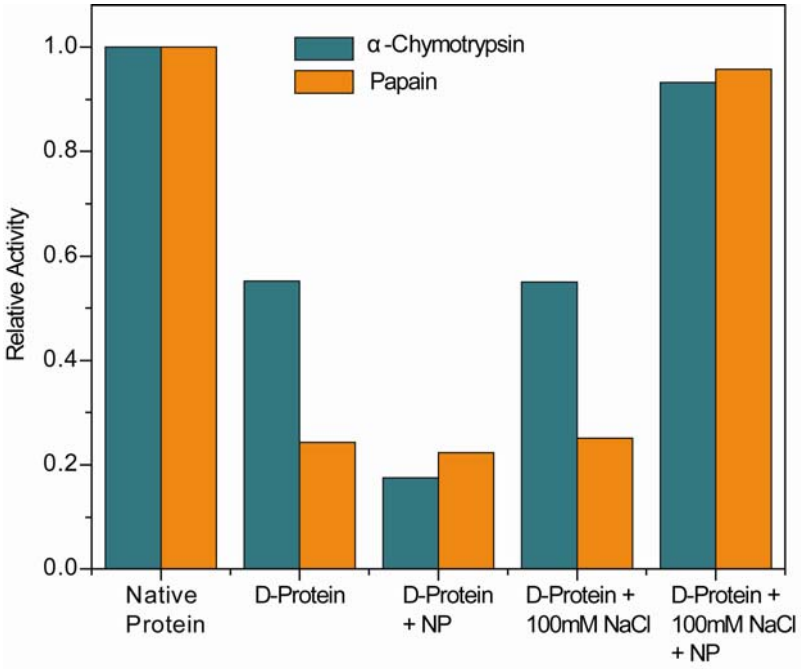

Figure 4.5. Enzymatic activity of thermally denatured ChT and papain (3.2μM) in the presence of NP_MA (0.8 μM) and 100 mM NaCl solution in 5 mM sodium phosphate buffer (pH = 7.4).

4.2.1.2 Restoration of Secondary Structure

The circular dichroism (CD) spectrum of a protein is particularly more potential for the characterization of secondary structure of a protein.[41, 42] Hence to determine the degree of protein refolding we measure and compare the CD spectra of native, denatured and refolded proteins. CD spectra of protein with 100 mM NaCl could not be monitored at wavelengths shorter than 200 nm due to its high absorbance from the increased salt concentration.

The CD spectrum of native ChT has two characteristic minimum at 202 nm and 230 nm.[43] This two minimum are lost or changed when ChT loses its native structure and hence the enzymatic activity.[44] As expected, during the thermal denaturation the minimum at 230 nm completely disappears and the minimum at 202 nm enlarged and

shifted to 199 nm (Figure 4.6a). The addition of 100 mM NaCl does not show any spectral change but after the incubation with AuDA the minimum at 202 nm was regenerated. Although we didn't see any minimum at 230 nm, but the spectra has high similarity with native one compared to thermally denatured ChT, which is consistent with the increased activity observed in activity assays. Also the calculation of secondary structures (Helices, strand, turn and random coil) using DICHROWEB suggests significant refolding of protein structure. According to the calculation, although the α-helices are not entirely recovered, β-strand and turns increase with decrease of random coil compared to the native ChT which implies the extensive refolding of thermally denatured protein (Figure 4.6d). Similar experiment also performed with the other two cationic proteins, lysozyme and papain with consistent result. In case of lysozyme, the native protein has one minimum at 208 nm and one maximum at 192 nm primarily due to its high α-helix content.[45] When lysozyme was thermally denatured the content of α-helix decreases to ~6% from ~37% and the random coil increases accordingly. But in the presence of **NP_MA** the α-helicity increases and random coil decreases significantly which is similar to the native structure (Figure 4.6e). The removal of **NP_MA** by increasing ionic strength further improves the protein structure as we can see from figure 3b. In the similar way thermally denatured papain refolded to regenerate the two minimum at 208 nm and 222 nm, which is observed in native protein.[46] The secondary structure analysis also suggests considerable refolding of denatured protein in the presence of **NP_MA** consistent with the enzymatic activity recovery (Figure 4.6c and f).

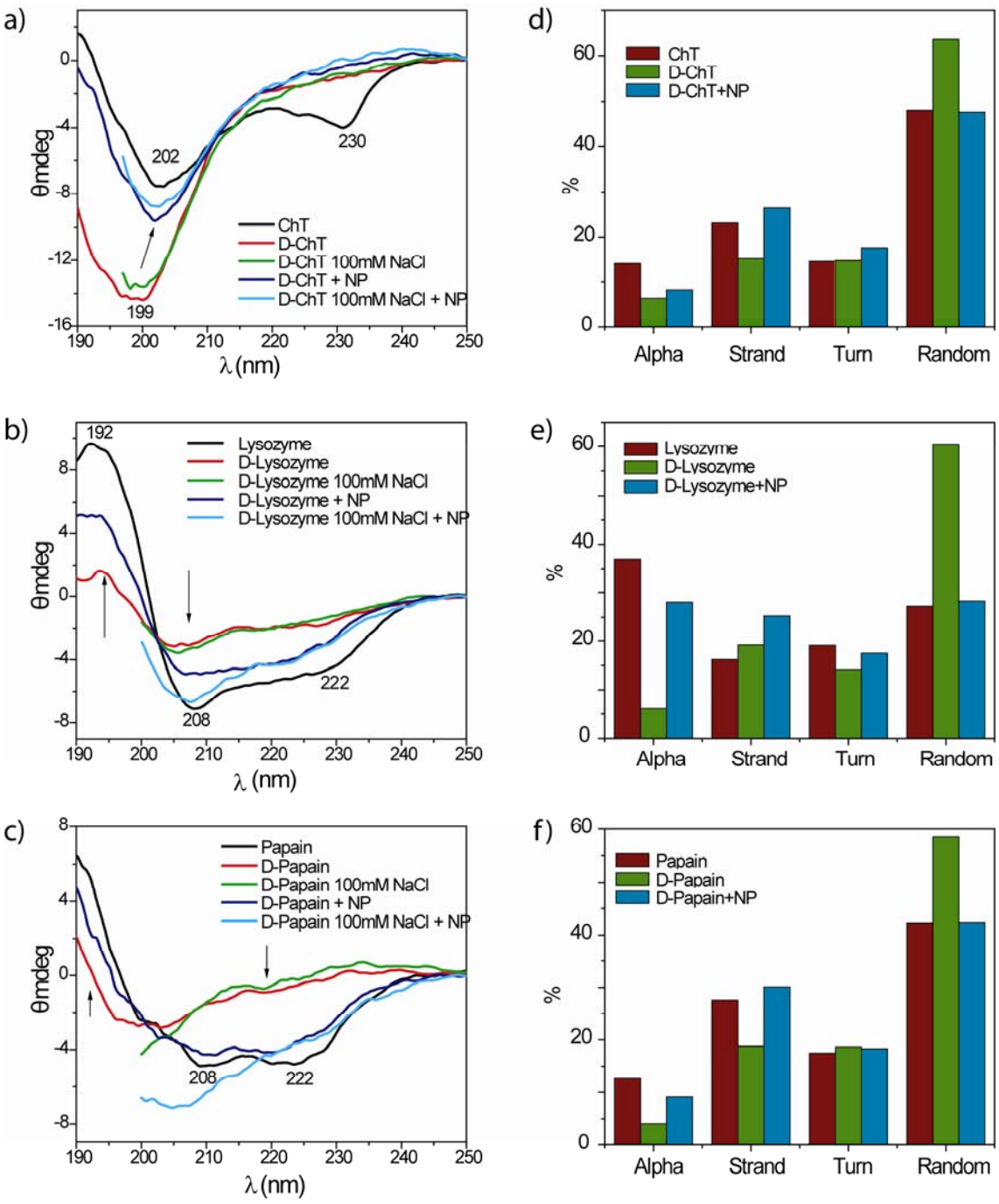

Figure 4.6. CD spectra of native, thermally denatured (5 μM) and denatured proteins with nanoparticles (NP) (1.25 μM) and in presence of 100 mM NaCl after 4h incubation. (a), (b) and (c) are CD spectra for α-chymotrypsin, lysozyme and papain respectively. (d-e) The percentage of secondary structure elements of native, thermally denatured and refolded proteins as estimated from far-UV CD spectra using CDSSTR method.

It was well known that the native structure has the hydrophilic residues present at the surface of the protein to prevent aggregation as it is hydrated. In our study the cationic proteins have positive residues (i.e. arginin and lysin) on the surface which prevent the protein aggregation by hydration and electrostatic repulsion. But during the thermal denaturation the hydrophobic inner core gets well exposed and causes the possible aggregation by intermolecular association of the hydrophobic core.[47,48] But employment of negatively charged nanoparticles (**NP_MA**) prevents the aggregation by binding with unfolded proteins through the electrostatic interaction with positive residues and promotes correct refolding. The overall high negative charge of these complexes, as evident from the Zeta potential measurement (Table 4.2 in experimental section), prevents the aggregation, thereby promoting correct refolding (Figure 4.7). Thereby the nanoparticles preventing aggregation and misfolding act as an artificial chaperon.

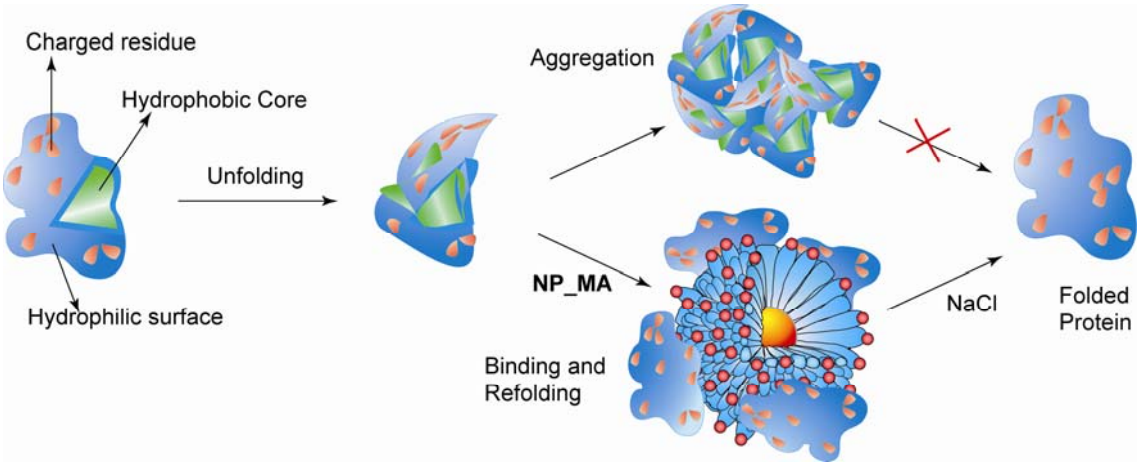

Figure 4.7. Illustration of the thermally induced protein unfolding process and the exposure of hydrophobic core followed by either aggregation in absence of nanoparticle or binding and refolding in presence of nanoparticle.

In presence of nanoparticle the charged residues are reorganized on the surface and hydrophobic part regenerate the inner core with probable secondary structure. Upon removal of negatively charged nanoparticle by increasing salt concentration the released partially refolded proteins are not further aggregated due to its hydrophilic surface becoming similar to native protein. After the rescue from nanoparticle surface the protein is refolded towards its native structure to minimize the potential energy. During this self refolding towards the native structure the protein passes through several intermediate structures which are already established by several studies such as NMR analysis,[49] which is consistent with our experimental results. It was also reported that for some proteins one intermediate structure is present at equilibrium with other structures. In case of lysozyme an isosbestic point at 202 nm observed in CD study suggests clearly the equilibrium between the intermediate states. Although for the other two proteins this point is not prominent as lysozyme (212 nm and 201 nm for ChT and papain respectively).

4.2.2 Conclusion

In conclusion here we demonstrate the application of nanoparticles in protein refolding. In the present study we used highly charged negative particles, **NP_MA** for extensive refolding of thermally denatured cationic proteins. In this report we achieved considerable refolding of thermally denatured cationic proteins in presence of anionic nanoparticles. Also this perception opens the possibility of refolding the anionic proteins by using positively charged nanoparticles. This fundamental study offer promising opportunities in developing protein stabilization and refolding system for further application.

4.3 Experimental

4.3.1 Materials

All the reagents, α-Chymotrypsin (Type II from bovine pancreas, ChT), Lysozyme (from chicken egg white), Papain (from *Carica papaya*), *N*-succinyl-L-phenylalanine *p*-nitroanilide (SPNA) and Nα-benzoyl-L-arginine *p*-nitroanilide (BAPNA) was purchased from Sigma and used as received.

4.3.2 Synthesis of Ligand and Nanoparticle

Synthesis of 2-(10-mercaptodecyl)-malonic acid (**1**) ligand and fabrication of 2 nm gold particle was done according to the following procedure. In brief, 1,10-dibromodecane was added to the solution of malonic diethyl ester and sodium ethoxide solution in ethanol. After the completion of the reaction, ethanol was evaporated and residues are redissolved in water-dichloromethane mixture. After the separation the crude product was purified using silica gel column chromatography to obtain 2-(10-bromodecyl)-malonic acid diethyl ester (**2**). The compound **2** was refluxed with sodium thioacetate in ethanol for overnight for the thioacetate substitution followed by aqueous NaOH hydrolysis to produce the 2-(10-mercaptodecyl)- malonic acid (**1**) which was purified using silica gel column chromatography.

Pentanethiol coated gold nanoparticles (d = 2 nm) were prepared according to the previously reported protocol.[50] Place-exchange reactions[51] were carried out to replace the 1-pentanethiol ligand on the nanoparticle surface with malonic acid functionalized ligand **1** to obtain the **NP_MA** nanoparticle.

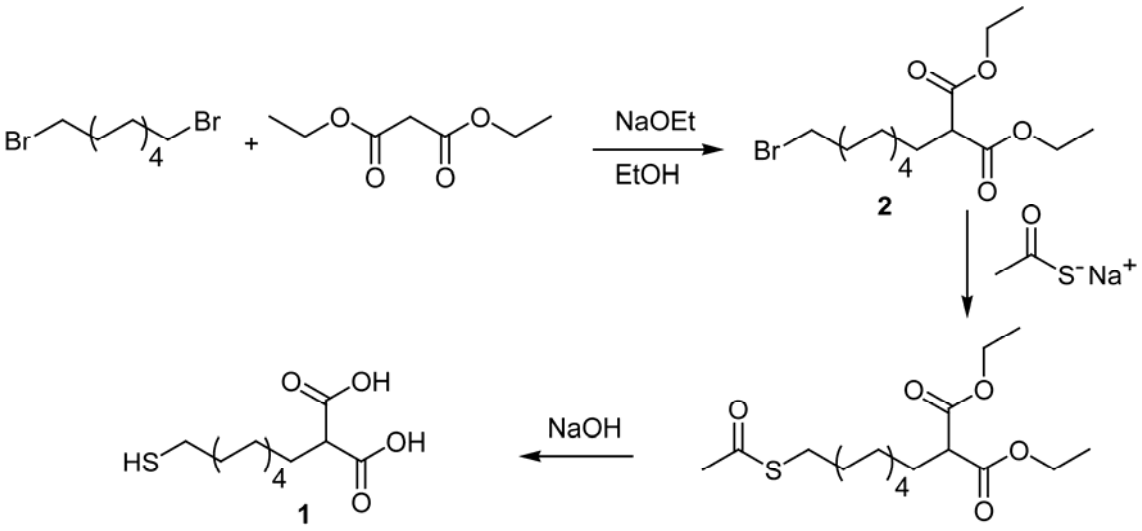

Scheme 4.1. Synthesis of malonic acid derivative for NP_MA nanoparticle.

4.3.3 Thermal Denaturation of Proteins

Proteins were dissolved in aqueous 5 mM sodium phosphate buffer solution (Na_2HPO_4 / NaH_2PO_4), pH 7.4 to make a concentration of 10 μM. The protein solutions were thermally denatured by incubating at 60°C (for lysozyme) to 80°C (for α-chymotrypsin and papain) for 30 min in airtight micro-centrifuge tubes. Following incubation, the proteins were transferred to an icewater bath to quench the denaturation process and the protein solution was used for activity assay and Circular dichroism study.

4.3.4 Activity assay

Activity assay of α-Chymotrypsin. Thermally denatured α-Chymotrypsin (3.48 μM) was incubated with AuDA (0.87 μM) in 5 mM sodium phosphate buffer (pH 7.4) for 4h, then at 100 mM NaCl concentrations for 1h. Thereafter, 184 μL of the each solution were taken in a 96-well flat bottom microplate along with native and denatured

α-Chymotrypsin followed by the addition of 16 μL of 25.9 mM SPNA dissolved in ethanol, resulting in final concentrations of 3.2 μM for ChT, 0.8 μM for NPs and 2.0 mM for SPNA. Activity was followed by monitoring the absorption changes at 405 nm with an Ultra Microplate Reader (EL808 Bio-Tek Instruments, Inc.). The obtained activity was normalized to that of ChT without NPs. Each sample was measured in triplicate and the average was reported.

Activity assay of Papain. Papain enzyme activity was also assayed with the chromogenic reagent BAPNA. The enzyme was activated by incubating in 2-mercaptoethanol at concentration of 142 mM. In this experiment thermally denatured papain was incubated with AuDA for 4h and then 1h with 100 mM NaCl at same concentration of ChT activity assay. Similarly 182 μL of each solution with 16 μL BAPNA and 2 μL mercaptoethanol was taken in a 96-well flat bottom microplate. The activity of papain on BAPNA was followed spectrophotometrically at 405 nm using same microplate reader. The obtained activity was normalized to that of native papain. Each sample was measured in triplicate and the average was reported.

4.3.5 Circular Dichroism

Far-UV circular dichroism (CD) spectra of ChT (3.2 μM) were measured on a JASCO J-720 spectropolarimeter with quartz cuvettes of 1 mm path length at 25 °C. The spectra were recorded from 190 to 250 nm as an average of 3 scans at a rate of 20 nm/min. The concentration of proteins is fixed at 5 μM and 0.8 μM for AuDA. The final spectra were obtained by subtracting the blank to eliminate background effects. The resultant CD spectra was fitted into secondary structure algorithm CDSSTR

(protein ref. set 7 comprising of 49 proteins) using DICHROWEB to determine the change in secondary structures (Table 4.1).

Table 4.1. The percentage of secondary structure elements of native proteins and thermally denatured proteins in the absence and presence of gold nanoparticles as estimated from far-UV CD spectra using CDSSTR method.[52]

Sample	α–Helix	β–Sheets	β–Turn	Random coil
ChT	14.1	23.1	14.6	48.1
DChT	6.5	15.2	14.7	63.7
DChT-AuDA	8.3	26.4	17.6	47.7
Lys	37.0	16.2	19.1	27.3
DLys	6.1	19.2	14.2	60.5
DLys-AuDA	28.0	25.3	17.5	28.2
Pap	12.6	27.6	17.5	42.3
DPap	4.1	18.8	18.6	58.5
DPap-AuDA	9.1	30.1	18.3	42.4

4.3.6 Zeta Potential

AuDA gold nanoparticles were dissolved in 5 mM sodium phosphate buffer, pH 7.4 to make a 1 μM solution and their zeta potentials were measured on a MALVERN Zetasizer Nano ZS instrument. The similar experiment was repeated with three denatured proteins at 4 μM concentration. Three rounds of assays of each solution have been performed and the average values were reported.

Table 4.2. Zeta-potentials for AuDA nanoparticle and in presence of three denatured proteins in 5 mM sodium phosphate buffer, pH 7.4 at 25.0 °C

Sample	**zeta-potential / mV**
AuDA	–44.7±1.5
AuDA + α-Chymotrypsin	–42.8±1.4
AuDA + Papain	–30.6±2.5
AuDA + Lysozyme	–22.1±1.5

4.4 References

1 Platis, D.; Foster, G. R., *Protein Expression Purif.* **2003,** *31*, 222-230.

2 Clark, E. D., *Curr. Opin. Biotechnol.* **2001,** *12*, 202-207.

3 Saibil, H. R., *Curr. Opin. Struct. Biol.* **2008,** *18*, 35-42.

4 Caplan, A. J.; Mandal, A. K.; Theodoraki, M. A., *Trends in Cell Biology* **2007,** *17*, 87-92.

5 Boylan, J. F.; Gudas, L. J., *J. Biol. Chem.* **1992,** *267*, 21486-21491.

6 Thomas, J. G.; Ayling, A.; Baneyx, F., *Applied Biochemistry and Biotechnology* **1997,** *66*, 197-238.

7 Fink, A. L., *Physiological Reviews* **1999,** *79*, 425-449.

8 Hartl, F. U., *Nature* **1996,** *381*, 571-580.

9 Glover, J. R.; Lindquist, S., *Cell* **1998,** *94*, 73-82.

10 Lin, Z.; Madan, D.; Rye, H. S., *Nat. Struct. Mol. Biol.* **2008,** *15*, 303-311.

11 Langer, T.; Lu, C.; Echols, H.; Flanagan, J.; Hayer, M. K.; Hartl, F. U., *Nature* **1992,** *356*, 683-689.

12 Fawzi, N. L.; Chubukov, V.; Clark, L. A.; Brown, S.; Head-Gordon, T., *Protein Sci.* **2005,** *14*, 993-1003.

13 Silow, M.; Oliveberg, M., *Biochemistry* **1997,** *36*, 7633-7637.

14 Wang, J.; Onuchic, J.; Wolynes, P., *Phys. Rev. Lett.* **1996,** *76*, 4861-4864.

15 Mittal, J.; Best, R. B., *Proc. Natl. Acad. Sci. U. S. A.* **2008,** *105*, 20233-20238.

16 Lei, H. X.; Wu, C.; Liu, H. G.; Duan, Y., *Proc. Natl. Acad. Sci. U. S. A.* **2007,** *104*, 4925-4930.

17 Fink, A. L.; Oberg, K. A.; Seshadri, S., *Folding & Design* **1998,** *3*, 19-25.

18 Lindner, A. B.; Madden, R.; Dernarez, A.; Stewart, E. J.; Taddei, F., *Proc. Natl. Acad. Sci. U. S. A.* **2008,** *105*, 3076-3081.

19 Armstrong, N.; De Lencastre, A.; Gouaux, E., *Protein Sci.* **1999,** *8*, 1475-1483.

20 Kudou, M.; Shiraki, K.; Fujiwara, S.; Imanaka, T.; Takagi, M., *Eur. J. Biochem.* **2003,** *270*, 4547-4554.

21 Ito, L.; Kobayashi, T.; Shiraki, K.; Yamaguchi, H., *Journal of Synchrotron Radiation* **2008,** *15*, 316-318.

22 Cleland, J. L.; Hedgepeth, C.; Wang, D. I. C., *J. Biol. Chem.* **1992,** *267*, 13327-13334.

23 Feltham, J. L.; Gierasch, L. M., *Cell* **2000,** *100*, 193-196.

24 Chapman, E.; Farr, G. W.; Fenton, W. A.; Johnson, S. M.; Horwich, A. L., *Proc. Natl. Acad. Sci. U. S. A.* **2008,** *105*, 19205-19210.

25 Rozema, D.; Gellman, S. H., *Biochemistry* **1996,** *35*, 15760-15771.

26 Rozema, D.; Gellman, S. H., *J. Biol. Chem.* **1996,** *271*, 3478-3487.

27 Cavalieri, F.; Chiessi, E.; Paradossi, G., *Soft Matter* **2007,** *3*, 718-724.

28 Sundari, C. S.; Raman, B.; Balasubramanian, D., *FEBS Lett.* **1999,** *443*, 215-219.

29 Nomura, Y.; Ikeda, M.; Yamaguchi, N.; Aoyama, Y.; Akiyoshi, K., *FEBS Lett.* **2003,** *553*, 271-276.

30 Yoshimoto, N.; Hashimoto, T.; Felix, M. M.; Umakoshi, H.; Kuboi, R., *Biomacromolecules* **2003,** *4*, 1530-1538.

31 Yoshimoto, M.; Shimanouchi, T.; Umakoshi, H.; Kuboi, R., *Journal of Chromatography B* **2000,** *743*, 93-99.

32 Furuta, T.; Wang, S. S. H.; Dantzker, J. L.; Dore, T. M.; Bybee, W. J.; Callaway, E. M.; Denk, W.; Tsien, R. Y., *Proc. Natl. Acad. Sci. U. S. A.* **1999,** *96*, 1193-1200.

33 Fischer, N. O.; Verma, A.; Goodman, C. M.; Simard, J. M.; Rotello, V. M., *J. Am. Chem. Soc.* **2003,** *125*, 13387-13391.

34 Goodman, C. A.; Frankamp, B. L.; Cooper, B. A.; Rotello, V. A., *Colloids and Surfaces B-Biointerfaces* **2004,** *39*, 119-123.

35 Chiti, F.; Dobson, C. M., *Annu. Rev. Biochem.* **2006,** *75*, 333-366.

36 Cobb, N. J.; Sonnichsen, F. D.; McHaourab, H.; Surewicz, W. K., *Proc. Natl. Acad. Sci. U. S. A.* **2007,** *104*, 18946-18951.

37 Dobson, C. M., *Nature* **2003,** *426*, 884-890.

38 Shiraki, K.; Kudou, M.; Fujiwara, S.; Imanaka, T.; Takagi, M., *Journal of Biochemistry* **2002,** *132*, 591-595.

39 Simard, J. M.; Szymanski, B.; Rotello, V. M., *Med. Chem.* **2005,** *1*, 153-158.

40 Verma, A.; Simard, J. M.; Rotello, V. M., *Langmuir* **2004,** *20*, 4178-4181.

41 Greenfield, N. J., *Anal. Biochem.* **1996,** *235*, 1-10.

42 Greenfield, N. J., *Nature Protocols* **2006,** *1*, 2876-2890.

43 Schechter, N. M.; Eng, G. Y.; Selwood, T.; McCaslin, D. R., *Biochemistry* **1995,** *34*, 10628-10638.

44 McConn, J.; Fasman, G. D.; Hess, G. P., *J. Mol. Biol.* **1969,** *39*, 551-562.

45 de Laureto, P. P.; Frare, E.; Gottardo, R.; van Dael, H.; Fontana, A., *Protein Sci.* **2002,** *11*, 2932-2946.

46 Naeem, A.; Fatima, S.; Khan, R. H., *Biopolymers* **2006,** *83*, 1-10.

47 Summers, C. A.; II, R. A. F., *Protein Sci.* **2000,** *9*, 2001-2008.

48 IbarraMolero, B.; SanchezRuiz, J. M., *Biochemistry* **1997,** *36*, 9616-9624.

49 Mok, K. H.; Kuhn, L. T.; Goez, M.; Day, I. J.; Lin, J. C.; Andersen, N. H.; Hore, P. J., *Nature* **2007,** *447*, 106-109.

50 Brust, M.; Walker, M.; Bethell, D.; Schiffrin, D. J.; Whyman, R., *J. Chem. Soc., Chem. Commun.* **1994**, 801-802.

51 Hostetler, M. J.; Templeton, A. C.; Murray, R. W., *Langmuir* **1999,** *15*, 3782-3789.

52 Sreerama, N.; Woody, R. W., *Anal. Biochem.* **2000,** *287*, 252-260.

CHAPTER 5

SENSING OF PROTEINS USING NANOPARTICLE-GREEN FLUORESCENCE PROTEIN CONJUGATES

5.1 Introduction

5.1.1 Protein Sensing

Protein sensors provide an important tool for the early diagnosis of diseases in biomedical research and practice,[1, 2] as the presence of biomarker proteins or irregular protein concentrations is a consequence of cancer and other disease states.[3, 4] Protein detection is however always a challenging target due to its structural and charge diversity and complexity, mainly to construct general sensor for multiple protein analyte.

Current protein sensors are highly engineered detection systems that rely on highly specific and selective interactions between receptors and proteins, such as enzyme-linked immunosorbent assay (ELISA),[5] artificial oligionucelotides (aptamers),[6] and protein chip technologies.[7] In these systems receptors are immobilized onto a device surface and binding of the target protein induces either an optical or electrochemical signal.[8, 9] As an example, So *et. al.* reported the real-time detection of protein using single-walled carbon nanotube field effect transistor (SWNT-FET) based biosensors consist of DNA aptamers as protein recognition elements (Figure 5.1).[10] Anti-thrombin aptamers that are highly specific to thrombin were immobilized on the sidewall of a SWNT-FET. The binding of thrombin aptamers to SWNT-FETs causes a rightward shift of the threshold gate voltages, whereas the addition of thrombin solution

causes an abrupt decrease in the conductance of the thrombin aptamer immobilized SWNT-FET. This change in voltage was used to detect the thrombin protein. The sensitivity of this system was saturated around protein concentrations of 300 nM. Although the lowest detection limit was around 10 nM.

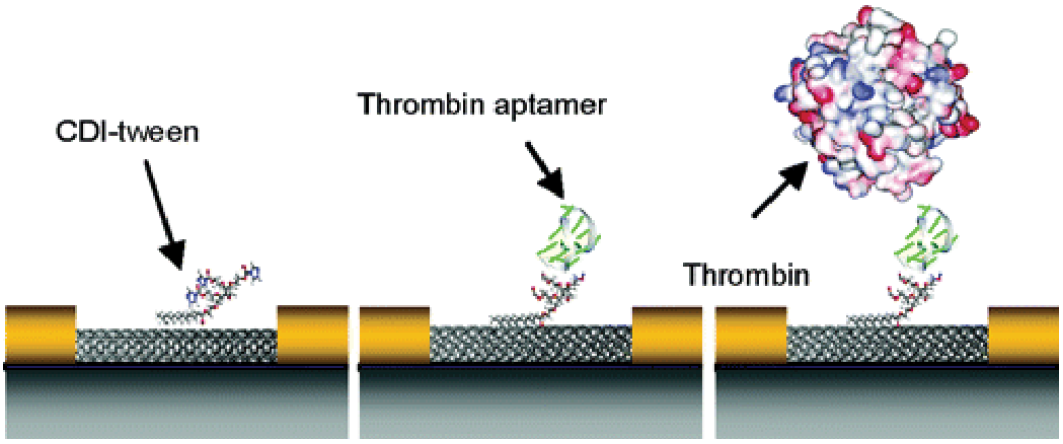

Figure 5.1. Binding and detection of thrombin on a SWNT-FET and aptamer based sensor. Carbodiimidazole-activated Tween 20 (CDI-Tween) was used to link the thrombin aptamer. Reprinted from reference no. 10.

The advantage of this specific "lock and key" mechanism is a highly sensitive detection system that can eliminate false positives. Affinity and catalytic-based protein sensors relying on antibodies as the recognition elements dominate commercial biosensor markets.[11] These protein detection systems are effective, however high production costs for antibodies, protein stability on surfaces, and extensive sample preparation has encouraged the demand for other multi-protein array detection system.

5.1.2 Chemical tongue/nose sensors

In biology most biomolecular interaction takes place by specific recognitions. Mimicking that interaction various sensor systems are reported, which are limited to specific analyte sensing. Other sensory processes such as taste and smell use

"differential" binding where the receptors bind to their analytes by different binding characteristics that are selective rather then specific.[12] These arrays, also known as "electronic tongues"[13] and "nose"[14] provide highly versatile sensors. For instance,

Greene and Shimizu reported a colorimetric sensor array composed of seven molecularly imprinted polymers to identify seven different aromatic amines (Figure 5.2).[15] Using the colorimetric response they systematically identified the amines using linear discriminant analysis with 94% classification accuracy.

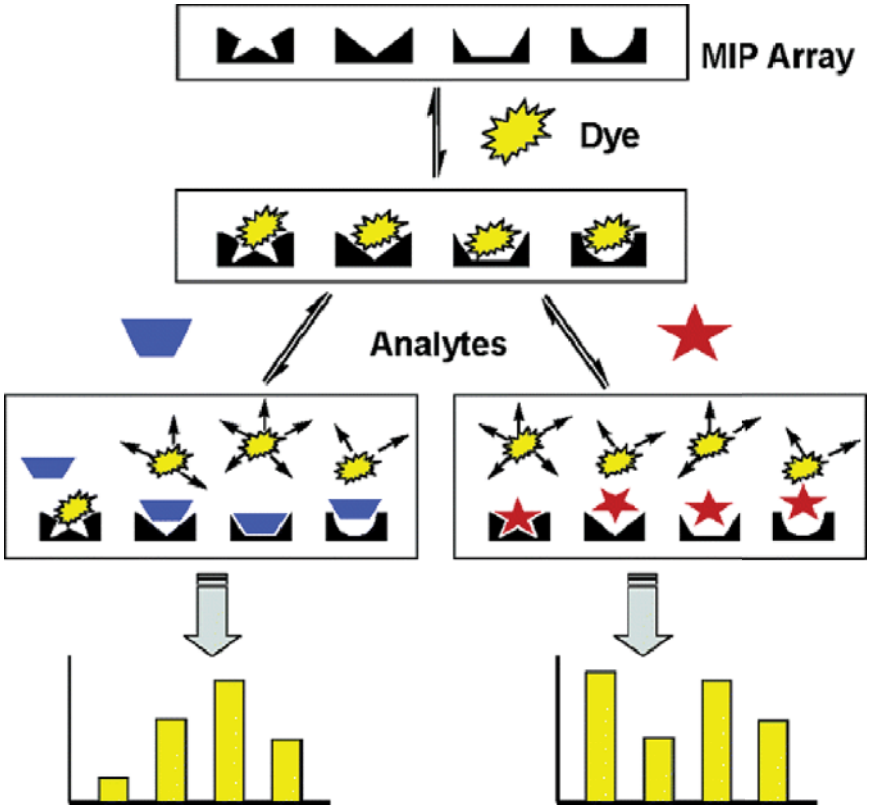

Figure 5.2. A Representative Scheme of an MIP Sensor Array that Uses a Dye-Displacement Strategy to Give an Easily Visualized and Unique Colorimetric Response Pattern for Each Analyte.

This method also has been used to sense calcium and metal ions, pH levels, sugars as well as cholesterol levels in blood, cocaine in urine, and toxins in water.[16, 17]

A variety of other analytes such as including metal ions,[18] volatile agents,[19] aromatic amines and nitrates,[15, 20] amino acids,[21, 22] and carbohydrates[23] have also been successfully identified using this approach.

5.1.3 Protein sensing using chemical noses

The emergences of abnormal proteins and/or irregular protein concentrations are indicative of cancers and diseases.[24] Therefore, sensitive, convenient, and precise protein sensing methods are required to obtain early diagnosis of diseases and successful treatment of patients. Currently, the most extensively used detection method for proteins is enzyme-linked immunosorbent array (ELISA).[25] In this system, the capture antibodies immobilized onto surfaces bind the antigen through a "lock-key" approach and another enzyme-coupled antibody is combined to react with chromogenic or fluorogenic substrates to generate detectable signals. Despite of the high sensitivity, the application of this method is restricted due to its high production cost, instability, and challenges for quantification. On the other hand, synthetic agents with high affinity and specificity for proteins are scarcely available although they possess better chemical and thermal stability.

Recently, the "chemical nose/tongue" approach has been applied to protein sensing. Hamilton's group has used eight tetra-*meso*-carboxylphenyl-porphyrins carrying peripheral amino acid functionalities to identify four metal and nonmetal-containing proteins, with a detection limit between 7.5 ~ 15 μM (Figure 5.3a).[26, 27] Anslyn et al. have employed 29 boronic acid-containing oligopeptide functionalized

resin beads to differentiate 5 proteins and glycoproteins through an indicator-uptake colorimetric analysis, with a limit of detection of 355 μM (Figure 5.3b).[28]

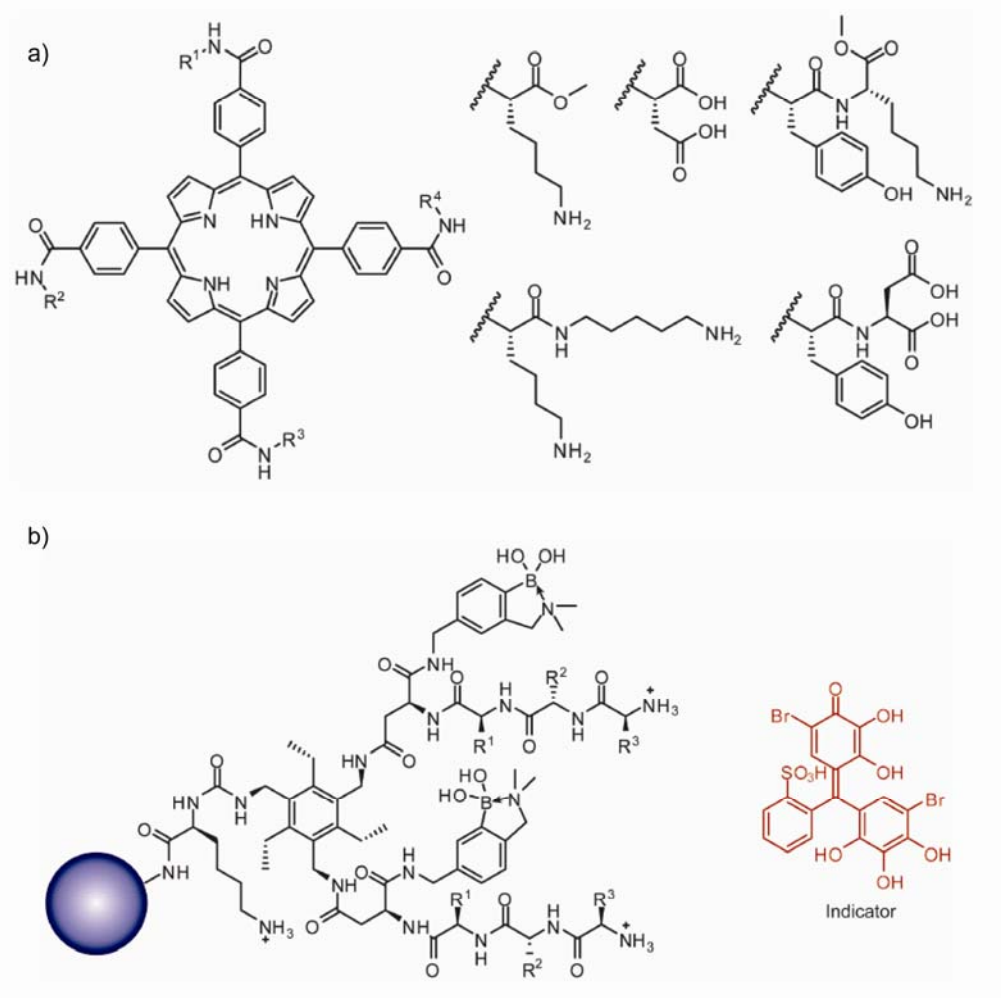

Figure 5.3. a) A library of tetra-meso-carboxylphenylporphyrin (TCPPs) conjugated with amino acids or amino acid derivatives used for protein sensing by Hamilton's group (reprinted from reference no. 26, 27). b) Structure of receptors which incorporates one of 19 natural amino acids at each of three sites that are biased towards particular analyte classes. Bromopyrogallol red is used for the indicator-uptake colorimetric analysis (reprinted from reference no. 28).

It has more recently been shown that non-selective electrostatic interaction in combination with covalently or non-covalently bound fluorophores are sufficient to differentiate between a numbers of biological relevant metalloproteins. Thayumanavan et al. exploited eight different fluorescence dye molecules non-covalently bound to the

micellar interiors of an amphiphilic homopolymer to generate a pattern and differentiate four different metalloproteins, with limits of detection between 1-200 μM.[29, 30]

5.1.4 Protein sensing using particle-polymer complexes

Based on pattern based sensing our group also created a sensor array which contains six structurally related cationic gold nanoparticles (**NP 1**-**NP 6**) as noncovalent protein receptors to create protein sensors (Figure 5.4a).[31] The nanoparticle end groups carry additional hydrophobic, aromatic or hydrogen-bonding functionality to tune the interaction between nanoparticles and proteins. For the signal transduction element, highly fluorescent poly(*p*-phenyleneethynylene) (PPE)[32, 33] derivative, **PPE-CO_2**,[34] was used a as a fluorescence indicator (Figure 5.4a). To establish the efficiency of this sensor, seven proteins with diverse structural features (Mw, pI) with variable concentrations levels were used as the target analytes.

As the **PPE-CO_2** backbone is anionic in nature, in presence of cationic nanoparticles the polymer fluorescence is quenched by gold nanoparticles. But in presence of analyte proteins, due to the competitive interaction between polymer and protein, disrupted the nanoparticle-polymer interaction, producing distinct fluorescence response patterns. These patterns were highly reproducible and characteristic for individual proteins, depending on the size and charge of the corresponding protein (Figure 5.4b). As all proteins vary their charge and size, they can be distinguished by this pattern. Also the response pattern fluctuates with the concentration of the analyte proteins but the reproducibility was observed even at nanomolar concentration.

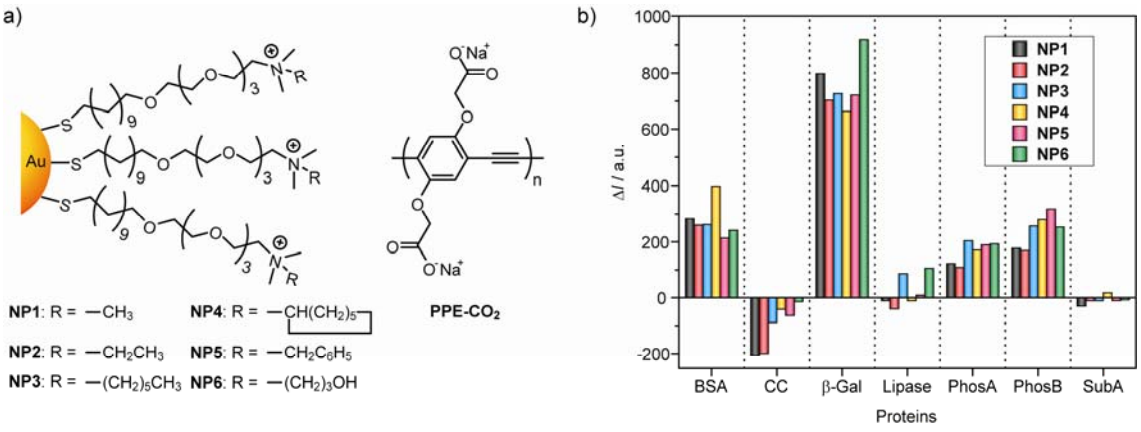

Figure 5.4. a) Structure of cationic gold nanoparticles (NP 1-NP 6) and anionic fluorescent polymer PPE-CO_2 (n~12). b) Fluorescence response (ΔI) patterns of the NP-PPE sensor array (NP 1 – NP 6) against various proteins (5 μM).

The raw data obtained were subjected to linear discriminant analysis (LDA) to differentiate the fluorescence response patterns of the nanoparticle-PPE systems against the different protein targets. LDA can maximize the ratio of between-class variance to the within-class variance in any particular data set thereby enabling maximal reparability.

The response patterns obtained from LDA for 5 μM proteins ware giving 100% separation accuracy (Figure 5.5a). Furthermore, another 56 protein samples were prepared randomly and used as unknowns in a "blind" experiment, i.e. the individual performing the analysis did not know the identity of the solutions. Out of 56 cases, 54 were correctly classified, affording an identification accuracy of 96.4%. But the detection and identification of proteins with both unknown identity and concentration is necessary for real world application. To make possible the detection of unknown proteins, a protocol was designed with the combination of LDA and UV measurements. In this approach, a set of fluorescence response patterns were generated at protein concentrations with an identical UV absorption value at 280 nm (A_{280} = 0.005) which is

the lowest concentration to get the substantial difference in responses. Using this protocol this sensor system were able to identify and quantify proteins at unknown concentrations with LDA classification accuracy of 97.6% (41 out of 42), according to the Jackknifed classification matrix (Figure 5.5b). This measurement also successfully used to identify and quantify 52 unknown proteins with an accuracy of 94.2% with concentrations within ±5-10%.

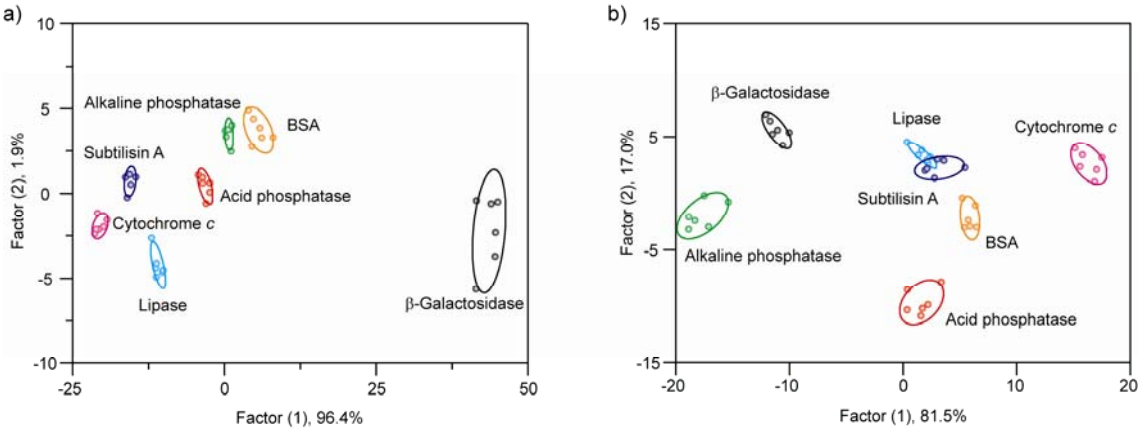

Figure 5.5. Canonical score plot as calculated by LDA for the identification of seven proteins, with 95% confidence for a) 5 μM proteins and b) proteins with identical absorption values of A = 0.005 at 280 nm.

5.2 Protein Detection using Nanoparticle-GFP Conjugates

In gold nanoparticle-fluorescent conjugated polymer based array array we used six different functionalized cationic nanoparticles and a fluorescent polymer to detect seven target proteins at detection limit of 4 nM for β-galactosidase (β-gal) with the accuracy of 94%.[31] Alternative to that system we also construct a biomolecules-based chemical nose approach that provides lowered limits of detection coupled with enhanced biocompatibility. In this approach an array of green fluorescent protein (GFP)-nanoparticle complexes was fashioned and used for the identification of proteins. The biocompatibility of the nanoparticles and GFP allows us to use this conjugated

system without any effect on target protein conformation during their detection.[35, 36] GFP is a beta barrel shaped marker protein that is negatively charged at physiological conditions (3.0 x 4.0 nm, MW = 27 KDa, pH 7.4, pI = 5.92),[37, 38] with an excitation peak at 490 nm and emission peak at 510 nm (Figure 5.6a). Due to its negative charge, GFP forms complexes with cationic gold nanoparticles, quenching GFP fluorescence. We hypothesized that displacement of the GFP from the particle by analyte proteins would regenerate GFP fluorescence.

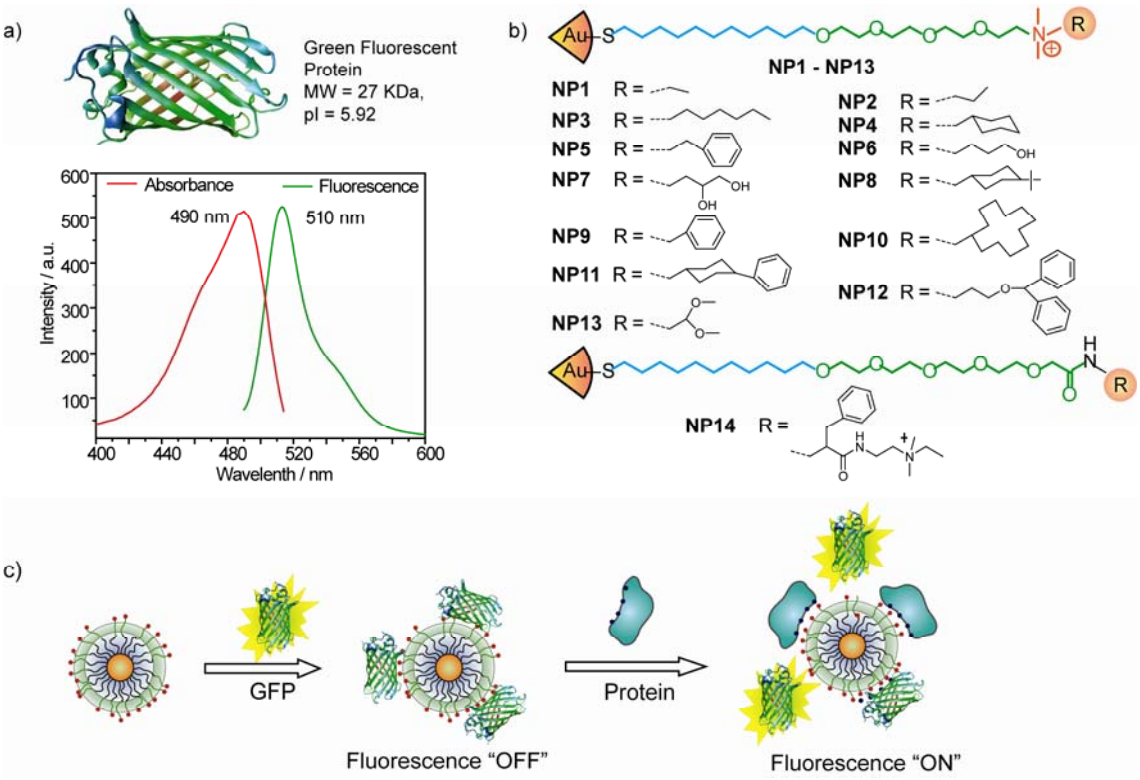

Figure 5.6. a) Structure, absorbance and fluorescence spectra of GFP in 5 mM sodium phosphate buffer, pH 7.40. b) Chemical structure of cationic gold nanoparticles (NP1-NP14). The nanoparticles highlited with green and blue color are used for low and high detection limit and red are used for both. c) Schematic illustration of the competitive binding between protein and quenched nanoparticle-GFP complexes leading to the fluorescence light-up.

To test this hypothesis, fourteen cationic gold nanoparticles (**NP1**–**NP14**) were synthesized and used to sense proteins. In addition to their cationic charges, these

nanoparticles varied hydrophobicity, aromaticity, and hydrogen bonding functionality (Figure 5.6b). We expected that in the presence of protein targets, GFP-nanoparticle interactions would be disrupted and generating distinct fluorescent signal patterns. Based on the affinity between protein target and GFP-nanoparticle adducts that could then be used to identify proteins (Figure 5.6c)

5.2.1 Result and Discussion

5.2.1.1 Fluorescence titration and Sensor Design

To optimize the binding ratio between GFP and nanoparticles for sensing, fluorescence titration was first conducted to assess the complexation between anionic GFP and cationic gold nanoparticles **NP1**-**NP6**. The intrinsic fluorescence of GFP was significantly quenched upon addition of all nanoparticles (Figure 5.7). The absorption effect of gold cores was obtained through control experiments using neutral particles[39, 40] and the normalized fluorescence intensities of GFP at 510 nm were subsequently plotted versus the ratio of nanoparticle to GFP. The complex stability constants (K_S) and association stoichiometries (n) were obtained through nonlinear least-squares curve-fitting analysis (Table 5.1).[41] Complex stabilities vary within *ca.* one order of magnitude ($\Delta\Delta G \sim 15$ kJ mol^{-1}), while the binding stoichiometry varies from ~2 to ~10. The observation indicates that the subtle structural changes of nanoparticle end groups significantly affect their affinity for the protein surface. It is noteworthy that all particle-GFP conjugates were optically transparent over the concentration range studied.

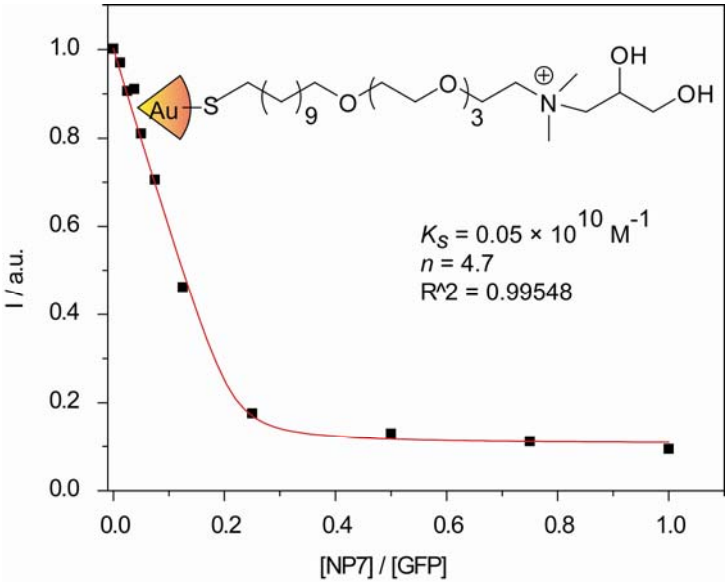

Figure 5.7. Fluorescence titration curves for the complexation of GFP with cationic gold nanoparticles NP 7. The changes of fluorescence intensity at 510 nm were measured following the addition of cationic nanoparticles (0-100 nM) with an excitation wavelength of 475 nm. The red solid lines represent the best curve fitting using the model of single set of identical binding sites.

Table 5.1. Binding constants (K_S), Gibbs free energy changes ($-\Delta G$) and binding stoichiometries (n) between GFP and various cationic nanoparticles (NP1–NP14) as determined from fluorescence titration.

Nanoparticle	*Ks* (10^9 M^{-1})	$-\Delta G$ (kJ mol^{-1})	*n*
NP1	22.7	59.11	3.9
NP2	2.6	53.74	2.8
NP3	51.3	61.13	2.2
NP4	15.9	58.23	3.6
NP5	30.7	59.86	4.1
NP6	9.4	56.93	1.8
NP7	0.5	49.65	4.7
NP8	1.1	51.61	7.9
NP9	0.2	47.38	1.6
NP10	0.5	49.65	9.7
NP11	9.3	56.90	4.4
NP12	83.9	62.35	3.3
NP13	0.1	45.66	6.2
NP14	0.2	47.38	3.3

5.2.1.2 Proteins Identification and Determination of the Detection Limit

Once the optimal binding ratios were determined, eleven target proteins with diverse sizes and charges were used to test the efficacy of the method (Table 1). Once the different binding characteristics of GFP with **NP1**-**NP14** were established, the optimal binding ratios were determined. According to that, nanoparticle-GFP conjugates were used to sense eleven proteins. The proteins were chosen to display a variety of sizes and charges: the isoelectric points (pI) of the eleven proteins vary from 4.6 to 10.7 and molecular weights range from 12.3 to 540 kDa (Table 5.2). Within this set there are several pairs of proteins that have comparable molecular weights and/or pI values, providing a challenging testbed for protein discrimination. In the initial sensing study, 200 μL of GFP (100 nM) and stoichiometric nanoparticles **NP1**-**NP14** (the stoichiometric values were taken from Table 5.1) were respectively loaded onto 96-well plates for recording the initial fluorescence intensities at 510 nm. Under these conditions, it is estimated that > 80% of polymer is bound to the nanoparticles based on the binding constants listed in Table 5.1, allowing fluorescent enhancement via subsequent displacement.

Table 5.2.Analyte proteins and concentrations used in study

Proteins	MW (kDa)	pI	ε_{280} (M^{-1} cm^{-1})	Conc. (nM)	
				A_{280} 0.005	A_{280} 0.0005
Bovine serum alb. (BSA)	66.3	4.8	46860	107	10.7
Acid phosphatase (PhosA)	110	5.2	257980	19	1.9
α-amylase (α-Am)	50	5.0	130000	38	3.8
β-galactosidase (β-Gal)	540	4.6	1128600	4	0.4
Subtilisin A (SubA)	30.3	9.4	26030	192	19.2
Hemoglobin (Hem)	64.5	6.8	125000	40	4.0
Human serum alb. (HSA)	69.4	5.2	37800	132	13.2
Alk. phosphatase (PhosB)	140	5.7	62780	80	8.0
Myoglobin (Myo)	17.0	7.2	13940	359	35.9
Lipase (Lip)	58	5.6	54350	92	9.2
Histone (His)	21.5	10.8	3840	1302	130

Following the previous protocol we can identify the unknown protein with unknown concentrations. The protocol is based on the combination of LDA and UV measurements. In brief, according to this protocol, a set of fluorescence response patterns were generated at analyte protein concentrations that generated a standard UV absorption value at 280 nm. We will determine the lowest absorbance that the proteins could be substantially differentiated using the given sensor array followed by LDA. Therefore, the absorbance followed by the corresponding protein concentration (can be obtained from ε_{280}) could also be treated as the detection limit of this assay. Another part is the identification of unknown protein with unidentified concentration. According to our protocol, the A_{280} value of the protein will be determined, and an aliquot subsequently diluted to A_{280} for recording the fluorescence response pattern against the nanoparticle-GFP sensing array. Once the identity of the protein was established by LDA, its initial concentration could be determined from the initial A_{280} value and corresponding molar extinction coefficient (ε_{280}) according to Beer-Lambert Law.

To determine the feasibility and efficiency of this system we first started with $A_{280} = 0.005$, which was the detection limit for the previous nanoparticle-polymer system. Using that concentration of all eleven analyte proteins we generated its fluorescence response against the corresponding GFP-nanoparticle complexes (GFP-**NP1** to **NP14)** using six duplicates.

In the first matrix set, addition of proteins into GFP-nanoparticle complexes at the same absorbance value ($A_{280} = 0.005$) resulted in unique fluorescence response patterns, as the affinity between the analyte proteins and nanoparticles differs depending on the surface characteristics of protein. At $A_{280} = 0.005$ we found maximum

classification accuracy of single nanoparticle-GFP conjugate was 80% (**NP14** and **NP2**). We also found that at A_{280} = 0.005 three GFP-nanoparticle complexes (**NP7**, **NP9**, **NP12**) afford an optimal classification of 100% accuracy (3 factors x 11 proteins x 6 replicates, Jackknifed classification matrix = 100%) (Figure 5.8a, b). This efficiency was mirrored in our unknown studies, where 48 unknown protein samples from the 11 target analytes were randomly prepared and identified with 100% identification accuracy.

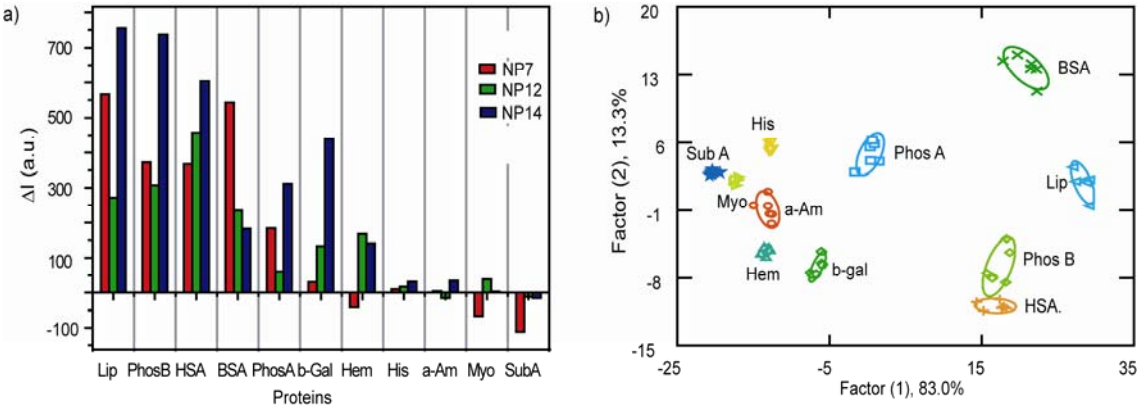

Figure 5.8. a) Fluorescence response (ΔI) patterns of the nanoparticle-GFP conjugate (NP7, NP12 and NP14) in the presence of various proteins at identical absorbance value of 0.005. Each value is an average of six parallel measurements. b) Canonical score plot for the fluorescence patterns as obtained from LDA against 11 protein analytes at fixed absorbance values A_{280} = 0.005. The 95% confidence ellipses for the individual proteins are also shown.

After getting the better efficiency in protein detection using nanoparticle-GFP conjugates, the next step will be the determination of the detection limit of this system. For that we run the trial at various lower absorbances of those eleven proteins. We found out that the lowest absorbance, where we can generate reproducible response pattern is A_{280} = 0.0005. The fluorescence response patterns where the protein concentration is A_{280} = 0.0005 are distinctly different from those generated from A_{280} = 0.005, but retain a high degree of reproducibility. In the case of A_{280} = 0.0005, the

biosensor accuracy was reduced to 70% using the above three nanoparticles. We found that accuracy was restored using six GFP-nanoparticle complexes (**NP1**, **NP2**, **NP4**, **NP7**, **NP12, NP14**), obtaining 98% accuracy (6 factors x 11 proteins x 6 replicates, Jackknifed classification matrix = 98%) (Figure 5.9).The canonical fluorescence response patterns display excellent separation, except for a minor overlap between hemoglobin and subtilisin A.

A series of unknown protein solutions were subsequently used for quantitative detection. For this set, 45 out of 48 unknown samples were correctly identified, affording an identification accuracy of 94 % with a detection limit as low as 400 picomolar for β-gal. This result unambiguously manifests that our sensor array holds substantial promise for both the identification and quantification of protein analytes.

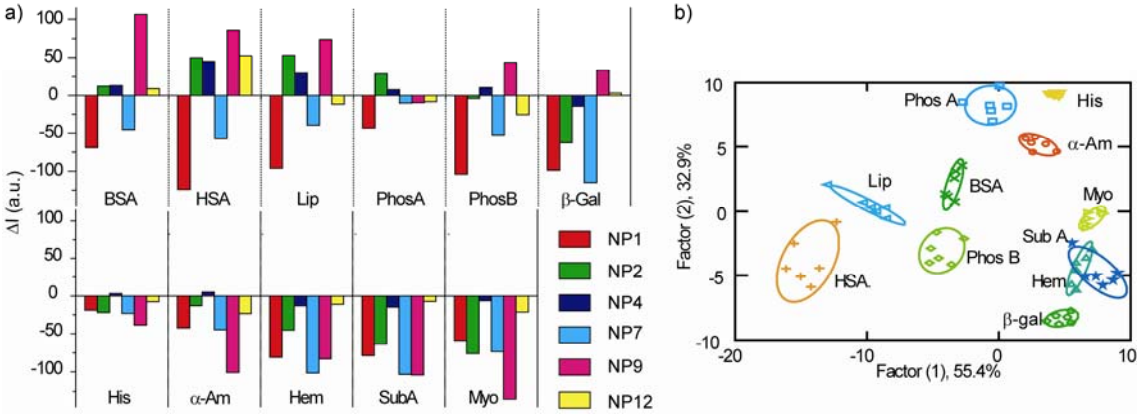

Figure 5.9. a) Fluorescence response (ΔI) patterns of the nanoparticle-GFP conjugate (NP1, NP2, NP4, NP7, NP9 and NP12) in the presence of various proteins at identical absorbance value of 0.0005. Each value is an average of six parallel measurements. b) LDA analysis of the fluorescence patterns as obtained from 11 protein analytes at fixed absorbance values A_{280} = 0.005. The little overlap between SubA and Hem was observed.

5.2.2 Conclusion

In summary, we have demonstrated that GFP-nanoparticle conjugates can effectively identify the wide range of proteins at nano/picomolar concentrations (400 pM for β-Gal). In this approach the competitive complexation between GFP and analyte proteins with nanoparticles make this system comparable to natural protein-protein interaction. Moreover the use of GFP and gold nanoparticle make this system biocompatible which can detect protein without any possible chance of protein deconformation. Hence these efficient characteristics of this system make it extremely promising in detection of proteins for biomedical diagnostics.

5.3 Detection of Serum Protein in Human Serum

Personalized medicine[42, 43] requires *personalized* diagnostics to achieve *personalized* treatment of specific diseases. While treatment with personalized drugs is the final goal, a necessary prerequisite is the early determination of the disease status and causes. It was evident that the most acute and chronic disease states will result in subtle or dramatic changes in the relative composition of a person's blood serum.[44, 45] This hypothesis has strong support from regular clinical tools, where simple electrophoresis of plasma leads to the identification and semiquantitative "fingerprinting" of proteins that are abundant in blood serum. The presence of specific electrophoresis patterns can interpreted by physicians to diagnose a significant number of disorders.[46] Changes in protein electrophoresis patterns are diagnostic for liver and renal failure, as well to states of massive malnutrition, systemic shock or other large scale inflammatory events. Simple one-dimensional agarose electrophoresis of protein

serum is an effective but slow and insensitive tool for the detection of gross protein imbalances. The reason of the difficulty for the detection of protein composition in serum is arising from its complex composition. Human blood serum contains >20,000 different proteins, some of which are present in concentrations > 50 gL^{-1} such as albumin, down to specific disease markers including cardiac troponin or natriuretic peptide that are found after a myocardial infarct or in patients with congestive heart failure respectively in concentrations of 2-9 μgL^{-1} and 0.6-1.4 μgL^{-1} respective. Besides albumin, the other proteins found in plasma at high concentrations are prealbumin (0.2-0.4 gL^{-1}), antitrypsin (a protease inhibitor 0.5 gL^{-1}), macroglobulin (1.5-3.5 gL^{-1}), lipoprotein (3-7 gL^{-1}), transferrin (2-4 gL^{-1}), and immunoglobulins A, D, E, G (8-17 gL^{-1}). About 20 proteins constitute 99 weight% of all of the serum protein content. Table 5.3 displays the isoelectric point, molecular weight and approximate concentrations of the 20 most common proteins in human serum. Most of the serum proteins are negatively charged, but their molecular weights vary from 28 to 900 kDa. It is important to note that some of these proteins such as transferrin display a quite significant range in concentration.

Table 5.3. Approximate Weight Content of High Abundant Proteins in Serum/Plasma for a healthy adult.[46, 47]

Protein	gL^{-1}	Mw^a	PI^b
Albumin	50	65	5.2
IgG	10	150	7.5-7.8
Transferrin	2-4	80	5.6
Fibrinogen	2	340	5.6
IgA Total	1.5	350	4.9
α-Macroglobulin	1.5	750	5.3-6.3
IgM	0.5	900	5-7
α-Antitrypsin	0.5	52	5.4
C3-Complement	0.5	180	5.8
Haptoglobin	0.2	41	5.1-7
Apolipoprotein A1	0.2	28	5.4-5.6
Apolipoprotein B	0.2	515	5.0-5.3
α-1-acid glycoprotein	0.2	40	2.7
Lipoprotein(a)	0.1	400-700	?
Factor H	0.2	139	?
Ceruloplasmin	0.2	135	4.4
C4-Complement	0.2	200	6
Complement B	0.2	100	5.9-6.1
Prealbumin	0.2	60	?
C9-Complement	0.1	71	5.60

a) molecular weight in kDa. b) isoelectric point.

The plasma protein composition can change for various reasons[48] such as, i) inter- and intradaily changes in serum composition, ii) age related changes in serum composition, iii) nutritional status, iv) differences in serum composition for each individual and v) disease related changes in serum composition.

The detection of the vast number of proteins acquired with proteomic techniques such as surface-enhanced laser desorption/ionization (SELDI)[49, 50] technique allows the determination of patterns of protein distribution that in comparison with normal sera

may allow to find specific protein signatures for specific diseases. But here the instrumentation is expensive, the throughput is low and the dynamic range is limited. If specific fractions of proteins are removed from the serum, then mass spectrometry is more sensitive and a tool for the discovery of hitherto unknown serum proteins. However mass spectrometry is at the moment not well suited as a high throughput tool for the economical screening of large numbers of serum samples, and is certainly unrealistic as a tool for personalized diagnostics.

With 2-D-SDS-PAGE electrophoresis, the specific proteins identified may also be sequenced.[51] Isoelectric focusing allows separation of proteins according to their charge, while in the second dimension the proteins are separable according to their molecular weight. This technique has led to the discovery of signature protein patterns in patients with ovarian carcinomas and in patients with inflammatory bowel disease.[52, 53] But these chromatograms are examined by eye and therefore only significant changes in serum composition are recognized. Plasma proteins that are present in much smaller amounts are specifically detected by monoclonal antibodies, with enhanced troponin or myoglobin levels being used to diagnose myocardial infarcts and increased PSA antigen used to detect prostate cancers.[54]

The third group is composed of specific disease markers that are present in small quantities to signal the early stage of a specific disease or a group of disorders. In such a case the gross plasma composition may be changed either significantly or subtly. Classic examples for such markers include those for neoplastic diseases, where the debris produced by the large number of dead and therefore lysed cells significantly increases the DNA content of the plasma.[55] While the use of monoclonal antibodies is

powerful, each monoclonal antibody has to be raised and can only detect one specific protein. Moreover, the technical difficulties as regards to quantification are significant.[56] We pose the hypothesis that most disease states will leave their "fingerprint" in the overall plasma composition, leading to an altered serum content of specific proteins or protein groups. The development of generalized and easy access "serum sensors" should give fast, reliable, and accurate readings of a person's health status.

Considering the high sensitivity of the nanoparticle-GFP conjugates as a sensor, we hypothesized that in presence of different composition of proteins the binding equilibrium between GFP and nanoparticle would be altered due to competitive binding, which will affect the fluorescence response. We are also expecting that those fluroscence responses will be reproducible to detect the particular composition. For that purpose, we consider some human serum protein. According to commercial availability we choose five serum proteins: albumin, IgG, transferrin, fibrinogen and α-antitrypsin. Table 5.3 displays the isoelectric point, molecular weight and approximate concentrations of the five proteins in healthy adult human serum. We spiked these proteins in commercially available human serum and differentiate those spiked serum from each other by LDA analysis.

5.3.1 Result and Discussion

5.3.1.1 Nanoparticle-GFP Complexation in Human Serum

Sensing of proteins in human serum is different than detection of single protein in buffer. As expected, the rate fluorescence quenching is not similar to buffer solution.

Due the opacity of pure human serum the required concentration of GFP to get sufficient response is higher than the previous study and the suitable concentration we found was 250 nM (in buffer solution we need 100 nM). According to the titration curve (Figure 5.10) we observed we did not reach the saturation in fluorescence quenching even in presence of 2 μM nanoparticles. This behavior can easily explain by the presence of several other proteins from human serum which are always competing with GFP to bind with nanoparticle. Also due to the existence of this multiple equilibrium constant it is very difficult to determine the binding characteristics of GFP with nanoparticles in serum. For our study we choose the middle point of the curve (500 nm of nanoparticles) as an optimum point.

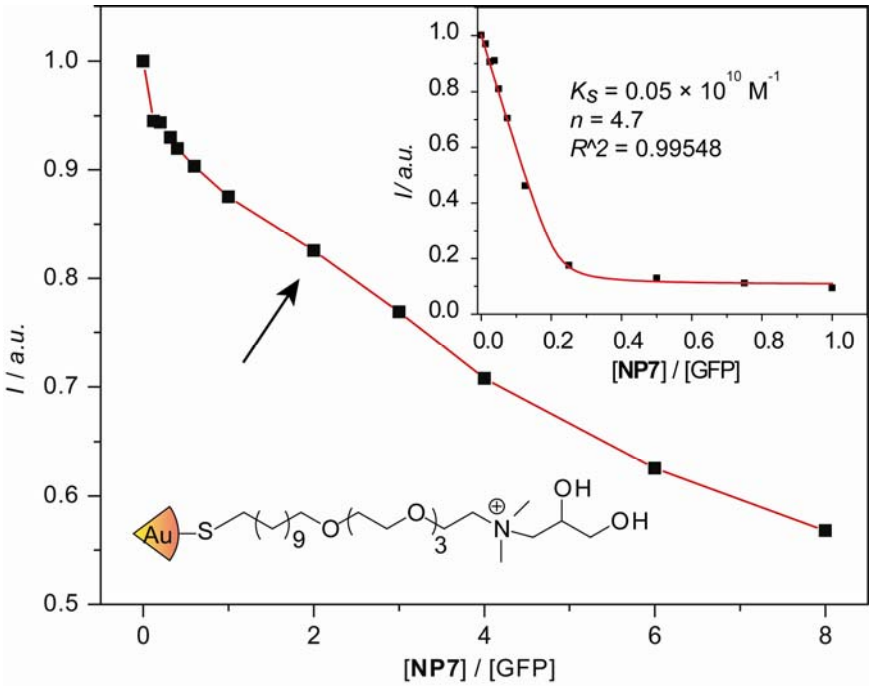

Figure 5.10. The changes of fluorescence intensity of GFP (250 nM) at 510 nm were measured following the addition of cationic nanoparticle NP7 (0-2 μM) with an excitation wavelength of 475 nm. Inset shows the change of Fluorescence intensity of GFP (100 nM) at 510 nm upon addition of NP7 in 5 mM sodium phosphate buffer.

5.3.1.2 Sensing of Protein in Human Serum

Similar to fluorescence titration, in serum we need to detect the protein in presence of several other proteins with variable concentration. In case of human serum solution the only albumin concentration is around 769 μM and total protein concentration is ~1mM. To detect the change of concentration of particular protein at certain level we ware considered the nanoparticles that showed the maximum selectivity in serum protein detection according to the result obtained from previous section. To determine the efficiency and detection limit of this system in serum we will spike the human serum with five proteins (Table 5.3) with various concentrations to generate a training matrix. We will then run the experiment with those spiked serum for multiple times (6 runs/ protein) and the results will be subjected to linear discriminate analysis (LDA).[57] Based on "jackknife classification analysis",[58] if we get a sufficient degree of separation accuracy (~>90%) then we will use that concentration as our detection limit and will use unknown identification as a proof of our concept. The minimum concentration we fond to get reproducible and well separable protein pattern is 500 nM using five nanoparticle-GFP conjugates (**NP1**, **NP3**, **NP7**, **NP8** and **NP14**). Hence we spiked the commercial human serum with additional protein with final concentration 500 nM and were used to create training matrix (5 nanoparticle-GFP conjugates × 5 proteins × 6 replicates) with various nanoparticle-GFP conjugates. The fluorescence response patterns of proteins are distinctly different from those generated from 25 nM in buffer solution, but each protein generates a distinguishable response pattern and retain the reproducibility (Figure 5.11a). As before, these patterns were further subjected to LDA analysis, providing a 97% of accuracy as α-antitrypsin slightly

overlap with IgG. Similar to the previous analysis the four canonical factors are 76.9%, 20.3%, 2.7%, 0.1% and the plot of the first two factors with 95% confidence ellipses as presented in Figure 4b. A series of unknown protein solutions were subsequently used to validate this system and out of 30 samples 28 samples were correctly identified affording 93.3% identification accuracy. This result indicate that we were able to identify target proteins in the complex serum matrix at the sub-micromolar range, corresponding to ~0.05% of the analyte by molarity relative to the total serum proteins. Successful identification of those proteins when spiked into this commercially available human serum demonstrates the superb sensitivity of this sensory system, which is able to detect subtle concentration changes (500 nM) in this complex matrix containing a significant quantity of other proteins.

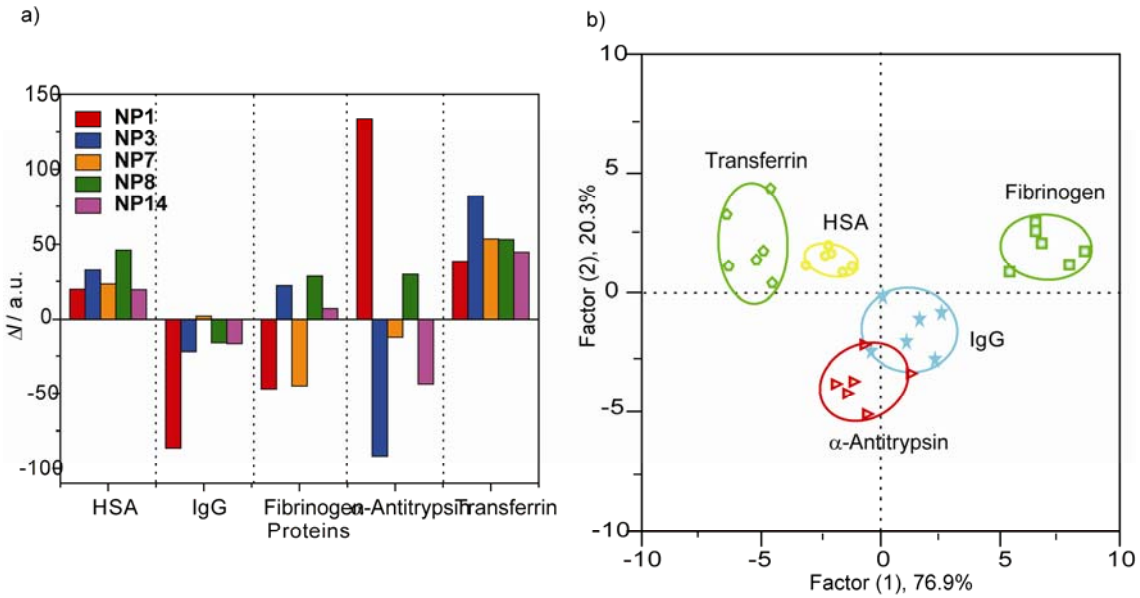

Figure 5.11. a) Fluorescence response (ΔI) pattern of the five nanoparticle-GFP adducts in the presence of serum proteins spiked in human serum at 500 nM concentration (average of six measurements). b)Canonical score plot for the fluorescence patterns as obtained from LDA against five protein analytes at fixed concentration 500 nM, with 95% confidence ellipses.

5.3.2 Conclusion

In conclusion, we have demonstrated a nanoparticle-GFP array based biosensor that can effectively identify most abundant serum proteins rang at very low concentration with higher efficiency. We also successfully extend this efficiency in detection of proteins in highly complex system i.e., human serum which is composed of several proteins with variable concentrations. This result indicate that the simple nanoparticle-GFP array can efficiently recognize biological analyst in serum simply and instantaneously with reliable fashion. In this approach the competitive complexation between GFP and analyte proteins with nanoparticles makes this system comparable to natural protein-protein interaction, providing potential for further optimization via engineering of both the synthetic and biological components. We also believe that optimization of this methodology potentially modernize the medical diagnostics, both in the clinic and as a tool for personalized diagnostics.

5.4 Experimental

5.4.1 Materials

Green fluorescence protein (GFP) was expressed according to the known procedure. In brief, Starter cultures from a glycerol stock of GFP in BL21(DE3) was grown overnight in 50 ml culture media at 37 ^{o}C. The following day, 5 ml of the starter cultures was added to a Fernbach flask containing 1 L culture media and shaken until the OD_{600} = 0.6 - 0.7. The culture was then induced by adding isopropyl-β-D-thiogalactopyranoside (IPTG) (1 mM final concentration) and shaken at 28 ^{o}C. After three hours, the cells were harvested by centrifugation and the pellet was then

resuspended in lysis buffer. Once lysed, the solution was pelleted and the supernatant was further purified using HisPur Cobalt columns. The Mw and pI of the expressed GFP is 26.9KDa and 5.92 respectively. The maximum λ_{ex} and λ_{em} are 490 nm and 510 nm (Figure S1).

The analyte proteins, bovine serum albumin (BSA), acid phosphatase (PhosA, frompotato), α-amylase (α-Am, from *Bacillus Licheniformis*), lipase (Lip, from *Candida Rugosa*, type *VII*), β-galactosidase (β-Gal, from *Escherichia Coli*), Subtilisin A (SubA, from *Bacillus Licheniformis*), hemoglobin (Hem, from human), human serum albumin (HAS), alkaline phosphatase (PhosB, from bovine intestinal mucosa), Histone (His, from calf thymus, type III-S) and myoglobin (Myo, from equine heart) for sensing of common proteins in clear buffer solution were purchased from Sigma-Aldrich and used as received. For sensing in serum, the analyte proteins, serum albumin (HSA), immunoglobulins (IgG), transferrin, fibrinogen and α-antitrypsin all from human serum were purchased from the same supplier.

Cationic nanoparticles **NP1**–**NP6**,[31] were synthesized according to the reported procedure and **NP7–NP14** were prepared according to the similar procedure as described below.

5.4.2 Synthesis of ligand and nanoparticles

General procedure for L1-L13. Compound **2** bearing ammonium end groups were synthesized through the reaction of 1,1,1-triphenyl-14,17,20,23-tetraoxa-2-thiapentacosan-25-yl methanesulphonate (**1**) with corresponding substituted N,N-dimethylamines during 48 h at ~35 ^{o}C. The trityl protected thiol ligand **(2)** was

dissolved in dry DiChloroMethane (Methylene Chloride, DCM) and an excess of trifluoroacetic acid (TFA, ~ 20 equivalents) was added. The color of the solution was turned to yellow immediately. Subsequently, triisopropylsilane (TIPS, ~ 1.2 equivalents) was added to the reaction mixture. The reaction mixture was stirred for ~5 h under Ar condition at room temperature. The solvent and most TFA and TIPS were distilled off under reduced pressure. The pale yellow residue was further dried in high vacuum. The product (**L**) formation was quantitative and their structure was confirmed by NMR. The yields were >95%.

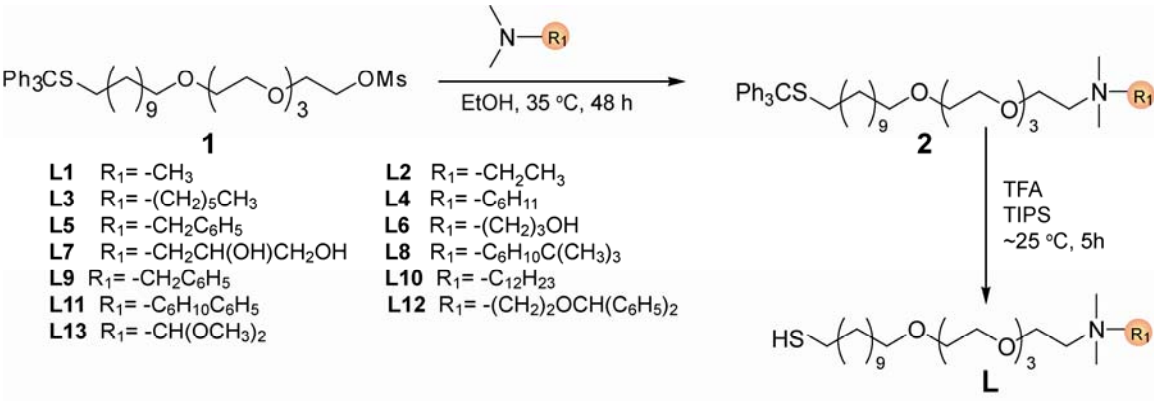

Scheme 5.1. Synthesis of ligands (L1-L13).

General procedure for L14. Compound **4** bearing L-Phe group was synthesized through the reaction of 26-mercapto-3,6,9,12,15-pentaoxahexacosan-1-oic acid (**3**) with corresponding 2-amino-N-(2-(dimethylamino)ethyl)-3-phenylpropanamide. The reaction was done in a mixture of DiChloroMethane (Methylene Chloride, DCM) and N, N-Dimethylformamide (DMF). After 2 days, the solution was poured into ethyl acetate (EtOAc) and water. The organic layer was collected and washed with bride, and dried with Na_2SO_4. After removal of the solvent, the residue was charged in SiO_2 column for purification. EtOAc/MeOH (90:10) and EtOAc/MeOH/NH_4OH (90:10:1) were used as gradient eluent. Compound **5** was

obtained through nucleophilic substitution of compound **4** with bromothane. The trityl protected thiol ligand (**5**) was dissolved in dry DCM and an excess of trifluoroacetic acid (TFA, ~ 20 equivalents) was added. The color of the solution was turned to yellow immediately. Subsequently, triisopropylsilane (TIPS, ~ 1.2 equivalents) was added to the reaction mixture. The reaction mixture was stirred for ~5 h under Ar condition at room temperature. The solvent and most TFA and TIPS were distilled off under reduced pressure. The pale yellow residue was further dried in high vacuum. The product **L14** (5-benzyl-N-ethyl-32-mercapto-N,N-dimethyl-4,7-dioxo-9,12,15,18,21-pentaoxa-3,6-diazadotriacontan-1-aminium) formation was quantitative and their structure was confirmed by NMR. The yields were >93%.

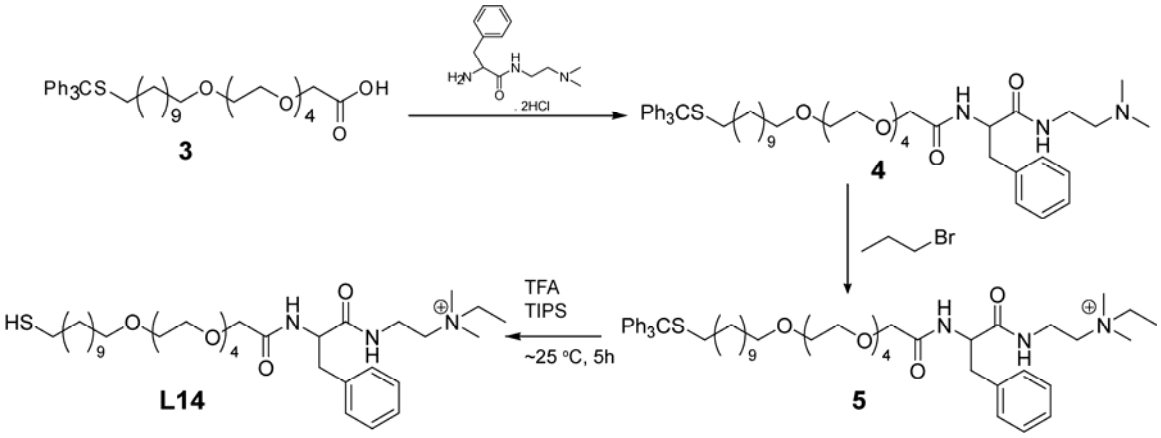

Scheme 5.2. Synthesis of ligand L14.

General procedure: 1-Pentanethiol coated gold nanoparticles (d = ~2 nm) were prepared according to the previously reported protocol.[59] Place-exchange reaction[60] of compound **Ls** dissolved in DCM with pentanethiol-coated gold nanoparticles (d~2 nm) was carried out for 3 days at environmental temperature. Then, DCM was evaporated under reduced pressure. The residue was dissolved in a small amount of distilled water

and dialyzed (membrane MWCO = 1,000) to remove excess ligands, acetic acid and the other salts present with the nanoparticles. After dialysis, the particles were lyophilized to afford a brownish solid. The nanoparticles are redispersed in water and/or ionized water (18 MΩ-cm). ^{1}H NMR spectra in D_2O showed substantial broadening of the proton signals and no free ligands were observed.

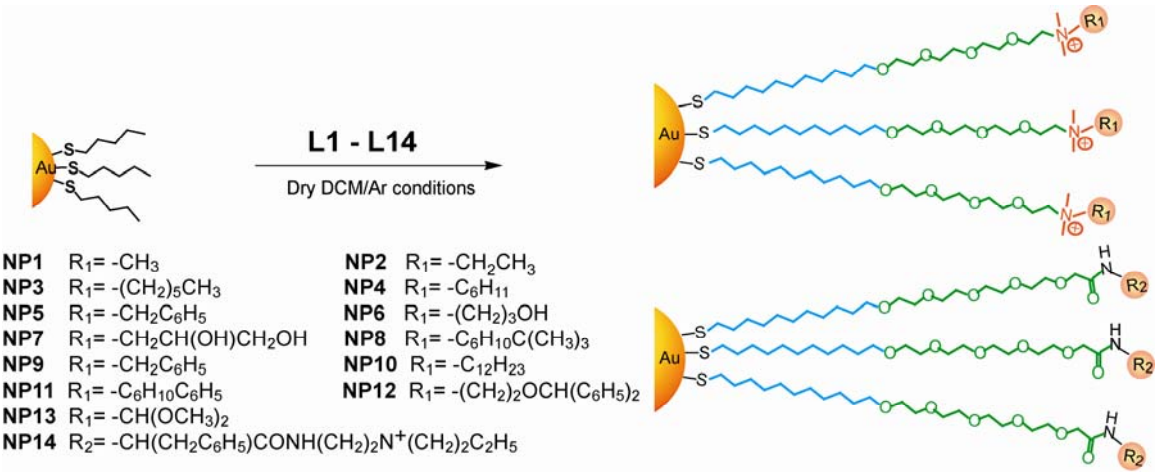

Scheme 5.3. Fabrication of cationic gold nanoparticles by place exchange method.

5.4.3 Fluorescence Titration

In the fluorescence titration between nanoparticles and GFP, the change of fluorescence intensity at 510 nm was measured with an excitation wavelength of 475 nm at various concentrations of nanoparticles from 0 to 100 nM on a Molecular Devices SpectaMax M5 microplate reader at 25 ^{o}C in 5 mM sodium phosphate buffer. The change of fluorescence intensity against increasing nanoparticle concentrations was plotted, using a non-interacting gold nanoparticle (e.g. PEG-NP) as a control to compensate for particle absorption. Nonlinear least-squares curve-fitting analysis was employed to estimate the binding constant (*Ks*) and association stoichiometry (*n*) using the model in which the nanoparticle is assumed to possess *n* equivalent of independent

binding sites. In case of human serum, similar procedure was followed, but the only modification was the concentration of GFP (250 nM) and the nanoparticles (0-2 μM).

5.4.4 Training Matrix

To create the training matrix, GFP and nanoparticles are mixed in the ratio obtained from fluorescence titration. In case of 5 mM sodium phosphate buffer solution the final concentration of nanoparticle and GFP were 100 nM each. On the other hand, in serum solution study the final concentration of nanoparticle and GFP were 500 nM and 250 nM respectively. After 30 min of incubation 200 μL of each solution was loaded into a well on a 96-well plate (300 μL Whatman black bottom micropalte) and the fluorescence intensity at 510 nm recorded using fluorescence microplate reader (Molecular Devices SpectraMax M5). Subsequently, 10 μL of protein solution of two different concentrations with absorbance value at 280 nm was added. In case of sensing in serum 10.5 μM of protein solution, was added so that the final concentrations were 500 nM. After incubation for 30 min the fluorescence intensity at 510 nm was recorded again. The difference between the two intensities before and after addition of proteins was considered as the fluorescence response. This process was repeated for five serum proteins with five selective cationic nanoparticles in six replicates. This data was used to generate the 6 × 5 × 5 (6 replicates × 5 proteins × 5 nanoparticles) training matrix. This training matrix was used for classical linear discriminant analysis (LDA) in SYSTAT (version 11.0).

5.4.5 Unknown Detection

For the unknown detection, we prepared the protein solutions out of the eleven common protein or five serum proteins according to buffer or serum study. From this prepared solution we randomly choose 48 or 30 samples for each system (buffer or serum) and the same method was followed using the nanoparticle-GFP motif. We replicated each unknown samples three times instead of six for preparing training matrix. We considered the average response of three replicates for a single unknown sample and analyzed with known proteins in LDA analysis.

5.5 References

1 Kingsmore, S. F., *Nat. Rev. Drug Discovery* **2006,** *5*, 310-320.

2 Sawyers, C. L., *Nature* **2008,** *452*, 548-552.

3 Daniels, M. J.; Wang, Y. M.; Lee, M. Y.; Venkitaraman, A. R., *Science* **2004,** *306*, 876-879.

4 Meyer-Luehmann, M.; Spires-Jones, T. L.; Prada, C.; Garcia-Alloza, M.; de Calignon, A.; Rozkalne, A.; Koenigsknecht-Talboo, J.; Holtzman, D. M.; Bacskai, B. J.; Hyman, B. T., *Nature* **2008,** *451*, 720-U5.

5 MacBeath, G., *Nat. Genet.* **2002,** *32*, 526-532.

6 Mairal, T.; Ozalp, V. C.; Sanchez, P. L.; Mir, M.; Katakis, I.; O'Sullivan, C. K., *Anal. Bioanal. Chem.* **2008,** *390*, 989-1007.

7 Henares, T. G.; Mizutani, F.; Hisamoto, H., *Anal. Chim. Acta* **2008,** *611*, 17-30.

8 Siwy, Z.; Trofin, L.; Kohli, P.; Baker, L. A.; Trautmann, C.; Martin, C. R., *J. Am. Chem. Soc.* **2005,** *127*, 5000-5001.

9 Meiring, J. E.; Schmid, M. J.; Grayson, S. M.; Rathsack, B. M.; Johnson, D. M.; Kirby, R.; Kannappan, R.; Manthiram, K.; Hsia, B.; Hogan, Z. L.; Ellington, A. D.; Pishko, M. V.; Willson, C. G., *Chem. Mater.* **2004,** *16*, 5574-5580.

10 So, H. M.; Won, K.; Kim, Y. H.; Kim, B. K.; Ryu, B. H.; Na, P. S.; Kim, H.; Lee, J. O., *J. Am. Chem. Soc.* **2005,** *127*, 11906-11907.

11 Rich, R. L.; Myszka, D. G., *J. Mol. Recognit.* **2008,** *21*, 355-400.

12 Lavigne, J. J.; Anslyn, E. V., *Angew. Chem., Int. Ed.* **2001,** *40*, 3119-3130.

13 Ciosek, P.; Wroblewski, W., *Analyst* **2007,** *132*, 963-978.

14 Gardner, J. W.; Bartlett, P. N., *Electronic Noses. Principles and Applications*. Oxford University Press, USA: 1999.

15 Greene, N. T.; Shimizu, K. D., *J. Am. Chem. Soc.* **2005,** *127*, 5695-5700.

16 Wiskur, S. L.; Floriano, P. N.; Anslyn, E. V.; McDevitt, J. T., *Angew. Chem., Int. Ed.* **2003,** *42*, 2070-2072.

17 Lavigne, J. J.; Savoy, S.; Clevenger, M. B.; Ritchie, J. E.; McDoniel, B.; Yoo, S. J.; Anslyn, E. V.; McDevitt, J. T.; Shear, J. B.; Neikirk, D., *J. Am. Chem. Soc.* **1998,** *120*, 6429-6430.

18 Lee, J. W.; Lee, J. S.; Kang, M.; Su, A. I.; Chang, Y. T., *Chem.Eur. J.* **2006,** *12*, 5691-5696.

19 Rakow, N. A.; Suslick, K. S., *Nature* **2000,** *406*, 710-713.

20 Hughes, A. D.; Glenn, I. C.; Patrick, A. D.; Ellington, A.; Anslyn, E. V., *Chem.Eur. J.* **2008,** *14*, 1822-1827.

21 Folmer-Andersen, J. F.; Kitamura, M.; Anslyn, E. V., *J. Am. Chem. Soc.* **2006,** *128*, 5652-5653.

22 Leung, D.; Folmer-Andersen, J. F.; Lynch, V. M.; Anslyn, E. V., *J. Am. Chem. Soc.* **2008,** *130*, 12318-12327.

23 Wright, A. T.; Anslyn, E. V., *Chem. Soc. Rev.* **2006,** *35*, 14-28.

24 Anderson, N. L.; Anderson, N. G., *Molecular & Cellular Proteomics* **2002,** *1*, 845-867.

25 Haab, B. B., *Curr. Opin. Biotechnol.* **2006,** *17*, 415-421.

26 Baldini, L.; Wilson, A. J.; Hong, J.; Hamilton, A. D., *J. Am. Chem. Soc.* **2004,** *126*, 5656-5657.

27 Zhou, H. C.; Baldini, L.; Hong, J.; Wilson, A. J.; Hamilton, A. D., *J. Am. Chem. Soc.* **2006,** *128*, 2421-2425.

28 Wright, A. T.; Griffin, M. J.; Zhong, Z. L.; McCleskey, S. C.; Anslyn, E. V.; McDevitt, J. T., *Angew. Chem., Int. Ed.* **2005,** *44*, 6375-6378.

29 Sandanaraj, B. S.; Demont, R.; Aathimanikandan, S. V.; Savariar, E. N.; Thayumanavan, S., *J. Am. Chem. Soc.* **2006,** *128*, 10686-10687.

30 Sandanaraj, B. S.; Demont, R.; Thayumanavan, S., *J. Am. Chem. Soc.* **2007,** *129*, 3506-+.

31 You, C. C.; Miranda, O. R.; Gider, B.; Ghosh, P. S.; Kim, I. B.; Erdogan, B.; Krovi, S. A.; Bunz, U. H. F.; Rotello, V. M., *Nature Nanotechnology* **2007,** *2*, 318-323.

32 Bunz, U. H. F., Synthesis and structure of PAEs. In *Poly(Arylene Ethynylene)S: from Synthesis to Application*, 2005; Vol. 177, pp 1-52.

33 Juan, Z.; Swager, T. M., Poly(arylene ethynylene)s in chemosensing and biosensing. In *Poly(Arylene Ethynylene)S: from Synthesis to Application*, 2005; Vol. 177, pp 151-179.

34 Kim, I. B.; Dunkhorst, A.; Gilbert, J.; Bunz, U. H. F., *Macromolecules* **2005,** *38*, 4560-4562.

35 De, M.; You, C. C.; Srivastava, S.; Rotello, V. M., *J. Am. Chem. Soc.* **2007,** *129*, 10747-10753.

36 Hong, R.; Fischer, N. O.; Verma, A.; Goodman, C. M.; Emrick, T.; Rotello, V. M., *J. Am. Chem. Soc.* **2004,** *126*, 739-743.

37 Tsien, R. Y., *Annu. Rev. Biochem.* **1998,** *67*, 509-544.

38 Chalfie, M.; KainIn, S. R., *Green Fluorescent Protein: Properties, Applications, and Protocols*. Wiley-Interscience: Hoboken, N.J., 2006.

39 Aguila, A.; Murray, R. W., *Langmuir* **2000,** *16*, 5949-5954.

40 Zhang, F.; Skoda, M. W. A.; Jacobs, R. M. J.; Zorn, S.; Martin, R. A.; Martin, C. M.; Clark, G. F.; Goerigk, G.; Schreiber, F., *J. Phys. Chem. A* **2007,** *111*, 12229-12237.

41 You, C. C.; De, M.; Han, G.; Rotello, V. M., *J. Am. Chem. Soc.* **2005,** *127*, 12873-12881.

42 Hood, L.; Heath, J. R.; Phelps, M. E.; Lin, B. Y., *Science* **2004,** *306*, 640-643.

43 Ginsburg, G. S.; McCarthy, J. J., *Trends Biotechnol.* **2001,** *19*, 491-496.

44 Issaq, H. J.; Xiao, Z.; Veenstra, T. D., *Chem. Rev.* **2007,** *107*, 3601-3620.

45 Pieper, R.; Gatlin, C. L.; Makusky, A. J.; Russo, P. S.; Schatz, C. R.; Miller, S. S.; Su, Q.; McGrath, A. M.; Estock, M. A.; Parmar, P. P.; Zhao, M.; Huang, S. T.; Zhou, J.; Wang, F.; Esquer-Blasco, R.; Anderson, N. L.; Taylor, J.; Steiner, S., *Proteomics* **2003,** *3*, 1345-1364.

46 McPherson, R. A.; Pincus, M. R., *Henry's Clinical Diagnosis and Manangement by Laboratory Methods*. 21st ed.; Saunders-Elsevier: 2007; Vol. Chapter 19.

47 Anderson, N. L.; Anderson, N. G., *Molecular & Cellular Proteomics* **2002,** *1*, 845-867.

48 Steil, L.; Thiele, T.; Hammer, E.; Bux, J.; Kalus, M.; Volker, U.; Greinacher, A., *Transfusion* **2008,** *48*, 2356-2363.

49 Hu, Y.; Zhang, S. Z.; Yu, J. K.; Liu, J.; Zheng, S., *Breast* **2005,** *14*, 250-255.

50 Li, J. N.; Zhang, Z.; Rosenzweig, J.; Wang, Y. Y.; Chan, D. W., *Clinical Chemistry* **2002,** *48*, 1296-1304.

51 Adam, B. L.; Vlahou, A.; Semmes, O. J.; Wright, G. L., *Proteomics* **2001,** *1*, 1264-1270.

52 Petricoin, E. F.; Ardekani, A. M.; Hitt, B. A.; Levine, P. J.; Fusaro, V. A.; Steinberg, S. M.; Mills, G. B.; Simone, C.; Fishman, D. A.; Kohn, E. C.; Liotta, L. A., *Lancet* **2002,** *359*, 572-577.

53 Fiocchi, C., *Gastroenterology* **1998,** *115*, 182-205.

54 Wu, G. H.; Datar, R. H.; Hansen, K. M.; Thundat, T.; Cote, R. J.; Majumdar, A., *Nat. Biotechnol.* **2001,** *19*, 856-860.

55 Bastian, P. J.; Ellinger, J.; Wittkamp, V.; Albers, P.; von Rucker, A.; Muller, S. C., *Journal of Urology* **2008,** *179*, 272-272.

56 Milam, R. A.; Milam, M. R.; Iyer, R. B., *Journal of Clinical Oncology* **2007,** *25*, 5657-5658.

57 Massart, D. L.; Kaufman, L., *The Interpretation of Analytical Chemical Data by the Use of Cluster Analysis*. John Wiley and Sons: New York, 1983.

58 Gong, G., *Journal of the American Statistical Association* **1986,** *81*, 108-113.

59 Brust, M.; Walker, M.; Bethell, D.; Schiffrin, D. J.; Whyman, R., *J. Chem. Soc., Chem. Commun.* **1994**, 801-802.

60 Hostetler, M. J.; Wingate, J. E.; Zhong, C. J.; Harris, J. E.; Vachet, R. W.; Clark, M. R.; Londono, J. D.; Green, S. J.; Stokes, J. J.; Wignall, G. D.; Glish, G. L.; Porter, M. D.; Evans, N. D.; Murray, R. W., *Langmuir* **1998,** *14*, 17-30.

APPENDIX

ENTHALPY-ENTROPY CORRELATION PLOTS

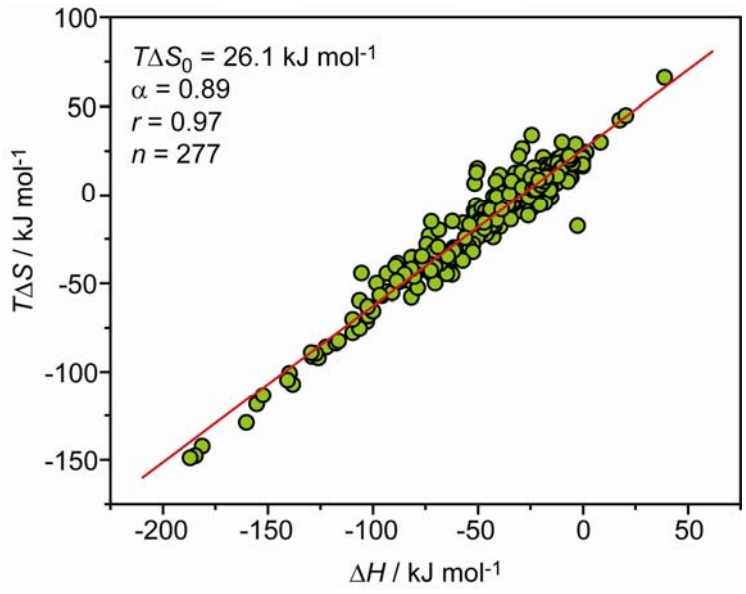

Figure A.1. Plots of entropy ($T\Delta S$) versus enthalpy (ΔH) for the protein-ligand (nonpeptide) interactions from Table A.2.

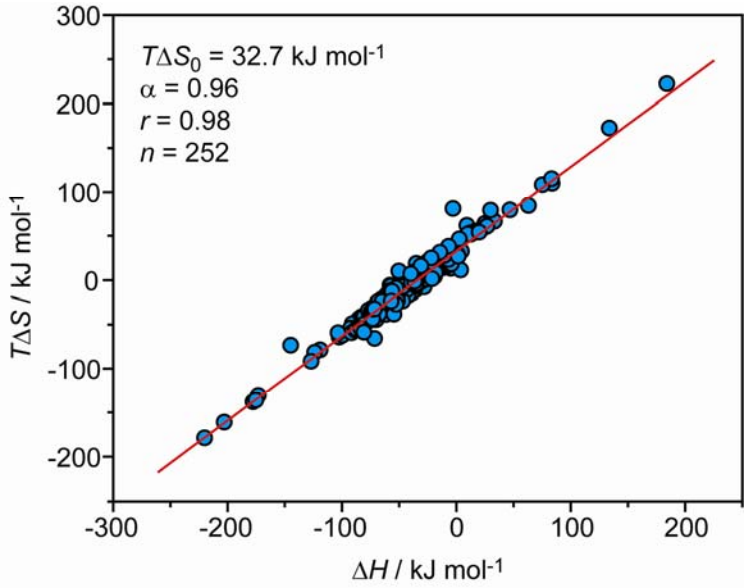

Figure A.2. Plots of entropy ($T\Delta S$) versus enthalpy (ΔH) for the protein-peptide interactions from Table A.3.

Table A.1. Thermodynamic Parameters for Some Protein-Protein Interactions (continues on the next page).

Complex	Solvent	T / °C	ΔG / kJ mol^{-1}	ΔH / kJ mol^{-1}	$T\Delta S$ / kJ mol^{-1}	Ref.
Trypsin/soybean inhibitor	200 mM KCl, 50 mM $CaCl_2$, pH 5.0	25.0	-51.5	36.0	87.1	1
Trypsin/cleaved soybean inhibitor	200 mM KCl, 50 mM $CaCl_2$, pH 5.0	25.0	-45.2	52.7	98.0	1
Trypsin/ovomucoid	200 mM KCl, 50 mM $CaCl_2$, pH 5.0	25.0	-42.7	23.4	66.2	1
Trypsin/lima bean inhibitor	200 mM KCl, 50 mM $CaCl_2$, pH 5.0	25.0	-53.1	8.8	62.0	1
Chymotrypsin/bovine pancreatic trypsin inhibitor	50 mM Tris/HCl, 20 mM $CaCl_2$, 0.005% Triton X-100, pH 8.2	22.0	-44.8	10.5	55.2	2
Chymotrypsin/subtilisin inhibitor	25 mM potassium phosphate, ionic strength = 100 mM with KCl, pH 7.0	25.0	-29.9	18.7	47.7	3
Chymotrypsin/OMTKY3	50 mM acetic acid/sodium acetate, 20 mM NaCl, pH 4.5	25.0	-39.3	52.3	91.6	4
Subtilisin/subtilisin inhibitor	25 mM potassium phosphate, ionic strength = 100 mM with KCl, pH 7.0	25.0	-57.9	-19.8	38.1	5
Calmodulin Ca^{2+}/myosin light chain kinase	50 mM Pipes/NaOH, 150 mM NaCl, 0.5 mM $CaCl_2$, pH 7.5	25.0	-48.1	-84.9	-36.4	6
Calmodulin Ca^{2+}/seminal plasmin	50 mM Pipes/NaOH, 150 mM NaCl, 0.5 mM $CaCl_2$, pH 7.5	25.0	-50.2	-50.2	0	6
Calmodulin/myosin light chain kinase	50 mM Pipes/NaOH, 150 mM NaCl, pH 7.5	25.0	-30.1	0	30.1	6
Calmodulin/seminal plasmin	50 mM Pipes/NaOH, 150 mM NaCl, pH 7.5	25.0	-33.9	0	33.9	6
Ch4D5 Fab/p185$^{HER2\text{-}ECD}$	20 mM sodium phosphate, 100 mM NaCl, pH 7.5	25.0	-56.5	-72.0	-15.0	7
HyHEL-5/hen egg lysozyme	10 mM sodium phosphate, pH 8.0	25.0	-60.7	-94.6	-33.9	8
HyHEL-10/hen egg lysozyme	50 mM phosphate, 200 mM NaCl, pH 7.2	30.0	-50.2	-91.6	-41.4	9
HyHEL-10/hen egg lysozyme	50 mM phosphate, 200 mM NaCl, pH 7.2	30.0	-51.7	-99.7	-47.9	10
Fv D1.3/hen egg lysozyme	10 mM sodium phosphate, 150 mM NaCl, pH 7.1	49.8	-42.6	-129.0	-86.0	11
mAb D1.3/hen egg lysozyme	10 mM sodium phosphate, 150 mM NaCl, pH 7.1	24.2	-48.0	-90.8	-42.8	11
F9.13.7/hen egg lysozyme	10 mM sodium phosphate, 150 mM NaCl, pH 7.1	23.9	-50.2	-46.4	4.1	12
D44.1/hen egg lysozyme	10 mM sodium phosphate, 150 mM NaCl, pH 7.1	24.2	-40.6	-43.1	-2.9	12
D11.15/hen egg lysozyme	10 mM sodium phosphate, 150 mM NaCl, pH 7.1	24.9	-50.6	-79.5	-28.7	12
D1.3/E5.2	10 mM sodium phosphate, 150 mM NaCl, pH 7.1	25.0	-43.5	-279.1	-235.0	13
D1.3/E225	10 mM sodium phosphate, 150 mM NaCl, pH 7.1	28.3	-30.5	7.5	38.3	13
Ferredoxin/ferredoxin :NADP$^{+reductase}$	50 mM Tris/HCl, pH 7.5	27.0	-39.1	-1.3	37.8	14
Colicin N/OmpF	20 mM Tris, 300 mM NaCl, 1% octyl-polyoxyethylene, pH 7.4	25.0	-32.4	-51.5	-19.1	15
Colicin N/OmpC	20 mM Tris, 300 mM NaCl, 1% octyl-polyoxyethylene, pH 7.4	25.0	-29.5	-15.5	14.0	15
Colicin N/PhoE	20 mM Tris, 300 mM NaCl, 1% octyl-polyoxyethylene, pH 7.4	25.0	-30.8	-25.0	5.9	15
Barstar/barnase	50 mM Pipes, pH 7.0	25.0	-73.2	-58.0	15.2	16
Human tissue factor/coagulation factor VII	20 mM Tris/HCl, 100 mM NaCl, 5 mM $CaCl_2$, pH 7.5	25.0	-46.9	-133.9	-87.3	17
Cytochrome *c*/cytochrome *c* peroxidase	50 mM ionic strength, potessium phosphate/KNO_3, pH 6.0	26.0	-29.1	9.6	38.8	18
Cytochrome *c*/cytochrome *c* peroxidase	50 mM DMG, pH 6.0	25.0	-32.2	-9.6	22.2	19
Cytochrome *c*/cytochrome *c* peroxidase, site 1	50 mM DMG, 200 mM melezitose, pH 6.0	25.0	-41.8	-15.5	26.3	19
Cytochrome *c*/cytochrome *c* peroxidase, site 2	50 mM DMG, 200 mM melezitose, pH 6.0	25.0	-33.5	-2.5	31.0	19
Cytochrome *c*/cytochrome *b5*	2 mM Tris/HCl, pH 7.4	25.0	-38.1	4.2	42.3	20
Cytochrome *c*/Ab E3	20 mM sodium/potassium phosphate, 0.8% NaCl, 0.02% KCl, pH 7.2	25.0	-40.6	-30.5	11.0	21

Cytochrome *c*/Ab E8	20 mM sodium/potassium phosphate, 0.8% NaCl, 0.02% KCl, pH 7.2	25.0	-39.7	-39.7	0.4	21
Cytochrome *c*/MAb 2B5	100 mM sodium phosphate, pH 7.0	25.0	-52.7	-87.9	-35.2	22
Cytochrome *c*/MAb 5F8	100 mM sodium phosphate, pH 7.0	25.0	-58.2	-90.8	-32.8	22
CheY/$CheA_{1-233}$	20 mM sodium phosphate, 20 mM NaCl, 1 mM EDTA, 1 mM PMSF, 10% (v/v) glycerol, pH 7.4	28.0	-33.9	-51.9	-18.1	23
CheB/$CheA_{1-233}$	20 mM sodium phosphate, 20 mM NaCl, 1 mM EDTA, 1 mM PMSF, 10% (v/v) glycerol, pH 7.4	28.0	-31.4	-42.3	-11.0	23
Interleukin 5-IL5 receptor α subunit	20 mM potassium phosphate, 150 mM NaCl, pH 7.4	25.0	-48.5	-47.7	0.8	24
Erythropoietin/EPO receptor site 1	Dulbecco's phosphate buffered saline, pH 7.0	25.0	-49.0	-6.3	42.7	25
Erythropoietin/EPO receptor site 2	Dulbecco's phosphate buffered saline, pH 7.0	25.0	-35.1	-14.2	21.0	25
Human growth hormone G120R/hGHbp	10 mM sodium phosphate, 137 mM NaCl, 2.7 mM KCl, pH 7.2	26.2	-49.0	-39.3	9.6	26
Phosphocarrier protein/enzyme I N-domain	10 mM potassium phosphate, 100 mM KCl, 1 mM EDTA, pH 7.5	25	-29.3	36.7	66.0	27
Stem cell factor/Kit extracellular domain	Phosphate buffered saline	25	-37.7	-54.4	-16.7	28
Hck SH3 domain/HIV-1 Nef	50 mM HEPES, 150 mM NaCl, 3.4 mM EDTA, 2 mM DTT, pH 7.4	25	-38.5	-53.6	-15.0	29
Fyn SH3 domain/PI3-Kinase p85 subunit	10 mM phosphate, pH 6.0	30	-31.8	44.4	76.4	30
Elastase/ovomucoid third domain	50 mM imidazole chloride, pH 7.0	25	-60.7	-4.2	56.5	31
Chaperonin GroEL/reduced α-lactalbumin	25 mM Tris/HCl, 200 mM KCl, 1 mM DTT, 1 mM EDTA, pH 7.8	10.0	-28.4	49.7	78.1	32
Chaperonin GroEL/reduced α-lactalbumin	25 mM Tris/HCl, 1 mM DTT, 1 mM EDTA, pH 7.8	10.5	-31.6	82.2	113.8	32
Champeronin GroEL/denatured pepsin	25 mM Tris/HCl, 200 mM KCl, 1 mM DTT, 1 mM EDTA, pH 7.8	25.1	-32.1	47.4	79.6	32
Glycoprotein gp120/CD4	3 mM sodium phosphate, 100 mM NaCl, pH 7.4	37.0	-49.4	-263.6	-214.2	33
Dihydrolipoyl dehydrogenase/PSBD of E2	10 mM HEPES, 150 mM NaCl, 3.4 mM EDTA, pH 7.4	25.0	-52.7	9.2	61.9	34
Human factor X/NAPc2	20 mM HEPES, 150 mM NaCl, 2 mM Ca^{2+}, pH 7.4	25.0	-51.7	-57.8	-6.1	35
Human factor Xa/NAPc2	20 mM HEPES, 150 mM NaCl, 2 mM Ca^{2+}, pH 7.4	25.0	-52.0	-71.5	-19.5	35
CBFβ protein/Runx 1 Runt domain	-------	30.0	-42.2	-18.9	23.3	36
CBFβ-$SMMHC_{47}$ protein/Runx 1 Runt domain	-------	30.0	-47.0	-16.9	30.1	36
A. niger xylanase/xylanase-inhibiting protein I	McIlvaine buffer, pH 5.5	25.0	-42.1	-48.5	-6.3	37
α-Hemoglobin stabilizing protein/α-globin	20 mM sodium phosphate buffer, 150 mM NaCl, pH 7.0	20.0	-39.3	-36.6	2.7	38
β-Lactoglobulin/pectin, site 1	5 mM sodium phosphate, pH 4.0	22.0	-43.5	-52.7	-10.5	39
β-Lactoglobulin/pectin, site 2	5 mM sodium phosphate, pH 4.0	22.0	-38.1	-23.0	14.6	39
α-Amylase 2/BASI	40 mM HEPES, 200 mM NaCl, 5 mM $CaCl_2$, pH 6.8	25.0	-45.0	-98.0	-53.0	40
α-Amylase 2/BASI	40 mM sodium acetate, 5 mM $CaCl_2$, pH 5.5	27.0	-43.5	-69.0	-26.0	40
Thrombin/monoclonal antibody	25 mM potassium phosphate, 150 mM NaCl, pH 6.5	25.0	-44.8	-34.3	10.5	41
Xanthine oxidase/Cu, Zn-SOD	10 mM HEPES, 150 mM NaCl, 1 mM EDTA, pH 7.4	25.0	-34.0	-201.1	-161.1	42
Human growth hormone/hGHR ECD1	20 mM HEPES, 150 mM NaCl, pH 7.4	25.0	-51.0	-37.6	13.4	43
E colicin DNase E2/immunity protein Im2	50 mM Mops, 200 mM NaCl, pH 7.0	25.0	-82.2	-161.7	-79.5	44
E colicin DNase E7/immunity protein Im9	50 mM Mops, 200 mM NaCl, pH 7.0	25.0	-82.8	-237.4	-154.4	44
E colicin DNase E9/immunity protein Im9	50 mM Mops, 200 mM NaCl, pH 7.0	25.0	-77.7	-79.5	-1.8	44

Table A.2. Thermodynamic Parameters for Some Protein-Ligand (nonpeptide) Interactions (continues on the next page).

Complex	Solvent	T / °C	ΔG / kJ mol^{-1}	ΔH / kJ mol^{-1}	$T\Delta S$ / kJ mol^{-1}	Ref.
AAC(6')-Iy/kanamycin B	50 mM Tris, 50 mM NaCl, 0.1% $HS(CH_2)_2OH$, 0.01% Tween-80, pH 7.5	27	-29.3	-54.4	-25.1	45
AAC(6')-Iy/tobramycin	50 mM Tris, 50 mM NaCl, 0.1% $HS(CH_2)_2OH$, 0.01% Tween-80, pH 7.5	27	-30.5	-50.6	-20.1	45
AAC(6')-Iy/dibekacin	50 mM Tris, 50 mM NaCl, 0.1% $HS(CH_2)_2OH$, 0.01% Tween-80, pH 7.5	27	-31.0	-53.6	-22.6	45
AAC(6')-Iy/gentamicin C	50 mM Tris, 50 mM NaCl, 0.1% $HS(CH_2)_2OH$, 0.01% Tween-80, pH 7.5	27	-26.8	-33.9	-7.1	45
AAC(6')-Iy/kanamycin A	50 mM Tris, 50 mM NaCl, 0.1% $HS(CH_2)_2OH$, 0.01% Tween-80, pH 7.5	27	-27.6	-40.2	-13.8	45
AAC(6')-Iy/amikacin	50 mM Tris, 50 mM NaCl, 0.1% $HS(CH_2)_2OH$, 0.01% Tween-80, pH 7.5	27	-27.6	-23.8	3.8	45
AAC(6')-Iy/sisomicin	50 mM Tris, 50 mM NaCl, 0.1% $HS(CH_2)_2OH$, 0.01% Tween-80, pH 7.5	27	-30.1	-37.2	-7.1	45
AAC(6')-Iy/netilmicin	50 mM Tris, 50 mM NaCl, 0.1% $HS(CH_2)_2OH$, 0.01% Tween-80, pH 7.5	27	-30.5	-25.1	5.4	45
AAC(6')-Iy/ribostamycin	50 mM Tris, 50 mM NaCl, 0.1% $HS(CH_2)_2OH$, 0.01% Tween-80, pH 7.5	27	-34.7	-83.3	-48.5	45
AAC(6')-Iy/butirosin	50 mM Tris, 50 mM NaCl, 0.1% $HS(CH_2)_2OH$, 0.01% Tween-80, pH 7.5	27	-33.9	-52.7	-18.8	45
AAC(6')-Iy/neomycin B	50 mM Tris, 50 mM NaCl, 0.1% $HS(CH_2)_2OH$, 0.01% Tween-80, pH 7.5	27	-31.4	-61.5	-30.1	45
AAC(6')-Iy/paromomycin	50 mM Tris, 50 mM NaCl, 0.1% $HS(CH_2)_2OH$, 0.01% Tween-80, pH 7.5	27	-28.5	-31.4	-2.9	45
AAC(6')-Iy/lividomycin A	50 mM Tris, 50 mM NaCl, 0.1% $HS(CH_2)_2OH$, 0.01% Tween-80, pH 7.5	27	-30.5	-44.4	-8.8	45
Epoxyalkane:CoM transferase/CoM	50 mM Tris-HCl, pH 8.0	30	-31.4	-102.9	-71.5	46
Epoxyalkane:CoM transferase/ethanethiol	50 mM Tris-HCl, pH 8.0	30	-20.1	-2.5	-17.6	46
Epoxyalkane:CoM transferase/ethanesulfonate	50 mM Tris-HCl, pH 8.0	30	-13.8	-15.1	-1.3	46
Epoxyalkane:CoM transferase/propanethiol	50 mM Tris-HCl, pH 8.0	30	-23.4	-0.8	22.6	46
Biotin holoenzyme synthetase/biotin	10 mM Tris-HCl, 200 mM KCl, 2.5 mM $MgCl_2$, pH 7.5	20	-41.4	-39.3	2.1	47
Biotin holoenzyme synthetase/bio-5'-AMP	10 mM Tris-HCl, 200 mM KCl, 2.5 mM $MgCl_2$, pH 7.5	20	-58.6	-24.3	33.9	47
Adenosine deaminase/inosine	50 mM sodium phosphate, pH 7.5	27	-22.1	-32.0	-9.9	48
YajQ/ATP	50 mM Tris-HCl, pH 7.4	25	-22.8	1.5	24.4	49
DNA gyrase/clorobiocin	20 mM Tris, 1 mM EDTA, pH 7.5	25	-51.0	-39.6	11.4	50
DNA gyrase/RU 64135	20 mM Tris, 1 mM EDTA, pH 7.5	25	-40.3	-18.9	21.4	50
DNA gyrase/RU 64136	20 mM Tris, 1 mM EDTA, pH 7.5	25	-35.1	-18.0	17.1	50
DNA gyrase/novobiocin	20 mM Tris, 1 mM EDTA, pH 7.5	25	-42.7	-51.8	-9.1	50
HIV-1 protease/TMC-126	10 mM sodium acetate, 2% DMSO, pH 5	25	-65.3	-50.2	15.1	51
HIV-1 protease/amprenavir	10 mM sodium acetate, 2% DMSO, pH 5	25	-55.2	-28.9	26.4	51
Peanut agglutinin/ Galactose	20 mM citrate buffer, pH 7.4	25	-17.0	-23.0	-6.0	52
Peanut agglutinin/ GalEMA	20 mM citrate buffer, pH 7.4	25	-21.4	-39.4	-18	52
Peanut agglutinin/ pGalEMA-A	20 mM citrate buffer, pH 7.4	25	-26.6	-5.8	20.8	52
Peanut agglutinin/ pGalEMA-B	20 mM citrate buffer, pH 7.4	25	-22.7	-19.8	2.8	52
Peanut agglutinin/ Galactose$_c$	20 mM citrate buffer, 150 mM NaCl, pH 7.4	25	-16.5	-23.9	-7.4	52
Peanut agglutinin/ pGalEMA-A	20 mM citrate buffer, 150 mM NaCl, pH 7.4	25	-21.7	-10.8	10.9	52
Peanut agglutinin/ pGalEMA-B	20 mM citrate buffer, 150 mM NaCl, pH 7.4	25	-21.2	-8.3	12.9	52

Peanut agglutinin/ pGalEMA-A	20 mM citrate buffer, 150 mM NaCl, pH 7.4, heats of dilution subtracted	25	-20.6	-6.4	14.2	52
Peanut agglutinin/ pGalEMA-A	50 mM Tris-HCl buffer, 500mM $MgCl_2$, 1mM $MnCl_2$, 1mM $CaCl_2$, pH 6.9	25	-17.9	-15.8	2.1	52
Peanut agglutinin/ pGalEMA-A	50 mM Tris-HCl buffer, 500mM $MgCl_2$, 1mM $MnCl_2$, 1mM $CaCl_2$, pH 6.9, heats of dilution subtracted	25	-18.6	-42.6	-24.0	52
Wild-Type MUP/ IBMP	PBS, pH 7.4	35	-38.5	-47.9	-9.4	53
Y120F MUP/ IBMP	PBS, pH 7.4	15	-34.9	-25.8	9.1	53
Y120F MUP/ IBMP	PBS, pH 7.4	25	-35.3	-31.4	3.9	53
Y120F MUP/ IBMP	PBS, pH 7.4	35	-33.6	-35.9	-2.3	53
Rho/ Bicyclomycin	40 mM Tris HCl 400 mM KCl, 0.1 mM EDTA, and 0.1 mM DTT, pH 7.9	26	-25.1	-3.3	21.8	54
Rho/ Bicyclomycin analogue	40 mM Tris HCl 400 mM KCl, 0.1 mM EDTA, and 0.1 mM DTT, pH 7.9	26	-32.2	-11.5	20.7	54
BirA/ Biotin	10 mM Tris-HCl, 200 mM KCl, 2.5 mM MgCl2, pH 7.50	20	-41.4	-80.3	-38.9	55
BirA/ Btn-SA	10 mM Tris-HCl, 200 mM KCl, 2.5 mM MgCl2, pH 7.50	20	-40.6	-83.3	-42.7	55
BirA/ BtnOH-AMP	10 mM Tris-HCl, 200 mM KCl, 2.5 mM MgCl2, pH 7.50	20	-49.5	-41.4	7.9	55
BirA/ Bio-5'-AMP	10 mM Tris-HCl, 200 mM KCl, 2.5 mM MgCl2, pH 7.50	20	-58.2	-51.5	6.7	55
ConA/methyl α-D-mannopyranoside	0.1 M sodium acetate, 0.1 M NaCl, 5 mM each $CaCl_2$ and $MnCl_2$, pH 5.2	27	-23.4	-35.1	-11.7	56
ConA/ Bivalant sugar derivative 1	0.1 M sodium acetate, 0.1 M NaCl, 5 mM each $CaCl_2$ and $MnCl_2$, pH 5.2	27	-25.1	-46.9	-21.8	56
ConA/ Bivalant sugar derivative 2	0.1 M sodium acetate, 0.1 M NaCl, 5 mM each $CaCl_2$ and $MnCl_2$, pH 5.2	27	-25.1	-59.0	-33.9	56
ConA/ Bivalant sugar derivative 3	0.1 M sodium acetate, 0.1 M NaCl, 5 mM each $CaCl_2$ and $MnCl_2$, pH 5.2	27	-24.7	-53.1	-28.0	56
ConA/ Bivalant sugar derivative 4	0.1 M sodium acetate, 0.1 M NaCl, 5 mM each $CaCl_2$ and $MnCl_2$, pH 5.2	27	-25.1	-47.7	-22.6	56
ConA/ Bivalant sugar derivative 5	0.1 M sodium acetate, 0.1 M NaCl, 5 mM each $CaCl_2$ and $MnCl_2$, pH 5.2	27	-26.4	-43.1	-16.7	56
ConA/ Bivalant sugar derivative 6	0.1 M sodium acetate, 0.1 M NaCl, 5 mM each $CaCl_2$ and $MnCl_2$, pH 5.2	27	-26.8	-56.1	-29.3	56
ConA/ Bivalant sugar derivative 7	0.1 M sodium acetate, 0.1 M NaCl, 5 mM each $CaCl_2$ and $MnCl_2$, pH 5.2	27	-26.8	-61.5	-34.7	56
ConA/ Bivalant sugar derivative 8	0.1 M sodium acetate, 0.1 M NaCl, 5 mM each $CaCl_2$ and $MnCl_2$, pH 5.2	27	-27.2	-63.6	-36.4	56
ConA/ Bivalant sugar derivative 9	0.1 M sodium acetate, 0.1 M NaCl, 5 mM each $CaCl_2$ and $MnCl_2$, pH 5.2	27	-26.8	-71.1	-44.4	56
ConA/ Bivalant sugar derivative 10	0.1 M sodium acetate, 0.1 M NaCl, 5 mM each $CaCl_2$ and $MnCl_2$, pH 5.2	27	-27.2	-69.5	-42.3	56
ConA/ Bivalant sugar derivative 11	0.1 M sodium acetate, 0.1 M NaCl, 5 mM each $CaCl_2$ and $MnCl_2$, pH 5.2	27	-27.6	-64.4	-36.8	56
ConA/ Bivalant sugar derivative 12	0.1 M sodium acetate, 0.1 M NaCl, 5 mM each $CaCl_2$ and $MnCl_2$, pH 5.2	27	-27.6	-59.8	-32.2	56
ConA/ Bivalant sugar derivative 13	0.1 M sodium acetate, 0.1 M NaCl, 5 mM each $CaCl_2$ and $MnCl_2$, pH 5.2	27	-27.2	-66.5	-39.3	56
DGL/methyl α-D-mannopyranoside	0.1 M sodium acetate, 0.1 M NaCl, 5 mM each $CaCl_2$ and $MnCl_2$, pH 5.2	27	-20.5	-34.3	-13.8	56
DGL/ Bivalant sugar derivative 1	0.1 M sodium acetate, 0.1 M NaCl, 5 mM each $CaCl_2$ and $MnCl_2$, pH 5.2	27	-24.3	-42.3	-18.0	56
DGL/ Bivalant sugar derivative 2	0.1 M sodium acetate, 0.1 M NaCl, 5 mM each $CaCl_2$ and $MnCl_2$, pH 5.2	27	-24.7	-45.2	-20.5	56
DGL/ Bivalant sugar derivative 3	0.1 M sodium acetate, 0.1 M NaCl, 5 mM each $CaCl_2$ and $MnCl_2$, pH 5.2	27	-24.7	-46.9	-22.2	56
DGL/ Bivalant sugar derivative 4	0.1 M sodium acetate, 0.1 M NaCl, 5 mM each $CaCl_2$ and $MnCl_2$, pH 5.2	27	-23.8	-46.0	-22.2	56
DGL/ Bivalant sugar derivative 5	0.1 M sodium acetate, 0.1 M NaCl, 5 mM each $CaCl_2$ and $MnCl_2$, pH 5.2	27	-26.4	-43.5	-17.2	56
DGL/ Bivalant sugar derivative 6	0.1 M sodium acetate, 0.1 M NaCl, 5 mM each $CaCl_2$ and $MnCl_2$, pH 5.2	27	-27.2	-48.5	-21.3	56
DGL/ Bivalant sugar derivative 7	0.1 M sodium acetate, 0.1 M NaCl, 5 mM each $CaCl_2$ and $MnCl_2$, pH 5.2	27	-28.0	-54.0	-25.9	56
DGL/ Bivalant sugar derivative 8	0.1 M sodium acetate, 0.1 M NaCl, 5 mM each $CaCl_2$ and $MnCl_2$, pH 5.2	27	-28.9	-61.9	-33.0	56
DGL/ Bivalant sugar derivative 9	0.1 M sodium acetate, 0.1 M NaCl, 5 mM each $CaCl_2$ and $MnCl_2$, pH 5.2	27	-23.8	-59.8	-36.0	56
DGL/ Bivalant sugar derivative 10	0.1 M sodium acetate, 0.1 M NaCl, 5 mM each $CaCl_2$ and $MnCl_2$, pH 5.2	27	-25.1	-61.9	-36.8	56

DGL/ Bivalant sugar derivative 11	0.1 M sodium acetate, 0.1 M NaCl, 5 mM each $CaCl_2$ and $MnCl_2$, pH 5.2	27	-26.8	-65.3	-38.5	56
DGL/ Bivalant sugar derivative 12	0.1 M sodium acetate, 0.1 M NaCl, 5 mM each $CaCl_2$ and $MnCl_2$, pH 5.2	27	-25.9	-50.2	-24.3	56
DGL/ Bivalant sugar derivative 13	0.1 M sodium acetate, 0.1 M NaCl, 5 mM each $CaCl_2$ and $MnCl_2$, pH 5.2	27	-25.1	-64.0	-38.9	56
BSA/ Naproxen	50 mM sodium phosphate buffer, pH 7.4.	25	-44.8	-50.7	-5.8	57
TtgV/ 1-Naphthol	25mM Tris-HOAc,8mM $Mg(OAc)_2$,1mM KCl,1mM dithiothreitol,pH 8.0	30	-31.4	-36.0	-4.6	58
TtgV-DNA complex/ 1-Naphthol	25mM Tris-HOAc,8mM $Mg(OAc)_2$,1mM KCl,1mM dithiothreitol,pH 8.0	30	-30.5	-21.8	8.8	58
TtgV/ 2,3-Dihydroxynaphthalene	25mM Tris-HOAc,8mM $Mg(OAc)_2$,1mM KCl,1mM dithiothreitol,pH 8.0	30	-32.2	-3.4	28.9	58
TtgV/ 4-Nitrotoluene	25mM Tris-HOAc,8mM $Mg(OAc)_2$,1mM KCl,1mM dithiothreitol,pH 8.0	30	-26.8	-62.3	-35.6	58
TtgV/ Benzonitrile	25mM Tris-HOAc,8mM $Mg(OAc)_2$,1mM KCl,1mM dithiothreitol,pH 8.0	30	-24.3	-52.3	-28.0	58
TtgV/ Indole	25mM Tris-HOAc,8mM $Mg(OAc)_2$,1mM KCl,1mM dithiothreitol,pH 8.0	30	-23.8	-54.4	-30.5	58
TtgV/ Tolune	25mM Tris-HOAc,8mM $Mg(OAc)_2$,1mM KCl,1mM dithiothreitol,pH 8.0	30	-22.6	-26.4	-3.8	58
TtgV/ 1-Hexanol	25mM Tris-HOAc,8mM $Mg(OAc)_2$,1mM KCl,1mM dithiothreitol,pH 8.0	30	-17.2	-62.3	-45.2	58
Porcine odorant binding protein/ Halothane	130 mm NaCl, 20 mm sodium phosphate, pH 7.0	20	-23.0	-5.9	17.2	59
Porcine odorant binding protein/ Isoflurane	130 mm NaCl, 20 mm sodium phosphate, pH 7.0	20	-22.6	-10.0	12.6	59
Tetracycline Repressor/ Tetracycline	10 mM Tris, 150 mM NaCl, and 2 mM DTT with 1 mM EDTA, pH 8.0	25	-27.7	-32.9	-5.3	60
Tetracycline Repressor/ Tetracycline with Mg^{2+}	10 mM Tris, 150 mM NaCl, and 2 mM DTT with 10 mM $MgCl_2$, pH 8.0	25	-39.7	-51.5	-11.6	60
β-trypsin/ Benzamidine/ Glycine-0.00	50 mM Tris buffer, with 25 mM $CaCl_2$, at pH 8.0	25	-26.8	-15.2	11.6	61
β-trypsin/ Benzamidine/ Glycine-0.25	50 mM Tris buffer, with 25 mM $CaCl_2$, at pH 8.0	25	-26.8	-12.5	14.3	61
β-trypsin/ Benzamidine/ Glycine-0.50	50 mM Tris buffer, with 25 mM $CaCl_2$, at pH 8.0	25	-26.1	-7.1	19.1	61
β-trypsin/ Benzamidine/ Glycine-1.00	50 mM Tris buffer, with 25 mM $CaCl_2$, at pH 8.0	25	-25.7	-6.5	19.2	61
β-trypsin/ Benzamidine/ Glucose-0.00	50 mM Tris buffer, with 25 mM $CaCl_2$, at pH 8.0	25	-26.8	-15.2	11.6	61
β-trypsin/ Benzamidine/ Glucose-0.38	50 mM Tris buffer, with 25 mM $CaCl_2$, at pH 8.0	25	-26.7	-15.2	11.6	61
β-trypsin/ Benzamidine/ Glucose-0.75	50 mM Tris buffer, with 25 mM $CaCl_2$, at pH 8.0	25	-26.2	-11.4	14.7	61
β-trypsin/ Berenil/ Glycine-0.00	50 mM Tris buffer, with 25 mM $CaCl_2$, at pH 8.0	25	-33.0	-17.2	15.8	61
β-trypsin/ Berenil/ Glycine-0.38	50 mM Tris buffer, with 25 mM $CaCl_2$, at pH 8.0	25	-32.8	-12.3	20.5	61
β-trypsin/ Berenil/ Glycine-0.75	50 mM Tris buffer, with 25 mM $CaCl_2$, at pH 8.0	25	-32.2	-12.3	19.9	61
β-trypsin/ Berenil/ Glycine-1.00	50 mM Tris buffer, with 25 mM $CaCl_2$, at pH 8.0	25	-32.2	-10.0	22.2	61
β-trypsin/ Berenil/ Glucose-0.00	50 mM Tris buffer, with 25 mM $CaCl_2$, at pH 8.0	25	-33.0	-17.2	15.8	61
β-trypsin/ Berenil/ Glucose-0.25	50 mM Tris buffer, with 25 mM $CaCl_2$, at pH 8.0	25	-32.2	-18.3	13.9	61
β-trypsin/ Berenil/ Glucose-0.50	50 mM Tris buffer, with 25 mM $CaCl_2$, at pH 8.0	25	-32.0	-14.1	17.9	61
β-trypsin/ Berenil/ Glucose-1.00	50 mM Tris buffer, with 25 mM $CaCl_2$, at pH 8.0	25	-32.2	-10.5	21.7	61
MUP-I-wild type/SBT	10 mM phosphate, 0.02% NaN_3, pH 6.3	30	-34.7	-45.6	-10.9	62
MUP-I-wild type/HMH	10 mM phosphate, 0.02% NaN_3, pH 6.3	30	-25.1	-54.4	-29.3	62
MUP-I/ IPMP	PBS, pH 7.4	35	-33.9	-44.5	-10.6	63
MUP-I/IBMP	PBS, pH 7.4	35	-38.5	-47.9	-9.4	63
Integrin I-domain/ inhibitor **1**	20 mM Tris base, 150 mM NaCl, and 1 mM MgCl2, 2% DMSO, pH 7.5	30	-44.9	-32.2	12.7	64
GH1 β-glucosidase/Aza sugar glycosidase inhibitor **6**	100 mM sodium citrate buffer, pH 5.8	27	-41.2	-28.5	12.9	65
GH1 β-glucosidase/Aza sugar glycosidase inhibitor **1**	100 mM sodium citrate buffer, pH 5.8	27	-36.3	-46.7	-10.5	65

GH1 β-glucosidase/Aza sugar glycosidase inhibitor **5**	100 mM sodium citrate buffer, pH 5.8	27	-29.0	-33.2	-3.9	65
Cellobiohydrolase I / (*S*)-alprenolol	sodium acetate buffer, pH 5.5	25	-24.1	17.6	42.4	66
Cellobiohydrolase I / (*S*)-alprenolol	sodium acetate buffer, pH 5.8	25	-25.2	20.5	44.9	66
Cellobiohydrolase I / (*S*)-alprenolol	sodium acetate buffer, pH 6.8	25	-26.9	38.9	66.1	66
Cellobiohydrolase I / (*R*)-alprenolol	sodium acetate buffer, pH 6.8	25	-21.3	8.4	29.9	66
HIV protease 1/ APV	10mM Na acetate, 2%DMSO, 2mM Tris(2-carboxyethyl)phosphine, pH 5	20	-52.7	-30.5	22.2	67
HIV protease 1/ TMC114	10mM Na acetate, 2%DMSO, 2mM Tris(2-carboxyethyl)phosphine, pH 5	20	-63.6	-50.6	13.0	67
hGSTA1-1_High-affinity site/ BSP	sodium phosphate, 150 mM NaCl , pH 6.5	20	-38.9	-23.5	15.5	68
hGSTA1-1_Low-affinity site/ BSP	sodium phosphate, 150 mM NaCl , pH 6.5	20	-28.3	-7.2	19.7	68
HAS/ Halothane (variable n)	20 mM Sodium phosphate buffer, 130 mM NaCl, pH 7.0	20	-15.6	-5.5	10.2	69
HAS/ Halothane (fixed n)	20 mM Sodium phosphate buffer, 130 mM NaCl, pH 7.0	20	-15.6	-6.0	9.6	69
HAS/ Propofol	20 mM Sodium phosphate buffer, 130 mM NaCl, pH 7.0	20	-23.5	-21.8	1.7	69
APH(3')-IIIa (Binary Complex)/ kanamycine A	50 mM Tris buffer, 100 mM KCl, pH 7.5	37	-31.0	-138.1	-107.1	70
APH(3')-IIIa (Binary Complex)/ kanamycine A	50 mM Bicine buffer, 100 mM KCl, pH 7.5	37	-31.4	-160.2	-128.9	70
APH(3')-IIIa (Binary Complex)/ kanamycine B	50 mM Tris buffer, 100 mM KCl, pH 7.5	37	-38.5	-93.7	-55.2	70
APH(3')-IIIa (Binary Complex)/ kanamycine B	50 mM Bicine buffer, 100 mM KCl, pH 7.5	37	-37.7	-128.9	-91.2	70
APH(3')-IIIa (Binary Complex)/ tobramycin	50 mM Tris buffer, 100 mM KCl, pH 7.5	37	-36.4	-122.2	-85.8	70
APH(3')-IIIa (Binary Complex)/ tobramycin	50 mM Bicine buffer, 100 mM KCl, pH 7.5	37	-36.8	-155.2	-118.4	70
APH(3')-IIIa (Binary Complex)/ amikacin	50 mM Tris buffer, 100 mM KCl, pH 7.5	37	-23.8	-81.6	-57.7	70
APH(3')-IIIa (Binary Complex)/ amikacin	50 mM Bicine buffer, 100 mM KCl, pH 7.5	37	-25.9	-78.7	-52.7	70
APH(3')-IIIa (Binary Complex)/ ribostamycin	50 mM Tris buffer, 100 mM KCl, pH 7.5	37	-33.9	-125.9	-92.0	70
APH(3')-IIIa (Binary Complex)/ ribostamycin	50 mM Bicine buffer, 100 mM KCl, pH 7.5	37	-33.9	-117.6	-83.7	70
APH(3')-IIIa (Binary Complex)/ meomycine B	50 mM Tris buffer, 100 mM KCl, pH 7.5	37	-38.9	-139.7	-100.8	70
APH(3')-IIIa (Binary Complex)/ meomycine B	50 mM Bicine buffer, 100 mM KCl, pH 7.5	37	-38.9	-181.2	-142.3	70
APH(3')-IIIa (Binary Complex)/ paromomycine I	50 mM Tris buffer, 100 mM KCl, pH 7.5	37	-37.7	-127.2	-89.5	70
APH(3')-IIIa (Binary Complex)/ paromomycine I	50 mM Bicine buffer, 100 mM KCl, pH 7.5	37	-38.9	-152.3	-113.4	70
APH(3')-IIIa (Binary Complex)/ lividomycine A	50 mM Tris buffer, 100 mM KCl, pH 7.5	37	-36.0	-140.6	-104.6	70
APH(3')-IIIa (Binary Complex)/ lividomycine A	50 mM Bicine buffer, 100 mM KCl, pH 7.5	37	-36.8	-184.5	-147.7	70
APH(3')-IIIa (Ternery Complex)/ kanamycine A	50 mM Tris buffer, 100 mM KCl, pH 7.5	37	-35.6	-39.3	-3.8	70
APH(3')-IIIa (Ternery Complex)/ kanamycine A	50 mM Bicine buffer, 100 mM KCl, pH 7.5	37	-34.7	-79.5	-44.8	70
APH(3')-IIIa (Ternery Complex)/ kanamycine B	50 mM Tris buffer, 100 mM KCl, pH 7.5	37	-39.3	-34.3	5.0	70
APH(3')-IIIa (Ternery Complex)/ kanamycine B	50 mM Bicine buffer, 100 mM KCl, pH 7.5	37	-38.1	-73.2	-35.1	70
APH(3')-IIIa (Ternery Complex)/ tobramycin	50 mM Tris buffer, 100 mM KCl, pH 7.5	37	-39.3	-38.1	1.3	70
APH(3')-IIIa (Ternery Complex)/ tobramycin	50 mM Bicine buffer, 100 mM KCl, pH 7.5	37	-37.2	-78.2	-41.0	70
APH(3')-IIIa (Ternery Complex)/ amikacin	50 mM Tris buffer, 100 mM KCl, pH 7.5	37	-26.4	-20.1	6.3	70
APH(3')-IIIa (Ternery Complex)/ amikacin	50 mM Bicine buffer, 100 mM KCl, pH 7.5	37	-27.2	-63.2	-36.0	70
APH(3')-IIIa (Ternery Complex)/ ribostamycin	50 mM Tris buffer, 100 mM KCl, pH 7.5	37	-38.9	-48.5	-9.6	70
APH(3')-IIIa (Ternery Complex)/ ribostamycin	50 mM Bicine buffer, 100 mM KCl, pH 7.5	37	-37.2	-54.0	-16.7	70
APH(3')-IIIa (Ternery Complex)/ meomycine B	50 mM Tris buffer, 100 mM KCl, pH 7.5	37	-41.0	-51.0	-10.0	70

APH(3')-IIIa (Ternery Complex)/ meomycine B	50 mM Bicine buffer, 100 mM KCl, pH 7.5	37	-38.9	-95.8	-56.9	70
APH(3')-IIIa (Ternery Complex)/ paromomycine I	50 mM Tris buffer, 100 mM KCl, pH 7.5	37	-40.6	-48.1	-7.5	70
APH(3')-IIIa (Ternery Complex)/ paromomycine I	50 mM Bicine buffer, 100 mM KCl, pH 7.5	37	-41.0	-78.7	-37.7	70
APH(3')-IIIa (Ternery Complex)/ lividomycine A	50 mM Tris buffer, 100 mM KCl, pH 7.5	37	-36.4	-43.9	-7.5	70
APH(3')-IIIa (Ternery Complex)/ lividomycine A	50 mM Bicine buffer, 100 mM KCl, pH 7.5	37	-37.2	-92.5	-55.2	70
APH(3')-IIIa (Ternery Complex)/ kanamycine A	50 mM Tris buffer, 100 mM KCl, pH 8.5	37	-27.2	-15.5	11.7	70
APH(3')-IIIa (Ternery Complex)/ kanamycine A	50 mM Bicine buffer, 100 mM KCl, pH 8.5	37	-27.2	-72.0	-44.8	70
APH(3')-IIIa (Ternery Complex)/ kanamycine B	50 mM Tris buffer, 100 mM KCl, pH 8.5	37	-29.7	-35.6	-5.4	70
APH(3')-IIIa (Ternery Complex)/ kanamycine B	50 mM Bicine buffer, 100 mM KCl, pH 8.5	37	-31.8	-109.6	-77.8	70
APH(3')-IIIa (Ternery Complex)/ tobramycin	50 mM Tris buffer, 100 mM KCl, pH 8.5	37	-29.3	-29.3	-0.4	70
APH(3')-IIIa (Ternery Complex)/ tobramycin	50 mM Bicine buffer, 100 mM KCl, pH 8.5	37	-31.0	-106.3	-75.3	70
APH(3')-IIIa (Ternery Complex)/ meomycine B	50 mM Tris buffer, 100 mM KCl, pH 8.5	37	-37.2	-46.4	-9.2	70
APH(3')-IIIa (Ternery Complex)/ meomycine B	50 mM Bicine buffer, 100 mM KCl, pH 8.5	37	-40.2	-129.3	-89.1	70
APH(3')-IIIa (Ternery Complex)/ paromomycine I	50 mM Tris buffer, 100 mM KCl, pH 8.5	37	-32.6	-45.6	-13.0	70
APH(3')-IIIa (Ternery Complex)/ paromomycine I	50 mM Bicine buffer, 100 mM KCl, pH 8.5	37	-33.9	-116.3	-82.4	70
Tetrameric human PAH/ BH_4	20 mM NaHepes, 0.2 M NaCl, pH 7.0	5	-33.1	-23.8	9.1	71
Tetrameric human PAH/ BH_4	20 mM NaHepes, 0.2 M NaCl, pH 7.0	15	-34.5	-33.8	0.8	71
Tetrameric human PAH/ BH_4	20 mM NaHepes, 0.2 M NaCl, pH 7.0	25	-35.0	-49.3	-14.3	71
Tetrameric human PAH/ BH_4	20 mM NaHepes, 0.2 M NaCl, pH 7.0	35	-35.2	-68.8	-33.6	71
Tetrameric human PAH/ 6M-PH_4	20 mM NaHepes, 0.2 M NaCl, pH 7.0	10	-28.2	-9.0	19.1	71
Tetrameric human PAH/ 6M-PH_4	20 mM NaHepes, 0.2 M NaCl, pH 7.0	25	-27.3	-14.0	13.3	71
Tetrameric human PAH/ 6M-PH_4	20 mM NaHepes, 0.2 M NaCl, pH 7.0	35	-28.7	-15.5	13.2	71
Tetrameric human PAH/ BH_4	20 mM MES, 0.2 M NaCl, pH 6.0	25	-29.4	-40.8	-11.8	71
Tetrameric human PAH/ BH_4	20 mM NaPhosphate, 0.2 M NaCl, pH 6.5	25	-33.8	-42.8	-8.9	71
Tetrameric human PAH/ BH_4	20 mM NaHepes, 0.2 M NaCl, pH 7.5	25	-33.9	-41.3	-7.4	71
Tetrameric human PAH/ BH_4	20 mM NaHepes, 0.2 M NaCl, pH 8.0	25	-35.7	-43.9	-8.1	71
Tetrameric human PAH/ 6M-PH_4	20 mM NaHepes, 0.2 M NaCl, pH 8.0	25	-27.8	-12.7	15.1	71
Tetrameric human PAH/ BH_4	20 mM Hepes, 200 mM NaCl, pH 7.0, 1 mM L-Phe	25	-31.8	-27.7	4.1	71
Tetrameric human PAH/ 6M-PH_4	20 mM Hepes, 200 mM NaCl, pH 7.0, 1mM L-Phe	25	-27.6	-7.7	19.8	71
wt FabI/ PD048890	10 mM Na-phosphate Buffer, 2% DMSO, 1 mM EDTA, and 1% Glycerol, 0.5 mM NAD+, pH 7.5	15	-41.7	-42.5	-0.7	72
wt FabI/ PD048890	10 mM Na-phosphate Buffer, 2% DMSO, 1 mM EDTA, and 1% Glycerol, 0.5 mM NAD+, pH 7.5	20	-40.8	-56.9	-15.9	72
wt FabI/ PD048890	10 mM Na-phosphate Buffer, 2% DMSO, 1 mM EDTA, and 1% Glycerol, 0.5 mM NAD+, pH 7.5	25	-39.0	-84.9	-45.8	72
wt FabI/ PD048890	10 mM Na-phosphate Buffer, 2% DMSO, 1 mM EDTA, and 1% Glycerol, 0.5 mM NAD+, pH 7.5	30	-40.5	-95.0	-54.5	72
wt FabI/ PD0200828	10 mM Na-phosphate Buffer, 2% DMSO, 1 mM EDTA, and 1% Glycerol, 0.5 mM NAD+, pH 7.5	20	-46.6	-72.8	-26.1	72

wt FabI/ PD200828	10 mM Na-phosphate Buffer, 2% DMSO, 1 mM EDTA, and 1% Glycerol, 0.5 mM NAD+, pH 7.5	25	-45.8	-81.2	-35.4	72
wt FabI/ PD200828	10 mM Na-phosphate Buffer, 2% DMSO, 1 mM EDTA, and 1% Glycerol, 0.5 mM NAD+, pH 7.5	30	-46.5	-106.3	-59.8	72
wt FabI/ PD2002165	10 mM Na-phosphate Buffer, 2% DMSO, 1 mM EDTA, and 1% Glycerol, 0.5 mM NAD+, pH 7.5	25	-50.2	-73.2	-23.1	72
wt FabI/ PD2002165	10 mM Na-phosphate Buffer, 2% DMSO, 1 mM EDTA, and 1% Glycerol, 0.5 mM NAD+, pH 7.5	27.5	-49.5	-88.3	-38.8	72
wt FabI/ PD2002165	10 mM Na-phosphate Buffer, 2% DMSO, 1 mM EDTA, and 1% Glycerol, 0.5 mM NAD+, pH 7.5	30	-48.2	-98.3	-50.1	72
wt FabI/ PD205405	10 mM Na-phosphate Buffer, 2% DMSO, 1 mM EDTA, and 1% Glycerol, 0.5 mM NAD+, pH 7.5	25	-49.0	-68.7	-19.8	72
wt FabI/ PD205405	10 mM Na-phosphate Buffer, 2% DMSO, 1 mM EDTA, and 1% Glycerol, 0.5 mM NAD+, pH 7.5	27.5	-46.0	-81.6	-35.6	72
wt FabI/ PD205405	10 mM Na-phosphate Buffer, 2% DMSO, 1 mM EDTA, and 1% Glycerol, 0.5 mM NAD+, pH 7.5	30	-48.8	-93.3	-44.5	72
BSA/ desflurane	150 mM NaCl and 10 mM HEPES at pH 7.2	20	-19.3	-12.7	6.6	73
BSA/ isoflurane	150 mM NaCl and 10 mM HEPES at pH 7.2	20	-17.5	-16.5	1.0	73
BSA/ enflurane	150 mM NaCl and 10 mM HEPES at pH 7.2	20	-16.6	-25.0	-8.4	73
BSA/halothane	150 mM NaCl and 10 mM HEPES at pH 7.2	20	-14.6	-26.1	-11.5	73
BSA/sevoflurane	150 mM NaCl and 10 mM HEPES at pH 7.2	20	-13.6	-18.0	-4.4	73
HSA/ desflurane	150 mM NaCl and 10 mM HEPES at pH 7.2	20	-20.0	-15.4	4.6	73
HSA/ isoflurane	150 mM NaCl and 10 mM HEPES at pH 7.2	20	-18.5	-15.6	2.9	73
HSA/ enflurane	150 mM NaCl and 10 mM HEPES at pH 7.2	20	-17.8	-22.0	-4.2	73
HSA/halothane	150 mM NaCl and 10 mM HEPES at pH 7.2	20	-14.9	-20.4	-5.5	73
HSA/sevoflurane	150 mM NaCl and 10 mM HEPES at pH 7.2	20	-15.1	-7.1	7.9	73
Disabled-1 PTB native/ PI-4,5P2	20 mM PIPES buffer, 150 mM NaCl, 0.2 mM DTT, pH 7.0	25	-33.8	-80.3	-46.4	74
Disabled-1 PTB mutant H81A/ PI-4,5P2	20 mM PIPES buffer, 150 mM NaCl, 0.2 mM DTT, pH 7.0	25	-26.4	-46.9	-19.2	74
Disabled-1 PTB mutant H81Q/ PI-4,5P2	20 mM PIPES buffer, 150 mM NaCl, 0.2 mM DTT, pH 7.0	25	-27.1	-41.0	-14.2	74
Disabled-1 PTB mutant S114Y/ PI-4,5P2	20 mM PIPES buffer, 150 mM NaCl, 0.2 mM DTT, pH 7.0	25	-33.8	-102.1	-68.2	74
Disabled-1 PTB mutant F158V/ PI-4,5P2	20 mM PIPES buffer, 150 mM NaCl, 0.2 mM DTT, pH 7.0	25	-35.5	-75.7	-40.2	74
HAS/ Sodium Penicillins Cloxacillin, first binding	Aqueous Buffered Solutions, pH 4.5	25	-21.7	-0.4	21.3	75
HAS/ Sodium Penicillins Cloxacillin, second binding	Aqueous Buffered Solutions, pH 4.5	25	-19.1	-0.1	19.0	75
HSA/ Sodium Penicillins Cloxacillin, first binding	Aqueous Buffered Solutions, pH 7.4	25	-20.5	-0.1	20.4	75
HSA/ Sodium Penicillins Cloxacillin, second binding	Aqueous Buffered Solutions, pH 7.4	25	-16.6	-0.1	16.5	75
HSA/ Sodium Penicillins Dicloxacillin, first binding	Aqueous Buffered Solutions, pH 4.5	25	-22.3	-0.3	22.0	75
HSA/ Sodium Penicillins Dicloxacillin, 2nd bindin	Aqueous Buffered Solutions, pH 4.5	25	-19.5	-0.1	19.4	75

HSA/ Sodium Penicillins Dicloxacillin, first binding	Aqueous Buffered Solutions, pH 7.4	25	-21.0	-0.1	20.9	75
HSA/ Sodium Penicillins Dicloxacillin, second binding	Aqueous Buffered Solutions, pH 7.4	25	-17.5	-0.1	17.4	75
S. japonicum-GST/ ANS	Standard phosphate buffer, pH 6.5	25	-20.0	-52.4	-32.4	76
S. japonicum-GST/ ANS	Standard phosphate buffer, pH 6.5	30	-19.9	-57.2	-37.2	76
S. japonicum-GST/ ANS	Standard phosphate buffer, pH 6.5	35	-20.0	-64.8	-44.8	76
S. japonicum-GST/ ANS	Standard phosphate buffer, pH 6.5	40	-20.2	-70.3	-50.1	76
S. japonicum-GST/ BS	Standard phosphate buffer, pH 6.5	25	-30.2	-12.0	18.2	76
S. japonicum-GST/ BS	Standard phosphate buffer, pH 6.5	30	-29.5	-29.1	0.5	76
S. japonicum-GST/ BS	Standard phosphate buffer, pH 6.5	35	-30.7	-38.7	-8.1	76
S. japonicum-GST/ BS	Standard phosphate buffer, pH 6.5	40	-33.5	-49.0	-15.6	76
Wild-Type HasASM/ Heme	Sodium Phosphate Buffer, pH 7.3	25	-61.1	-105.4	-44.3	77
H32A Mutated HasASM/ Heme	Sodium Phosphate Buffer, pH 7.3	25	-57.1	-72.2	-15.1	77
Y75A Mutated HasASM/ Heme	Sodium Phosphate Buffer, pH 7.3	25	-46.4	-74.4	-28.0	77
H83A Mutated HasASM/ Heme	Sodium Phosphate Buffer, pH 7.3	25	-47.3	-62.2	-14.9	77
H83Q Mutated HasASM/ Heme	Sodium Phosphate Buffer, pH 7.3	25	-48.7	-89.1	-40.4	77
H32A-Y75A Mutated HasASM/ Heme	Sodium Phosphate Buffer, pH 7.3	25	-27.2	-25.8	-1.4	77
H32A-H83A Mutated HasASM/ Heme	Sodium Phosphate Buffer, pH 7.3	25	-42.0	-41.1	-0.9	77
H32A-H83Q Mutated HasASM/ Heme	Sodium Phosphate Buffer, pH 7.3	25	-42.3	-29.2	13.1	77
Y75A-H83A Mutated HasASM/ Heme	Sodium Phosphate Buffer, pH 7.3	25	-35.7	-35.0	0.6	77
Y75A-H83Q Mutated HasASM/ Heme	Sodium Phosphate Buffer, pH 7.3	25	-36.9	-54.0	-17.0	77
Glycyl-tRNA Synthetase/ ATP	20 mM HEPES-KOH, 5 mM MgCl2, 0.5 mM DTT, 50 mM NaCl, pH 7.2	25	-30.6	-72.0	-36.9	78
Glycyl-tRNA Synthetase/ AMPPNP	20 mM HEPES-KOH, 5 mM MgCl2, 0.5 mM DTT, 50 mM NaCl, pH 7.2	25	-31.7	-68.0	-38.9	78
Glycyl-tRNA Synthetase/ AMPPCP	20 mM HEPES-KOH, 5 mM MgCl2, 0.5 mM DTT, 50 mM NaCl, pH 7.2	25	-36.3	-70.7	-31.7	78
Glycyl-tRNA Synthetase/ GSAd	20 mM HEPES-KOH, 5 mM MgCl2, 0.5 mM DTT, 50 mM NaCl, pH 7.2	25	-37.4	-187	-149	78
MAP2C/ DHEA	50 mM MES, pH 6.8	25	-42.0	-34.0	8.0	79
MAP2C/ DHEA	50 mM phosphate buffer, pH 7.5	25	-40.0	-10.0	30.0	79
Human AAG/ Indinavir	10 mM sodium acetate, 2% DMSO, pH 5.0	35	-26.9	-7.5	19.4	80
Human AAG/Saquinavir	10 mM sodium acetate, 2% DMSO, pH 5.0	25	-30.7	-60.7	-30.0	80
Human AAG/ KNI-764	10 mM sodium acetate, 2% DMSO, pH 5.0	25	-33.3	-28.9	4.4	80
Human AAG/ Nelfinavir	10 mM sodium acetate, 2% DMSO, pH 5.0	25	-33.4	-22.2	11.2	80
Human AAG/ Ritonavir	10 mM sodium acetate, 2% DMSO, pH 5.0	25	-34.9	-24.7	10.2	80
Trypsin/ p-Alkylbenzamidinium Chlorides	50 mM Tris, 10 mM $CaCl_2$ buffer at pH 8.0	20	-26.9	-17.0	9.9	81
Trypsin/ p-Alkylbenzamidinium Chlorides	50 mM Tris, 10 mM $CaCl_2$ buffer at pH 8.0	37	-26.7	-23.7	3.0	81
Trypsin/Me- p-Alkylbenzamidinium Chlorides	50 mM Tris, 10 mM $CaCl_2$ buffer at pH 8.0	20	-27.5	-16.7	10.8	81
Trypsin/Me- p-Alkylbenzamidinium Chlorides	50 mM Tris, 10 mM $CaCl_2$ buffer at pH 8.0	37	-27.4	-23.8	3.6	81
Trypsin/Et- p-Alkylbenzamidinium Chlorides	50 mM Tris, 10 mM $CaCl_2$ buffer at pH 8.0	20	-25.5	-10.6	14.9	81
Trypsin/ Et-p-Alkylbenzamidinium Chlorides	50 mM Tris, 10 mM $CaCl_2$ buffer at pH 8.0	37	-25.6	-22.4	3.2	81
Trypsin/ nPr-p-Alkylbenzamidinium Chlorides	50 mM Tris, 10 mM $CaCl_2$ buffer at pH 8.0	20	-25.7	-9.7	16.0	81

Trypsin/ nPr-p-Alkylbenzamidinium Chlorides	50 mM Tris, 10 mM $CaCl_2$ buffer at pH 8.0	37	-25.6	-19.9	5.7	81
Trypsin/ iPr-p-Alkylbenzamidinium Chlorides	50 mM Tris, 10 mM $CaCl_2$ buffer at pH 8.0	20	-22.6	-4.9	18	81
Trypsin/ i-Pr-p-Alkylbenzamidinium Chlorides	50 mM Tris, 10 mM $CaCl_2$ buffer at pH 8.0	37	-22.7	-12.0	11	81
Trypsin/ nBu-p-Alkylbenzamidinium Chlorides	50 mM Tris, 10 mM $CaCl_2$ buffer at pH 8.0	20	-26.2	-6.1	20.1	81
Trypsin/ nBu-p-Alkylbenzamidinium Chlorides	50 mM Tris, 10 mM $CaCl_2$ buffer at pH 8.0	37	-26.3	-18.5	7.8	81
Trypsin/ nPent- p-Alkylbenzamidinium Chlorides	50 mM Tris, 10 mM $CaCl_2$ buffer at pH 8.0	20	-26.8	-6.6	20.3	81
Trypsin/ nPent-p-Alkylbenzamidinium Chlorides	50 mM Tris, 10 mM $CaCl_2$ buffer at pH 8.0	37	-27.9	-17.5	10.4	81
Trypsin/ nHex-p-Alkylbenzamidinium Chlorides	50 mM Tris, 10 mM $CaCl_2$ buffer at pH 8.0	20	-28.9	-6.6	22.2	81
Trypsin/ nHex-p-Alkylbenzamidinium Chlorides	50 mM Tris, 10 mM $CaCl_2$ buffer at pH 8.0	37	-29.7	-21.0	8.7	81
Anti-NP antibody N1G9/NP-Cap	5 mM sodium phosphate buffer, 200 mM NaCl, pH 8.0	25.5	-31.0	-46.9	-15.7	82
Anti-NP antibody N1G9/NP-Cap	5 mM sodium phosphate buffer, 200 mM NaCl, pH 8.0	30	-31.3	-56.1	-24.5	82
Anti-NP antibody N1G9/NP-Cap	5 mM sodium phosphate buffer, 200 mM NaCl, pH 8.0	34.7	-29.9	-61.5	-31.5	82
Anti-NP antibody N1G9/NP-Cap	5 mM sodium phosphate buffer, 200 mM NaCl, pH 8.0	37.5	-29.8	-64.4	-34.9	82
Anti-NP antibody N1G9/NP-Cap	5 mM sodium phosphate buffer, 200 mM NaCl, pH 8.0	41	-29.7	-70.3	-40.7	82
Anti-NP antibody N1G9/NP-Cap	5 mM sodium phosphate buffer, 200 mM NaCl, pH 8.0	45.2	-29.5	-72.4	-42.9	82
Anti-NP antibody 3B44/NP-Cap	5 mM sodium phosphate buffer, 200 mM NaCl, pH 8.0	25.5	-39.4	-69.0	-29.6	82
Anti-NP antibody 3B44/NP-Cap	5 mM sodium phosphate buffer, 200 mM NaCl, pH 8.0	30	-39.7	-77.0	-37.6	82
Anti-NP antibody 3B44/NP-Cap	5 mM sodium phosphate buffer, 200 mM NaCl, pH 8.0	33.1	-39.1	-81.6	-42.0	82
Anti-NP antibody 3B44/NP-Cap	5 mM sodium phosphate buffer, 200 mM NaCl, pH 8.0	37.2	-38.2	-87.4	-49.3	82
Anti-NP antibody 3B44/NP-Cap	5 mM sodium phosphate buffer, 200 mM NaCl, pH 8.0	40.3	-35.6	-90.8	-55.4	82
Anti-NP antibody 3B44/NP-Cap	5 mM sodium phosphate buffer, 200 mM NaCl, pH 8.0	45.2	-34.1	-100.0	-65.6	82
Anti-NP antibody 3B62/NP-Cap	5 mM sodium phosphate buffer, 200 mM NaCl, pH 8.0	25.2	-41.5	-76.6	-34.8	82
Anti-NP antibody 3B62/NP-Cap	5 mM sodium phosphate buffer, 200 mM NaCl, pH 8.0	30	-40.1	-84.9	-45.0	82
Anti-NP antibody 3B62/NP-Cap	5 mM sodium phosphate buffer, 200 mM NaCl, pH 8.0	33	-39.6	-88.7	-48.9	82
Anti-NP antibody 3B62/NP-Cap	5 mM sodium phosphate buffer, 200 mM NaCl, pH 8.0	36.8	-39.9	-96.7	-56.9	82
Anti-NP antibody 3B62/NP-Cap	5 mM sodium phosphate buffer, 200 mM NaCl, pH 8.0	39.8	-39.3	-102.5	-63.2	82
Anti-NP antibody 3B62/NP-Cap	5 mM sodium phosphate buffer, 200 mM NaCl, pH 8.0	44.6	-39.6	-109.6	-70.2	82

Table A.3. Thermodynamic Parameters for Some Protein-Peptide Interactions (continues on the next page).

Complex	Solvent	T / °C	ΔG / kJ mol^{-1}	ΔH / kJ mol^{-1}	$T\Delta S$ / kJ mol^{-1}	Ref.
nGLP1R/GLP-1	0.25 M L-arginine, 50 mM phosphate, 1 mM EDTA, pH 7.3	20	-38.4	-102.5	-64.1	83
Fibrinogen/*S*-nitrosoglutathione	Phosphate buffered saline, pH 7.4	25	-31.3	46.9	79.5	84
Nematode anticoagulant protein c2/factor X	20 mM hepes, 0.15 M NaCl, 2.0 mM Ca^{2+}, pH 7.4	25	-51.7	-57.8	-6.1	85
Nematode anticoagulant protein c2/factor X	20 mM hepes, 0.15 M NaCl, pH 7.4	25	-50.2	-57.1	-6.9	85

Nematode anticoagulant protein c2/factor Xa	20 mM hepes, 0.15 M NaCl, 2.0 mM Ca^{2+}, pH 7.4	25	-52.0	-71.5	-65.6	85
Calmodulin/nitric oxide synthase I peptide	10 mM hepes, 150 mM NaCl, 10 mM $MgCl_2$, 3 mM $CaCl_2$, 2 mM EGTA, 0.005% Tween 20, pH 7.4	25	-41.1	-30.4	10.8	86
Src homology 2/phosphotyrosyl peptide inhibitor	20 mM hepes, 1 mM $HS(CH_2)_2OH$, 1 mM EDTA, 100 mM NaCl, pH 7.3	25	-37.7	-25.4	12.3	87
Src homology 2/phosphotyrosyl peptide inhibitor	20 mM hepes, 1 mM $HS(CH_2)_2OH$, 1 mM EDTA, 100 mM NaCl, pH 7.3	25	-40	-24.7	21.2	87
Src homology 2/phosphotyrosyl peptide inhibitor	20 mM hepes, 1 mM $HS(CH_2)_2OH$, 1 mM EDTA, 100 mM NaCl, pH 7.3	25	-41	-30.7	10.4	87
Src homology 2/phosphotyrosyl peptide inhibitor	20 mM hepes, 1 mM $HS(CH_2)_2OH$, 1 mM EDTA, 100 mM NaCl, pH 7.3	25	-38.7	-21	17.8	87
Src homology 2/phosphotyrosyl peptide inhibitor	20 mM hepes, 1 mM $HS(CH_2)_2OH$, 1 mM EDTA, 100 mM NaCl, pH 7.3	25	-40.7	-29	11.7	87
Human protein S100P/melittin	50 mM Tris, 0.2 mM EDTA, 1.5 mM TCEP, pH 7.5	25	-21.4	63	84.4	88
Dihydrolipoyl dehydrogenase/PSBD of dihydrolipoyl acetyltransferase	10 mM Hepes, 150 mM NaCl, 3.4 mM EDAT, pH 7.4	25	-52.7	9.2	61.9	89
Pyruvate decarboxylase/ PSBD of dihydrolipoyl acetyltransferase	10 mM Hepes, 150 mM NaCl, 3.4 mM EDAT, pH 7.4	25	-54.0	-35.1	18.8	89
FRS2α PTB domain/FGFR1 peptide	20 mM Tris-HCl, pH 8.0	25	-27.6	-5.0	22.6	90
FRS2α PTB domain/FGFR1 peptide	50mM phosphate,200mM NaCl,1 mM EDTA,5 mM $HS(CH_2)_2OH$,pH 7.0	25	-28.5	-7.5	20.9	90
FRS2α PTB domain/TRKB, pY61 peptide	20 mM Tris-HCl, pH 8.0	25	-28.9	-20.1	8.8	90
FRS2α PTB domain/TRKB, pY61 peptide	50mM phosphate,200mM NaCl,1 mM EDTA,5 mM $HS(CH_2)_2OH$,pH 7.0	25	-30.1	-33.5	-3.3	90
FRS2α PTB domain/TRKA, pY490 peptide	20 mM Tris-HCl, pH 8.0	25	-27.2	-20.9	6.3	90
FRS2α PTB domain/TRKA, pY490 peptide	50mM phosphate,200mM NaCl,1 mM EDTA,5 mM $HS(CH_2)_2OH$,pH 7.0	25	-29.3	-27.2	2.1	90
FRS2α PTB domain/TRKA (A-5) peptide	20 mM Tris-HCl, pH 8.0	25	-25.5	-19.7	5.4	90
FRS2α PTB domain/TRKA (A-5) peptide	50mM phosphate,200mM NaCl,1 mM EDTA,5 mM $HS(CH_2)_2OH$,pH 7.0	25	-26.4	-23.0	3.3	90
FRS2α PTB domain/IL-4R, pY497 peptide	20 mM Tris-HCl, pH 8.0	25	-34.3	-43.1	-8.8	90
SOCS3(Δ101–133)/ gp130 peptide	50 mm NaCl, 50 mm arginine, 50 mm glutamate, 5 mm 2-mercaptoethanol, pH 6.7	25	-40.6	-27.0	13.6	91
Wild type SOCS3/ gp130 peptide	50 mm NaCl, 50 mm arginine, 50 mm glutamate, 5 mm 2-mercaptoethanol, pH 6.7	25	-38.7	-25.9	12.7	91
Hemextin AB complex/ FVIIα	50 mM Tris-HCl buffer and 10 mM $CaCl_2$, pH 7.4	37	-33.3	-33.2	-1.6	92
Tetratricopeptide repeat domain/ MEEVD peptide	50 mM Mes, 5 mM DTT, pH 6.0	10	-40.6	-33.0	7.6	93
Tetratricopeptide repeat domain/ MEEVD peptide	50 mM Mes, 5 mM DTT, pH 6.0	15	-40.3	-52.9	-12.7	93
Tetratricopeptide repeat domain/ MEEVD peptide	50 mM Mes, 5 mM DTT, pH 6.0	17.5	-39.3	-63.4	-24.1	93
Tetratricopeptide repeat domain/ MEEVD peptide	50 mM Mes, 5 mM DTT, pH 6.0	20	-41.2	-84.9	-43.7	93
Tetratricopeptide repeat domain/ MEEVD peptide	50 mM Mes, 5 mM DTT, pH 6.0	22.5	-41.7	-90.9	-49.1	93
Tetratricopeptide repeat domain/ MEEVD peptide	50 mM Mes, 5 mM DTT, pH 6.0	25	-41.4	-144.7	-73.3	93
Tetratricopeptide repeat domain/ MEEVD peptide	50 mM Mes, 5 mM DTT, pH 6.0	25	-40.3	-119.0	-78.6	93
Tetratricopeptide repeat domain/ MEEVD peptide	50 mM Mes, 5 mM DTT, pH 6.0	27.5	-42.2	-123.7	-81.4	93
Tetratricopeptide repeat domain/ MEEVD peptide	50 mM Mes, 5 mM DTT, pH 6.0	30	-42.6	-173.2	-130.5	93
Tetratricopeptide repeat domain/ MEEVD peptide	50 mM Mes, 5 mM DTT, pH 6.0	32	-39.8	-177.7	-137.9	93
Tetratricopeptide repeat domain/ MEEVD peptide	50 mM Mes, 5 mM DTT, pH 6.0	34	-42.8	-202.8	-161.0	93
Tetratricopeptide repeat domain/ MEEVD peptide	50 mM Mes, 5 mM DTT, pH 6.0	36	-41.1	-219.9	-178.8	93
SjGST(Y7F)/ *S*-methyl-GSH	20 mM MES, 2 mM DTT, and 1 mM EDTA, pH 6.5	25	-26.2	-19.2	7.0	94

SjGST(Y7F)/ *S*-methyl-GSH	20 mM MES, 2 mM DTT, and 1 mM EDTA, pH 6.5	30	-25.5	-26.5	-1.0	94
SjGST(Y7F)/ *S*-methyl-GSH	20 mM MES, 2 mM DTT, and 1 mM EDTA, pH 6.5	35	-24.5	-32.4	-7.9	94
SjGST(Y7F)/ S-hexyl-GSH	20 mM MES, 2 mM DTT, and 1 mM EDTA, pH 6.5	25	-30.1	-31.3	-1.1	94
SjGST(Y7F)/ S-hexyl-GSH	20 mM MES, 2 mM DTT, and 1 mM EDTA, pH 6.5	30	-30.1	-36.9	-6.7	94
SjGST(Y7F)/ S-hexyl-GSH	20 mM MES, 2 mM DTT, and 1 mM EDTA, pH 6.5	35	-30.7	-42.4	-11.7	94
SjGST(Y7F)/ S-octyl-GSH	20 mM MES, 2 mM DTT, and 1 mM EDTA, pH 6.5	20	-32.2	-27.9	4.3	94
SjGST(Y7F)/ S-octyl-GSH	20 mM MES, 2 mM DTT, and 1 mM EDTA, pH 6.5	25	-32.5	-30.4	2.1	94
SjGST(Y7F)/ S-octyl-GSH	20 mM MES, 2 mM DTT, and 1 mM EDTA, pH 6.5	30	-32.8	-33.5	-0.7	94
SjGST(Y7F)/ S-octyl-GSH	20 mM MES, 2 mM DTT, and 1 mM EDTA, pH 6.5	35	-32.5	-38.1	-5.6	94
FadR protein- *E. coli*/ Leoyl-CoA	20mM Tris-HCl, 50mM NaCl, 1 mM EDTA, 0.1 mM Tris(2-carboxyethyl)phosphine hydrochloride), pH 7.0	30	-41.4	-82.9	-41.5	95
FadR protein- *S. enterica*/ Leoyl-CoA	20mM Tris-HCl, 50mM NaCl, 1 mM EDTA, 0.1 mM Tris(2-carboxyethyl)phosphine hydrochloride), pH 7.0	30	-39.7	-80.8	-41.0	95
FadR protein- *V. cholerae*/ Leoyl-CoA	20mM Tris-HCl, 50mM NaCl, 1 mM EDTA, 0.1 mM Tris(2-carboxyethyl)phosphine hydrochloride), pH 7.0	30	-44.0	-49.0	-5.0	95
FadR protein- *P. multocida*/ Leoyl-CoA	20mM Tris-HCl, 50mM NaCl, 1 mM EDTA, 0.1 mM Tris(2-carboxyethyl)phosphine hydrochloride), pH 7.0	30	-32.7	-36.0	-3.3	95
FadR protein- *H. influenzae*/ Leoyl-CoA	20mM Tris-HCl, 50mM NaCl, 1 mM EDTA, 0.1 mM Tris(2-carboxyethyl)phosphine hydrochloride), pH 7.0	30	-32.2	-34.3	-2.1	95
Grb7-SH2/ erbB2 peptide pY1139	50 mM sodium acetate, 100 mM NaCl, 5 mM DTT, 1 mM NaN3, and 1 mM EDTA, pH 6.6	25	-32.2	-19.5	12.7	96
Molecular Chaperone, $ClpA_6$/ SsrA peptide	50 mM Tris, 0.1 M KCl, 10% glycerol, 10 mM MgCl2, 2 mM ATPγS, 7.5	4	-26.4	83.7	110.0	97
Molecular Chaperone, $ClpA_6$/ SsrA peptide	50 mM Tris, 0.1 M KCl, 10% glycerol, 10 mM MgCl2, 2 mM ATPγS, 7.5	10	-33.1	75.3	108.4	97
Molecular Chaperone, $ClpA_6$/ SsrA peptide	50 mM Tris, 0.1 M KCl, 10% glycerol, 10 mM MgCl2, 2 mM ATPγS, 7.5	15	-34.7	25.1	59.8	97
Molecular Chaperone, $ClpA_6$/ SsrA peptide	50 mM Tris, 0.1 M KCl, 10% glycerol, 10 mM MgCl2, 2 mM ATPγS, 7.5	20	-38.1	-16.7	21.3	97
Molecular Chaperone, $ClpA_6$/ SsrA peptide	50 mM Tris, 0.1 M KCl, 10% glycerol, 10 mM MgCl2, 2 mM ATPγS, 7.5	28	-38.9	-20.9	18.0	97
Molecular Chaperone, $ClpA_6$/ SsrA peptide	20mM MOPS, 0.1M KCl, 10% glycerol, 10mM MgCl2, 2mM ATPγS, 7.5	10	-38.9	12.6	51.5	97
Molecular Chaperone, $ClpA_6$/ SsrA peptide	20mM MOPS, 0.1M KCl, 10% glycerol, 10mM MgCl2, 2mM ATPγS, 7.5	28	-83.7	-2.9	80.8	97
Molecular Chaperone, $ClpA_6$/ DNS-SsrA peptide	50 mM Tris, 0.1 M KCl, 10% glycerol, 10 mM MgCl2, 2 mM ATPγS, 7.5	12	-38.5	16.7	55.2	97
Molecular Chaperone, $ClpA_6$/ DNS-SsrA peptide	50 mM Tris, 0.1 M KCl, 10% glycerol, 10 mM MgCl2, 2 mM ATPγS, 7.5	28	-40.6	-8.4	32.2	97
Molecular Chaperone, $ClpA_6$/ αSsrA peptide	50 mM Tris, 0.1 M KCl, 10% glycerol, 10 mM MgCl2, 2 mM ATPγS, 75	6	-38.1	184.1	222.2	97

Molecular Chaperone, $ClpA_6$/ αSsrA peptide	50 mM Tris, 0.1 M KCl, 10% glycerol, 10 mM MgCl2, 2 mM ATPγS, 7.5	10	-38.5	133.9	172.4	97
Molecular Chaperone, $ClpA_6$/ αSsrA peptide	50 mM Tris, 0.1 M KCl, 10% glycerol, 10 mM MgCl2, 2 mM ATPγS, 7.5	18	-38.9	25.1	64.0	97
CaM/ RS20 peptide	50 mM Hepes, 2 mM CaCl2, pH 7.5	25	-43.3	-55.3	-11.8	98
CaMox/ RS20 peptide	50 mM Hepes, 2 mM CaCl2, pH 7.5	25	-36.3	-32.4	3.9	98
CaMox + MsrA/ RS20 peptide	50 mM Hepes, 2 mM CaCl2, pH 7.5	25	-42.8	-56.3	-13.5	98
CaMox + MsrB/ RS20 peptide	50 mM Hepes, 2 mM CaCl2, pH 7.5	25	-37.8	-54.7	-17.7	98
CaMox + MsrAB/ RS20 peptide	50 mM Hepes, 2 mM CaCl2, pH 7.5	25	-41.9	-58.1	-16.2	98
PDZ3 from PSD-95/ peptide **1**	20 mM MES, 10 mM NaCl, pH 6.0	25	-27.6	-7.7	19.8	99
PDZ3 from PSD-95/ peptide **2**	20 mM MES, 10 mM NaCl, pH 6.0	25	-29.4	-14.4	15.0	99
PDZ3 from PSD-95/ peptide **3**	20 mM MES, 10 mM NaCl, pH 6.0	25	-30.3	-16.2	14.1	99
PDZ3 from PSD-95/ peptide **4**	20 mM MES, 10 mM NaCl, pH 6.0	25	-31.0	-7.8	23.1	99
PDZ3 from PSD-95/ peptide **5**	20 mM MES, 10 mM NaCl, pH 6.0	25	-31.0	-7.7	23.2	99
PDZ3 from PSD-95/ peptide **6**	20 mM MES, 10 mM NaCl, pH 6.0	25	-29.7	-14.6	15.1	99
PDZ3 from PSD-95/ peptide **7**	20 mM MES, 10 mM NaCl, pH 6.0	25	-27.5	-11.1	16.4	99
PDZ3 from PSD-95/ peptide **8**	20 mM MES, 10 mM NaCl, pH 6.0	25	-27.6	-13.9	13.7	99
src homology 3 (SH3)/ peptide p1	10 mM phosphate buffer, pH 7.5	25	-17.8	-4.7	13.1	100
src homology 3 (SH3)/ peptide p2	10 mM phosphate buffer, pH 7.5	25	-7.6	3.8	11.4	100
ApoCaM/ NOS-II V511K peptide	10 mM HEPES, 150 mM NaCl, 2 mM $MgCl_2$, 10 mM EGTA, and 0.005% (v/v) Tween 20, pH 7.4	25	-34.8	25.9	60.7	101
ApoCaM/ NOS-II F517K peptide	10 mM HEPES, 150 mM NaCl, 2 mM $MgCl_2$, 10 mM EGTA, and 0.005% (v/v) Tween 20, pH 7.4	25	-37.9	31.2	69.1	101
ApoCaM/ NOS-II M521K peptide	10 mM HEPES, 150 mM NaCl, 2 mM $MgCl_2$, 10 mM EGTA, and 0.005% (v/v) Tween 20, pH 7.4	25	-41.3	11.9	53.2	101
ApoCaM/ NOS-II 3K peptide	10 mM HEPES, 150 mM NaCl, 2 mM $MgCl_2$, 10 mM EGTA, and 0.005% (v/v) Tween 20, pH 7.4	25	-33.0	33.3	66.3	101
ApoCaM/ NOS-II E3K peptide	10 mM HEPES, 150 mM NaCl, 2 mM $MgCl_2$, 10 mM EGTA, and 0.005% (v/v) Tween 20, pH 7.4	25	-33.7	27.0	60.8	101
Ab1-SH3/ RP1 peptide	20 mM phosphate buffer, pH 7.0	25	-25.8	-63.2	-37.6	102
Ab1-SH3/ APR-RP1 peptide	20 mM phosphate buffer, pH 7.0	25	-23.0	-61.5	-38.5	102
Native IL-8/ *CXCR1N*	*50 mM NaCl, 50 mM HEPES, pH 8.0*	25	-30.5	-29.3	1.3	103
Native IL-8 monomer/ *CXCR1N*	*50 mM NaCl, 50 mM HEPES, pH 8.0*	25	-29.7	-43.9	-14.2	103
Sem-5 C-SH3/ SosY I	20 mM Tris and 200 mM NaCl, pH 9.0	25.1	-25.5	-39.3	-13.80	104
Sem-5 C-SH3/ SosY I	20 mM Tris and 200 mM NaCl, pH 8.5	25.1	-25.1	-36.0	-10.9	104
Sem-5 C-SH3/ SosY I	20 mM Tris and 200 mM NaCl, pH 8.0	25.1	-25.1	-38.1	-13.0	104
Sem-5 C-SH3/ SosY III	20 mM Tris and 200 mM NaCl, pH 7.5	15.2	-25.1	-27.6	-2.5	104
Sem-5 C-SH3/ SosY III	20 mM Tris and 200 mM NaCl, pH 7.5	20.2	-25.1	-31.4	-6.3	104
Sem-5 C-SH3/ SosY III	20 mM Tris and 200 mM NaCl, pH 7.5	35.2	-25.1	-34.7	-9.6	104
Sem-5 C-SH3/ SosY III	20 mM Tris and 200 mM NaCl, pH 7.5	25.1	-25.1	-37.7	-12.6	104

Sem-5 C-SH3/ SosY III	20 mM Tris and 200 mM NaCl, pH 7.5	25.1	-24.7	-41.8	-17.2	104
Sem-5 C-SH3/ SosY II	20 mM Tris and 200 mM NaCl, pH 7.5	25.1	-25.1	-38.1	-13.0	104
Sem-5 C-SH3/ SosY II	20 mM imidazole and 200 mM NaCl, pH 7.5	25.1	-25.1	-33.9	-8.8	104
Sem-5 C-SH3/ SosY II	20 mM Hepes and 200 mM NaCl, pH 7.5	25.1	-25.1	-31.8	-6.7	104
Sem-5 C-SH3/ SosY II	20 mM phosphate and 200 mM NaCl, pH 7.5	25.1	-25.1	-33.5	-8.4	104
Sem-5 C-SH3/ SosY III	20 mM imidazole and 200 mM NaCl, pH 7.0	25.1	-24.7	-35.1	-10.5	104
Sem-5 C-SH3/ SosY III	20 mM imidazole and 200 mM NaCl, pH 6.5	25.1	-24.3	-38.9	-14.6	104
Sem-5 C-SH3/ SosY III	50 mM sodium acetate, 100 mM NaCl and 10 mM $CaCl_2$. pH 4.8	25.1	-20.1	-28.0	-7.9	104
Wild type FAT/ LD2 peptide (Helix 1,4 site)	50 mM HEPES, 100 mM NaCl, and 2 mM NaN_3 at pH 7.0	26	-28.9	-30.1	-1.3	105
E949A/K956A/R963A/ LD2 peptide (Helix 1,4 site)	50 mM HEPES, 100 mM NaCl, and 2 mM NaN_3 at pH 7.0	26	-30.7	-23.0	7.5	105
Pyk2/ LD2 peptide (Helix 1,4 site)	50 mM HEPES, 100 mM NaCl, and 2 mM NaN_3 at pH 7.0	26	-24.9	-41.8	-16.7	105
Wild type FAT/ LD2 peptide (Helix 2,3 site)	50 mM HEPES, 100 mM NaCl, and 2 mM NaN_3 at pH 7.0	26	-28.3	4.6	32.6	105
1937A/ LD2 peptide (Helix 2,3 site)	50 mM HEPES, 100 mM NaCl, and 2 mM NaN_3 at pH 7.0	26	-27.9	1.3	28.9	105
Pyk2/ LD2 peptide (Helix 2,3 site)	50 mM HEPES, 100 mM NaCl, and 2 mM NaN_3 at pH 7.0	26	-26.8	1.3	28.0	105
C3/ *V4W/H9A* peptide	PBS, pH 7.4	15	-39.5	-61.1	-21.8	106
C3/ *V4W/H9A* peptide	PBS, pH 7.4	20	-39.9	-70.7	-31.0	106
C3/ *V4W/H9A* peptide	PBS, pH 7.4	25	-39.3	-75.9	-36.8	106
C3/ *V4W/H9A* peptide	PBS, pH 7.4	37	-37.9	-99.6	-61.9	106
C3/ *V4W/H9A* peptide	Tris, pH 7.4	25	-40.3	-61.5	-21.5	106
C3/ *V4W/H9A* peptide	MOPS, pH 7.4	25	-39.6	-66.2	-26.8	106
C3/ *V4W/H9A* peptide	PBS, pH 6.7	25	-40.4	-75.0	-34.7	106
C3/ *V4W/H9A* peptide	Tris, pH 6.7	25	-40.8	-54.0	-13.4	106
C3/ *V4W/H9A* peptide	MOPS, pH 6.7	25	-40.4	-65.3	-25.0	106
C3/ *V4W/H9A* peptide	PB, pH 7.4	25	-39.9	-66.5	-26.8	106
C3/ *V4W/H9A* peptide	PBS, 0.5 M glycerol, pH 7.4	25	-39.7	-126.8	-91.6	106
C3/ *V4W/H9A* peptide	PBS, 1 M glycerol, pH 7.4	25	-38.7	-92.5	-54.0	106
C3/ *V4H9* peptide	PBS, pH 7.4	15	-34.6	-39.7	-5.3	106
C3/ *V4H9* peptide	PBS, pH 7.4	20	-32.6	-46.5	-14.1	106
C3/ *V4H9* peptide	PBS, pH 7.4	25	-33.8	-50.7	-17.1	106
C3/ *V4H9* peptide	PBS, pH 7.4	37	-31.2	-58.5	-27.4	106
C3/ *V4H9* peptide	Tris, pH 7.4	25	-33.8	-66.9	-33.4	106
C3/ *V4H9* peptide	MOPS, pH 7.4	25	-31.6	-62.8	-31.4	106
C3/ *V4H9* peptide	PBS, pH 6.7	25	-34.6	-53.7	-19.2	106
C3/ *V4H9* peptide	Tris, pH 6.7	25	-32.9	-57.3	-24.6	106
C3/ *V4H9* peptide	MOPS, pH 6.7	25	-33.8	-49.7	-16.1	106
C3/ *V4H9* peptide	PB, pH 7.4	25	-34.2	-52.6	-18.6	106
C3/ *V4H9* peptide	PBS, 0.5 M glycerol, pH 7.4	25	-33.5	-46.6	-13.2	106
C3/ *V4H9* peptide	PBS, 1 M glycerol, pH 7.4	25	-32.8	-76.8	-44.2	106
PDZ3 fromPSD-95/ peptide ligand **2**	20 mM MES, pH 6.0	25	-24.0	-8.6	15.4	107

PDZ3 fromPSD-95/ peptide ligand **4**	20 mM MES, pH 6.0	25	-23.9	-5.1	18.7	107
PDZ3 fromPSD-95/ peptide ligand **5**	20 mM MES, pH 6.0	25	-27.0	-10.3	16.7	107
PDZ3 fromPSD-95/ peptide ligand **6**	20 mM MES, pH 6.0	25	-25.8	-12.3	13.5	107
PDZ3 fromPSD-95/ peptide ligand **7**	20 mM MES, pH 6.0	25	-25.4	-10.3	15.2	107
PDZ3 fromPSD-95/ peptide ligand **8**	20 mM MES, pH 6.0	25	-30.5	-9.6	21.0	107
PDZ3 fromPSD-95/ peptide ligand **9**	20 mM MES, pH 6.0	25	-28.7	-11.5	17.3	107
PDZ3 fromPSD-95/ peptide ligand **10**	20 mM MES, pH 6.0	25	-26.8	-5.9	21.0	107
PDZ3 fromPSD-95/ peptide ligand **11**	20 mM MES, pH 6.0	25	-29.7	-14.2	15.6	107
PDZ3 fromPSD-95/ peptide ligand **12**	20 mM MES, pH 6.0	25	-30.0	-20.0	10.0	107
PDZ3 fromPSD-95/ peptide ligand **13**	20 mM MES, pH 6.0	25	-24.9	-5.8	19.1	107
PDZ3 fromPSD-95/ peptide ligand **14**	20 mM MES, pH 6.0	25	-24.4	-6.8	17.7	107
PDZ3 fromPSD-95/ peptide ligand 15	20 mM MES, pH 6.0	25	-30.2	-12.9	17.4	107
Abl-SH3 domain/ p41	20 mM sodium phosphate, pH 7.0	25	-32.2	-91.6	-59.4	108
Abl-SH3 domain/ p41	20 mM sodium phosphate, pH 7.0	25	-32.2	-88.3	-56.1	108
Abl-SH3 domain/ p40	20 mM sodium phosphate, pH 7.0	25	-31.8	-76.6	-44.8	108
Abl-SH3 domain/ p7	20 mM sodium phosphate, pH 7.0	25	-28.9	-73.2	-44.4	108
Abl-SH3 domain/ p0	20 mM sodium phosphate, pH 7.0	25	-28.9	-71.1	-42.3	108
Abl-SH3 domain/ 3BP1	20 mM sodium phosphate, pH 7.0	25	-25.5	-69.9	-44.4	108
PDZ3 from PSD-95/ KKETE*X* (X=Ala, Me)	20 mM MES, 10 mM NaCl, pH 6.0	25	-23.1	-19.1	4.0	109
PDZ3 from PSD-95/ KKETE*X* (X=Aib, Me,Me)	20 mM MES, 10 mM NaCl, pH 6.0	25	-22.5	-4.3	18.2	109
PDZ3 from PSD-95/ KKETE*X* (X=Abu, Et)	20 mM MES, 10 mM NaCl, pH 6.0	25	-30.6	-31.8	-1.3	109
PDZ3 from PSD-95/ KKETE*X* (X=Val, i-Pr)	20 mM MES, 10 mM NaCl, pH 6.0	25	-32.6	-26.1	6.6	109
PDZ3 from PSD-95/ KKETE*X* (X=Ape, nPr)	20 mM MES, 10 mM NaCl, pH 6.0	25	-34.2	-31.0	3.2	109
PDZ3 from PSD-95/ KKETE*X* (X=Tle, t-Bu)	20 mM MES, 10 mM NaCl, pH 6.0	25	-31.0	-18.7	12.3	109
PDZ3 from PSD-95/ KKETE*X* (X=Ile, s-Bu)	20 mM MES, 10 mM NaCl, pH 6.0	25	-29.2	-18.0	11.2	109
PDZ3 from PSD-95/ KKETE*X* (X=Leu, i-Bu)	20 mM MES, 10 mM NaCl, pH 6.0	25	-29.2	-17.2	11.9	109
PDZ3 from PSD-95/ KKETE*X* (X=Ahx, n-Bu)	20 mM MES, 10 mM NaCl, pH 6.0	25	-29.4	-26.9	2.6	109
Disabled-1 PTB native/ ApoER2 Peptide	20 mM PIPES buffer, 150 mM NaCl, 0.2 mM DTT, pH 7.0	25	-32.2	-40.2	-7.9	74
Disabled-1 PTB mutant H81Q/ ApoER2 Peptide	20 mM PIPES buffer, 150 mM NaCl, 0.2 mM DTT, pH 7.0	25	-33.1	-45.2	-12.1	74
Disabled-1 PTB mutant K45A/ ApoER2 Peptide	20 mM PIPES buffer, 150 mM NaCl, 0.2 mM DTT, pH 7.0	25	-32.2	-42.3	-10.0	74
Disabled-1 PTB mutant K45Q/ ApoER2 Peptide	20 mM PIPES buffer, 150 mM NaCl, 0.2 mM DTT, pH 7.0	25	-31.6	-33.9	-2.5	74
Disabled-1 PTB mutant K45E/ ApoER2 Peptide	20 mM PIPES buffer, 150 mM NaCl, 0.2 mM DTT, pH 7.0	25	-32.3	-44.4	-12.1	74
Disabled-1 PTB mutant K82A/ ApoER2 Peptide	20 mM PIPES buffer, 150 mM NaCl, 0.2 mM DTT, pH 7.0	25	-33.4	-46.0	-12.6	74
Disabled-1 PTB mutant K82Q/ ApoER2 Peptide	20 mM PIPES buffer, 150 mM NaCl, 0.2 mM DTT, pH 7.0	25	-32.9	-60.7	-27.6	74
Disabled-1 PTB mutant K45A/K82A/ ApoER2 Peptide	20 mM PIPES buffer, 150 mM NaCl, 0.2 mM DTT, pH 7.0	25	-31.5	-36.8	-5.4	74
Disabled-1 PTB mutant K45Q/K82Q/ ApoER2 Peptide	20 mM PIPES buffer, 150 mM NaCl, 0.2 mM DTT, pH 7.0	25	-31.8	-38.9	-7.1	74
Disabled-1 PTB mutant K45E/K82Q/ ApoER2 Peptide	20 mM PIPES buffer, 150 mM NaCl, 0.2 mM DTT, pH 7.0	25	-32.4	-42.7	-10.5	74

Cob B/ H4-11 peptide	20 mM Hepes, 100 mM NaCl, 10 mM DTT, pH 7.5	15	-35.1	-38.0	-2.9	110
Cob B/ p53-11 peptide	20 mM Hepes, 100 mM NaCl, 10 mM DTT, pH 7.5	15	-32.0	-16.0	15.5	110
Cob B/ Acs-11 peptide	20 mM Hepes, 100 mM NaCl, 10 mM DTT, pH 7.5	15	-31.6	-8.8	23.2	110
Cob B/ Acs-15 peptide	20 mM Hepes, 100 mM NaCl, 10 mM DTT, pH 7.5	15	-30.0	-7.0	23.1	110
SjGST-Y7F/ GSH	20mM phosphate, 2mM DTT, 1mM EDTA, pH 6.5	16	-28.0	-17.2	10.8	111
SjGST-Y7F/ GSH	20mM phosphate, 2mM DTT, 1mM EDTA, pH 6.5	20	-28.1	-22.0	6.1	111
SjGST-Y7F/ GSH	20mM phosphate, 2mM DTT, 1mM EDTA, pH 6.5	25	-28.2	-28.7	0.5	111
SjGST-Y7F/ GSH	20mM phosphate, 2mM DTT, 1mM EDTA, pH 6.5	30	-28.1	-34.9	-6.8	111
WT Human GSH Transferase/ GSH	5 mM NaCl, 0.1 mM EDTA, 1 mM DTT, 50 mM Na phosphate, pH 6.5	25	-23.1	-46.9	-23.6	112
Y49F mutant Human GSH Transferase/ GSH	5 mM NaCl, 0.1 mM EDTA, 1 mM DTT, 50 mM Na phosphate, pH 6.5	25	-20.4	-54.6	-38.4	112
WT Human GSH Transferase/ S-hexyl-GSH	5 mM NaCl, 0.1 mM EDTA, 1 mM DTT, 50 mM Na phosphate, pH 6.5	25	-33.6	-67.5	-33.6	112
Y49F mut. Human GSH Trf./ S-hexyl-GSH	5 mM NaCl, 0.1 mM EDTA, 1 mM DTT, 50 mM Na phosphate, pH 6.5	25	-32.0	-71.7	-39.5	112
SurA/ WEYIPNV peptide	150 mM NaCl, 20 mM NaH_2PO_4, pH 7.3	20	-31.7	-83.3	-51.6	113
SurA/ WEYIPNV peptide	150 mM NaCl, 20 mM NaH_2PO_4, pH 7.3	25	-31.1	-81.2	-50.1	113
SurA/ WEYIPNV peptide	150 mM NaCl, 20 mM NaH_2PO_4, pH 7.3	30	-30.8	-77.4	-46.6	113
SurA/ WEYIPNV peptide	150 mM NaCl, 20 mM NaH_2PO_4, pH 7.3	37	-29.5	-67.4	-37.9	113
SurA(ΔP2)/ WEYIPNV peptide	150 mM NaCl, 20 mM NaH_2PO_4, pH 7.3	20	-32.4	-87.4	-55.0	113
SurA(ΔP2)/ WEYIPNV peptide	150 mM NaCl, 20 mM NaH_2PO_4, pH 7.3	25	-32.3	-84.3	-52.0	113
SurA(ΔP2)/ WEYIPNV peptide	150 mM NaCl, 20 mM NaH_2PO_4, pH 7.3	30	-31.4	-81.0	-49.6	113
SurA(ΔP2)/ WEYIPNV peptide	150 mM NaCl, 20 mM NaH_2PO_4, pH 7.3	37	-28.9	-83.3	-54.5	113
Fab/e-pep	50 mM sodium phosphate, 0.15 M NaCl, pH 7.2	10	-41.4	-46.9	-5.4	114
CB4-1/ e-pep	50 mM sodium phosphate, 0.15 M NaCl, pH 7.2	10	-42.3	-45.2	2.9	114
Fab/e-pep	50 mM sodium phosphate, 0.15 M NaCl, pH 7.2	25	-43.1	-65.3	-22.2	114
CB4-1/ e-pep	50 mM sodium phosphate, 0.15 M NaCl, pH 7.2	25	-43.5	-65.3	-21.8	114
CB4-1/ e-pep	50 mM MOPS, 0.15 M NaCl, pH 7.2	25	-43.5	-64.9	-21.3	114
Fab/e-pep	50 mM sodium phosphate, 0.15 M NaCl, pH 7.2	35	-42.3	-74.5	-32.2	114
CB4-1/ e-pep	50 mM sodium phosphate, 0.15 M NaCl, pH 7.2	35	43.1	-77.0	-33.9	114
Fab/h-pep	50 mM sodium phosphate, 0.15 M NaCl, pH 7.2	10	-41.8	-40.6	1.3	114
CB4-1/ h-pep	50 mM sodium phosphate, 0.15 M NaCl, pH 7.2	10	-42.3	-42.7	-0.4	114
Fab/h-pep	50 mM sodium phosphate, 0.15 M NaCl, pH 7.2	25	-43.5	-58.6	-15.1	114
CB4-1/ h-pep	50 mM sodium phosphate, 0.15 M NaCl, pH 7.2	25	-43.9	-58.2	-14.2	114
CB4-1/ h-pep	50 mM MOPS, 0.15 M NaCl, pH 7.2	25	-44.4	-60.7	-16.3	114
Fab/h-pep	50 mM sodium phosphate, 0.15 M NaCl, pH 7.2	35	-43.9	-69.0	-25.1	114
CB4-1/ h-pep	50 mM sodium phosphate, 0.15 M NaCl, pH 7.2	35	43.9	-67.8	-23.8	114
Fab/u-pep	50 mM sodium phosphate, 0.15 M NaCl, pH 7.2	10	-39.7	-49.0	-9.2	114
CB4-1/ u-pep	50 mM sodium phosphate, 0.15 M NaCl, pH 7.2	10	-40.2	-50.2	10.0	114
Fab/u-pep	50 mM sodium phosphate, 0.15 M NaCl, pH 7.2	25	-40.2	-64.9	-24.7	114
CB4-1/ u-pep	50 mM sodium phosphate, 0.15 M NaCl, pH 7.2	25	-41.4	-64.0	-22.6	114
CB4-1/ u-pep	50 mM MOPS, 0.15 M NaCl, pH 7.2	25	-40.6	-64.9	-24.3	114
Fab/u-pep	50 mM sodium phosphate, 0.15 M NaCl, pH 7.2	35	-38.9	-74.5	-35.6	114

CB4-1/ u-pep	50 mM sodium phosphate, 0.15 M NaCl, pH 7.2	35	-39.7	-73.2	-33.5	114
CB4-1/ d-pep	50 mM sodium phosphate, 0.15 M NaCl, pH 7.2	25	-32.2	-51.5	-19.2	114
CB4-1/ GA-pep	50 mM sodium phosphate, pH 7.2	25	-40.6	-45.2	-4.6	114
CB4-1/ GA-pep	50 mM sodium phosphate, 0.15 M NaCl, pH 7.2	25	-41.4	-47.7	-6.3	114
CB4-1/ AT-pep	50 mM sodium phosphate, pH 7.2	25	-38.9	-46.4	-7.5	114
CB4-1/ SE-pep	50 mM sodium phosphate, pH 7.2	25	-29.3	-72.8	-43.5	114
Fab/ SE-pep	50 mM sodium phosphate, pH 7.2	25	-29.7	-73.2	-43.5	114
Ab 131/angiotensin II	20 mM buffer, 50 mM NaCl, pH 7.3	30	-46.0	-37.2	8.8	115
Endothiapepsin/pepstatin A	20 mM phosphate, pH 7.0	16.1	-38.1	-10.5	27.6	116
HK 565 peptide/PK 262 peptide	30 mM phosphate, pH 7.0	30	-24.7	1.7	26.8	117
human Grb2 (SH3)/human Sos peptide	50 mM potassium phosphate, 1 mM DTT, pH 8.0	25	-26.8	-25.9	0.9	118
Fyn SH3 domain/P2L peptide	10 mM phosphate, pH 6.0	30	-27.6	-51.5	-23.6	119
Lck SH2 domain/Lck phosphopeptide	50 mM Mops, 100 nM NaCl, 1 mM DTT, pH 6.8	25	-30.5	-35.1	-4.4	120
p85 SH2 domain/PDGFR phosphopeptide	50 mM Mops, 100 nM NaCl, 1 mM DTT, pH 6.8	25	-36.4	-39.3	-3.0	120
Src SH2 domain/pYHmT phosphopeptide	50 mM Mops, 100 nM NaCl, 1 mM DTT, pH 6.8	25	-36.0	-35.1	0.5	120
Fyn SH2 domain/pYHmT phosphopeptide	10 mM potassium phosphate, 30 mM NaCl, 5 mM DTT, pH 6.0	25	-26.4	-18.0	8.2	121
Fyn SH2 domain/pY531 phosphopeptide	10 mM potassium phosphate, 30 mM NaCl, 5 mM DTT, pH 6.0	25	-35.1	-36.4	-1.6	121
SHC N-term. Domain/EGFR1148 peptide	100 mM Hepes, 100 mM NaCl, 1 mM DTT, pH 7.5	25	-43.1	-22.8	20.2	122
SHC N-term. Domain/Trk490 peptide	100 mM Hepes, 100 mM NaCl, 1 mM DTT, pH 7.5	25	-42.3	10.0	52.0	122
Ab 13AD/peptide LZ	1.46 mM KH_2PO_4,6.46 mM Na_2HPO_4,0.14 M NaCl,0.27 mM KCl,pH 7.2	27	-43.9	-52.7	-8.9	123
Ab 13AD/peptide LZ(7P14P)	1.46 mM KH_2PO_4,6.46 mM Na_2HPO_4,0.14 M NaCl,0.27 mM KCl,pH 7.2	27	-39.7	-72.8	-32.7	123
Ab 29AB/peptide LZ	1.46 mM KH_2PO_4,6.46 mM Na_2HPO_4,0.14 M NaCl,0.27 mM KCl,pH 7.2	27	-46.0	-57.7	-11.9	123
Ab 29AB/peptide LZ(7P14P)	1.46 mM KH_2PO_4,6.46 mM Na_2HPO_4,0.14 M NaCl,0.27 mM KCl,pH 7.2	27	-39.7	-71.5	-32.4	123
Ab 42PF/peptide LZ(7P14P)	1.46 mM KH_2PO_4,6.46 mM Na_2HPO_4,0.14 M NaCl,0.27 mM KCl,pH 7.2	27	-43.5	-56.1	-12.6	123
calmodulinCa^{2+}/melittin	50 mM Pipes/NaOH, 150 mM NaCl, 0.5 mM CaCl2, pH 7.0	25	-49.0	30.1	79.0	124
Calmodulin/melittin	50 mM Pipes/NaOH, 150 mM NaCl, pH 7.0	25	-33.9	20.1	54.0	124
ribonuclease S/truncated S peptide	50 mM sodium acetate, 100 mM NaCl, pH 6.0	25	-39.3	-175.3	-136.0	125
Streptavidin/FSHPQNT peptide	50 mM potassium phosphate, pH 7.62	25	-22.2	-80.8	-58.6	126
Streptavidin/p*Strep*-tag	50 mM potassium phosphate, pH 7.62	25	-25.5	-52.7	-27.2	127
CheR/receptor pentapeptide	20 mM potassium phosphate, 20 mM NaCl, 1 mM EDTA, 1 mM PMSF, pH 7.0	28	-33.1	-56.9	-23.8	128
Profiling/Pro11	10 mM Tris, 75 mM KCl, 3.1 mM NaN_3, pH 7.5	28	-22.6	-21.3	1.4	129
A/B heterodimeric coiled coil	10 mM sodium phosphate, ionic strength 22 mM, pH 7.2	20	-44.4	-103.3	-59.2	130
GroEL/unfolded subtilisin BPN' mutant	50 mM Tris, 100 mM KCl, 1 mM DTT, 0.1 mM EDTA, pH 7.8	14.3	-31.8	83.3	115.1	131
Jel42 scFv/HPr	15 mM sodium phosphate buffer, pH 7.2	2	-43.5	2.7	46.4	132
Jel42 scFv/HPr	15 mM sodium phosphate buffer, pH 7.2	9	-44.8	-6.7	38.1	132
Jel42 scFv/HPr	15 mM sodium phosphate buffer, pH 7.2	15	-45.6	-14.2	31.4	132
Jel42 scFv/HPr	15 mM sodium phosphate buffer, pH 7.2	21	-46.0	-21.8	24.7	132
Jel42 scFv/HPr	15 mM sodium phosphate buffer, pH 7.2	29	-46.4	-31.0	15.9	132
Jel42 scFv/HPr	15 mM sodium phosphate buffer, pH 7.2	37	-46.9	-39.7	7.1	132

1. Baugh, R. J.; Trowbridge, C. G. *J. Biol. Chem.* **1972**, *247*, 7498.
2. Castro, M. J. M.; Anderson, S. *Biochemistry* **1996**, *35*, 11435-11446.
3. Fukada, H.; Takahashi, K.; Sturtevant, J. M. *Biochemistry* **1985**, *24*, 5109-5115.
4. Filfil, R.; Chalikian, T. V. *J. Mol. Biol.* **2003**, *326*, 1271-1288.
5. Takahashi, K.; Fukada, H. *Biochemistry* **1985**, *24*, 297-300.
6. Milos, M.; Schaer, J.-J.; Comte, M.; Cox, J. A. *J. Biol. Chem.* **1988**, *263*, 9218-9222.
7. Kelley, R. F.; O'Connell, M. P.; Carter, P.; Presta, L.; Eigenbrot, C.; Covarrubias, M.; Snedecor, B.; Bourell, J. H.; Vetterlein, D. *Biochemistry* **1992**, *31*, 5434-5441.
8. Hibbits, K. A.; Gill, D. S.; Willson, R. C. *Biochemistry* **1994**, *33*, 3584-3590.
9. Tsumoto, K.; Ueda, Y.; Maenaka, K.; Watanabe, K.; Ogasahara, K.; Yutani, K.; Kumagai, I. *J. Biol. Chem.* **1994**, *269*, 28777-28782
10. Yokota, A.; Tsumoto, K.; Shiroishi, M.; Kondo, H.; Kumagai, I. *J. Biol. Chem.* **2003**, *278*, 5410-5418.
11. Bhat, T. N.; Bentley, G. A.; Boulet, G.; Greene, M. I.; Tello, D.; Dall'Acqua, W.; Souchon, H.; Schwarz, F. P.; Mariuzza, R. A.; Poljak, R. J. *Proc. Nat. Acad. Sci. U.S.A.* **1994**, *91*, 1089-1093.
12. Schwarz, F. P.; Tello, D.; Goldbaum, F. A.; Mariuzza, R. A.; Poljak, R. J. *Eur. J. Biochem.* **1995**, *228*, 388-394.
13. Tello, D.; Eisenstein, E.; Schwarz, F. P.; Goldbaum, F. A.; Fields, B. A.; Mariuzza, R. A.; Poljak, R. J. *J. Mol. Recognit.* **1994**, *7*, 57-62
14. Jelesarov, I.; Bosshard, H. R. *Biochemistry* **1994**, *33*, 13321-13328
15. Evans, L. J. A.; Cooper, A.; Lakey, J. H. *J. Mol. Biol.* **1996**, *255*, 559-563.
16. Martinez, J. C.; Filimonov, V. V.; Mateo, P. L.; Schreiber, G.; Fersht, A. R. *Biochemistry* **1995**, *34*, 5224-5233.
17. Kelley, R. F.; Costas, K. E.; O'Connell, M. P.; Lazarus, R. A. *Biochemistry* **1995**, *34*, 10383´-10392.
18. Kresheck, G. C.; Vitello, L. B.; Erman, J. E. *Biochemistry* **1995**, *34*, 8398-8405.
19. Morar, A. S.; Pielak, G. J. *Biochemistry* **2002**, *41*, 547-551.
20. McLean, M. A.; Sligar, S. G. *Biochem. Biophys. Res. Commun.* **1995**, *215*, 316-320.
21. Murphy, K. P.; Freire, E.; Paterson, Y. *Proteins* **1995**, *21*, 83-90.
22. Raman, C. S.; Allen, M. J.; Nall, B. T. *Biochemistry* **1995**, *34*, 5831-5838.
23. Li, J.; Swanson, R. V.; Simon, M. I.; Weis, R. M. *Biochemistry* **1995**, *34*, 14626-.
24. Johanson, K.; Appelbaum, E.; Doyle, M.; Hensley, P.; Zhao, B.; Abdel-Meguid, S. S.; Young, P.; Cook, R.; Carr, S.; Matico, R.; Cusimano, D.; Dul, E.; Angelichio, M.; Brooks, I.; Winborne, E.; McDonnell, P.; Morton, T.; Bennett, D.; Sokoloski, T.; McNulty, D.; Rosenberg, M.; Chaiken, I. *J. Biol. Chem.* **1995**, *270*, 9459-9471.
25. Philo, J. S.; Aoki, K. H.; Arakawa, T.; Narhi, L. O.; Wen, J. *Biochemistry* **1996**, *35*, 1681-1691.
26. Pearce, K. H., Jr.; Ultsch, M. H.; Kelley, R. F.; de Vos, A. M.; Wells, J. A. *Biochemistry* **1996**, *36*, 10300-10307.
27. Chauvin, F.; Fomenkov, A.; Johnson, C. R.; Roseman, S. *Proc. Nat. Acad. Sci. U.S.A.* **1996**, *93*, 7028-7031.
28. Philo, J. S.; Wen, J.; Wypych, J.; Schwartz, M. G.; Mendiaz, E. A.; Langley, K. E. *J. Biol. Chem.* **1996**, *271*, 6895-6902.
29. Lee, C. H.; Leung, B.; Lemmon, M. A.; Zheng, J.; Cowburn, D.; Kuriyan, J.; Saksela, K. *EMBO J.* **1995**, *14*, 5006-5015.
30. Renzoni, D. A.; Pugh, D. J. R.; Siligardi, G.; Das, P.; Morton, C. J.; Rossi, C.; Waterfield, M. D.; Campbell, I. D.; Ladbury, J. E. *Biochemistry* **1996**, *35*, 15646-15653.

[31]. Baker, B. M.; Murphy, K. P. *J. Mol. Biol.* **1997**, *268*, 557-569.
[32]. Aoki, K.; Taguchi, H.; Shindo, Y.; Yoshida, M.; Ogasahara, K.; Yutani, K.; Tanaka, N. *J. Biol. Chem.* **1997**, *272*, 32158-32162.
[33]. Myszka, D. G.; Sweet, R. W.; Hensley, P.; Brigham-Burke, M.; Kwong, P. D.; Hendrickson, W. A.; Wyatt, R.; Sodroski, J.; Doyle, M. L. *Proc. Nat. Acad. Sci. U.S.A.* **2000**, *97*, 9026-9031.
[34]. Jung, H.-I.; Cooper, A.; Perham, R. N. *Biochemistry* **2002**, *41*, 10446-10453.
[35]. Buddai, S. K.; Toulokhonova, L.; Bergum, P. W.; Vlasuk, G. P.; Krishnaswamy, S. *J. Biol. Chem.* **2002**, *277*, 26689-26698.
[36]. Lukasik, S. M.; Zhang, L.; Corpora, T.; Tomanicek, S.; Li, Y.; Kundu, M.; Hartman, K.; Liu, P. P.: Laue, T. M.; Biltonen, R. L.; Speck, N. A.; Bushweller, J. H. *Nature Struct. Mol. Biol.* **2002**, *9*, 674-679.
[37]. Flatman, R.; McLauchlan, W. R.; Juge, N.; Furniss, C.; Berrin, J.-G.; Hughes, R. K.; Manzanares, P.; Ladbury, J. E.; O'Brien, R.; Williamson, G. *Biochem. J.* **2002**, *365*, 773-781.
[38]. Gell, D.; Kong, Y.; Eaton, S. A.; Weiss, M. J.; Mackay, J. P. *J. Biol. Chem.* **2002**, *277*, 40602-40609.
[39]. Girard, M.; Turgeon, S. L.; Gauthier, S. F. *J. Agric. Food Chem.* **2003**, *51*, 4450-4455.
[40]. Nielsen, P. K.; Bonsager, B. C.; Berland, C. R.; Sigurskjold, B. W.; Svensson, B. *Biochemistry* **2003**, *42*, 1478-1487.
[41]. Baerga-Ortiz, A.; Bergqvist, S.; Mandell, J. G.; Komives, E. A. *Protein Sci.* **2004**, *13*, 166-176.
[42]. Zhou, Y.-L.; Liao, J.-M.; Du, F.; Liang, Y. *Thermochim. Acta* **2005**, *426*, 173-178.
[43]. Kouadio, J.-L. K.; Horn, J. R.; Pal, G.; Kossiakoff, A. A. *J. Biol. Chem.* **2005**, *280*, 25524-25532.
[44]. Keeble, A. H.; Kirkpatrick, N.; Shimizu, S.; Kleanthous, C. *Biochemistry* **2006**, *45*, 3243-3254.
[45]. Hegde, S. S.; Dam, T. K.; Brewer, C. F., Blanchard, J. S. *Biochemistry* **2002**, *41*, 7519-7527.
[46]. Krum, J. G.; Ellsworth, H.; Sargeant, R. R.; Rich, G.; Ensign, S. A. *Biochemistry* **2002**, *41*, 5005-5014.
[47]. Kwon, K.; Streaker, E. D.; Beckett, D. *Protein Sci.* **2002**, *11*, 558-570.
[48]. Saboury, A. A.; Divsalar, A.; Jafari, G. A.; Moosavi-Movahedi, A. A.; Housaindokht, M. R.; Hakimelahi, G. H. *J. Biochem. Mol. Biol.* **2002**, *35*, 302-305.
[49]. Saveanu, C.; Miron, S.; Borza, T.; Craescu, C. T.; Labesse, G.; Gagyi, C.; Popescu, A.; Schaeffer, F.; Namane, A.; Laurent-Winter, C.; Barzu, O.; Gilles, A.-M. *Protein Sci.* **2003**, *11*, 2551-2560.
[50]. Lafitte, D.; Lamour, V.; Tsvetkov, P. O.; Makarov, A. A.; Klich, M.; Deprez, P.; Moras, D.; Briand, C.; Gilli, R. *Biochemistry* **2002**, *41*, 7217-7223.
[51]. Ohtaka, H.; Velazquez-Campoy, A.; Xie, D.; Preire, E. *Protein Sci.* **2002**, *11*, 1908-1916.
[52]. Ambrosi, M.; Cameron, N. R.; Davis, B. G.; Stolnik, S. *Org. Biomol. Chem.* **2005,** *3*, 1476-1480.
[53]. Barratt, E.; Bingham, R. J.; Warner, D. J.; Laughton, C. A.; Phillips, S. E. V.; Homans, S. W. *J. Am. Chem. Soc.* **2005,** *127*, 11827-11834.
[54]. Brogan, A. P.; Widger, W. R.; Bensadek, D.; Riba-Garcia, I.; Gaskell, S. J.; Kohn, H. *J. Am. Chem. Soc.* **2005,** *127*, 2741-2751.
[55]. Brown, P. H.; Beckett, D. *Biochemistry* **2005,** *44*, 3112-3121.
[56]. Dam, T. K.; Oscarson, S.; Roy, R.; Das, S. K.; Page, D.; Macaluso, F.; Brewer, C. F. *J. Biol. Chem.* **2005,** *280*, 8640-8646.
[57]. Fielding, L.; Rutherford, S.; Fletcher, D. *Magn. Reson. Chem.* **2005,** *43*, 463-470.
[58]. Guazzaroni, M. A. E.; Krell, T.; Felipe, A.; Ruiz, R.; Meng, C. X.; Zhang, X. D.; Gallegos, M. T.; Ramos, J. L. *J. Biol. Chem.* **2005,** *280*, 20887-20893.
[59]. Johansson, J. S.; Manderson, G. A.; Ramoni, R.; Grolli, S.; Eckenhoff, R. G. *FEBS Journal* **2005,** *272*, 573-581.
[60]. Kedracka-Krok, S.; Gorecki, A.; Bonarek, P.; Wasylewski, Z. *Biochemistry* **2005,** *44*, 1037-1046.
[61]. Pereira, M. T.; Silva-Alves, J. M.; Martins-Jose, A.; Lopes, J. C. D.; Santoro, M. M. *Brazil. J. Med.Biol. Res.* **2005,** *38*, 1593-1601.

[62]. Sharrow, S. D.; Edmonds, K. A.; Goodman, M. A.; Novotny, M. V.; Stone, M. J. *Protein Sci.* **2005,** *14*, 249-256.
[63]. Bingham, R. J.; Findlay, J. B. C.; Hsieh, S. Y.; Kalverda, A. P.; Kjeliberg, A.; Perazzolo, C.; Phillips, S. E. V.; Seshadri, K.; Trinh, C. H.; Turnbull, W. B.; Bodenhausen, G.; Homans, S. W. *J. Am. Chem. Soc.* **2004,** *126*, 1675-1681.
[64]. Crump, M. P.; Ceska, T. A.; Spyracopoulos, L.; Henry, A.; Archibald, S. C.; Alexander, R.; Taylor, R. J.; Findlow, S. C.; O'Connell, J.; Robinson, M. K.; Shock, A. *Biochemistry* **2004,** *43*, 2394-2404.
[65]. Gloster, T. M.; Macdonald, J. M.; Tarling, C. A.; Stick, R. V.; Withers, S. G.; Davies, G. J. *J. Biol. Chem.* **2004,** *279*, 49236-49242.
[66]. Gotmar, G.; Ozen, C.; Serpersu, E.; Guiochon, G. *J. Chromatogr. A* **2004,** *1046*, 49-53.
[67]. King, N. M.; Prabu-Jeyabalan, M.; Nalivaika, E. A.; Wigerinck, P.; de Bethune, M. P.; Schiffer, C. A. *J. Virol.* **2004,** *78*, 12012-12021.
[68]. Kolobe, D.; Sayed, Y.; Dirr, H. W. *Biochem. J.* **2004,** *382*, 703-709.
[69]. Liu, R. Y.; Meng, Q. C.; Xi, J.; Yang, J. S.; Ha, C. E.; Bhagavan, N. V.; Eckenhoff, R. G. *Biochem. J.* **2004,** *380*, 147-152.
[70]. Ozen, C.; Serpersu, E. H. *Biochemistry* **2004,** *43*, 14667-14675.
[71]. Pey, A. L.; Thorolfsson, M.; Teigen, K.; Ugarte, M.; Martinez, A. *J. Am. Chem. Soc.* **2004,** *126*, 13670-13678.
[72]. Protasevich, II; Brouillette, C. G.; Snow, M. E.; Dunham, S.; Rubin, J. R.; Gogliotti, R.; Siegel, K. *Biochemistry* **2004,** *43*, 13380-13389.
[73]. Sawas, A. H.; Pentyala, S. N.; Rebecchi, M. J. *Biochemistry* **2004,** *43*, 12675-12685.
[74]. Stolt, P. C.; Vardar, D.; Blacklow, S. C. *Biochemistry* **2004,** *43*, 10979-10987.
[75]. Taboada, P.; Fernandez, Y.; Mosquera, V. *Biomacromolecules* **2004,** *5*, 2201-2211.
[76]. Yassin, Z.; Ortiz-Salmeron, E.; Garcia-Maroto, F.; Baron, C.; Garcia-Fuentes, L. *Biochim. Biophys. Acta-Proteins & Proteomics* **2004,** *1698*, 227-237.
[77]. Deniau, C.; Gilli, R.; Izadi-Pruneyre, N.; Letoffe, S.; Delepierre, M.; Wandersman, C.; Briand, C.; Lecroisey, A. *Biochemistry* **2003,** *42*, 10627-10633.
[78]. Dignam, J. D.; Nada, S.; Chaires, J. B. *Biochemistry* **2003,** *42*, 5333-5340.
[79]. Laurine, E.; Lafitte, D.; Gregoire, C.; Seree, E.; Loret, E.; Douillard, S.; Michel, B.; Briand, C.; Verdier, J. M. *J. Biol. Chem.* **2003,** *278*, 29979-29986.
[80]. Schon, A.; Ingaramo, M. D.; Freire, E. *Biophys. Chem.* **2003,** *105*, 221-230.
[81]. Talhout, R.; Villa, A.; Mark, A. E.; Engberts, J. *J. Am. Chem. Soc.* **2003,** *125*, 10570-10579.
[82]. Torigoe, H.; Nakayama, T.; Imazato, M.; Shimada, I.; Arata, Y.; Sarai, A. *J. Biol. Chem.* **1995**, *270*, 22218-22222.
[83]. Bazarsuren, A.; Grauschopf, U.; Wozny, M.; Reusch, D.; Hoffmann, E.; Schaefer, W.; Panzner, S.; Rudolph, R. *Biophys. Chem.* **2002**, *96*, 305-318.
[84]. Akhter, S.; Vignini, A.; Wen, Z.; English, A.; Wang, P. G.; Mutus, B. *Proc. Natl. Acad. Sci. U. S. A.* **2002**, *99*, 9172-9177.
[85]. Buddai, S. K.; Toulokhonova, L.; Bergum, P. W.; Vlasuk, G. P.; Krishnaswamy, S. *J. Biol. Chem.* **2002**, *277*, 26689-26698.
[86]. Censarek, P.; Beyermann, M.; Koch, K.-W. *Biochemistry* **2002**, *41*, 8598-8604.
[87]. Davidson, J. P.; Lubman, O.; Rose, T.; Waksman, G.; Martin, S. F. *J. Am. Chem. Soc.* **2002**, *124*, 205-215.
[88]. Gribenko, A. V.; Guzman-Casado, M.; Lopez, M. M.; Makhatadze, G. I. *Protein Sci.* **2002**, *11*, 1367-1375.
[89]. Jung, H.-I.; Bowden, S. J.; Cooper, A.; Perham, R. N. *Protein Sci.* **2002**, *11*, 1091-1100.
[90]. Yan, K. S.; Kuti, M.; Yan, S.; Mujtaba, S.; Farooq, A.; Goldfarb, M. P.; Zhou, M.-M. *J. Biol. Chem.* **2002**, *277*, 17088-17094.
[91]. Babon, J. J.; Yao, S. G.; DeSouza, D. P.; Harrison, C. F.; Fabri, L. J.; Liepinsh, E.; Scrofani, S. D.; Baca, M.; Norton, R. S. *FEBS J.* **2005,** *272*, 6120-6130.
[92]. Banerjee, Y.; Mizuguchi, J.; Iwanaga, S.; Kini, R. M. *J. Biol. Chem.* **2005,** *280*, 42601-42611.
[93]. Cliff, M. J.; Williams, M. A.; Brooke-Smith, J.; Barford, D.; Ladbury, J. E. *J. Mol. Biol.* **2005,** *346*, 717-732.

[94]. Andujar-Sanchez, M.; Smith, A. W.; Clemente-Jimenez, J. M.; Rodriguez-Vico, F.; Heras-Vazquez, F. J. L.; Jara-Perez, V.; Camara-Artigas, A. *Biochemistry* 2005, *44*, 1174-1183.
[95]. Iram, S. H.; Cronan, J. E. *J. Biol. Chem.* **2005,** *280*, 32148-32156.
[96]. Ivancic, M.; Spuches, A. M.; Guth, E. C.; Daugherty, M. A.; Wilcox, D. E.; Lyons, B. A. *Protein Sci.* **2005,** *14*, 1556-1569.
[97]. Piszczek, G.; Rozycki, J.; Singh, S. K.; Ginsburg, A.; Maurizi, M. R. *J. Biol. Chem.* **2005,** *280*, 12221-12230.
[98]. Tsvetkov, P. O.; Ezraty, B.; Mitchell, J. K.; Devred, F.; Peyrot, V.; Derrick, P. J.; Barras, F.; Makarov, A. A.; Lafitte, D. *Biochimie* **2005,** *87*, 473-480.
[99]. Udugamasooriya, G.; Saro, D.; Spaller, M. R. *Org. Lett.* **2005,** *7*, 1203-1206.
[100]. Wylie, G. P.; Rangachari, V.; Bienkiewicz, E. A.; Marin, V.; Bhattacharya, N.; Love, J. F.; Murphy, J. R.; Logan, T. M. *Biochemistry* **2005,** *44*, 40-51.
[101]. Censarek, P.; Beyermann, M.; Koch, K. W. *FEBS Lett.* **2004,** *577*, 465-468.
[102]. Cobos, E. S.; Pisabarro, M. T.; Vega, M. C.; Lacroix, E.; Serrano, L.; Ruiz-Sanz, J.; Martinez, J. C. *J. Mol. Biol.* **2004,** *342*, 355-365.
[103]. Fernando, H.; Chin, C.; Rosgen, J.; Rajarathnam, K. *J. Biol. Chem.* **2004,** *279*, 36175-36178.
[104]. Ferreon, J. C.; Hilser, V. J. *Biochemistry* **2004,** *43*, 7787-7797.
[105]. Gao, G. H.; Prutzman, K. C.; King, M. L.; Scheswohl, D. M.; DeRose, E. F.; London, R. E.; Schaller, M. D.; Campbell, S. L. *J. Biol. Chem.* **2004,** *279*, 8441-8451.
[106]. Katragadda, M.; Morikis, D.; Lambris, J. D. *J. Biol. Chem.* **2004,** *279*, 54987-54995.
[107]. Li, T.; Saro, D.; Spaller, M. R. *Bioorg. Med. Chem. Lett.* **2004,** *14*, 1385-1388.
[108]. Palencia, A.; Cobos, E. S.; Mateo, P. L.; Martinez, J. C.; Luque, I. *J. Mol. Biol.* **2004,** *336*, 527-537.
[109]. Saro, D.; Klosi, E.; Paredes, A.; Spaller, M. R. *Org. Lett.* **2004,** *6*, 3429-3432.
[110]. Zhao, K. H.; Chai, X. M.; Marmorstein, R. *J. Mol. Biol.* **2004,** *337*, 731-741.
[111]. Andujar-Sanchez, M.; Clemente-Jimenez, J. M.; Las Heras-Vazquez, F. J.; Rodriguez-Vico, F.; Camara-Artigas, A.; Jara-Perez, V. *Int. J. Biol. Macromol.* **2003,** *32*, 77-82.
[112]. Ortiz-Salmeron, E.; Nuccetelli, M.; Oakley, A. J.; Parker, M. W.; Lo Bello, M.; Garcia-Fuentes, L. *J. Biol. Chem.* **2003,** *278*, 46938-46948.
[113]. Bitto, E.; McKay, D. B. *J. Biol. Chem.* **2003,** *278*, 49316-49322.
[114]. Welfle, K.; Misselwitz, R.; Hohne, W.; Welfle, H. *J. Mol. Recognit.* **2003,** *16*, 54-62.
[115]. Murphy, K. P.; Xie, D.; Garcia, K. C.; Amzel, L. M.; Freire, E. *Proteins* **1993**, *15*, 113-120.
[116]. Gomez, J.; Freire, E. *J. Mol. Biol.* **1995**, *252*, 337-350.
[117]. Page, J. D.; You, J.-L.; Harris, R. B.; Colman, R. W. *Arch. Biochem. Biophys.* **1994**, *314*, 159-164.
[118]. Lemmon, M. A.; Ladbury, J. E.; Mandiyan, V.; Zhou, M.; Schlessinger, J. *J. Biol. Chem.* **1994**, *269*, 31653-31658.
[119]. Renzoni, D. A.; Pugh, D. J. R.; Siligardi, G.; Das, P.; Morton, C. J.; Rossi, C.; Waterfield, M. D.; Campbell, I. D.; Ladbury, J. E. *Biochemistry* **1996**, *35*, 15646-15653.
[120]. Ladbury, J. E.; Lemmon, M. A.; Zhou, M.; Green, J.; Botfield, M. C.; Schlessinger, J. *Proc. Nat. Acad. Sci. U.S.A.* **1995**, *92*, 3199-3203.
[121]. Ladbury, J. E.; Hensmann, M.; Panayotou, F.; Campbell, I. D. *Biochemistry* **1996**, *35*, 11062-11069.
[122]. Mandiyan, V.; O'Brien, R.; Zhou, M.; Margolis, B.; Lemmon, M. A.; Sturtevant, J. M.; Schlessinger, J. *J. Biol. Chem.* **1996**, *271*, 4770-4775.
[123]. Leder, L.; Berger, C.; Bornhauser, S.; Wendt, H.; Ackerman, F.; Jelesarov, I.; Bosshard, H. R. *Biochemistry* **1995**, *34*, 16509-16518.
[124]. Milos, M.; Schaer, J.-J.; Comte, M.; Cox, J. A. *J. Biol. Chem.* **1987**, *262*, 2746-2749.

[125]. Varadarajan, R.; Connelly, P. R.; Sturtevant, J. M.; Richards, F. M. *Biochemistry* **1992**, *31*, 1421-1426.
[126]. Weber, P. C.; Pantoliano, M. W.; Thompson, L. D. *Biochemistry* **1992**, *31*, 9350-9354.
[127]. Schmidt, T. G. M.; Koepke, J.; Frank, R.; Skerra, A. *J. Mol. Biol.* **1996**, *255*, 753-766.
[128]. Wu, J.; Li, J.; Li, G.; Long, D. G.; Weis, R. M. *Biochemistry* **1996**, *35*, 4984-4993.
[129]. Petrella, E. C.; Machesky, L. M.; Kaiser, D. A.; Pollard, T. D. *Biochemistry* **1996**, *35*, 16535-16543.
[130]. Jelesarov, I.; Bosshard, H. R. *J. Mol. Biol.* **1996**, *263*, 344-358.
[131]. Lin, Z.; Schwarz, F. P.; Eisenstein, E. *J. Biol. Chem.* **1995**, *270*, 1011-1014.
[132]. Smallshaw, J. E.; Georges, F.; Lee, J. S.; Waygood, E. B. *Protein Eng.* **1999**, *12*, 623-630.

BIBLIOGRAPHY

1. Adam, B. L.; Vlahou, A.; Semmes, O. J.; Wright, G. L., *Proteomics* **2001,** *1*, 1264-1270.

2. Addadi, L.; Rubin, N.; Scheffer, L.; Ziblat, R., *Accounts of Chemical Research* **2008,** *41*, 254-264.

3. Aguila, A.; Murray, R. W., *Langmuir* **2000,** *16*, 5949-5954.

4. Akhter, S.; Vignini, A.; Wen, Z.; English, A.; Wang, P. G.; Mutus, B., *Proceedings of the National Academy of Sciences of the United States of America* **2002,** *99*, 9172-9177.

5. Ambrosi, M.; Cameron, N. R.; Davis, B. G.; Stolnik, S., *Organic & Biomolecular Chemistry* **2005,** *3*, 1476-1480.

6. Anderson, N. L.; Anderson, N. G., *Molecular & Cellular Proteomics* **2002,** *1*, 845-867.

7. Anderson, N. L.; Anderson, N. G., *Molecular & Cellular Proteomics* **2002,** *1*, 845-867.

8. Andujar-Sanchez, M.; Clemente-Jimenez, J. M.; Las Heras-Vazquez, F. J.; Rodriguez-Vico, F.; Camara-Artigas, A.; Jara-Perez, V., *International Journal of Biological Macromolecules* **2003,** *32*, 77-82.

9. Andujar-Sanchez, M.; Smith, A. W.; Clemente-Jimenez, J. M.; Rodriguez-Vico, F.; Heras-Vazquez, F. J. L.; Jara-Perez, V.; Camara-Artigas, A., *Biochemistry* **2005,** *44*, 1174-1183.

10. Aoki, K.; Taguchi, H.; Shindo, Y.; Yoshida, M.; Ogasahara, K.; Yutani, K.; Tanaka, N., *Journal of Biological Chemistry* **1997,** *272*, 32158-32162.

11. Armitage, B. A., Cyanine dye-DNA interactions: Intercalation, groove binding, and aggregation. In *DNA Binders and Related Subjects*, 2005; Vol. 253, pp 55-76.

12. Armstrong, N.; De Lencastre, A.; Gouaux, E., *Protein Science* **1999,** *8*, 1475-1483.

13. Arndt, H. D.; Hauschild, K. E.; Sullivan, D. P.; Lake, K.; Dervan, P. B.; Ansari, A. Z., *Journal of the American Chemical Society* **2003,** *125*, 13322-13323.

14. Babon, J. J.; Yao, S. G.; DeSouza, D. P.; Harrison, C. F.; Fabri, L. J.; Liepinsh, E.; Scrofani, S. D.; Baca, M.; Norton, R. S., *Febs Journal* **2005,** *272*, 6120-6130.

15. Backes, A. C.; Zech, B.; Felber, B.; Klebl, B.; Muller, G., *Expert Opinion on Drug Discovery* **2008,** *3*, 1409-1425.

16. Baerga-Ortiz, A.; Bergqvist, S.; Mandell, J. G.; Komives, E. A., *Protein Science* **2004,** *13*, 166-176.

17. Baker, B. M.; Murphy, K. P., *Journal of Molecular Biology* **1997,** *268*, 557-569.

18. Baldini, L.; Wilson, A. J.; Hong, J.; Hamilton, A. D., *Journal of the American Chemical Society* **2004,** *126*, 5656-5657.

19. Banerjee, Y.; Mizuguchi, J.; Iwanaga, S.; Kini, R. M., *Journal of Biological Chemistry* **2005,** *280*, 42601-42611.

20. Barratt, E.; Bingham, R. J.; Warner, D. J.; Laughton, C. A.; Phillips, S. E. V.; Homans, S. W., *Journal of the American Chemical Society* **2005,** *127*, 11827-11834.

21. Bastian, P. J.; Ellinger, J.; Wittkamp, V.; Albers, P.; von Rucker, A.; Muller, S. C., *Journal of Urology* **2008,** *179*, 272-272.

22. Battistuzzi, G.; Borsari, M.; Ranieri, A.; Sola, M., *Journal of Biological Inorganic Chemistry* **2004,** *9*, 781-787.

23. Baugh, R. J.; Trowbrid.Cg, *Journal of Biological Chemistry* **1972,** *247*, 7498-&.

24. Bazarsuren, A.; Grauschopf, U.; Wozny, M.; Reusch, D.; Hoffmann, E.; Schaefer, W.; Panzner, S.; Rudolph, R., *Biophysical Chemistry* **2002,** *96*, 305-318.

25. Benjamin, L. R.; Chung, H. J.; Sanford, S.; Kouzine, F.; Liu, J. H.; Levens, D., *Proceedings of the National Academy of Sciences of the United States of America* **2008,** *105*, 18296-18301.

26. Bhat, H. K.; Calaf, G.; Hei, T. K.; Loya, T.; Vadgama, J. V., *Proceedings of the National Academy of Sciences of the United States of America* **2003,** *100*, 3913-3918.

27. Bingham, R. J.; Findlay, J. B. C.; Hsieh, S. Y.; Kalverda, A. P.; Kjeliberg, A.; Perazzolo, C.; Phillips, S. E. V.; Seshadri, K.; Trinh, C. H.; Turnbull, W. B.; Bodenhausen, G.; Homans, S. W., *Journal of the American Chemical Society* **2004,** *126*, 1675-1681.

28. Birktoft, J. J.; Blow, D. M., *Journal of Molecular Biology* **1972,** *68*, 187-&.

29. Bitto, E.; McKay, D. B., *Journal of Biological Chemistry* **2003,** *278*, 49316-49322.

30. Bjerre, J.; Fenger, T. H.; Marinescu, L. G.; Bols, M., *European Journal of Organic Chemistry* **2007**, 704-710.

31. Blow, D. M., *Accounts of Chemical Research* **1976,** *9*, 145-152.

32. Boal, A. K.; Rotello, V. M., *Journal of the American Chemical Society* **2000,** *122*, 734-735.

33. Bogan, A. A.; Thorn, K. S., *Journal of Molecular Biology* **1998,** *280*, 1-9.

34. Boylan, J. F.; Gudas, L. J., *Journal of Biological Chemistry* **1992,** *267*, 21486-21491.

35. Braig, K.; Otwinowski, Z.; Hegde, R.; Boisvert, D. C.; Joachimiak, A.; Horwich, A. L.; Sigler, P. B., *Nature* **1994,** *371*, 578-586.

36. Brogan, A. P.; Widger, W. R.; Bensadek, D.; Riba-Garcia, I.; Gaskell, S. J.; Kohn, H., *Journal of the American Chemical Society* **2005,** *127*, 2741-2751.

37. Brown, P. H.; Beckett, D., *Biochemistry* **2005,** *44*, 3112-3121.

38. Bruchez, M.; Moronne, M.; Gin, P.; Weiss, S.; Alivisatos, A. P., *Science* **1998,** *281*, 2013-2016.

39. Brust, M.; Walker, M.; Bethell, D.; Schiffrin, D. J.; Whyman, R., *Journal of the Chemical Society, Chemical Communications* **1994**, 801-802.

40. Buddai, S. K.; Toulokhonova, L.; Bergum, P. W.; Vlasuk, G. P.; Krishnaswamy, S., *Journal of Biological Chemistry* **2002,** *277*, 26689-26698.

41. Bunz, U. H. F., Synthesis and structure of PAEs. In *Poly(Arylene Ethynylene)S: from Synthesis to Application*, 2005; Vol. 177, pp 1-52.

42. Capasso, C.; Rizzi, M.; Menegatti, E.; Ascenzi, P.; Bolognesi, M., *Journal of Molecular Recognition* **1997,** *10*, 26-35.

43. Caplan, A. J.; Mandal, A. K.; Theodoraki, M. A., *Trends in Cell Biology* **2007,** *17*, 87-92.

44. Castro, M. J. M.; Anderson, S., *Biochemistry* **1996,** *35*, 11435-11446.

45. Cavalieri, F.; Chiessi, E.; Paradossi, G., *Soft Matter* **2007,** *3*, 718-724.

46. Censarek, P.; Beyermann, M.; Koch, K. W., *Biochemistry* **2002,** *41*, 8598-8604.

47. Censarek, P.; Beyermann, M.; Koch, K. W., *Febs Letters* **2004,** *577*, 465-468.

48. Chakrabarti, R.; Klibanov, A. M., *J. Am. Chem. Soc.* **2003,** *125*, 12531-12540.

49. Chalfie, M.; KainIn, S. R., *Green Fluorescent Protein: Properties, Applications, and Protocols*. Wiley-Interscience: Hoboken, N.J., 2006.

50. Chan, W. C. W.; Nie, S. M., *Science* **1998,** *281*, 2016-2018.

51. Chapman, E.; Farr, G. W.; Fenton, W. A.; Johnson, S. M.; Horwich, A. L., *Proceedings of the National Academy of Sciences of the United States of America* **2008,** *105*, 19205-19210.

52. Chauvin, F.; Fomenkov, A.; Johnson, C. R.; Roseman, S., *Proceedings of the National Academy of Sciences of the United States of America* **1996,** *93*, 7028-7031.

53. Chen, C. P.; Hsu, C. H.; Su, N. Y.; Lin, Y. C.; Chiou, S. H.; Wu, S. H., *Journal of Biological Chemistry* **2001,** *276*, 45079-45087.

54. Cheon, J.; Lee, J. H., *Accounts of Chemical Research* **2008,** *41*, 1630-1640.

55. Chiti, F.; Dobson, C. M., *Annual Review of Biochemistry* **2006,** *75*, 333-366.

56. Ciosek, P.; Wroblewski, W., *Analyst* **2007,** *132*, 963-978.

57. Clark, E. D., *Current Opinion in Biotechnology* **2001,** *12*, 202-207.

58. Cleland, J. L.; Hedgepeth, C.; Wang, D. I. C., *Journal of Biological Chemistry* **1992,** *267*, 13327-13334.

59. Cliff, M. J.; Williams, M. A.; Brooke-Smith, J.; Barford, D.; Ladbury, J. E., *Journal of Molecular Biology* **2005,** *346*, 717-732.

60. Cobb, N. J.; Sonnichsen, F. D.; McHaourab, H.; Surewicz, W. K., *Proceedings of the National Academy of Sciences of the United States of America* **2007,** *104*, 18946-18951.

61. Cobos, E. S.; Pisabarro, M. T.; Vega, M. C.; Lacroix, E.; Serrano, L.; Ruiz-Sanz, J.; Martinez, J. C., *Journal of Molecular Biology* **2004,** *342*, 355-365.

62. Crump, M. P.; Ceska, T. A.; Spyracopoulos, L.; Henry, A.; Archibald, S. C.; Alexander, R.; Taylor, R. J.; Findlow, S. C.; O'Connell, J.; Robinson, M. K.; Shock, A., *Biochemistry* **2004,** *43*, 2394-2404.

63. Dam, T. K.; Oscarson, S.; Roy, R.; Das, S. K.; Page, D.; Macaluso, F.; Brewer, C. F., *Journal of Biological Chemistry* **2005,** *280*, 8640-8646.

64. Daniels, M. J.; Wang, Y. M.; Lee, M. Y.; Venkitaraman, A. R., *Science* **2004,** *306*, 876-879.

65. Davidson, J. P.; Lubman, O.; Rose, T.; Waksman, G.; Martin, S. F., *Journal of the American Chemical Society* **2002,** *124*, 205-215.

66. de la Fuente, J. M.; Barrientos, A. G.; Rojas, T. C.; Rojo, J.; Canada, J.; Fernandez, A.; Penades, S., *Angewandte Chemie-International Edition* **2001,** *40*, 2257-2261.

67. de Laureto, P. P.; Frare, E.; Gottardo, R.; van Dael, H.; Fontana, A., *Protein Science* **2002,** *11*, 2932-2946.

68. De, M.; Ghosh, P. S.; Rotello, V. M., *Advanced Materials* **2008,** *20*, 4225-4241.

69. De, M.; Rana, S.; Rotello, V. M., *Macromolecular Bioscience* **2009,** *9*, DOI: 10.1002/mabi.200800289.

70. De, M.; You, C. C.; Srivastava, S.; Rotello, V. M., *Journal of the American Chemical Society* **2007,** *129*, 10747-10753.

71. de Rinaldis, M.; Ausiello, G.; Cesareni, G.; Helmer-Citterich, M., *Journal of Molecular Biology* **1998,** *284*, 1211-1221.

72. De Souza, A. C.; Kamerling, J. P., *Methods in Enzymology* **2006,** *417*, 221-243.

73. Deniau, C.; Gilli, R.; Izadi-Pruneyre, N.; Letoffe, S.; Delepierre, M.; Wandersman, C.; Briand, C.; Lecroisey, A., *Biochemistry* **2003,** *42*, 10627-10633.

74. Derfus, A. M.; Chen, A. A.; Min, D. H.; Ruoslahti, E.; Bhatia, S. N., *Bioconjugate Chemistry* **2007,** *18*, 1391-1396.

75. Desie, G.; Boens, N.; Deschryver, F. C., *Biochemistry* **1986,** *25*, 8301-8308.

76. DeVries, G. A.; Brunnbauer, M.; Hu, Y.; Jackson, A. M.; Long, B.; Neltner, B. T.; Uzun, O.; Wunsch, B. H.; Stellacci, F., *Science* **2007,** *315*, 358-361.

77. Di Cera, E., *Chemical Reviews* **1998,** *98*, 1563-1591.

78. Di Fiore, A.; Monti, S. M.; Hilvo, M.; Parkkila, S.; Romano, V.; Scaloni, A.; Pedone, C.; Scozzafava, A.; Supuran, C. T.; De Simone, G., *Proteins-Structure Function and Bioinformatics* **2009,** *74*, 164-175.

79. Dignam, J. D.; Nada, S.; Chaires, J. B., *Biochemistry* **2003,** *42*, 5333-5340.

80. Dobson, C. M., *Nature* **2003,** *426*, 884-890.

81. Dubertret, B.; Calame, M.; Libchaber, A. J., *Nature Biotechnology* **2001,** *19*, 365-370.

82. Duellman, S. J.; Burgess, R. R., *Protein Expression and Purification* **2009,** *63*, 128-133.

83. Dunitz, J. D., *Chemistry & Biology* **1995,** *2*, 709-712.

84. Eigenbrot, C.; Randal, M.; Presta, L.; Carter, P.; Kossiakoff, A. A., *Journal of Molecular Biology* **1993,** *229*, 969-995.

85. Ernst, J. T.; Becerril, J.; Park, H. S.; Yin, H.; Hamilton, A. D., *Angewandte Chemie-International Edition* **2003,** *42*, 535-+.

86. Euliss, L. E.; DuPont, J. A.; Gratton, S.; DeSimone, J., *Chemical Society Reviews* **2006,** *35*, 1095-1104.

87. Evans, L. J. A.; Cooper, A.; Lakey, J. H., *Journal of Molecular Biology* **1996,** *255*, 559-563.

88. Fairlie, D. P.; West, M. L.; Wong, A. K., *Current Medicinal Chemistry* **1998,** *5*, 29-62.

89. Fan, H. Y.; Chen, Z.; Brinker, C. J.; Clawson, J.; Alam, T., *Journal of the American Chemical Society* **2005,** *127*, 13746-13747.

90. Fan, H. Y.; Leve, E. W.; Scullin, C.; Gabaldon, J.; Tallant, D.; Bunge, S.; Boyle, T.; Wilson, M. C.; Brinker, C. J., *Nano Letters* **2005,** *5*, 645-648.

91. Favero, G.; Campanella, L.; Cavallo, S.; D'Annibale, A.; Perrella, M.; Mattei, E.; Ferri, T., *Journal of the American Chemical Society* **2005,** *127*, 8103-8111.

92. Fawzi, N. L.; Chubukov, V.; Clark, L. A.; Brown, S.; Head-Gordon, T., *Protein Science* **2005,** *14*, 993-1003.

93. Fazal, M. A.; Roy, B. C.; Sun, S. G.; Mallik, S.; Rodgers, K. R., *Journal of the American Chemical Society* **2001,** *123*, 6283-6290.

94. Fechter, E. J.; Olenyuk, B.; Dervan, P. B., *Angewandte Chemie-International Edition* **2004,** *43*, 3591-3594.

95. Feltham, J. L.; Gierasch, L. M., *Cell* **2000,** *100*, 193-196.

96. Fernando, H.; Chin, C.; Rosgen, J.; Rajarathnam, K., *Journal of Biological Chemistry* **2004,** *279*, 36175-36178.

97. Ferrando, R.; Jellinek, J.; Johnston, R. L., *Chemical Reviews* **2008,** *108*, 845-910.

98. Ferreon, J. C.; Hilser, V. J., *Biochemistry* **2004,** *43*, 7787-7797.

99. Ferrer, M. L.; Duchowicz, R.; Carrasco, B.; de la Torre, J. G.; Acuna, A. U., *Biophysical Journal* **2001,** *80*, 2422-2430.

100. Fielding, L.; Rutherford, S.; Fletcher, D., *Magnetic Resonance in Chemistry* **2005,** *43*, 463-470.

101. Filfil, R.; Chalikian, T. V., *Journal of Molecular Biology* **2003,** *326*, 1271-1288.

102. Fink, A. L., *Physiological Reviews* **1999,** *79*, 425-449.

103. Fink, A. L.; Oberg, K. A.; Seshadri, S., *Folding & Design* **1998,** *3*, 19-25.

104. Fiocchi, C., *Gastroenterology* **1998,** *115*, 182-205.

105. Fischer, N. O.; McIntosh, C. M.; Simard, J. M.; Rotello, V. M., *Proc. Natl. Acad. Sci. U.S.A.* **2002,** *99*, 5018-5023.

106. Fischer, N. O.; Verma, A.; Goodman, C. M.; Simard, J. M.; Rotello, V. M., *Journal of the American Chemical Society* **2003,** *125*, 13387-13391.

107. Flajolet, M.; Wang, Z. F.; Futter, M.; Shen, W. X.; Nuangchamnong, N.; Bendor, J.; Wallach, I.; Nairn, A. C.; Surmeier, D. J.; Greengard, P., *Nature Neuroscience* **2008,** *11*, 1402-1409.

108. Flatman, R.; McLauchlan, W. R.; Juge, N.; Furniss, C.; Berrin, J. G.; Hughes, R. K.; Manzanares, P.; Ladbury, J. E.; O'Brien, R.; Williamson, G., *Biochemical Journal* **2002,** *365*, 773-781.

109. Fletchera, J. I.; Meusburger, S.; Hawkins, C. J.; Riglar, D. T.; Lee, E. F.; Fairlie, W. D.; Huang, D. C. S.; Adams, J. M., *Proceedings of the National Academy of Sciences of the United States of America* **2008,** *105*, 18081-18087.

110. Folmer-Andersen, J. F.; Kitamura, M.; Anslyn, E. V., *Journal of the American Chemical Society* **2006,** *128*, 5652-5653.

111. Fukada, H.; Takahashi, K.; Sturtevant, J. M., *Biochemistry* **1985,** *24*, 5109-5115.

112. Furuta, T.; Wang, S. S. H.; Dantzker, J. L.; Dore, T. M.; Bybee, W. J.; Callaway, E. M.; Denk, W.; Tsien, R. Y., *Proceedings of the National Academy of Sciences of the United States of America* **1999,** *96*, 1193-1200.

113. Gao, G. H.; Prutzman, K. C.; King, M. L.; Scheswohl, D. M.; DeRose, E. F.; London, R. E.; Schaller, M. D.; Campbell, S. L., *Journal of Biological Chemistry* **2004,** *279*, 8441-8451.

114. Gardner, J. W.; Bartlett, P. N., *Electronic Noses. Principles and Applications*. Oxford University Press, USA: 1999.

115. Gearhart, M. D.; Dickinson, L.; Ehley, J.; Melander, C.; Dervan, P. B.; Wright, P. E.; Gottesfeld, J. M., *Biochemistry* **2005,** *44*, 4196-4203.

116. Gell, D.; Kong, Y.; Eaton, S. A.; Weiss, M. J.; Mackay, J. P., *Journal of Biological Chemistry* **2002,** *277*, 40602-40609.

117. Gerion, D.; Herberg, J.; Bok, R.; Gjersing, E.; Ramon, E.; Maxwell, R.; Kurhanewicz, J.; Budinger, T. F.; Gray, J. W.; Shuman, M. A.; Chen, F. F., *Journal of Physical Chemistry C* **2007,** *111*, 12542-12551.

118. Gestwicki, J. E.; Cairo, C. W.; Strong, L. E.; Oetjen, K. A.; Kiessling, L. L., *Journal of the American Chemical Society* **2002,** *124*, 14922-14933.

119. Ginsburg, G. S.; McCarthy, J. J., *Trends in Biotechnology* **2001,** *19*, 491-496.

120. Girard, M.; Turgeon, S. L.; Gauthier, S. F., *Journal of Agricultural and Food Chemistry* **2003,** *51*, 4450-4455.

121. Gloster, T. M.; Macdonald, J. M.; Tarling, C. A.; Stick, R. V.; Withers, S. G.; Davies, G. J., *Journal of Biological Chemistry* **2004,** *279*, 49236-49242.

122. Glover, J. R.; Lindquist, S., *Cell* **1998,** *94*, 73-82.

123. Golumbfskie, A. J.; Pande, V. S.; Chakraborty, A. K., *Proceedings of the National Academy of Sciences of the United States of America* **1999,** *96*, 11707-11712.

124. Gomez, J.; Freire, E., *Journal of Molecular Biology* **1995,** *252*, 337-350.

125. Gong, G., *Journal of the American Statistical Association* **1986,** *81*, 108-113.

126. Goodman, C. A.; Frankamp, B. L.; Cooper, B. A.; Rotello, V. A., *Colloids and Surfaces B-Biointerfaces* **2004,** *39*, 119-123.

127. Gordon, E. J.; Sanders, W. J.; Kiessling, L. L., *Nature* **1998,** *392*, 30-31.

128. Gotmar, G.; Ozen, C.; Serpersu, E.; Guiochon, G., *Journal of Chromatography A* **2004,** *1046*, 49-53.

129. Granneman, J. G.; Moore, H. P. H.; Granneman, R. L.; Greenberg, A. S.; Obin, M. S.; Zhu, Z. X., *Journal of Biological Chemistry* **2007,** *282*, 5726-5735.

130. Greene, N. T.; Shimizu, K. D., *Journal of the American Chemical Society* **2005,** *127*, 5695-5700.

131. Greenfield, N. J., *Analytical Biochemistry* **1996,** *235*, 1-10.

132. Greenfield, N. J., *Numerical Computer Methods, Pt D* **2004,** *383*, 282-317.

133. Greenfield, N. J., *Nature Protocols* **2006,** *1*, 2876-2890.

134. Gribenko, A. V.; Guzman-Casado, M.; Lopez, M. M.; Makhatadze, G. I., *Protein Science* **2002,** *11*, 1367-1375.

135. Grueninger, D.; Treiber, N.; Ziegler, M. O. P.; Koetter, J. W. A.; Schulze, M. S.; Schulz, G. E., *Science* **2008,** *319*, 206-209.

136. Guazzaroni, M. A. E.; Krell, T.; Felipe, A.; Ruiz, R.; Meng, C. X.; Zhang, X. D.; Gallegos, M. T.; Ramos, J. L., *Journal of Biological Chemistry* **2005,** *280*, 20887-20893.

137. Haab, B. B., *Current Opinion in Biotechnology* **2006,** *17*, 415-421.

138. Han, G.; Martin, C. T.; Rotello, V. M., *Chemical Biology & Drug Design* **2006,** *67*, 78-82.

139. Hanessian, S.; Auzzas, L., *Accounts of Chemical Research* **2008,** *41*, 1241-1251.

140. Harrison, C. J.; Bohm, A. A.; Nelson, H. C. M., *Science* **1994,** *263*, 224-227.

141. Hartl, F. U., *Nature* **1996,** *381*, 571-580.

142. Hedstrom, L., *Chem. Rev.* **2002,** *102*, 4501-4524.

143. Hegde, S. S.; Dam, T. K.; Brewer, C. F.; Blanchard, J. S., *Biochemistry* **2002,** *41*, 7519-7527.

144. Henares, T. G.; Mizutani, F.; Hisamoto, H., *Analytica Chimica Acta* **2008,** *611*, 17-30.

145. Hibbits, K. A.; Gill, D. S.; Willson, R. C., *Biochemistry* **1994,** *33*, 3584-3590.

146. Hildebrandt, N.; Charbonniere, L. J.; Beck, M.; Ziessel, R. F.; Lohmannsroben, H. G., *Angew. Chem.-Int. Ed.* **2005,** *44*, 7612-7615.

147. Holdgate, G. A.; Tunnicliffe, A.; Ward, W. H. J.; Weston, S. A.; Rosenbrock, G.; Barth, P. T.; Taylor, I. W. F.; Pauptit, R. A.; Timms, D., *Biochemistry* **1997,** *36*, 9663-9673.

148. Hong, R.; Fischer, N. O.; Verma, A.; Goodman, C. M.; Emrick, T.; Rotello, V. M., *J. Am. Chem. Soc.* **2004,** *126*, 739-743.

149. Hong, R.; Han, G.; Fernandez, J. M.; Kim, B. J.; Forbes, N. S.; Rotello, V. M., *J. Am. Chem. Soc.* **2006,** *128*, 1078-1079.

150. Hood, L.; Heath, J. R.; Phelps, M. E.; Lin, B. Y., *Science* **2004,** *306*, 640-643.

151. Horne, W. S.; Gellman, S. H., *Accounts of Chemical Research* **2008,** *41*, 1399-1408.

152. Hostetler, M. J.; Templeton, A. C.; Murray, R. W., *Langmuir* **1999,** *15*, 3782-3789.

153. Hostetler, M. J.; Wingate, J. E.; Zhong, C. J.; Harris, J. E.; Vachet, R. W.; Clark, M. R.; Londono, J. D.; Green, S. J.; Stokes, J. J.; Wignall, G. D.; Glish, G. L.; Porter, M. D.; Evans, N. D.; Murray, R. W., *Langmuir* **1998,** *14*, 17-30.

154. Houk, K. N.; Leach, A. G.; Kim, S. P.; Zhang, X., *Angew. Chem. Int. Ed.* **2003,** *42*, 4872 – 4897.

155. Houseman, B. T.; Mrksich, M., *Journal of Organic Chemistry* **1998,** *63*, 7552-7555.

156. Hu, M. H.; Qian, L. P.; Brinas, R. P.; Lymar, E. S.; Hainfeld, J. F., *Angewandte Chemie-International Edition* **2007,** *46*, 5111-5114.

157. Hu, Y.; Zhang, S. Z.; Yu, J. K.; Liu, J.; Zheng, S., *Breast* **2005,** *14*, 250-255.

158. Hughes, A. D.; Glenn, I. C.; Patrick, A. D.; Ellington, A.; Anslyn, E. V., *Chemistry-a European Journal* **2008,** *14*, 1822-1827.

159. IbarraMolero, B.; SanchezRuiz, J. M., *Biochemistry* **1997,** *36*, 9616-9624.

160. Iram, S. H.; Cronan, J. E., *Journal of Biological Chemistry* **2005,** *280*, 32148-32156.

161. Issaq, H. J.; Xiao, Z.; Veenstra, T. D., *Chemical Reviews* **2007,** *107*, 3601-3620.

162. Ito, L.; Kobayashi, T.; Shiraki, K.; Yamaguchi, H., *Journal of Synchrotron Radiation* **2008,** *15*, 316-318.

163. Ivancic, M.; Spuches, A. M.; Guth, E. C.; Daugherty, M. A.; Wilcox, D. E.; Lyons, B. A., *Protein Science* **2005,** *14*, 1556-1569.

164. Jelesarov, I.; Bosshard, H. R., *Biochemistry* **1994,** *33*, 13321-13328.

165. Jelesarov, I.; Bosshard, H. R., *Journal of Molecular Biology* **1996,** *263*, 344-358.

166. Jelesarov, I.; Bosshard, H. R., *Journal of Molecular Recognition* **1999,** *12*, 3-18.

167. Jin, Y. H.; Kannan, S.; Wu, M.; Zhao, J. X. J., *Chemical Research in Toxicology* **2007,** *20*, 1126-1133.

168. Johanson, K.; Appelbaum, E.; Doyle, M.; Hensley, P.; Zhao, B.; Abdelmeguid, S. S.; Young, P.; Cook, R.; Carr, S.; Matico, R.; Cusimano, D.; Dul, E.; Angelichio, M.; Brooks, I.; Winborne, E.; McDonnell, P.; Morton, T.; Bennett, D.; Sokoloski, T.; McNulty, D.; Rosenberg, M.; Chaiken, I., *Journal of Biological Chemistry* **1995,** *270*, 9459-9471.

169. Johansson, J. S.; Manderson, G. A.; Ramoni, R.; Grolli, S.; Eckenhoff, R. G., *Febs Journal* **2005,** *272*, 573-581.

170. Johns, E. W., *Biochemical Journal* **1964,** *92*, 55-&.

171. Jones, S.; Thornton, J. M., *Proceedings of the National Academy of Sciences of the United States of America* **1996,** *93*, 13-20.

172. Jones, S.; Thornton, J. M., *Proceedings of the National Academy of Sciences of the United States of America* **1996,** *93*, 13-20.

173. Joshi, H.; Shirude, P. S.; Bansal, V.; Ganesh, K. N.; Sastry, M., *Journal of Physical Chemistry B* **2004,** *108*, 11535-11540.

174. Juan, Z.; Swager, T. M., Poly(arylene ethynylene)s in chemosensing and biosensing. In *Poly(Arylene Ethynylene)S: from Synthesis to Application*, 2005; Vol. 177, pp 151-179.

175. Jung, H. I.; Bowden, S. J.; Cooper, A.; Perham, R. N., *Protein Science* **2002,** *11*, 1091-1100.

176. Jung, H. I.; Cooper, A.; Perham, R. N., *Biochemistry* **2002,** *41*, 10446-10453.

177. Kanaras, A. G.; Kamounah, F. S.; Schaumburg, K.; Kiely, C. J.; Brust, M., *Chemical Communications* **2002**, 2294-2295.

178. Karaman, M. W.; Herrgard, S.; Treiber, D. K.; Gallant, P.; Atteridge, C. E.; Campbell, B. T.; Chan, K. W.; Ciceri, P.; Davis, M. I.; Edeen, P. T.; Faraoni, R.; Floyd, M.; Hunt, J. P.; Lockhart, D. J.; Milanov, Z. V.; Morrison, M. J.; Pallares, G.; Patel, H. K.; Pritchard, S.; Wodicka, L. M.; Zarrinkar, P. P., *Nature Biotechnology* **2008,** *26*, 127-132.

179. Karlsson, M.; Davidson, M.; Karlsson, R.; Karlsson, A.; Bergenholtz, J.; Konkoli, Z.; Jesorka, A.; Lobovkina, T.; Hurtig, J.; Voinova, M.; Orwar, O., *Annual Review of Physical Chemistry* **2004,** *55*, 613-649.

180. Karlsson, M.; Martensson, L. G.; Jonsson, B. H.; Carlsson, U., *Langmuir* **2000,** *16*, 8470-8479.

181. Katragadda, M.; Morikis, D.; Lambris, J. D., *Journal of Biological Chemistry* **2004,** *279*, 54987-54995.

182. Kedracka-Krok, S.; Gorecki, A.; Bonarek, P.; Wasylewski, Z., *Biochemistry* **2005,** *44*, 1037-1046.

183. Keeble, A. H.; Kirkpatrick, N.; Shimizu, S.; Kleanthous, C., *Biochemistry* **2006,** *45*, 3243-3254.

184. Kelley, R. F.; Costas, K. E.; Oconnell, M. P.; Lazarus, R. A., *Biochemistry* **1995,** *34*, 10383-10392.

185. Kelley, R. F.; Oconnell, M. P.; Carter, P.; Presta, L.; Eigenbrot, C.; Covarrubias, M.; Snedecor, B.; Bourell, J. H.; Vetterlein, D., *Biochemistry* **1992,** *31*, 5434-5441.

186. Khademhosseini, A.; Jon, S.; Suh, K. Y.; Tran, T. N. T.; Eng, G.; Yeh, J.; Seong, J.; Langer, R., *Advanced Materials* **2003,** *15*, 1995-2000.

187. Kim, I. B.; Dunkhorst, A.; Gilbert, J.; Bunz, U. H. F., *Macromolecules* **2005,** *38*, 4560-4562.

188. King, N. M.; Prabu-Jeyabalan, M.; Nalivaika, E. A.; Wigerinck, P.; de Bethune, M. P.; Schiffer, C. A., *Journal of Virology* **2004,** *78*, 12012-12021.

189. Kingsmore, S. F., *Nature Reviews Drug Discovery* **2006,** *5*, 310-320.

190. Koffas, T. S.; Kim, J.; Lawrence, C. C.; Somorjai, G. A., *Langmuir* **2003,** *19*, 3563-3566.

191. Kolobe, D.; Sayed, Y.; Dirr, H. W., *Biochemical Journal* **2004,** *382*, 703-709.

192. Koncki, R., *Analytica Chimica Acta* **2007,** *599*, 7-15.

193. Kouadio, J. L. K.; Horn, J. R.; Pal, G.; Kossiakoff, A. A., *Journal of Biological Chemistry* **2005,** *280*, 25524-25532.

194. Kresheck, G. C.; Vitello, L. B.; Erman, J. E., *Biochemistry* **1995,** *34*, 8398-8405.

195. Krum, J. G.; Ellsworth, H.; Sargeant, R. R.; Rich, G.; Ensign, S. A., *Biochemistry* **2002,** *41*, 5005-5014.

196. Kruzel, M.; Morawiecka, B., *Acta Biochimica Polonica* **1982,** *29*, 321-330.

197. Kudou, M.; Shiraki, K.; Fujiwara, S.; Imanaka, T.; Takagi, M., *European Journal of Biochemistry* **2003,** *270*, 4547-4554.

198. Kussie, P. H.; Gorina, S.; Marechal, V.; Elenbaas, B.; Moreau, J.; Levine, A. J.; Pavletich, N. P., *Science* **1996,** *274*, 948-953.

199. Kwon, K.; Streaker, E. D.; Beckett, D., *Protein Science* **2002,** *11*, 558-570.

200. Ladbury, J. E.; Hensmann, M.; Panayotou, G.; Campbell, I. D., *Biochemistry* **1996,** *35*, 11062-11069.

201. Ladbury, J. E.; Lemmon, M. A.; Zhou, M.; Green, J.; Botfield, M. C.; Schlessinger, J., *Proceedings of the National Academy of Sciences of the United States of America* **1995,** *92*, 3199-3203.

202. Lafitte, D.; Lamour, V.; Tsvetkov, P. O.; Makarov, A. A.; Klich, M.; Deprez, P.; Moras, D.; Briand, C.; Gilli, R., *Biochemistry* **2002,** *41*, 7217-7223.

203. Langer, T.; Lu, C.; Echols, H.; Flanagan, J.; Hayer, M. K.; Hartl, F. U., *Nature* **1992,** *356*, 683-689.

204. Larsericsdotter, H.; Oscarsson, S.; Buijs, J., *Journal of Colloid and Interface Science* **2001,** *237*, 98-103.

205. Larsericsdotter, H.; Oscarsson, S.; Buijs, J., *Journal of Colloid and Interface Science* **2005,** *289*, 26-35.

206. Laurine, E.; Lafitte, D.; Gregoire, C.; Seree, E.; Loret, E.; Douillard, S.; Michel, B.; Briand, C.; Verdier, J. M., *Journal of Biological Chemistry* **2003,** *278*, 29979-29986.

207. Lavigne, J. J.; Anslyn, E. V., *Angewandte Chemie-International Edition* **2001,** *40*, 3119-3130.

208. Lavigne, J. J.; Savoy, S.; Clevenger, M. B.; Ritchie, J. E.; McDoniel, B.; Yoo, S. J.; Anslyn, E. V.; McDevitt, J. T.; Shear, J. B.; Neikirk, D., *Journal of the American Chemical Society* **1998,** *120*, 6429-6430.

209. Leder, L.; Berger, C.; Bornhauser, S.; Wendt, H.; Ackermann, F.; Jelesarov, I.; Bosshard, H. R., *Biochemistry* **1995,** *34*, 16509-16518.

210. Lee, C. H.; Leung, B.; Lemmon, M. A.; Zheng, J.; Cowburn, D.; Kuriyan, J.; Saksela, K., *Embo Journal* **1995,** *14*, 5006-5015.

211. Lee, J. H.; Jun, Y. W.; Yeon, S. I.; Shin, J. S.; Cheon, J., *Angewandte Chemie-International Edition* **2006,** *45*, 8160-8162.

212. Lee, J. W.; Lee, J. S.; Kang, M.; Su, A. I.; Chang, Y. T., *Chemistry-a European Journal* **2006,** *12*, 5691-5696.

213. Lee, Y. C., *Faseb Journal* **1992,** *6*, 3193-3200.

214. Lei, H. X.; Wu, C.; Liu, H. G.; Duan, Y., *Proceedings of the National Academy of Sciences of the United States of America* **2007,** *104*, 4925-4930.

215. Lemmon, M. A.; Ladbury, J. E.; Mandiyan, V.; Zhou, M.; Schlessinger, J., *Journal of Biological Chemistry* **1994,** *269*, 31653-31658.

216. Leung, D.; Folmer-Andersen, J. F.; Lynch, V. M.; Anslyn, E. V., *Journal of the American Chemical Society* **2008,** *130*, 12318-12327.

217. Leung, D. K.; Yang, Z. W.; Breslow, R., *Proceedings of the National Academy of Sciences of the United States of America* **2000,** *97*, 5050-5053.

218. Li, J. N.; Zhang, Z.; Rosenzweig, J.; Wang, Y. Y.; Chan, D. W., *Clinical Chemistry* **2002,** *48*, 1296-1304.

219. Li, J. Y.; Swanson, R. V.; Simon, M. I.; Weis, R. M., *Biochemistry* **1995,** *34*, 14626-14636.

220. Li, T.; Saro, D.; Spaller, M. R., *Bioorganic & Medicinal Chemistry Letters* **2004,** *14*, 1385-1388.

221. Li, Z.; Lazaridis, T., *Journal of Physical Chemistry B* **2005,** *109*, 662-670.

222. Lijnzaad, P.; Argos, P., *Proteins-Structure Function and Genetics* **1997,** *28*, 333-343.

223. Lin, C. C.; Yeh, Y. C.; Yang, C. Y.; Chen, G. F.; Chen, Y. C.; Wu, Y. C.; Chen, C. C., *Chemical Communications* **2003**, 2920-2921.

224. Lin, Z.; Madan, D.; Rye, H. S., *Nature Structural & Molecular Biology* **2008,** *15*, 303-311.

225. Lin, Z. L.; Schwarz, F. P.; Eisenstein, E., *Journal of Biological Chemistry* **1995,** *270*, 1011-1014.
226. Lindman, S.; Lynch, I.; Thulin, E.; Nilsson, H.; Dawson, K. A.; Linse, S., *Nano Letters* **2007,** *7*, 914-920.

227. Lindner, A. B.; Madden, R.; Dernarez, A.; Stewart, E. J.; Taddei, F., *Proceedings of the National Academy of Sciences of the United States of America* **2008,** *105*, 3076-3081.

228. Lindsley, C. W.; Barnett, S. F.; Yaroschak, M.; Bilodeau, M. T.; Layton, M. E., *Current Topics in Medicinal Chemistry* **2007,** *7*, 1349-1363.

229. Linert, W., *Chemical Physics* **1989,** *129*, 381-393.

230. Link, S.; Wang, Z. L.; El-Sayed, M. A., *Journal of Physical Chemistry B* **1999,** *103*, 3529-3533.

231. Liu, L.; Guo, Q. X., *Chemical Reviews* **2001,** *101*, 673-695.

232. Liu, R. Y.; Meng, Q. C.; Xi, J.; Yang, J. S.; Ha, C. E.; Bhagavan, N. V.; Eckenhoff, R. G., *Biochemical Journal* **2004,** *380*, 147-152.

233. Liu, Y.; Tong, L.-H.; Huang, S.; Tian, B.-Z.; Inoue, Y.; Hakushi, T., *J. Phys. Chem.* **1990,** *94*, 2666-2670.

234. Lo Conte, L.; Chothia, C.; Janin, J., *Journal of Molecular Biology* **1999,** *285*, 2177-2198.

235. Lukasik, S. M.; Zhang, L. N.; Corpora, T.; Tomanicek, S.; Li, Y. H.; Kundu, M.; Hartman, K.; Liu, P. P.; Laue, T. M.; Biltonen, R. L.; Speck, N. A.; Bushweller, J. H., *Nature Structural Biology* **2002,** *9*, 674-679.

236. Ma, P. X., *Advanced Drug Delivery Reviews* **2008,** *60*, 184-198.

237. MacBeath, G., *Nature Genetics* **2002,** *32*, 526-532.

238. Macdonald, I. D. G.; Smith, W. E., *Langmuir* **1996,** *12*, 706-713.

239. Mahtab, R.; Harden, H. H.; Murphy, C. J., *Journal of the American Chemical Society* **2000,** *122*, 14-17.

240. Mairal, T.; Ozalp, V. C.; Sanchez, P. L.; Mir, M.; Katakis, I.; O'Sullivan, C. K., *Analytical and Bioanalytical Chemistry* **2008,** *390*, 989-1007.

241. Makhatadze, G. I.; Privalov, P. L., *Journal of Molecular Biology* **1993,** *232*, 639-659.

242. Mammen, M.; Choi, S. K.; Whitesides, G. M., *Angewandte Chemie-International Edition* **1998,** *37*, 2755-2794.

243. Mandiyan, V.; Obrien, R.; Zhou, M.; Margolis, B.; Lemmon, M. A.; Sturtevant, J. M.; Schlessinger, J., *Journal of Biological Chemistry* **1996,** *271*, 4770-4775.

244. Marsili, V.; Lupidi, G.; Berellini, G.; Calzuola, I.; Perni, S.; Cruciani, G.; Gianfranceschi, G. L., *Peptides* **2008,** *29*, 2232-2242.

245. Martinez, J. S.; Olivera, B. M.; Gray, W. R.; Craig, A. G.; Groebe, D. R.; Abramson, S. N.; McIntosh, J. M., *Biochemistry* **1995,** *34*, 14519-14526.

246. Massart, D. L.; Kaufman, L., *The Interpretation of Analytical Chemical Data by the Use of Cluster Analysis*. John Wiley and Sons: New York, 1983.

247. McConn, J.; Fasman, G. D.; Hess, G. P., *Journal of Molecular Biology* **1969,** *39*, 551-562.

248. McIntosh, C. M.; Esposito, E. A.; Boal, A. K.; Simard, J. M.; Martin, C. T.; Rotello, V. M., *Journal of the American Chemical Society* **2001,** *123*, 7626-7629.

249. McLean, M. A.; Sligar, S. G., *Biochemical and Biophysical Research Communications* **1995,** *215*, 316-320.

250. McMillan, R. A.; Paavola, C. D.; Howard, J.; Chan, S. L.; Zaluzec, N. J.; Trent, J. D., *Nature Materials* **2002,** *1*, 247-252.

251. McPherson, R. A.; Pincus, M. R., *Henry's Clinical Diagnosis and Manangement by Laboratory Methods*. 21st ed.; Saunders-Elsevier: 2007; Vol. Chapter 19.

252. Medarova, Z.; Pham, W.; Farrar, C.; Petkova, V.; Moore, A., *Nature Medicine* **2007,** *13*, 372-377.

253. Meiring, J. E.; Schmid, M. J.; Grayson, S. M.; Rathsack, B. M.; Johnson, D. M.; Kirby, R.; Kannappan, R.; Manthiram, K.; Hsia, B.; Hogan, Z. L.; Ellington, A. D.; Pishko, M. V.; Willson, C. G., *Chemistry of Materials* **2004,** *16*, 5574-5580.

254. Merchant, K. A.; Best, R. B.; Louis, J. M.; Gopich, I. V.; Eaton, W. A., *Proceedings of the National Academy of Sciences of the United States of America* **2007,** *104*, 1528-1533.

255. Meyer-Luehmann, M.; Spires-Jones, T. L.; Prada, C.; Garcia-Alloza, M.; de Calignon, A.; Rozkalne, A.; Koenigsknecht-Talboo, J.; Holtzman, D. M.; Bacskai, B. J.; Hyman, B. T., *Nature* **2008,** *451*, 720-U5.

256. Milam, R. A.; Milam, M. R.; Iyer, R. B., *Journal of Clinical Oncology* **2007,** *25*, 5657-5658.

257. Milos, M.; Schaer, J. J.; Comte, M.; Cox, J. A., *Journal of Biological Chemistry* **1987,** *262*, 2746-2749.

258. Milos, M.; Schaer, J. J.; Comte, M.; Cox, J. A., *Journal of Biological Chemistry* **1988,** *263*, 9218-9222.

259. Mirkin, C. A.; Letsinger, R. L.; Mucic, R. C.; Storhoff, J. J., *Nature* **1996,** *382*, 607-609.

260. Mittal, J.; Best, R. B., *Proceedings of the National Academy of Sciences of the United States of America* **2008,** *105*, 20233-20238.

261. Mok, K. H.; Kuhn, L. T.; Goez, M.; Day, I. J.; Lin, J. C.; Andersen, N. H.; Hore, P. J., *Nature* **2007,** *447*, 106-109.

262. Monera, O. D.; Sereda, T. J.; Zhou, N. E.; Kay, C. M.; Hodges, R. S., *J Pept Sci* **1995,** *1*, 319-29.

263. Morar, A. S.; Pielak, G. J., *Biochemistry* **2002,** *41*, 547-551.

264. Mrksich, M.; Whitesides, G. M., *Annual Review of Biophysics and Biomolecular Structure* **1996,** *25*, 55-78.

265. Murphy, C. J.; Gole, A. M.; Stone, J. W.; Sisco, P. N.; Alkilany, A. M.; Goldsmith, E. C.; Baxter, S. C., *Accounts of Chemical Research* **2008,** *41*, 1721-1730.

266. Murphy, K. P.; Freire, E.; Paterson, Y., *Proteins-Structure Function and Genetics* **1995,** *21*, 83-90.

267. Murphy, K. P.; Xie, D.; Garcia, K. C.; Amzel, L. M.; Freire, E., *Proteins-Structure Function and Genetics* **1993,** *15*, 113-120.

268. Myszka, D. G.; Sweet, R. W.; Hensley, P.; Brigham-Burke, M.; Kwong, P. D.; Hendrickson, W. A.; Wyatt, R.; Sodroski, J.; Doyle, M. L., *Proceedings of the National Academy of Sciences of the United States of America* **2000,** *97*, 9026-9031.

269. Nadassy, K.; Wodak, S. J.; Janin, J., *Biochemistry* **1999,** *38*, 1999-2017.

270. Naeem, A.; Fatima, S.; Khan, R. H., *Biopolymers* **2006,** *83*, 1-10.

271. Nam, J. M.; Stoeva, S. I.; Mirkin, C. A., *Journal of the American Chemical Society* **2004,** *126*, 5932-5933.

272. Nielsen, P. K.; Bonsager, B. C.; Berland, C. R.; Sigurskjold, B. W.; Svensson, B., *Biochemistry* **2003,** *42*, 1478-1487.

273. Nissink, J. W. M.; van der Maas, J. H., *Applied Spectroscopy* **1999,** *53*, 33-39.

274. Nomura, Y.; Ikeda, M.; Yamaguchi, N.; Aoyama, Y.; Akiyoshi, K., *Febs Letters* **2003,** *553*, 271-276.

275. Oh, E.; Hong, M. Y.; Lee, D.; Nam, S. H.; Yoon, H. C.; Kim, H. S., *Journal of the American Chemical Society* **2005,** *127*, 3270-3271.

276. Ohtaka, H.; Velazquez-Campoy, A.; Xie, D.; Freire, E., *Protein Science* **2002,** *11*, 1908-1916.

277. Oishi, M.; Nakaogami, J.; Ishii, T.; Nagasaki, Y., *Chemistry Letters* **2006,** *35*, 1046-1047.

278. Olsson, T. S. G.; Williams, M. A.; Pitt, W. R.; Ladbury, J. E., *Journal of Molecular Biology* **2008,** *384*, 1002-1017.

279. Ortiz-Salmeron, E.; Nuccetelli, M.; Oakley, A. J.; Parker, M. W.; Lo Bello, M.; Garcia-Fuentes, L., *Journal of Biological Chemistry* **2003,** *278*, 46938-46948.

280. Ostuni, E.; Grzybowski, B. A.; Mrksich, M.; Roberts, C. S.; Whitesides, G. M., *Langmuir* **2003,** *19*, 1861-1872.

281. Oyewumi, M. O.; Liu, S. Q.; Moscow, J. A.; Mumper, R. J., *Bioconjugate Chemistry* **2003,** *14*, 404-411.

282. Ozen, C.; Serpersu, E. H., *Biochemistry* **2004,** *43*, 14667-14675.

283. Page, J. D.; You, J. L.; Harris, R. B.; Colman, R. W., *Archives of Biochemistry and Biophysics* **1994,** *314*, 159-164.

284. Palencia, A.; Cobos, E. S.; Mateo, P. L.; Martinez, J. C.; Luque, I., *Journal of Molecular Biology* **2004,** *336*, 527-537.

285. Park, H. S.; Lin, Q.; Hamilton, A. D., *Proceedings of the National Academy of Sciences of the United States of America* **2002,** *99*, 5105-5109.

286. Pearce, K. H.; Ultsch, M. H.; Kelley, R. F.; deVos, A. M.; Wells, J. A., *Biochemistry* **1996,** *35*, 10300-10307.

287. Pengo, P.; Baltzer, L.; Pasquato, L.; Scrimin, P., *Angewandte Chemie-International Edition* **2007,** *46*, 400-404.

288. Pengo, P.; Broxterman, Q. B.; Kaptein, B.; Pasquato, L.; Scrimin, P., *Langmuir* **2003,** *19*, 2521-2524.

289. Pereira, M. T.; Silva-Alves, J. M.; Martins-Jose, A.; Lopes, J. C. D.; Santoro, M. M., *Brazilian Journal of Medical and Biological Research* **2005,** *38*, 1593-1601.

290. Petrella, E. C.; Machesky, L. M.; Kaiser, D. A.; Pollard, T. D., *Biochemistry* **1996,** *35*, 16535-16543.

291. Petricoin, E. F.; Ardekani, A. M.; Hitt, B. A.; Levine, P. J.; Fusaro, V. A.; Steinberg, S. M.; Mills, G. B.; Simone, C.; Fishman, D. A.; Kohn, E. C.; Liotta, L. A., *Lancet* **2002,** *359*, 572-577.

292. Pey, A. L.; Thorolfsson, M.; Teigen, K.; Ugarte, M.; Martinez, A., *Journal of the American Chemical Society* **2004,** *126*, 13670-13678.

293. Philo, J. S.; Aoki, K. H.; Arakawa, T.; Narhi, L. O.; Wen, J., *Biochemistry* **1996,** *35*, 1681-1691.

294. Philo, J. S.; Wen, J.; Wypych, J.; Schwartz, M. G.; Mendiaz, E. A.; Langley, K. E., *Journal of Biological Chemistry* **1996,** *271*, 6895-6902.

295. Pieper, R.; Gatlin, C. L.; Makusky, A. J.; Russo, P. S.; Schatz, C. R.; Miller, S. S.; Su, Q.; McGrath, A. M.; Estock, M. A.; Parmar, P. P.; Zhao, M.; Huang, S. T.; Zhou, J.; Wang, F.; Esquer-Blasco, R.; Anderson, N. L.; Taylor, J.; Steiner, S., *Proteomics* **2003,** *3*, 1345-1364.

296. Piszczek, G.; Rozycki, J.; Singh, S. K.; Ginsburg, A.; Maurizi, M. R., *Journal of Biological Chemistry* **2005,** *280*, 12221-12230.

297. Platis, D.; Foster, G. R., *Protein Expression and Purification* **2003,** *31*, 222-230.

298. Prakash, S.; Piruska, A.; Gatimu, E. N.; Bohn, P. W.; Sweedler, J. V.; Shannon, M. A., *Ieee Sensors Journal* **2008,** *8*, 441-450.

299. Prime, K. L.; Whitesides, G. M., *Journal of the American Chemical Society* **1993,** *115*, 10714-10721.

300. Protasevich, II; Brouillette, C. G.; Snow, M. E.; Dunham, S.; Rubin, J. R.; Gogliotti, R.; Siegel, K., *Biochemistry* **2004,** *43*, 13380-13389.

301. Provencher, S. W.; Glockner, J., *Biochemistry* **1981,** *20*, 33-37.

302. Pulido, R.; van Huijsduijnen, R. H., *Febs Journal* **2008,** *275*, 848-866.

303. Qi, K.; Ma, Q. G.; Remsen, E. E.; Clark, C. G.; Wooley, K. L., *Journal of the American Chemical Society* **2004,** *126*, 6599-6607.

304. Rakow, N. A.; Suslick, K. S., *Nature* **2000,** *406*, 710-713.

305. Raman, C. S.; Allen, M. J.; Nall, B. T., *Biochemistry* **1995,** *34*, 5831-5838.

306. Ray, P. C.; Fortner, A.; Darbha, G. K., *Journal of Physical Chemistry B* **2006,** *110*, 20745-20748.

307. Rekharsky, M. V.; Inoue, Y., *Chemical Reviews* **1998,** *98*, 1875-1917.

308. Renzoni, D. A.; Pugh, D. J. R.; Siligardi, G.; Das, P.; Morton, C. J.; Rossi, C.; Waterfield, M. D.; Campbell, I. D.; Ladbury, J. E., *Biochemistry* **1996,** *35*, 15646-15653.

309. Reynolds, R. A.; Mirkin, C. A.; Letsinger, R. L., *J. Am. Chem. Soc.* **2000,** *122*, 3795-3796.

310. Rich, R. L.; Myszka, D. G., *Journal of Molecular Recognition* **2008,** *21*, 355-400.

311. Roberts, C.; Chen, C. S.; Mrksich, M.; Martichonok, V.; Ingber, D. E.; Whitesides, G. M., *Journal of the American Chemical Society* **1998,** *120*, 6548-6555.

312. Robinson, J. A., *Accounts of Chemical Research* **2008,** *41*, 1278-1288.

313. Ron, D.; Walter, P., *Nature Reviews Molecular Cell Biology* **2007,** *8*, 519-529.

314. Rosi, N.; Mirkin, C. A., *Chem. Rev.* **2005,** *105*, 1547-1562.

315. Ross, M.; Gerke, V.; Steinem, C., *Biochemistry* **2003,** *42*, 3131-3141.

316. Rothrock, A. R.; Donkers, R. L.; Schoenfisch, M. H., *Journal of the American Chemical Society* **2005,** *127*, 9362-9363.

317. Rozema, D.; Gellman, S. H., *Biochemistry* **1996,** *35*, 15760-15771.

318. Rozema, D.; Gellman, S. H., *Journal of Biological Chemistry* **1996,** *271*, 3478-3487.

319. Russell, R. B.; Aloy, P., *Nature Chemical Biology* **2008,** *4*, 666-673.

320. Saboury, A. A.; Divsalar, A.; Jafari, G. A.; Moosavi-Movahedi, A. A.; Housaindokht, M. R.; Hakimelahi, G. H., *Journal of Biochemistry and Molecular Biology* **2002,** *35*, 302-305.

321. Saibil, H. R., *Current Opinion in Structural Biology* **2008,** *18*, 35-42.

322. Sandanaraj, B. S.; Demont, R.; Aathimanikandan, S. V.; Savariar, E. N.; Thayumanavan, S., *Journal of the American Chemical Society* **2006,** *128*, 10686-10687.

323. Sandanaraj, B. S.; Demont, R.; Thayumanavan, S., *Journal of the American Chemical Society* **2007,** *129*, 3506-+.

324. Saro, D.; Klosi, E.; Paredes, A.; Spaller, M. R., *Organic Letters* **2004,** *6*, 3429-3432.

325. Saveanu, C.; Miron, S.; Borza, T.; Craescu, C. T.; Labesse, G.; Gagyi, C.; Popescu, A.; Schaeffer, F.; Namane, A.; Laurent-Winter, C.; Barzu, O.; Gilles, A. M., *Protein Science* **2002,** *11*, 2551-2560.

326. Sawas, A. H.; Pentyala, S. N.; Rebecchi, M. J., *Biochemistry* **2004,** *43*, 12675-12685.

327. Sawyers, C. L., *Nature* **2008,** *452*, 548-552.

328. Schechter, N. M.; Eng, G. Y.; Selwood, T.; McCaslin, D. R., *Biochemistry* **1995,** *34*, 10628-10638.

329. Schellenberger, E. A.; Sosnovik, D.; Weissleder, R.; Josephson, L., *Bioconjugate Chemistry* **2004,** *15*, 1062-1067.

330. Schmidt, T. G. M.; Koepke, J.; Frank, R.; Skerra, A., *Journal of Molecular Biology* **1996,** *255*, 753-766.

331. Schon, A.; Ingaramo, M. D.; Freire, E., *Biophysical Chemistry* **2003,** *105*, 221-230.

332. Schwarz, F. P.; Tello, D.; Goldbaum, F. A.; Mariuzza, R. A.; Poljak, R. J., *European Journal of Biochemistry* **1995,** *228*, 388-394.

333. Selmer, M.; Dunham, C. M.; Murphy, F. V.; Weixlbaumer, A.; Petry, S.; Kelley, A. C.; Weir, J. R.; Ramakrishnan, V., *Science* **2006,** *313*, 1935-1942.

334. Sharp, K., *Protein Science* **2001,** *10*, 661-667.

335. Sharrow, S. D.; Edmonds, K. A.; Goodman, M. A.; Novotny, M. V.; Stone, M. J., *Protein Science* **2005,** *14*, 249-256.

336. Shimohigashi, Y.; Nose, T.; Yamauchi, Y.; Maeda, I., *Biopolymers* **1999,** *51*, 9-17.

337. Shimokhina, N.; Bronowska, A.; Homans, S. W., *Angewandte Chemie-International Edition* **2006,** *45*, 6374-6376.

338. Shiraki, K.; Kudou, M.; Fujiwara, S.; Imanaka, T.; Takagi, M., *Journal of Biochemistry* **2002,** *132*, 591-595.

339. Shultz, M. D.; Chmielewski, J., *Bioorganic & Medicinal Chemistry Letters* **1999,** *9*, 2431-2436.

340. Silow, M.; Oliveberg, M., *Biochemistry* **1997,** *36*, 7633-7637.

341. Simard, J. M.; Szymanski, B.; Rotello, V. M., *Med. Chem.* **2005,** *1*, 153-158.

342. Siwy, Z.; Trofin, L.; Kohli, P.; Baker, L. A.; Trautmann, C.; Martin, C. R., *Journal of the American Chemical Society* **2005,** *127*, 5000-5001.

343. Slowing, II; Trewyn, B. G.; Lin, V. S. Y., *Journal of the American Chemical Society* **2007,** *129*, 8845-8849.

344. Smallshaw, J. E.; Georges, F.; Lee, J. S.; Waygood, E. B., *Protein Engineering* **1999,** *12*, 623-630.

345. So, H. M.; Won, K.; Kim, Y. H.; Kim, B. K.; Ryu, B. H.; Na, P. S.; Kim, H.; Lee, J. O., *Journal of the American Chemical Society* **2005,** *127*, 11906-11907.

346. So, M. K.; Xu, C. J.; Loening, A. M.; Gambhir, S. S.; Rao, J. H., *Nature Biotechnology* **2006,** *24*, 339-343.

347. Sosnovik, D. E.; Nahrendorf, M.; Weissleder, R., *Circulation* **2007,** *115*, 2076-2086.

348. Sosnovik, D. E.; Weissleder, R., *Current Opinion in Biotechnology* **2007,** *18*, 4-10.

349. Sperling, R. A.; Gil, P. R.; Zhang, F.; Zanella, M.; Parak, W. J., *Chemical Society Reviews* **2008,** *37*, 1896-1908.

350. Sreerama, N.; Woody, R. W., *Analytical Biochemistry* **2000,** *287*, 252-260.

351. Srivastava, S.; Samanta, B.; Jordan, B. J.; Hong, R.; Xiao, Q.; Tuominen, M. T.; Rotello, V. M., *Journal of the American Chemical Society* **2007,** *129*, 11776-11780.

352. Stavens, K. B.; Pusztay, S. V.; Zou, S. H.; Andres, R. P.; Wei, A., *Langmuir* **1999,** *15*, 8337-8339.

353. Steil, L.; Thiele, T.; Hammer, E.; Bux, J.; Kalus, M.; Volker, U.; Greinacher, A., *Transfusion* **2008,** *48*, 2356-2363.

354. Stites, W. E., *Chemical Reviews* **1997,** *97*, 1233-1250.

355. Stolt, P. C.; Vardar, D.; Blacklow, S. C., *Biochemistry* **2004,** *43*, 10979-10987.

356. Storhoff, J. J.; Lucas, A. D.; Garimella, V.; Bao, Y. P.; Muller, U. R., *Nature Biotechnology* **2004,** *22*, 883-887.

357. Strater, N.; Sun, L.; Kantrowitz, E. R.; Lipscomb, W. N., *Proceedings of the National Academy of Sciences of the United States of America* **1999,** *96*, 11151-11155.

358. Summers, C. A.; II, R. A. F., *Protein Science* **2000,** *9*, 2001-2008.

359. Sundari, C. S.; Raman, B.; Balasubramanian, D., *Febs Letters* **1999,** *443*, 215-219.

360. Taboada, P.; Fernandez, Y.; Mosquera, V., *Biomacromolecules* **2004,** *5*, 2201-2211.

361. Takahashi, K.; Fukada, H., *Biochemistry* **1985,** *24*, 297-300.

362. Talhout, R.; Villa, A.; Mark, A. E.; Engberts, J., *Journal of the American Chemical Society* **2003,** *125*, 10570-10579.

363. Taylor, J. D.; Ababou, A.; Fawaz, R. R.; Hobbs, C. J.; Williams, M. A.; Ladbury, J. E., *Proteins-Structure Function and Bioinformatics* **2008,** *73*, 929-940.

364. Tello, D.; Eisenstein, E.; Schwarz, F. P.; Goldbuam, F. A.; Fields, B. A.; Mariuzza, R. A.; Poljak, R. J., *Journal of Molecular Recognition* **1994,** *7*, 57-62.

365. Templeton, A. C.; Wuelfing, M. P.; Murray, R. W., *Accounts of Chemical Research* **2000,** *33*, 27-36.

366. Thomas, C. M.; Ward, T. R., *Chemical Society Reviews* **2005,** *34*, 337-346.

367. Thomas, J. G.; Ayling, A.; Baneyx, F., *Applied Biochemistry and Biotechnology* **1997,** *66*, 197-238.

368. Thordarson, P.; Bijsterveld, E. J. A.; Rowan, A. E.; Nolte, R. J. M., *Nature* **2003,** *424*, 915-918.

369. Torigoe, H.; Nakayama, T.; Imazato, M.; Shimada, I.; Arata, Y.; Sarai, A., *Journal of Biological Chemistry* **1995,** *270*, 22218-22222.

370. Tsien, R. Y., *Annual Review of Biochemistry* **1998,** *67*, 509-544.

371. Tsukada, H.; Blow, D. M., *Journal of Molecular Biology* **1985,** *184*, 703-711.

372. Tsukihara, T.; Aoyama, H.; Yamashita, E.; Tomizaki, T.; Yamaguchi, H.; ShinzawaItoh, K.; Nakashima, R.; Yaono, R.; Yoshikawa, S., *Science* **1996,** *272*, 1136-1144.

373. Tsumoto, K.; Ueda, Y.; Maenaka, K.; Watanabe, K.; Ogasahara, K.; Yutani, K.; Kumagai, I., *Journal of Biological Chemistry* **1994,** *269*, 28777-28782.

374. Tsvetkov, P. O.; Ezraty, B.; Mitchell, J. K.; Devred, F.; Peyrot, V.; Derrick, P. J.; Barras, F.; Makarov, A. A.; Lafitte, D., *Biochimie* **2005,** *87*, 473-480.

375. Udugamasooriya, G.; Saro, D.; Spaller, M. R., *Organic Letters* **2005,** *7*, 1203-1206.

376. Varadarajan, R.; Connelly, P. R.; Sturtevant, J. M.; Richards, F. M., *Biochemistry* **1992,** *31*, 1421-1426.

377. Verma, A.; Nakade, H.; Simard, J. M.; Rotello, V. M., *Journal of the American Chemical Society* **2004,** *126*, 10806-10807.

378. Verma, A.; Simard, J. M.; Rotello, V. M., *Langmuir* **2004,** *20*, 4178-4181.

379. Verma, A.; Srivastava, S.; Rotello, V. M., *Chemistry of Materials* **2005,** *17*, 6317-6322.

380. Wada, A.; Mie, M.; Aizawa, M.; Lahoud, P.; Cass, A. E. G.; Kobatake, E., *Journal of the American Chemical Society* **2003,** *125*, 16228-16234.

381. Wang, G. L.; Zhang, J.; Murray, R. W., *Analytical Chemistry* **2002,** *74*, 4320-4327.

382. Wang, J.; Onuchic, J.; Wolynes, P., *Physical Review Letters* **1996,** *76*, 4861-4864.

383. Weber, P. C.; Pantoliano, M. W.; Thompson, L. D., *Biochemistry* **1992,** *31*, 9350-9354.

384. Wegner, G. J.; Lee, N. J.; Marriott, G.; Corn, R. M., *Analytical Chemistry* **2003,** *75*, 4740-4746.

385. Wei, G. B.; Ma, P. X., *Advanced Functional Materials* **2008,** *18*, 3568-3582.

386. Welfle, K.; Misselwitz, R.; Hohne, W.; Welfle, H., *Journal of Molecular Recognition* **2003,** *16*, 54-62.

387. Williams, D. H.; Stephens, E.; O'Brien, D. P.; Zhou, M., *Angewandte Chemie-International Edition* **2004,** *43*, 6596-6616.

388. Willner, I.; Katz, E., *Angewandte Chemie-International Edition* **2000,** *39*, 1180-1218.

389. Wilson, A. J.; Groves, K.; Jain, R. K.; Park, H. S.; Hamilton, A. D., *Journal of the American Chemical Society* **2003,** *125*, 4420-4421.

390. Wiskur, S. L.; Floriano, P. N.; Anslyn, E. V.; McDevitt, J. T., *Angewandte Chemie-International Edition* **2003,** *42*, 2070-2072.

391. Witt, D.; Klajn, R.; Barski, P.; Grzybowski, B. A., *Current Organic Chemistry* **2004,** *8*, 1763-1797.

392. Wright, A. T.; Anslyn, E. V., *Chemical Society Reviews* **2006,** *35*, 14-28.

393. Wright, A. T.; Griffin, M. J.; Zhong, Z. L.; McCleskey, S. C.; Anslyn, E. V.; McDevitt, J. T., *Angewandte Chemie-International Edition* **2005,** *44*, 6375-6378.

394. Wroblowski, B.; Diaz, J. F.; Schlitter, J.; Engelborghs, Y., *Protein Engineering* **1997,** *10*, 1163-1174.

395. Wu, G. H.; Datar, R. H.; Hansen, K. M.; Thundat, T.; Cote, R. J.; Majumdar, A., *Nature Biotechnology* **2001,** *19*, 856-860.

396. Wu, H. L.; Lace, D. A.; Bender, M. L., *Proceedings of the National Academy of Sciences of the United States of America-Biological Sciences* **1981,** *78*, 4118-4119.

397. Wu, J. G.; Li, J. Y.; Li, G. Y.; Long, D. G.; Weis, R. M., *Biochemistry* **1996,** *35*, 4984-4993.

398. Wunderbaldinger, P.; Josephson, L.; Weissleder, R., *Academic Radiology* **2002,** *9*, S304-S306.

399. Wylie, G. P.; Rangachari, V.; Bienkiewicz, E. A.; Marin, V.; Bhattacharya, N.; Love, J. F.; Murphy, J. R.; Logan, T. M., *Biochemistry* **2005,** *44*, 40-51.

400. Xu, C. J.; Xu, K. M.; Gu, H. W.; Zhong, X. F.; Guo, Z. H.; Zheng, R. K.; Zhang, X. X.; Xu, B., *Journal of the American Chemical Society* **2004,** *126*, 3392-3393.

401. Yan, K. S.; Kuti, M.; Yan, S.; Mujtaba, S.; Farooq, A.; Goldfarb, M. P.; Zhou, M. M., *Journal of Biological Chemistry* **2002,** *277*, 17088-17094.

402. Yassin, Z.; Ortiz-Salmeron, E.; Garcia-Maroto, F.; Baron, C.; Garcia-Fuentes, L., *Biochimica Et Biophysica Acta-Proteins and Proteomics* **2004,** *1698*, 227-237.

403. Yokota, A.; Tsumoto, K.; Shiroishi, M.; Kondo, H.; Kumagai, I., *Journal of Biological Chemistry* **2003,** *278*, 5410-5418.

404. Yoshida, R., *Current Organic Chemistry* **2005,** *9*, 1617-1641.

405. Yoshimoto, M.; Shimanouchi, T.; Umakoshi, H.; Kuboi, R., *Journal of Chromatography B* **2000,** *743*, 93-99.

406. Yoshimoto, N.; Hashimoto, T.; Felix, M. M.; Umakoshi, H.; Kuboi, R., *Biomacromolecules* **2003,** *4*, 1530-1538.

407. You, C. C.; Agasti, S. S.; De, M.; Knapp, M. J.; Rotello, V. M., *Journal of the American Chemical Society* **2006,** *128*, 14612-14618.

408. You, C. C.; De, M.; Han, G.; Rotello, V. M., *Journal of the American Chemical Society* **2005,** *127*, 12873-12881.

409. You, C. C.; De, M.; Rotello, V. M., *Organic Letters* **2005,** *7*, 5685-5688.

410. You, C. C.; Miranda, O. R.; Gider, B.; Ghosh, P. S.; Kim, I. B.; Erdogan, B.; Krovi, S. A.; Bunz, U. H. F.; Rotello, V. M., *Nature Nanotechnology* **2007,** *2*, 318-323.

411. Young, M.; Willits, D.; Uchida, M.; Douglas, T., *Annual Review of Phytopathology* **2008,** *46*, 361-384.

412. Zambelli, B.; Turano, P.; Musiani, F.; Neyroz, P.; Ciurli, S., *Proteins-Structure Function and Bioinformatics* **2009,** *74*, 222-239.

413. Zhang, F.; Skoda, M. W. A.; Jacobs, R. M. J.; Zorn, S.; Martin, R. A.; Martin, C. M.; Clark, G. F.; Goerigk, G.; Schreiber, F., *Journal of Physical Chemistry A* **2007,** *111*, 12229-12237.

414. Zhao, K. H.; Chai, X. M.; Marmorstein, R., *Journal of Molecular Biology* **2004,** *337*, 731-741.

415. Zheng, M.; Huang, X. Y., *Journal of the American Chemical Society* **2004,** *126*, 12047-12054.

416. Zhong, D. P., *Current Opinion in Chemical Biology* **2007,** *11*, 174-181.

417. Zhou, H. C.; Baldini, L.; Hong, J.; Wilson, A. J.; Hamilton, A. D., *Journal of the American Chemical Society* **2006,** *128*, 2421-2425.

418. Zhou, Y. L.; Liao, J. M.; Du, F.; Liang, Y., *Thermochimica Acta* **2005,** *426*, 173-178.